7-29-2014 12:00 AM

The Role of c-Kit Receptor Tyrosine Kinase in Beta-Cell Proliferation, Function and Survival

Zhi Chao Feng
The University of Western Ontario

Supervisor
Dr.Rennian Wang
The University of Western Ontario

Graduate Program in Pharmacology and Toxicology
A thesis submitted in partial fulfillment of the requirements for the degree in Doctor of Philosophy

THE ROLE OF C-KIT RECEPTOR TYROSINE KINASE IN BETA-CELL PROLIFERATION, FUNCTION AND SURVIVAL

(Thesis format: Integrated Article)

by

Zhi-Chao Feng

Graduate Program in Pharmacology and Toxicology

A thesis submitted in partial fulfillment
of the requirements for the degree of
Doctor of Philosophy

The School of Graduate and Postdoctoral Studies
The University of Western Ontario
London, Ontario, Canada

Abstract

c-Kit, a receptor tyrosine kinase, interacts with Stem Cell Factor (SCF), mediating cell differentiation, function, and survival. c-Kit is critical for the development and maintenance of beta-cell function in both rodents and humans. The mutation of *c-Kit* at *W* locus (*c-Kit*$^{Wv/+}$) in mice results in an early onset of diabetes. However, the underlying mechanisms by which c-Kit deficiency leads to beta-cell failure are unknown. Therefore, studying SCF/c-Kit downstream signaling pathways is essential to understanding the precise mechanism by which c-Kit regulates beta-cell survival and function *in vivo*.

We identified that dysregulated Akt/Glycogen synthase kinase 3β (Gsk3β)/cyclin D1 pathway, downstream of c-Kit, is responsible for reduced beta-cell proliferation, leading to a severe loss of beta-cell mass in *c-Kit*$^{Wv/+}$ mice. An up-regulation of Fas-mediated caspase-dependent apoptotic machinery is also associated with beta-cell death in *c-Kit*$^{Wv/+}$ mouse islets. The loss of functional Fas (*lpr* mutation) reversed beta-cell apoptosis and dysfunction in *c-Kit*$^{Wv/+}$*;Fas*$^{lpr/lpr}$ double mutant mice, demonstrating that a balance between c-Kit and Fas signaling is critical for beta-cell survival and function. To further delineate the primary functional role of c-Kit in beta-cells, we developed a transgenic (*c-KitβTg*) mouse model with beta-cell specific *c-KIT* overexpression. *c-KitβTg* mice exhibited increased beta-cell mass with improved insulin secretion, which is mediated by up-regulation of Akt/Gsk3β/cyclin D1 pathway. *c-KIT* overexpression in beta-cells not only protected islet function from 4 weeks of high-fat-diet (HFD) challenge, but also recused the onset of diabetes observed in *c-Kit*$^{Wv/+}$ mice. We also found that c-Kit signaling plays a critical role in islet vascularization. c-Kit mediates VEGF-A production via the Akt/mTOR pathway *in vivo*. *c-KIT* overexpression in beta-cells rescued the islet vascular defects in *c-Kit*$^{Wv/+}$ mice. However, under long-term HFD challenge, *c-KitβTg* mouse islets displayed dilated vessels with reduced beta-cell mass and increased beta-cell apoptosis. The observed beta-cell failure was likely associate with expanded islet vasculature causing increased islet inflammatory response.

In conclusion, this series of studies represent an integrated *in vitro* and *in vivo* approach aimed at unraveling the cellular mechanisms by which SCF/c-Kit regulates beta-cell survival and function.

Keywords

c-Kit, Stem Cell Factor, diabetes, pancreas, islet, beta-cell survival and insulin secretory function, islet vasculature, glucose metabolism

Co-Authorship Statement

Zhi-Chao Feng performed most experiments, and contributed to the writing of manuscripts in Chapters 3-6 with assistance of the co-authors named below in the laboratory of Dr. Rennian Wang.

Chapter 3 is adapted from **Feng ZC**, Donnelly L, Li J, Krishnamurthy M, Riopel M, Wang R. (2012) Inhibition of Gsk3β activity improves beta-cell function in *c-Kit*$^{Wv/+}$ male mice. *Lab Invest.* 92:543-555. Donnelly L contributed to some of morphometric analyses. Li J contributed to qRT-PCR analyses, and assisted with mouse islet isolation. Krishnamurthy M contributed to some of western blots analyses. Riopel M assisted with the manuscript revision. Wang R contributed to the conception and design of the study, assisted with data interpretation and analyses, and revised the manuscript.

Chapter 4 is adapted from **Feng ZC**, Riopel M, Li J, Donnelly L, Wang R. **(**2013) Improved beta-cell proliferation and function in *c-Kit*$^{Wv/+}$*;Fas*$^{lpr/lpr}$ double mutant mice. *Am J Physiol Endocrinol Metab.* 304:E557-E565. Riopel M contributed to some of morphometric analyses, and assisted with the manuscript revision. Li J contributed to qRT-PCR analyses, and assisted with mouse genotyping, mouse islet isolation. Donnelly L contributed to the double mutant mice breeding, phenotype characterization, and manuscript revision. Wang R contributed to the conception and design of the study, assisted with data interpretation and analyses, and revised the manuscript.

Chapter 5 is partially adapted from **Feng ZC***, Li J*, Turco B, Riopel M, Yee SP, Wang R. (2012) Critical role of c-Kit in beta-cell function: *increased insulin secretion and protection against diabetes in a mouse model. Diabetologia* 55:2214-2225. *equal contribution, Turco B contributed to some of morphometric analyses, Riopel M assisted with the manuscript revision. Yee SP generated the *c-KitβTg* mouse model and assisted with the manuscript revision. Wang R contributed to the conception and design of the study, assisted with data interpretation and analyses, as well as wrote and revised the manuscript.

Chapter 6 is partially adapted from **Feng ZC**, Popell A, Li J, Silverstein J, Yee SP, Wang R. (2014) c-Kit receptor tyrosine signaling regulates pancreatic islet microvasculature, beta-cell

survival and function *in vivo*. Popell A assisted with some data collection and interpretation, Li J contributed to qRT-PCR analyses and mouse islet isolation. Silverstein J contributed to some of morphometric analyses. Yee SP generated the *c-KitβTg* mouse model and assisted with the manuscript revision. Wang R contributed to the conception and design of the study, assisted with data interpretation and analyses, and revised the manuscript.

Dedication

To my father Yao-Qiang Feng and mother Jian-Xin Zhang, as well as my Ph.D. supervisor Dr.Rennian Wang, and her husband Jinming Li

Acknowledgments

First of all, I would like to extend my deepest gratitude to my Ph.D. supervisor Dr. Rennian Wang. You offered me the opportunity to pursue my Ph.D. studies in your laboratory. You taught me many indispensible skills to further my academic career. More importantly, you taught me more than what one could learn from books. I am extremely humbled and grateful for your guidance.

I would like to thank my Ph.D. advisory committee, Dr. Andy V. Babwah, Dr. Sean P. Cregan, and Dr. John DiGuglielmo, for their support.

I would like to thank all present and past members of the Wang Lab, especially Jinming Li, Matthew Riopel, Alex Popell, Jenna Silverstein, Byren Turco, Amanda Oakie, and Jason Peart.

The work presented in this thesis was supported by grants from the Canadian Institute of Health Research, and the Doctoral Student Research Award from the Canadian Diabetes Association.

Table of Contents

Abstract ii

Co-Authorship Statement iv

Dedication vi

Acknowledgments vii

List of Figures xiv

List of Appendices xviii

List of Abbreviations xix

Chapter 1 1

1 General introduction 1

1.1 Significance of the study 2

1.2 Pancreas and islet of Langerhans 2

1.2.1 Pancreas 2

1.2.2 Pancreas development in rodents 3

1.2.3 Morphogenesis signals in islet development 3

1.2.4 Vasculature in the pancreas and the pancreatic islets 4

1.2.5 Pancreatic beta-cell mass 5

1.2.6 Pancreatic beta-cell insulin secretion 6

1.3 Diabetes mellitus and current therapies 7

1.3.1 Type 1 diabetes mellitus 8

1.3.2 Type 2 diabetes mellitus 9

1.3.3 High-fat diet induced diabetes in C57BL/6J mice 10

1.3.4 Diagnosis of diabetes and current therapies 11

1.4 c-Kit and Stem Cell Factor 12

1.4.1 Structure of c-Kit and Stem Cell Factor 12
1.4.2 SCF/c-Kit signaling pathways 16
1.4.3 SCF/c-Kit function in organ development 20
1.5 c-Kit function in the pancreas 21
1.5.1 c-Kit in the developing rodent pancreas 21
1.5.2 SCF/c-Kit in islet cell differentiation 22
1.5.3 c-Kit in the regenerating pancreas 23
1.5.4 c-Kit in pancreatic disease 24
1.6 Rationales, objectives and hypotheses 25
1.6.1 Overall objective and hypothesis 25
1.6.2 Beta-cell survival and function in *c-Kit*$^{Wv/+}$ mice 25
1.6.3 Beta-cell apoptosis in *c-Kit*$^{Wv/+}$ mice 26
1.6.4 c-Kit directly affects beta-cell function 27
1.6.5 VEGF-A and islet vasculature in c-Kit mutant and transgenic mouse 28
1.7 References 30
Chapter 2 44
2 Summary of materials and methods for Chapters 3, 4, 5 and 6 44
2.1 Mouse models 45
2.1.1 Mouse models used in Chapter 3 45
2.1.2 Mouse models used in Chapter 4 50
2.1.3 Mouse models used in Chapter 5 53
2.1.4 Mouse models used in Chapter 6 56
2.2 DNA extraction and PCR genotyping 56
2.3 Body weight, food intake, and *in vivo* metabolic studies 56
2.4 *In vivo* and *ex vivo* glucose stimulated insulin secretion assay 57

2.5 Insulin ELISA analyses 57
2.6 Cell culture and treatment 58
2.6.1 Treatment with Gsk3β inhibitor on isolated islets in Chapter 3 58
2.6.2 INS-1 cell culture in Chapter 4 and 5 58
2.7 Immunofluorescence and morphometric analyses 59
2.8 Protein extraction and western blot analyses 61
2.9 RNA extraction and real-time RT-PCR analyses 61
2.10 Statistical analyses 62
2.11 References 63
Chapter 3 64
3 Inhibition of Gsk3β activity improves beta-cell function in *c-Kit*$^{Wv/+}$ mice 64
3.1 Introduction 65
3.2 Materials and methods 66
3.3 Results 68
3.3.1 Reduction of phospho-Akt, phospho-Gsk3β and cyclin D1 in *c-Kit*$^{Wv/+}$ mice 68
3.3.2 Inhibition of Gsk3β activity prevents early onset of diabetes in *c-Kit*$^{Wv/+}$ mice 75
3.3.3 Inhibition of Gsk3β activity preserves beta-cell mass in *c-Kit*$^{Wv/+}$ mice 80
3.3.4 Inhibition of Gsk3β activity preserves β-catenin, cyclin D1, Pdx-1, and MafA expression and increases the proliferative capacity of beta-cells of *c-Kit*$^{Wv/+}$ mice 83
3.4 Discussion 93
3.5 References 97
Chapter 4 101
4 Down-regulation of Fas activity rescues early onset of diabetes in *c-Kit*$^{Wv/+}$ mice 101
4.1 Introduction 102

4.2 Materials and methods 103

4.3 Results 104

4.3.1 *c-Kit*$^{Wv/+}$ mice show increased beta-cell apoptosis due to increased p53 signaling and resulting up-regulated Fas activity 104

4.3.2 Down-regulation of Fas in *c-Kit*$^{Wv/+}$ mice leads to improved beta-cell function 114

4.3.3 Increased beta-cell mass and proliferation, and decreased beta-cell apoptosis observed in c-*Kit*$^{Wv/+}$;*Fas*$^{lpr/lpr}$ double mutant mice 119

4.3.4 Down-regulation of Fas in the absence of c-Kit signaling activates the cFlip/NF-κB pathway, and increases islet transcription factor expression 122

4.4 Discussion 129

4.5 References 133

Chapter 5 136

5 Critical role of c-Kit in beta-cell function: *increased insulin secretion and protection against diabetes* 136

5.1 Introduction 137

5.2 Materials and methods 137

5.3 Results 139

5.3.1 Generation of transgenic mouse model with *c-KIT* overexpression specifically in beta-cells 139

5.3.2 Improved glucose tolerance and insulin secretion in *c-KitβTg* mice 144

5.3.3 Increased islet transcription factors, beta-cell mass and proliferation in *c-KitβTg* mice 149

5.3.4 Increased PI3K/Gsk3β/cyclin D1 signaling pathway in *c-KitβTg* mouse islets 156

5.3.5 *c-KitβTg* mice tolerate HFD-induced diabetes 159

5.3.6 *c-Kit*$^{Wv/+}$ mice with specific overexpression of *c-KIT* in beta-cells display normal glucose metabolism 164

5.4 Discussion 169

5.5 References 172

Chapter 6 175

6 c-Kit-mediated VEGF-A production regulates islet microvasculature, beta-cell survival, and function *in vivo* 175

6.1 Introduction 176

6.2 Materials and methods 177

6.3 Results 178

6.3.1 c-Kit function is required for maintaining the normal islet microvasculature *in vivo* 178

6.3.2 Beta-cell specific c-Kit maintains islet microvasculature via the PI3K/Akt/mTOR pathway and VEGF-A production *in vivo* 181

6.3.3 *c-KIT* overexpression in beta-cell promotes islet angiogenesis *in vivo* .. 186

6.3.4 *c-KIT* overexpression exaggerates islet hyper-vasculature in 28-week-old *c-KitβTg* mice under long-term HFD. 189

6.3.5 *c-KIT* overexpression-induced hyper-vasculature impairs beta-cell function in 28-week-old *c-KitβTg* mice under long-term HFD 192

6.3.6 *c-KIT* overexpression-induced hyper-vasculature is associated with islet inflammatory response and cytokine production in 28-week-old *c-KitβTg* mice under long-term HFD 201

6.4 Discussion 206

6.5 References 210

Chapter 7 214

7 Summary, limitations and future directions 214

7.1 Summary 215

7.1.1 Overall rationale and main objective 215

7.1.2 The *c-Kit* W^{v} mutation causes beta-cell loss and dysfunction via the dysregulated Akt/Gsk3β pathway and up-regulated Fas-mediated apoptotic signaling in *c-Kit*$^{Wv/+}$ mouse model 218

7.1.3 *c-KIT* overexpression positively regulates beta-cell proliferation and function via an up-regulation of the Akt/Gsk3β/cyclin D1 pathway in *c-KitβTg* mice 219

7.1.4 c-Kit signaling positively regulates islet vascular formation via the Akt/mTOR/VEGF-A pathway 219

7.2 Limitations 220

7.2.1 Chapter 3 220

7.2.2 Chapter 4 222

7.2.3 Chapter 5 223

7.2.4 Chapter 6 225

7.3 Concluding remarks 225

7.4 Future directions 226

7.5 References 228

Appendices 231

Curriculum Vitae 243

List of Figures

Figure 1-1. Structure of c-Kit and Stem Cell Factor (SCF). 15

Figure 1-2. c-Kit signaling pathways. 19

Figure 2-1. Breeding schematic for *c-Kit*$^{Wv/+}$ mice. 46

Figure 2-2. Experimental design of 1-AKP treatments for *c-Kit*$^{Wv/+}$ mice. 48

Figure 2-3. Breeding schematic for *c-Kit*$^{Wv/+}$*;Fas*$^{lpr/lpr}$ double mutant mice. 51

Figure 2-4. Breeding schematic for *c-KitβTg;Wv* mice. 54

Figure 3-1. Down-regulation of phospho-Akt/Gsk3β signaling in the pancreata and isolated islets from *c-Kit*$^{Wv/+}$ mice. 69

Figure 3-2. Western blot analyses of phospho-Akt^{T308}, and phospho-Gsk3β^{Y216} protein levels in isolated islets from *c-Kit*$^{Wv/+}$ mice. 71

Figure 3-3. Decreased cyclin D1 protein levels in isolated islets of *c-Kit*$^{Wv/+}$ mice. 73

Figure 3-4. Effect of Gsk3β inhibitor on glucose homeostasis of *c-Kit*$^{Wv/+}$*/1-AKP* mice..... 76

Figure 3-5. Effect of Gsk3β inhibitor on beta-cell function of *c-Kit*$^{Wv/+}$*/1-AKP* mice. 78

Figure 3-6. Effect of Gsk3β inhibitor on pancreatic morphology of *c-Kit*$^{Wv/+}$*/1-AKP* mice. . 81

Figure 3-7. Inhibition of Gsk3β maintains β-catenin and cyclin D1 level in *c-Kit*$^{Wv/+}$*/1-AKP* mouse islets. 85

Figure 3-8. Inhibition of Gsk3β results in increased Pdx-1 and MafA expression in *c-Kit*$^{Wv/+}$*/1-AKP* mice. 87

Figure 3-9. Inhibition of Gsk3β results in increased beta-cell proliferation in *c-Kit*$^{Wv/+}$*/1-AKP* mice. 89

Figure 3-10. A proposed model involving c-Kit/Akt/Gsk3β signaling pathways in beta-cell survival and function in *c-Kit*$^{Wv/+}$ mice. 91

Figure 4-1. Up-regulation of p53 and Fas signaling in isolated islets from *c-Kit*$^{Wv/+}$ mice.. 105

Figure 4-2. Increased SCF/c-Kit interaction in INS-1 cells results in decrease of p53 and Fas expression via the PI3K pathway. 108

Figure 4-3. Absence of c-Kit signaling induces the p53/Fas-mediated caspase-dependent apoptotic signaling. 110

Figure 4-4. Knockdown of Fas decreases cell apoptosis. 112

Figure 4-5. Fasting blood glucose and glucose tolerance on *c-Kit*$^{Wv/+}$*;Fas*$^{lpr/lpr}$ *(Wv;-/-)* mice at 8 weeks of age. 115

Figure 4-6. GSIS and insulin content in *c-Kit*$^{Wv/+}$*;Fas*$^{lpr/lpr}$*(Wv;-/-)* mice at 8 weeks of age. 117

Figure 4-7. Islet morphology and immunohistochemical analysis of endocrine cell mass, cell proliferation, and cell death in *c-Kit*$^{Wv/+}$*;Fas*$^{lpr/lpr}$*(Wv;-/-)* mice at 8 weeks of age. 120

Figure 4-8. Expression of transcription factors, endocrine genes, and signaling molecules in *c-Kit*$^{Wv/+}$*;Fas*$^{lpr/lpr}$*(Wv;-/-)* mice. 123

Figure 4-9. Expression of cleaved caspase 8 and 3 in *c-Kit*$^{Wv/+}$*;Fas*$^{lpr/lpr}$ (*Wv;-/-*) mice at 8 weeks of age. 125

Figure 4-10. Proposed model of c-Kit and Fas signaling that mediates beta-cell proliferation, function, and survival. 127

Figure 5-1. Generation of C57BL/6J transgenic mice with *c-KIT* overexpression specifically in beta-cells (*c-KitβTg*). 140

Figure 5-2. Expression of SCF levels in C57BL/6J transgenic mice with *c-KIT* overexpression specifically in beta-cells (*c-KitβTg*). 142

Figure 5-3. Body weight, food intake and blood glucose level in *c-KitβTg* mice. 145

Figure 5-4. Glucose tolerance, GSIS, and insulin content in *c-KitβTg* mice. 147

Figure 5-5. Islet morphology in *c-KitβTg* mice at 8 weeks of age. 150

Figure 5-6. Expression of islet transcription factors in *c-KitβTg* mice at 8 weeks of age. ... 152

Figure 5-7. Expression of islet endocrine genes, Glut2, and Glp1 receptors in *c-KitβTg* mice at 8 weeks of age. 154

Figure 5-8. Levels of phosphorylated Akt/Gsk3β/cyclin D1 signaling and downstream signaling molecules in *c-KitβTg* mice at 8 weeks of age. 157

Figure 5-9. Effect of a HFD on *c-KitβTg* mice. 160

Figure 5-10. Effect of a HFD on islet morphology of *c-KitβTg* mice. 162

Figure 5-11. Glucose tolerance and insulin secretion in *c-KitβTg;Wv* mice. 165

Figure 5-12. A proposed model of SCF/c-Kit signaling to mediate beta-cell proliferation and function. 167

Figure 6-1. Overexpressing *c-KIT* in beta-cells rescues loss of islet microvasculature in *c-Kit*$^{Wv/+}$ mice. 179

Figure 6-2. Rescued islet microvasculature is associated with increased c-Kit-mediated VEGF-A production via the PI3K/mTOR pathway in *c-KitβTg;Wv* mice. 182

Figure 6-3. Expression of islet transcription factors in *c-KitβTg;Wv* mice. 184

Figure 6-4. Beta-cell specific *c-KIT* overexpression promotes islet angiogenesis *in vivo*. .. 187

Figure 6-5. Increased vessel dilation in 28-week-old *c-KitβTg* mice under long-term HFD. 190

Figure 6-6. Glucose tolerance and islet morphology in 28-week-old *c-KitβTg* mice. 193

Figure 6-7. Expression of islet transcription factors in 28-week-old *c-KitβTg* mice. 195

Figure 6-8. Islet hypervascularization results in impaired glucose tolerance in 28-week-old *c-KitβTg* mice under long-term HFD. 197

Figure 6-9. Altered islet morphology is observed in 28-week-old *c-KitβTg* mice under long-term HFD. 199

Figure 6-10. Increased islet inflammation and cytokine production is induced by islet hypervascularization in 28-week-old *c-KitβTg* mice under long-term HFD. 202

Figure 6-11. Proposed model of c-Kit signaling that mediates VEGF-A production and modulates islet vasculature, affecting beta-cell function and survival. 204

Figure 7-1. Summary of c-Kit signaling in the beta-cell. 216

List of Appendices

Appendix I. Animal used protocol. 231

Appendix II. Biosafety approval. 232

Appendix III. Sequences of primers. 233

Appendix IV. Sequences of siRNA 234

Appendix V. List of antibodies for immunofluorescence. 235

Appendix VI. List of antibodies for western blot. 236

Appendix VII. Sequences of primers for real-time RT-PCR. 237

Appendix VIII. Copyright of Chapter 3. 238

Appendix IX. Copyright of Chapter 5. 239

List of Abbreviations

ADP	Adenosine diphosphate
ATP	Adenosine triphosphate
AUC	Area under curve
cDNA	Complementary deoxyribonucleic acid
CTL	Cytotoxic T lymphocyte
c-KitβTg	Beta-cell specific overexpression of *c-KIT*
DAPI	4'-6'-diamidino-2-phenylindol
eGFP	Enhanced green fluorescent protein
ER	Endoplasmic reticulum
ERK	Extracellular signal-regulated kinases
E-cad	E-cadherin
FasL	Fas ligand
FBG	Fasting blood glucose
GAPDH	Glyceraldehyde 3-phosphate dehydrogenase
Glp-1r	Glucagon-like peptide-1 receptor
Glut2	Glucose transporter 2
GNNK	Gly-Asn-Asn-Lys sequence
GSIS	Glucose stimulated insulin secretion
Gsk3β	Glycogen synthase kinase 3 β
HFD	High-fat diet
HLA	Human leukocyte antigen
HSCs	Hematopoietic stem cells
IL-1β	Interleukin-1 β
INS-1	Rat insulinoma cell lines

IPITT	Intraperitoneal insulin tolerance test
IPGTT	Intraperitoneal glucose tolerance test
JAK/STAT	Janus kinase and signal transducers and activtors of transcription
Mac-2	Galectin-3
MafA	V-maf musculoaponeurotic fibrosarcoma oncogene homolog A
MAP	Mitogen-activated protein
mSCF	Membrane-bound Stem Cell Factor
MTT	(3-(4,5-Dimethylthiazol-2-yl)-2,5-diphenyltetrazolium bromide
Ngn3	Neurogenin 3
Nkx2.2	NK2 homeobox 2
Nkx6.1	NK6 homeobox 1
NOD/SCID	Non-obese diabetic/severe combined immune deficient
ON	Overnight
PANC-1	Human pancreatic carcinoma epithelial-like cell lines
PARP	Poly ADP ribose polymerase
Pax4	Paired box protein 4
Pax6	Paired box protein 6
PDGFR	Platelet-derived growth factor receptor
Pdx-1	Pancreatic duodenal homeobox-1
PECAM-1	Platelet endothelial cell adhesion molecule-1
PFT-α	Pifithrin-alpha
PI3K	Phosphoinositide 3-kinase
PLC-γ	Phospholipase C-gamma
qRT-PCR	quantitative RT-PCR
RIP	Rat insulin promoter

RTK	Receptor tyrosine kinase
RT	Reverse transcription
SDS-PAGE	Sodium dodecyl sulfate-polyacrylamide gel electrophoresis
Src	V-src avian sarcoma
sSCF	Soluble Stem Cell Factor
TNF	Tumor necrosis factor
TUNEL	Terminal deoxynucleotidyl transferase dUTP nick end labeling
T1D	Type 1 diabetes mellitus
T2D	Type 2 diabetes mellitus
VEGFs	Vascular endothelial growth factors
VNTR	Variable number of tandem repeats
W^v	Viable dominant spotting
1-AKP	1-Azakenpaullone

Chapter 1

1 General introduction[1]

[1] Parts of this chapter have been modified and adapted from the following manuscript:

- Feng ZC, Riopel M, Popell A, Wang R. A survival Kit for the pancreatic beta-cell. Manuscript in submission 2014.

1.1 Significance of the study

The incidence of diabetes mellitus is rising globally. One major cause behind the progression of diabetes is the decline in pancreatic beta-cell mass and function. Repopulating insulin-producing cell-based therapy remains a highly promising therapeutic modality that could provide the solution for treating diabetes. Donor islet availability is limited, so a greater understanding of how cellular machinery maintains islet function and survival is needed. c-Kit, a receptor tyrosine kinase (RTK), plays an important role in mediating islet cell neogenesis, proliferation, differentiation, and function. The objective of this work is to determine the intracellular mechanisms of c-Kit and its ligand, Stem Cell Factor (SCF), in regulating beta-cell survival and function in both physiological and pathological settings. The resulting data from this work will contribute to new and more physiologically relevant cell replacement therapies for treating diabetes.

1.2 Pancreas and islet of Langerhans

1.2.1 Pancreas

The pancreas is a glandular organ that consists of two major functional compartments: exocrine and endocrine. The exocrine pancreas constitutes almost 99% of the total pancreatic mass and is comprised of acinar cells and ducts. Acinar cells release pancreatic juices containing protease, lipases, and amylases to assist in the digestion and absorption of nutrients in the small intestine. The pancreatic ducts join to the common bile duct, which transports the pancreatic juices to the duodenum. The endocrine pancreas is comprised of the islets of Langerhans, and account for only 1-2% of the total pancreatic mass. Islets possess a remarkable architecture and varying levels of cellular organization across different species. In rodents, five primary endocrine cell types are found within islets: insulin-producing beta-cells are the major endocrine cell population in the core of islets (60-80%), and are surrounded by the glucagon-secreting alpha-cells (15-20%). The remaining 5% of endocrine cells are somatostatin-secreting delta-cells, pancreatic polypeptide-secreting F-cells, and ghrelin-secreting epsilon-cells, which appear as single cells or in small groups that are scattered within islets. The levels of glucose in the blood

are rapidly and precisely regulated by hormone production from islets [1, 2]. Thus, islet dysfunction is central to the development of hyperglycemia, and multiple efforts have been made to improve islet survival and function.

1.2.2 Pancreas development in rodents

The development of the pancreas is conserved among species, and the mouse model has been a powerful research tool for examining pancreatic organogenesis. In rodents, the pancreas begins to develop from the mid-gut endoderm on embryonic day e8.5 [3, 4]. The 'primary transition' commences when the dorsal bud develops in proximity to the notochord at e9.5, and the ventral bud grows as the pancreatic epithelium evaginations derivate at e10.25. The twisting of the gut tube brings the dorsal and ventral buds together in close proximity, which leads to projections of the epithelium invading into surrounding mesenchyme at approximately e12.5 [3]. The first wave of the pancreatic endocrine differentiation begins during the primary transition. Endocrine cells that co-express both glucagon and insulin are first visible at e9.5 in the dorsal pancreas. Ghrelin- and somatostatin-expressing cells begin to appear between e9.5 and e12.5 at the tip of the dorsal pancreas, and a few pancreatic polypeptide-expressing cells clustered in the ventral pancreas are seen at e11.5 [3]. Following the primary transition, the pancreatic epithelium undergoes a massive wave of expansion and differentiation, marking the 'secondary transition'. During this transition, the pancreatic primordium branches off, differentiates, and commits to an endocrine or exocrine pancreatic lineage. This indicates the second wave of the pancreatic endocrine cell differentiation, with the majority differentiating into beta-cells or alpha-cells. This is followed by the expansion and maturation of epsilon-cells, delta-cells, and F-cells [3]. Mature islet aggregates with capillaries form during the third transition, and the endocrine pancreas continues to mature, expand, and remodel until the end of the third postnatal week [1, 3-5].

1.2.3 Morphogenesis signals in islet development

The morphogenesis of the pancreas relies on inductive signals from the notochord. Specifically, growth factor activin-β and fibroblast growth factor-2 from the notochord repress expression of the sonic hedgehog (Shh) morphogen in the primitive gut endoderm

[6]. Inhibition of Shh signaling promotes pancreatic and duodenal homeobox 1 (Pdx-1) expression at e8.5, marking the onset of the pancreas development [7]. Following Pdx-1 expression, Pancreas transcription factor (Ptf1a) and Homeobox transcription factor (Hlxb9) appear, which are required for ventral and dorsal pancreas formation, respectively. The initial step that specifies pancreatic endocrine cell fate occurs with the expression of the bHLH transcription factor Neurogenin 3 (Ngn3) at e9-9.5 [8]. Mice lacking Ngn3 expression failed to develop any endocrine cells [9]. Ngn3-expressing islet progenitors adopt the pancreatic endocrine cell fate with a specific combinations of lineage-determining transcription factors. In brief, alpha-cell fate is primarily specified by the appearance of aristaless related homebox, and subsequent expression of brain 4, V-maf musculoaponeurotic fibrosarcoma oncogene homolog B, and paired box protein 6 (Pax6) [8]. In contrast, beta-cell phenotype is determined by transient expression of paired box protein (Pax4), which is followed by the appearance of V-maf musculoaponeurotic fibrosarcoma oncogene homolog A (MafA), NK2 homeobox 2 (Nkx 2.2), NK6 homeobox 1 (Nkx 6.1), Pax6, and Pdx-1 [8]. Many transcription factors, such as Pdx-1 and Pax6, appear to serve dual functions in determining the specification of endocrine cell lineage and in maintaining the phenotype and function of islet cells. Thus, loss of these transcriptional regulators correlates with defective pancreatic endocrine cells growth and function, and later corresponding manifestation of impaired glucose homeostasis.

1.2.4 Vasculature in the pancreas and the pancreatic islets

Blood vessels play an important role in pancreatic development. During the primary transition, most of the vessels in the early budding pancreas are not perfused; this provides non-nutrient cues to the developing pancreas. There is emerging evidence showing that the maintenance of Pdx-1, induction of Ptf1A, and subsequent pancreatic budding depends on signals from embryonic aortic endothelial cells [4, 10-12]. Blood vessels also appear to provide nutrient cues to trigger pancreatic growth from e14.5-15 onward [12]. Blood perfusion in vessels is coordinated with rapid pancreas branching and endocrine cell differentiation during the second transition. The capillary network also plays an important role in islet survival and function. The vasculature in the endocrine

pancreas is five-fold denser than in the exocrine pancreas [13]. Likewise, islets receive 10% of total pancreatic blood flow, and their vessels are approximately ten times more fenestrated than the exocrine pancreas [14]. The denser capillary networks correlate with high vascular endothelial growth factor (VEGF) production from beta-cells. Beta-cells exclusively express the soluble, diffusible splice-forms of VEGF-A 120, VEGF-A 164, and VEGF-A 188. VEGF-A 164 (the predominant form) has the highest bioavailability and biological potency [5, 8, 15]. As demonstrated in mouse models, VEGF-A acts as a messenger to maintain the intimate connection between islet endocrine cells and blood vessels. The dense islet capillary network supplies beta-cells with a nutrient filled environment necessary for survival and function. In return, constitutive release of VEGF-A by beta-cells promotes endothelial cell recruitment and maintains the integrity of islet vasculature. Overall, the efficient communication between blood and beta-cells is essential for the precise glucose sensing and systemic circulation of pancreatic hormone [16]. Thus, disturbance of VEGF-A signaling can lead to abnormal vasculature in islets, and ultimately affects beta-cell survival and function resulting in impaired glucose homeostasis.

1.2.5 Pancreatic beta-cell mass

Pancreatic beta-cell mass is determined by neogenesis, proliferation of pre-existing beta-cells, and apoptosis [17]. In rodent pancreatic development, the major expansion of beta-cells occurs during secondary transition and involves a rapid daily doubling of the beta-cell population. Neogenesis accounts for almost 80% of new beta-cells formed, whereas only a fraction (10-20%) of beta-cell growth is attributed to beta-cell proliferation [17]. Newly formed islet clusters appear adjacent to or are embedded in the ducts, suggesting that the islet cell precursors are a subpopulation found within the ducts or harboured in the ducts [17]. In contrast to gestational stages in rodents, beta-cell mass expansion only occurs at a rate of 2-3% per day [17], consisting of a transient surge in beta-cell neogenesis within the first week, and proliferation after the first week of birth in neonatal rodent pancreas [17]. Loss of some beta-cell mass due to apoptosis is seen around weaning age during the postnatal remodelling period. In the adult rodent pancreas, the mitotic rate of beta-cells slows down due to the limited proliferative capacity of the

terminally differentiated endocrine cells. The turnover rate is less than 0.25% beyond 3 months of age [17, 18]. Interestingly, beta-cells retain a remarkable degree of plasticity in response to a variety of stresses, including pregnancy, obesity, and insulin resistance. Under these scenarios, a robust beta-cell mass compensation is seen in an attempt to maintain insulin production and subsequent euglycemia. However, the underlying mechanism(s) by which beta-cells maintain their own survival and proliferation is (are) not fully determined.

1.2.6 Pancreatic beta-cell insulin secretion

The *Insulin* genes in rodents form a two-gene system in which *Insulin I* was retroposed from the partially processed mRNA of *Insulin II*. These two *Insulin* genes are located on different chromosomes, with *Insulin I* on chromosome 7, and *Insulin II* on chromosome 19 in mice [19]. This is in contrast to humans, in which one copy of the *INSULIN* gene was found on chromosome 11 [19]. *Preproinsulin gene I* (*Insulin I*) is a rodent specific retrogene that contains only one intron homologous to the first intron of *Preproinsulin gene II* (*Insulin II*). *Insulin II* is an ortholog to the *INSULIN* gene in humans that has three exons and two introns. Insulin production involves multiple intermediate steps. Preproinsulin is a large precursor translational product of either *Insulin I* or *Insulin II*, and it contains the N-terminal signal peptide, B chain, C-peptide, and A chain. Preproinsulin is rapidly cleaved to proinsulin by signal peptidases, which remove the signal peptide from its N-terminus. The modification of proinsulin to insulin is a relatively slow process, which comprises both the conversion of proinsulin to insulin in the Golgi apparatus, and the sorting out of insulin polypeptides on their way from the rough endoplasmic reticulum (ER) to the storage secretory granules [19]. Mechanically, proinsulin together with the proteolytic enzymes is stored in trans Golgi vesicles surrounded by a cisternae membrane that contains the adenosine triphosphate (ATP)-dependent proton pump. As ATP increases due to glucose metabolism in beta-cells, the proton pump transports H^+ into the trans Golgi vesicles. The acidic proteolytic enzymes are activated, and the C-peptide is cleaved from the A and B chains of insulin [20]. Mature insulin and cleaved C-peptides are then packaged into secretory granules for release into circulation.

Insulin is exclusively secreted by beta-cells in response to changes in blood glucose levels [21]. In rodents, insulin secretion occurs along a biphasic time course [22]. The first phase lasts approximately 10 minutes, peaking 5 minutes following glucose stimulation. The second phase is characterized by a prolonged slow release, which lasts until the blood glucose level returns to normal. Glucose transporter 2 (Glut2) is involved in metabolic glucose sensing by mediating glucose transport into rodent beta-cells. Subsequently, glucose is phosphorylated by the rate-limiting enzyme glucokinase, and is further metabolized to produce ATP via the mitochondrial tricarboxylic acid cycle in the mitochondria. Increased ATP: adenosine diphosphate ratio causes the closure of ATP-sensitive potassium channels. The increasing concentration of intracellular potassium ions in beta-cells leads to beta-cell depolarization, which triggers calcium influx from opened voltage-gated calcium channels. There is emerging evidence showing that the first phase of insulin secretion depends on the rapid and marked elevation of intracellular calcium level in beta-cells, and corresponds to the release of insulin granules from a readily releasable pool within 5 minutes of glucose stimulation. The second phase of insulin secretion requires paracrine signals other than the intracellular calcium rise, including the amplification of glucose and insulin that may serve to replenish the pool of granules that are releasable at the prevailing intracellular calcium level.

1.3 Diabetes mellitus and current therapies

Diabetes mellitus is a chronic metabolic disease that occurs when the body is either unable to sufficiently produce or properly use insulin. It is widely recognized as an epidemic in Canada. There are currently more than 9 millions Canadians living with diabetes or prediabetes [23]. The prevalence of diabetes translates into a huge economical burden for Canadian society. It is estimated that the total health care costs associated with diabetes is expected to increase to over 8 billion dollars annually by the year 2016 [23]. There are two major forms of diabetes. It is estimated that 5% to 10% of diabetic Canadians have type 1 diabetes mellitus (T1D), while 90% to 95% have type 2 diabetes mellitus (T2D) [23]. T1D, once known as ‘juvenile diabetes’ or ‘insulin dependent diabetes’, is characterized by an absolute deficiency of beta-cells due to an autoimmune attack, resulting in an insufficient supply of insulin that is unable to maintain euglycemia

[23]. In contrast, T2D, also referred to as 'non-insulin-dependent diabetes', is a metabolic disorder that occurs when there is insufficient insulin production to compensate for growing systemic insulin resistance [23]. The high secretory demand in overt hyperglycemia results in progressive deterioration of beta-cell function and induction of beta-cell apoptosis. Thus, beta-cell failure is regarded as the primary cause of both forms of diabetes.

1.3.1 Type 1 diabetes mellitus

T1D is an autoimmune disorder, meaning patients often exhibit features reflective of an immunological contribution to the disease. In most cases, genetic predisposition associated with the immune system plays a huge role in the onset of T1D. The region of the human leukocyte antigen (HLA) complex in T1D patients and non-obese diabetic mice is highly linked to T1D susceptibility. The majority of T1D patients carry HLA-DR3 and HLA-DR4, with around 30% being DR3/DR4 heterozygous [24]. Beyond the HLA, the variable number of tandem repeats (VNTR) located upstream of the *Insulin* gene is the second most susceptible region to T1D. Short VNTR confers high risk for T1D [25]. Other non-HLA genes associated with T1D are cytotoxic T lymphocyte (CTL) associated-4 and PTPN22. CTL associated-4 encodes a molecule that plays a regulatory role in T-cell functionality [26], and the PTPN22 phosphatase is thought to influence immune responsiveness [27]. The genes that confer a risk to T1D may also play an important role in beta-cell death.

Mechanistically, beta-cells develop specific autoantigens expressed as peptide-major histocompatibility complexes. This portends the development of activated CTLs and autoreactive helper T-cells (including $CD8^+$ and $CD4^+$ T-cells) capable of destroying beta-cells. Beta-cells can be selectively killed by the immune system via multiple pathways including: 1) activation of death receptor, 2) perforin and granzyme B released by $CD8^+$ T cells, and 3) interleukin-1 β (IL-1β). Activation of death receptors including Fas and tumor necrosis factor alpha (TNFα) receptors has also been implicated in beta-cell destruction in T1D [28]. While Fas receptor (Fas) expression is negligible in healthy islets, up-regulated Fas expression on beta-cells could be triggered by exposure to cytokine IL-1β. Extrinsic caspase 8 apoptotic pathway is mediated by the interaction

between Fas and Fas ligand (FasL), which contributes to beta-cell destruction in the progression of T1D. Perforin and granzyme B represent an alternative pathway of beta-cell apoptosis in T1D [28]. Perforin released by CTLs are able to integrate into the beta-cell membrane forming pores for granzyme B infiltration. Granzyme B is able to enter the cell and cleave multiple apoptotic proteins, including Bid, to activate apoptosis [29]. Additionally, IL-1β is detectable in islets, and confers another avenue in mediating beta-cell destruction in T1D. In rodent models, injection of recombinant IL-1β induced transient hyperglycemia, and high doses of IL-1β accelerated the onset of diabetes [30]. Furthermore, neutralization of IL-1β was able to delay and reduce diabetes in non-obese diabetic (NOD) mice [31].

1.3.2 Type 2 diabetes mellitus

T2D is characterized by beta-cell failure, hyperinsulinemia, and hyperlipidemia. There is emerging evidence showing that T2D stems from interactions between genetic predisposition and environment, including obesity. Genetically, calpain-10, a member of a ubiquitously expressed family of cysteine proteases, is associated with a high risk of T2D. About 30% of the T2D population is associated with this locus [32]. Obesity is associated with peripheral insulin resistance and systemic inflammation. In obese people, increased beta-cell mass and insulin secretion is required to compensate for the metabolic demand. A failure of this compensatory increase results in beta-cell dysfunction and insulin resistance, and eventually a loss of beta-cell mass during the course of T2D. Compared to weight-matched control subjects, a 40-60% loss of beta-cell mass is also found in T2D subjects, and at least 40% of the beta-cell mass is reduced in pre-diabetic patients [33]. Multiple proposed pathogenic mechanisms are responsible for beta-cell failure during the progression of T2D, including: 1) glucose toxicity, 2) beta-cell exhaustion, 3) lipotoxicity, and 4) pro-inflammatory cytokine. Glucose toxicity implies a direct effect of elevated blood glucose levels, which impairs beta-cell health via various mechanisms, such as Fas-mediated beta-cell apoptosis [34], toxic reactive oxygen species production from mitochondria [35], or induction of the pro-apoptotic protein TXNIP [36] and Bcl family members [37]. Beta-cell exhaustion is another proposed mechanism based on an indirect effect of hyperglycemia to impair beta-cell function by causing a

nonsustainable compensatory increase in insulin secretion. Increased beta-cell workload could result in an increase of misfolded protein production, and activation of the unfolded protein response in the ER and Golgi apparatus [38, 39]. Subsequently, an accumulation of these misfolded proteins can trigger beta-cell failure in T2D. There has been interest in examining excess fatty acids such as palmitate, as they may have toxic effects on beta-cell function and viability via the generation of ceramide and reactive oxygen species. Indeed, previous studies have demonstrated that palmitate is able to trigger beta-cell apoptosis via activation of caspase-mediated mitochondrial dysfunction and reduction of Bcl pro-survival proteins. Moreover, palmitate negatively impacts proinsulin's conversion to mature insulin by an induced calcium-dependent degradation of carboxypeptidase E [38]. Furthermore, palmitate has been demonstrated to impair the secretory pathways by partially depleting ER calcium stores [39]. Finally, considerable data supports that pro-inflammatory cytokines and immune cell infiltration of the islet are potential underlying mechanisms contributing to beta-cell failure in T2D. An elevated production of IL-1β can be detected in islets exposed to high glucose levels and hyperlipidemia. The induced local islet inflammation recruits subsequent islet infiltration by macrophages to promote beta-cell apoptosis [40]. There is emerging evidence that cytokines, such as IL-1β and TNFα, promote the production of NO, leading to depleted calcium influx into the ER, which in turn promotes ER stress mediated beta-cell apoptosis [41].

1.3.3 High-fat diet induced diabetes in C57BL/6J mice

Obesity represents a major risk factor, and often precedes the onset of T2D. In diabetes research, syndromes resembling T2D have been identified in obese C57BL/6J mice. Several genetic factors contained in the C57BL/6J background allow these mice to develop diabetes in a manner analogous to most cases of T2D in humans through dietary manipulation [42]. C57BL/6J mice fed with food enriched in fat spontaneously developed obesity along with hyperinsulinemia, hyperglycemia, and hypertension. However, lean C57BL/6J mice remain euglycemic when fed a normal diet. Noticeable weight gain is observed after 2 weeks of high-fat diet (HFD), and hyperglycemia usually develops

within 4 weeks of HFD [43], and the full manifestation of diet-induced diabetes develops after 16 weeks of HFD, with 20-30% weight gain, compared to normal diet-fed mice.

1.3.4 Diagnosis of diabetes and current therapies

Blood tests are used to diagnose diabetes and prediabetes, and the amount of glucose in the blood is measured in mmol/L. There are different tests that can be used for a diagnosis, including 1) a glycated hemoglobin (A1C) test; 2) fasting and/or random plasma glucose tests; or 3) an oral glucose tolerance test. The hemoglobin A1C (HbA1c) is a form of hemoglobin that is formed in a non-enzymatic glycation pathway by its exposure to plasma glucose. It is an indication of the average plasma glucose concentration over prlonged periods of time (the past 3 months). If a patient has test results of HbA1c ≥6.5%, fasting plasma glucose ≥7.0 mmol/L, or 2-hour plasma glucose in a 75g oral glucose tolerance test ≥11.1 mmol/L, they are diagnosed with diabetes. T1D patients require lifelong intensive insulin therapy. Most of them require two or more daily injections of insulin. In contrast, patients with T2D are usually obese, and therefore the first line of treatment includes diet modification and physical activity, with the end goal of weight management. If the blood glucose levels remain high, medications that increase peripheral insulin sensitivity and secretion are usually advised. Over a decade ago, the Edmonton Islet Transplantation Protocol created a new era of therapeutic promise for treating T1D diabetic patients with islet cell replacement. The success of this protocol was driven by a low risk of morbidity and hypoglycemia, normalization of glycosylated hemoglobin values, and sustained freedom from the need for exogenous insulin [44-46]. Unfortunately, many problems accompanied this success, including the shortage of cadaver islets and gradual loss of function and/or viability of transplanted islets due to immunosuppressive drug toxicity [45, 46]. These obstacles have limited islet cell replacement therapy for wide scale application [46]. For these reasons, an extraordinary amount of research is currently underway to search factors that promote beta-cell development and maintain beta-cell function and survival in the pancreas. One such factor currently being researched is c-Kit. Accumulating evidence from recent studies and the present work has demonstrated the prominent role of c-Kit in the formation of the islet of Langerhans. More importantly, c-Kit is a marker and

maintenance factor for putative pancreatic stem/progenitor cells, and activation of c-Kit signaling modulates beta-cell survival and function in normal and diabetic settings.

1.4 c-Kit and Stem Cell Factor

1.4.1 Structure of c-Kit and Stem Cell Factor

c-Kit is a cellular homologue of the v-Kit oncogene, found to be encoded by the *W* locus on chromosome 4 (4q11-21) in humans, and on chromosome 5 in rodents [47]. c-Kit is a member of the type III group of RTKs. The receptor structure and sequence within the kinase domain of c-Kit is closely related to Platelet-Derived Growth Factor Receptor (PDGFR), macrophage colony-stimulating factor receptor, and Fms-like tyrosine kinase 3 [48-51]. Structurally, c-Kit is characterized by the presence of an extracellular region comprised of five Ig-like domains, a single spanning transmembrane region, and a cytoplasmic region containing a hydrophilic kinase insert domain (Figure 1-1A). The specificity of c-Kit for binding Stem Cell Factor (SCF) depends on the concave surface of the ligand-binding pocket formed by the first three domains. The fourth and fifth domains play a critical role in c-Kit monomer positioning and dimerization [52]. The intracellular portion of c-Kit constitutes a juxtamembrane domain with an ATP-binding region, a phosphotransferase region split into two domains by a kinase insert, and a COOH-terminal tail. Most of the phosphorylation sites are located in the cytoplasmic region and are important in the transduction of intracellular activation signals.

Production of c-Kit is regulated at the mRNA level in both humans and rodents. Transcriptional regulation gives rise to two main isoforms, distinguished by the presence or absence of an in-frame insertion of a four amino acid sequence, Gly-Asn-Asn-Lys (GNNK), in the extracellular compartment [53-55]. Both isoforms of c-Kit are co-expressed in most tissues, with the dominant form lacking the GNNK (GNNK(-)) isoform [56]. Although receptor affinity to SCF is identical between both isoforms, there is a profound difference in the kinetics of receptor phosphorylation and signal transduction in the different isoform types. For instance, the GNNK(-) isoform of c-Kit displays rapid receptor phosphorylation, internalization, and degradation compared to the GNNK(+) isoform. Upon c-Kit phosphorylation, activation of both the extracellular

signal-regulated kinases (ERK) and phosphoinositide 3-kinase (PI3K) pathways are stronger in GNNK(-) expressing cells, as opposed to cells expressing the GNNK(+) isoform [57, 58].

SCF is a ligand for c-Kit and is a product of the *Sl* locus, mapped to chromosome 12 in humans and 10 in rodents [59]. There are six known SCF transcripts in humans, and four in rodents. Two alternative transcripts (220 and 248) are predominantly expressed (Figure 1-1B). Both transcripts encode for membrane-bound SCF (mSCF), constituting an extracellular domain, a transmembrane domain, and an intracellular region. In humans, SCF 248 contains a proteolytic cleavage site at exon 6, possibly accelerating the production of soluble SCF (sSCF) 165 by posttranscriptional modification. In contrast, both SCF 220 and 248 can be cleaved at exon 7 to generate the soluble from of SCF in rodents [60, 61]. Dimerization in mSCF makes it more biologically active than the monomeric form [16], but most sSCF proteins exist as monomers under physiological conditions [62]. Both mSCF and sSCF are considered biologically active, but with differential effects on c-Kit signal transduction in target cells [63, 64]. It is now apparent that mSCF results in persistent activation and a prolonged c-Kit lifespan, whereas sSCF induces transient receptor activation and enhances receptor degradation.

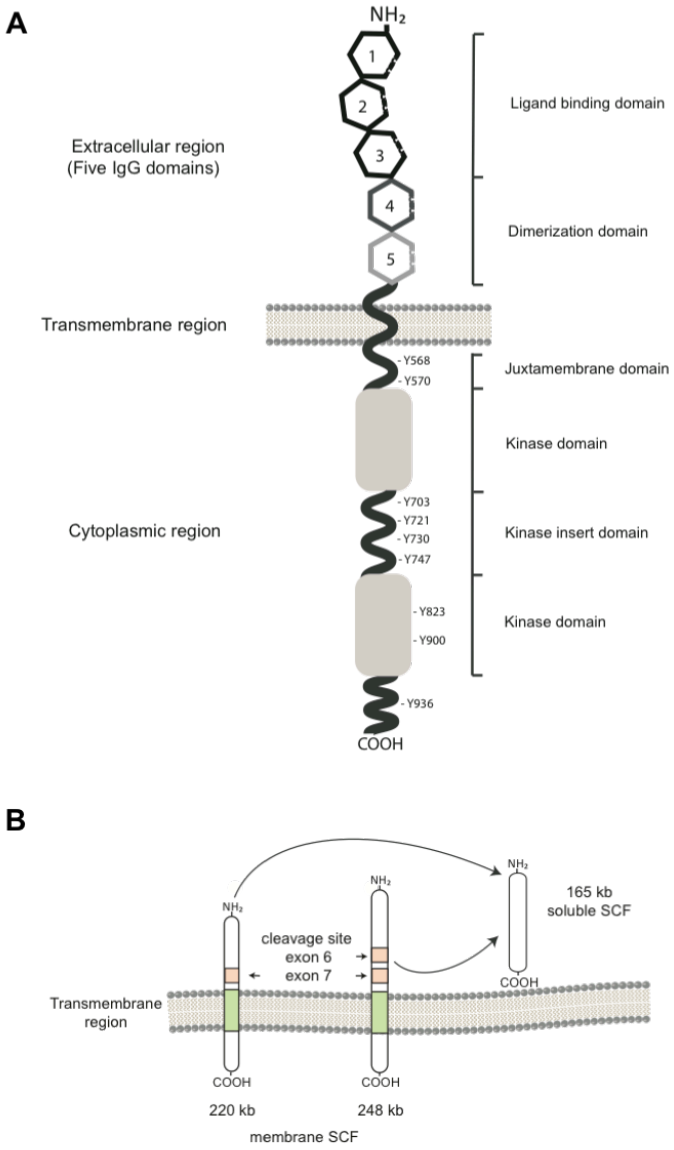
A
NH2
1
2
3
4
5
Extracellular region
(Five IgG domains)
Ligand binding domain
Dimerization domain
Transmembrane region
Y568
Y570
Juxtamembrane domain
Kinase domain
Y703
Y721
Y730
Y747
Cytoplasmic region
Kinase insert domain
Y823
Y900
Kinase domain
Y936
COOH
B
NH2
NH2
NH2
165 kb
soluble SCF
cleavage site
exon 6
exon 7
COOH
Transmembrane
region
COOH
COOH
220 kb
248 kb
membrane SCF

Figure 1-1. Structure of c-Kit and Stem Cell Factor (SCF).

(**A**) c-Kit has extracellular, transmembrane, and intracellular regions. The extracellular region consists of five Ig-like domains. The transmembrane region keeps c-Kit attached to the cell membrane. The intracellular region contains two kinase domains split into two parts by the kinase insert domain. (**B**) The soluble SCF 165 is generated by cleavage of membrane-bound SCF (220 or 248). The primary proteolytic cleavage sites are indicated by the arrows.

1.4.2 SCF/c-Kit signaling pathways

Receptor activation: c-Kit exists as a monomer on the cell membrane and SCF drives the formation of c-Kit homodimerization by binding to the first three Ig-like domains of the c-Kit monomers [65]. The subsequent interaction between Ig-like domain 4 and domain 5 in adjacent c-Kit monomers further stabilizes c-Kit dimerization, allowing for positioning and efficient trans-phosphorylation of cytoplasmic kinases [66-68]. The juxtamembrane domain plays a critical role in regulating c-Kit activity [69]. SCF stimulation promotes the release of the juxtamembrane domain from the activation loop, enabling catalytic function of the tyrosine kinase to convey its downstream signaling transduction [70, 71].

Molecular signal transduction: To date, nine tyrosine phosphorylation sites have been identified in c-Kit (Figure 1-1A). Trans-phosphorylation proceeds on the tyrosine kinase residues, which act as docking sites for signaling molecules containing the v-src avian sarcoma (Src) homology 2 domain and phosphotyrosine-binding domain. c-Kit phosphorylated at Y721 and Y900 activates the PI3K pathway, resulting in cell survival and proliferation (Figure 1-2) [72-74]. Phosphorylation of c-Kit at Y703 and Y936 activates the mitogen-activated protein (MAP) kinase pathway (Figure 1-2) [75]. The MAP kinases can act on transcription factors to affect gene transcription and proliferation [65]. c-Kit phosphorylation at Y568, Y570, and Y936 activates the Src pathway, which is associated with cell adhesion and cell motility (Figure 1-2) [76, 77]. Src also converges with the PI3K and MAP kinase pathways, as well as the janus kinase and signal transducers and activators of transcription (JAK/STAT) pathway [65, 78, 79]. The phospholipase c-gamma (PLC-γ) pathway can interact with tyrosine kinase residue Y730 of c-Kit [80], and was found to be important for suppressing cellular apoptosis (Figure 1-2) [81, 82]. There is also evidence indicating that SCF/c-Kit signaling pathways are not simple linear reactions. Indeed, integrated inputs from different pathways determine the biological consequences in different cellular contexts. This is accomplished by c-Kit cross-talking with other receptors, including erythropoietin receptor or interleukin receptors, to recruit common signaling molecules, such as PI3K, MAP kinase, JAK/STAT, and PLCγ, so that multiple physiological responses may be amplified [83-87].

Receptor down-regulation: A tight regulation of c-Kit signaling is crucial for proper cellular functions. Attenuation of c-Kit signaling can be achieved by several routes, including receptor internalization, tyrosine dephosphorylation, and kinase domain inactivation by serine phosphorylation. Phosphorylation at sites Y568 and Y936 and association with the E3 ubiquitin ligase c-Cbl is required for c-Kit internalization [76, 88, 89]. Studies have demonstrated that suppression of cytokine signaling proteins SOCS1 and SOCS6 negatively regulate c-Kit signaling by endocytosis and subsequent lysosomal degradation [90, 91]. In addition, negative feedback regulation contributes to c-Kit down-regulation: stimulation of ligand binding to c-Kit increases protein kinase C activity, which negatively regulates kinase activity by phosphorylating serine residues S741 and S746 of c-Kit. This results in shedding of the c-Kit extracellular domain from the cell surface [65, 92-95]. Furthermore, the adaptor protein, Lnk, preferentially binds to phosphorylated Y567 in the c-Kit juxtamembrane domain, mediating inhibition of c-Kit activity [96]. c-Kit signaling can also be regulated by tyrosine phosphatases, including SHP-1, even in the absence of SCF [97].

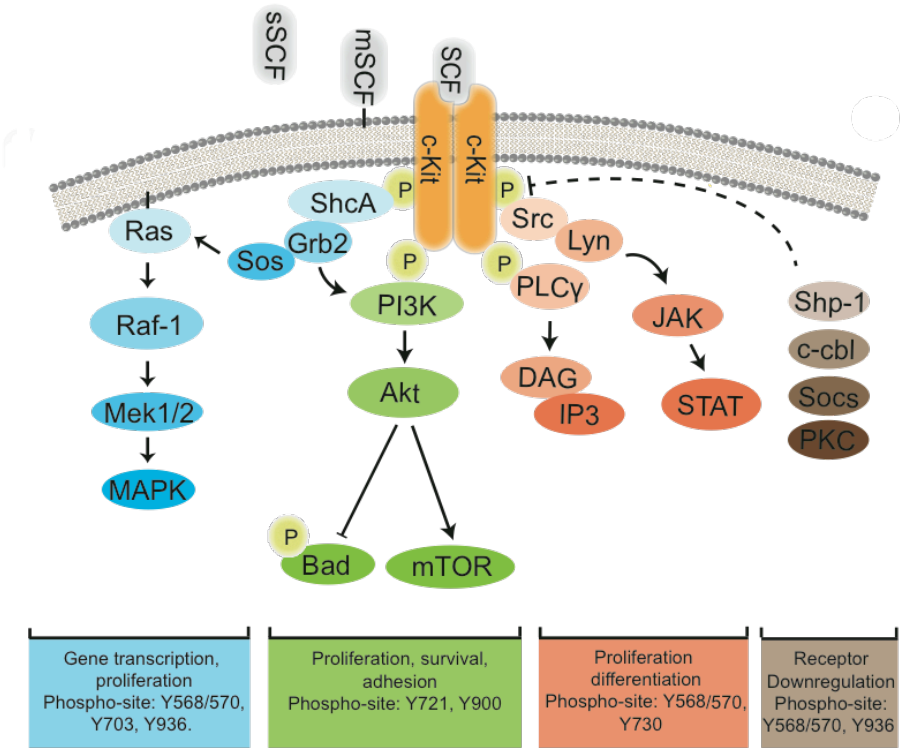
sSCF
mSCF
SCF
c-Kit
c-Kit
P
P
ShcA
Grb2
Sos
Ras
Raf-1
Mek1/2
MAPK
P
PI3K
Akt
P
Bad
mTOR
Src
Lyn
P
PLCγ
DAG
IP3
JAK
STAT
Shp-1
c-cbl
Socs
PKC
Gene transcription, proliferation Phospho-site: Y568/570, Y703, Y936.
Proliferation, survival, adhesion Phospho-site: Y721, Y900
Proliferation differentiation Phospho-site: Y568/570, Y730
Receptor Downregulation Phospho-site: Y568/570, Y936

Figure 1-2. c-Kit signaling pathways.

The MAPK pathway (blue) regulates gene transcription and proliferation. PI3K signaling (green) plays an important role in cellular proliferation, survival and adhesion. PLCγ and JAK/Stat pathways (orange) are implicated in proliferation and differentiation. Shp-1, c-Cbl, SOCs and PKC signal (brown) are involved c-Kit down-regulation. sSCF: soluble Stem Cell Factor; mSCF: membrane-bound Stem Cell Factor.

1.4.3 SCF/c-Kit function in organ development

c-Kit-mediated signal transduction governs proliferation, survival, and adhesion in hematopoietic stem cells (HSCs), mast cells, and dendrite cells. The mechanism involved in this phenomenon is suppression of cell apoptosis through either activation of anti-apoptotic genes, such as Bcl-2, or inactivation of pro-apoptotic genes, such as Bad via the PI3K pathway. SCF functions as a chemotactic factor for HSCs [98]. Cell adhesion, a process SCF is known to play a role in, is required for the maintenance of cells in their microenvironment [99]. sSCF promotes mast cell proliferation, whereas mSCF binds directly to c-Kit, and in mast cells increases the expression of proteins involved in cell-matrix attachment [100, 101]. Animal studies using *Sl* and *W* mutant mice demonstrate that defective SCF/c-Kit signaling results in deformity of erythrocytes, megakaryocytes, and mast cells, illustrating that these cells are dependent on c-Kit for their proliferation, survival, and function [102].

c-Kit and SCF play an indispensable role in the pigmentation of the epidermis and hair of mammals. Mice with a heterozygotic mutation in SCF or c-Kit exhibited a lack of hair pigmentation associated with loss of melanocytes [103]. In contrast, overexpression of epidermal SCF leads to hyperpigmentation in mice, and constitutively activated c-Kit results in uncontrolled proliferation of melanocytes, promoting melanogenesis and migration of pigment cells [104, 105]. SCF/c-Kit activity is essential in enabling melanocyte-lineage cell migration from the neural crest into developing mature hair follicles in rodents [106, 107]. Furthermore, c-Kit-activated Src family kinases regulate the microphthalmia-associated transcription factor to govern the proliferation, survival, and maturation of melanocytes [108, 109].

Expression and functional studies have shown that SCF/c-Kit is essential for germ cell development during both the fetal and postnatal periods of life. Humans with a mutation in SCF suffer from idiopathic male infertility [110]. Elevation of c-Kit expression is linked to the commitment of germ cell differentiation in rodents. Both *Sl* and *W* mutant mice show defective c-Kit signaling, which is associated with germ cell apoptosis and the corresponding degree of sterility [111]. Activation of the PI3K and MAP kinase pathways by stimulation of SCF has been found to promote germ cell proliferation [74,

112, 113]. Other studies have demonstrated that phosphorylation of Src family kinases, by the juxtamembrane kinase of c-Kit, regulates primitive germ cell migration [114]. In addition, downstream of c-Kit, the PLCγ pathway has been implicated in meiosis of fertilized eggs [115, 116], and the ERK cascade has been shown to act as a regulator of gene transcription involved in the maturation and proliferation of primitive germ cells [112, 114].

The physiological relevance of SCF and c-Kit has been characterized in mice with various naturally occurring mutations in the *Sl* and *W* loci. The loss-of-function mutations in these receptor/ligand-defective mice result in defective signaling pathways and underline the complexity of rodent phenotypes. Given the fact that SCF and c-Kit are expressed in a wide variety of normal tissues, it is not surprising that SCF/c-Kit interactions play a crucial role in hematopoiesis, pigmentation, and gametogenesis, as well as in the gastrointestinal tract, cardiovascular system, and neuronal network [117]. Recent studies suggest that c-Kit function may be linked to regulation of pancreatic endocrine cell development, particularly beta-cell maturation, proliferation and function, which will be highlighted in the following sections.

1.5 c-Kit function in the pancreas

1.5.1 c-Kit in the developing rodent pancreas

c-Kit expression was first detected in RINm5F rat insulinoma cell lines and fetal rat islets [118]. Subsequent immunohistochemistry studies revealed the localization of c-Kit to pancreatic ducts [119], and mRNA expression of the c-Kit gene was enriched in the e13 embryonic rat pancreata [120], suggesting that c-Kit expression is important for proper development of the pancreas. One cell-lineage tracing study utilizing *LacZ* murine embryos showed that c-Kit expression is detectable in a subpopulation of endocrine and epithelial cells [121]. The abundant c-Kit expression in early rodent pancreas development demonstrates that c-Kit might be involved in maintaining the endocrine cell precursor pool in fetal rodents. This statement was further supported by findings from our laboratory. We characterized dynamic changes of c-Kit expression in rodent pancreata during transition from the prenatal to postnatal period, and revealed that c-Kit was

localized to the ductal region and in newly formed islet endocrine cell clusters at e18, and progressively decreased during postnatal life [122]. These observations suggested that decreased c-Kit expression correlated with islet endocrine cell maturation. More recently, the presence of two distinct putative stem cell like populations, expressing either c-Kit or Sca-1, another stem cell antigen, in the developing rodent pancreas was characterized. Flow cytometry analysis revealed that the isolated c-Kit$^+$ cell population co-expressed markers of islet differentiation including Pdx-1 and Ngn3, but an isolated Sca-1$^+$ cell population lacked these markers [123]. This data indicates that c-Kit could be used a marker to identify putative islet precursor cells, thus playing a significant role in pancreas morphogenesis, particularly in the developing rodent endocrine pancreas. Interestingly, a report from Bernex *et al.* has documented pancreatic endocrine cells present in Wv^{LacZ}/Wv^{LacZ} mouse embryos with a null allele of c-Kit. Findings from this study suggested c-Kit might not be required for the determination and specification of pancreatic endocrine cells [124]. However, it is worth noting that PDGFR is also expressed in islets of Langerhans, which might represent a possible redundant RTK signaling pathway that compensates for the absence of c-Kit expression.

1.5.2 SCF/c-Kit in islet cell differentiation

Accumulating evidence has shown that c-Kit plays an important role in pancreatic morphogenesis and islet maturation. c-Kit-mediated islet differentiation was demonstrated across multiple species *in vitro*. It was demonstrated that stimulation of c-Kit promotes gene transcription [121] and proliferation in the INS-1 rat insulinoma cell line [125, 126]. Furthermore, exogenous SCF induced differentiation of human pancreatic carcinoma epithelial-like cell lines (PANC-1) into islet-like clusters [127]. In isolated primary rodent islet cultures, Oberg-Welsh *et al.* demonstrated that rat fetal islet clusters treated with SCF show augmented insulin and total DNA content [119]. The rat islet epithelial monolayer that expanded on collagen I contained an increased number of proliferating c-Kit-expressing cells, with constant expression of Pdx-1, Ngn3, Pax4, and multiple undifferentiated cell markers, including octamer-binding transcription factor-4, and α-fetoprotein [128]. Differentiation of these monolayers was greatly enhanced when cultured on laminin-rich matrigel. Islet-like clusters were formed and cells secreted

insulin in response to glucose [128]. It was found that SCF released from microencapsulated monolayered Sertoli cells significantly accelerated differentiation and maturation of neonatal porcine islets. Increased early islet differentiation markers and co-localization with c-Kit and insulin was found in these porcine islets, demonstrating that the c-Kit positive subpopulation represents islet precursors that can stimulate differentiation of porcine insulin producing cells *in vitro* [129]. Our group showed that SCF mediates the differentiation of c-Kit-expressing immature endocrine progenitors in the human fetal pancreas, and phosphorylated Akt may have a functional role downstream of c-Kit signaling in mediating their maturation [130]. Furthermore, c-Kit activation results in cellular proliferation via suppression of cell apoptosis in human fetal islet epithelia [131]. Conversely, silencing *c-Kit* mRNA disrupts islet differentiation in cells of the human fetal pancreas [131], highlighting the importance of c-Kit signaling in mediating early beta-cell differentiation and survival.

1.5.3 c-Kit in the regenerating pancreas

Although there is no consensus about the identity and origin of pancreatic stem/progenitor cells, c-Kit-expressing cells exhibit many stem cell-like features in the regenerating pancreas. Our group showed that following pancreatic duct ligation, pancreatic islets, exocrine acini, and ductal complexes regrew, indicating that c-Kit-expressing proliferating pancreatic progenitors may be a putative source for islet regeneration in rodents [132]. Our study revealed that c-Kit is expressed in the periphery of islets and co-localizes with ductal/progenitor markers cytokeratin 20 and Pdx-1 in the ligated rat pancreas 3 days post-ligation [133]. c-Kit-expressing cells in ligated regions displayed a high proliferative capacity, suggesting that beta-cell neogenesis may arise from these ductal progenitor cells. c-Kit has also been found to participate in islet regeneration in a streptozotocin-induced diabetic model. A few remaining beta-cells that express c-Kit have high proliferative capacity following streptozotocin-induced beta-cell damage, suggesting that these cells are involved in the regenerative process [134]. A similar study was reported in an acute pancreatitis rat model in which extensive pancreatic cellular damage was induced by cerulean and resulted in beta-cell replenishment due to replication of these highly proliferative pre-existing c-Kit

expressing beta-cells [135]. c-Kit-expressing cells from other cell sources may also be involved in beta-cell regeneration. Hess *et al.* showed that transplanted bone marrow-derived c-Kit-expressing cells initiate islet regeneration in streptozotocin-treated non-obese diabetic/severe combined immune deficient (NOD/SCID) recipient mice. Rapid engraftment of these GFP-tagged c-Kit^{+} bone marrow-derived cells to the damaged ductal and islet regions stimulated endogenous islet neogenesis [136]. Using multipotent stromal cells expressing surface markers (ALDH^{high}c-Kit^{+}CD113^{+}CD34^{+}) to treat the streptozotocin-treated NOD/SCID mice nearly restored glucose homeostasis, with formation of beta-cell clusters adjacent to the ductal epithelium [137]. By transferring these purified multipotent stromal cells from umbilical cord blood into the recipient NOD/SCID mice, hyperglycemia was reversed in the animals. Intriguingly, multipotent stromal cells purified from umbilical cord blood were able to augment endogenous beta-cell proliferation and revascularization [138].

1.5.4 c-Kit in pancreatic disease

Despite the necessity of c-Kit in the pancreas, it has also been identified to be a proto-oncogene [47]. Indeed, inappropriate expression of c-Kit or SCF has led to a wide range of pancreatic diseases ranging from pancreatitis (acute and chronic) to pancreatic cancer [117, 139, 140]. Chronic pancreatitis is characterized by chronic inflammation, fibrosis, and loss of pancreatic function [141]. The immune response in chronic pancreatitis is very powerful and contributes to a large portion of chronic pancreatitis pathophysiology. Indeed, increased mast cell presence correlates with inflammation and fibrosis in chronic pancreatitis [142]. It has been reported that SCF/c-Kit interactions have an influential effect on mast cells. During chronic pancreatitis, c-Kit expression is increased on mast cells near affected ducts, and weak immunoreactivity of c-Kit is observed on acini and islets [142]. c-Kit expression is also found in ducts during chronic pancreatitis, consistent with other studies that have shown increased ductal c-Kit expression after pancreatic ductal ligation in rodents [133]. Therefore, it can be concluded that c-Kit plays various important roles dependent upon the cell type in which it is expressed.

Pancreatic cancer is among the most lethal and least common of the human cancers [143]. Diabetes and chronic pancreatitis have been linked to pancreatic cancer, yet

smoking was shown to be responsible for 20-25% of pancreatic cancers. While cancer etiology is varied, SCF/c-Kit interactions play a role in promoting pancreatic cancer cell line proliferation, invasion, and differentiation into endocrine hormone producing cells [127, 144]. Other cell line experiments showed that hypoxia-inducible factor 1-alpha, a protein expressed under hypoxic conditions that can indicate tumor survival and proliferation, was influenced by c-Kit activity in pancreatic cancer cells independent of the oxygen level [145]. c-Kit is also present on neoplastic cells in the pancreas, as well as throughout the duct of the cancerous pancreas [146], indicating that SCF/c-Kit interactions have profound implications on pancreatic cancer cell proliferation and invasiveness. Therefore, the development of c-Kit inhibitors has been useful for the management of cancers by inhibiting proliferation as well as inducing apoptosis of cancer cells [147, 148].

1.6 Rationales, objectives and hypotheses

1.6.1 Overall objective and hypothesis

The **overall objective** is to understand the physiological role of c-Kit on beta-cells *in vivo*, and we **hypothesize** that activation of c-Kit and its downstream PI3K/Akt signaling pathway plays a critical role in determining beta-cell survival and function under normal and diabetic pathophysiological conditions.

1.6.2 Beta-cell survival and function in *c-Kit*$^{Wv/+}$ mice

The first reported evidence, *in vivo,* linking c-Kit activity with beta-cell survival and function utilized mice carrying the mutation, viable dominant spotting (W^v)[149]. The W^v point mutation refers to a threonine to methionine substitution at the first catalytic region of the c-Kit cytoplasmic kinase domain, greatly diminishing its kinase activity without altering the binding site to SCF. As a result, the autophosphorylation activity of c-Kit W^v mutant monomers is only ~10-20% of that observed in normal c-Kit monomers. More importantly, c-Kit W^v mutant monomer can act in a trans-dominant manner to prevent tyrosine phosphorylation of normal c-Kit by dimerization, reflected by ~60% reduction in c-Kit transduction activity [150]. Phenotypic analysis of *c-Kit*$^{Wv/+}$ mice showed high fasting plasma glucose and impaired glucose tolerance between 4 to 8 weeks of age.

Absence of insulin resistance in peripheral tissue was found, indicating that the development of a diabetic phenotype was due to a loss of beta-cell mass, along with a reduced proliferative capacity in *c-Kit*$^{Wv/+}$ mice. Islet morphology and Pdx-1 expression was altered in *c-Kit*$^{Wv/+}$ pancreatic islets when compared to controls. In addition, these mice demonstrated a significant reduction in plasma insulin levels 35 minutes after glucose stimulation, and isolated islets exhibited marked insulin secretory defects in response to glucose load [149]. Overall, beta-cell dysfunction emerges as the physiological defect, leading to early onset diabetes in *c-Kit*$^{Wv/+}$ mice, specifically in males. Interestingly, the female *c-Kit*$^{Wv/+}$ mice did not show the impaired glucose metabolism until 40 weeks of age [149]. The complex intracellular pathways downstream of c-Kit have been well studied in other cellular contexts, but such information is largely unknown in the context of beta-cell biology *in vivo*. Therefore, the **first objective** of this work was to identify the responsible intracellular machinery that had the most influence on beta-cell proliferation and function in *c-Kit*$^{Wv/+}$ male mice (**Chapter 3**). We **hypothesized** that the dysregulated Akt/Gsk3β pathway contributes to severe loss of beta-cell mass and impaired beta-cell function in *c-Kit*$^{Wv/+}$ mice.

1.6.3 Beta-cell apoptosis in *c-Kit*$^{Wv/+}$ mice

Beta-cell mass reflects a dynamic balance between cell proliferation and apoptosis. The increase in beta-cell apoptosis and decrease in beta-cell proliferation, followed by loss of beta-cell mass and eventual beta-cell failure, is a hallmark of diabetes. A high rate of apoptosis was detected in the beta-cell population of *c-Kit*$^{Wv/+}$ mice. However, our current understanding of apoptotic pathways induced by the *c-Kit W*^{v} mutation in beta-cells is lacking. One attractive candidate is Fas, also known as APO-1 or CD95, which belongs to the tumor necrosis superfamily. The gene coding *Fas* is located near the *lpr* locus of chromosome 19 in rodents [151]. The *lpr* mutation leads to the production of non-functional truncated *Fas* mRNA due to an early transposable element, similar to an endogenous retrovirus inserted into intron 2 [151]. Thus, the *Fas*$^{lpr/lpr}$ mouse model is an excellent system to study the effect of a deficiency in Fas signaling in any given tissue. FasL-binding and subsequent activation of Fas leads to programmed cell death in many systems. Experimental data from several studies showed that, at least in T1D models, that

Fas/FasL interaction has been implicated in beta-cell death. In transgenic mice expressing FasL on beta-cells, extensive beta-cell destruction was associated with autoimmune attack, whereas Fas-negative NOD mice with *lpr* mutation failed to develop T1D [151], and are resistant to adoptive transfer of diabetogenic NOD spleen cells [152]. More experiments using NOD-gld/+ mice, which have reduced FasL expression, also demonstrated that beta-cell apoptosis is possibly mediated by FasL-positive T-lymphocytes on activation of Fas. In addition, Fas deficient (*lpr/lpr*) NOD/SCID were protected from diabetes induced by adoptive transfer of diabetogenic T-cells [153]. Taking this further, more studies using dominant negative Fas mutation beta-cell specific NOD mice [154] and administration of FasL antibody treatment found that it prevented early onset of autoimmune diabetes [155], and prolonged survival and engraftment of NOD islets in diabetic NOD mice [156]. A conditional knockout of Fas improved beta-cell insulin releasing function [157]. Accumulating evidence demonstrates that Fas signaling contributes to cell apoptosis, which is accompanied by the absence of c-Kit signaling in melanocytes [158], gametes [159], oocytes [160], and HSCs [161], thus leaving an open question as described in **Chapter 4.** The **second objective** of this work was to assess the balance between c-Kit and Fas signaling on beta-cell survival and function using *c-Kit*$^{Wv/+}$ and *c-Kit*$^{Wv/+}$*;Fas*$^{lpr/lpr}$ mice, and *in vitro* rat insulinoma INS-1 cells. We **hypothesized** that loss of c-Kit signaling leads to activation of Fas-mediated beta-cell loss in *c-Kit*$^{Wv/+}$ mice, but that the Fas *lpr* mutation in *c-Kit*$^{Wv/+}$ mice would protect beta-cells from apoptosis, and improve beta-cell insulin release in the *c-Kit*$^{Wv/+}$ mouse model.

1.6.4 c-Kit directly affects beta-cell function

Homozygous *c-Kit* null mutant mice display relatively normal islet morphology, but they die shortly after birth and are not available for further functional studies [124]. We recently characterized *c-Kit*$^{Wv/+}$ mice with a loss of beta-cell function resulting in early-onset of diabetes [149]. However, the *c-Kit*$^{Wv/+}$ mice model may not be sufficient to reveal whether c-Kit plays a primary or secondary role in beta-cell survival and function, because the global c-Kit mutation may raise unknown confounding effects from other tissue. Thus, we further generated a novel transgenic mouse model containing beta-cell

specific overexpression of *c-KIT* (*c-KitβTg* mice). Using this novel *c-KitβTg* mouse model, the **third objective** of this work was to delineate the physiological role of c-Kit in normal, and HFD-induced diabetic and *c-Kit*$^{Wv/+}$ mice. This work is described in **Chapter 5**. It is **hypothesized** that elevated beta-cell c-Kit expression can improve beta-cell function and survival in normal and HFD-induced diabetic *c-KitβTg* mice, and *c-KIT* overexpression in beta-cells could reverse the onset of diabetes in *c-Kit*$^{Wv/+}$ mice.

1.6.5 VEGF-A and islet vasculature in c-Kit mutant and transgenic mouse

The formation of microvascular networks in the islet relies on vascular endothelial growth factors (VEGFs), a group of receptor tyrosine kinase signaling proteins able to stimulate vasculogenesis and angiogenesis through binding to three functionally distinct VEGF receptors 1-3. Beta-cells express high levels of VEGFs, in particular VEGF-A that binds to and activates VEGF receptors 2 present on the neighboring endothelial cells. This attracts endothelial cells and stimulates their proliferation and growth. By deleting VEGF-A in the pancreas, the fenestration of islet capillaries, required for fine-tuning of blood glucose regulation, is severely impaired [162]. This is further supported by studies using transgenic mice with beta-cell-specific loss of VEGF-A, driven by the rat insulin promoter (RIP)-Cre system. The substantial loss of islet vasculature results in severely impaired development of islet capillaries and beta-cell dysfunction [163, 164]. The causal link between c-Kit and VEGF-A production has been documented previously in multiple cancer pathologies: in lung cancer cells, SCF was shown to induce VEGF expression, and this was associated with increased PI3K signaling and hypoxia-inducible factor 1-alpha transcription, and the effect was blocked by inhibition of c-Kit [165]. Likewise, in neuroblastoma cells, inhibition of c-Kit resulted in a significant reduction in VEGF expression, which led to significant decreases in tumor vasculogenesis and angiogenesis [166]. In a pancreatic islet cancer model, treatment with both SU5416 (VEGFR inhibitor) and Gleevec (c-Kit inhibitor) significantly repressed tumor growth [167]. Therefore, the **fourth objective** was to assess the role of SCF/c-Kit signaling on islet microvasculature, and its subsequent effect on islet function and glucose homeostasis *in vivo* under both

normal and diabetic conditions (**Chapter 6**). It is **hypothesized** that c-Kit-dependent regulation of VEGF-A is critical for islet vasculature and beta-cell survival.

1.7 References

1. Steiner DJ, Kim A, Miller K, Hara M (2010) Pancreatic islet plasticity: interspecies comparison of islet architecture and composition. Islets 2:135–145.

2. Levetan CS, Pierce SM (2013) Distinctions between the islets of mice and men: implications for new therapies for type 1 and 2 diabetes. Endocrine Practice

3. Jørgensen MC, Ahnfelt-Rønne J, Hald J, et al. (2007) An illustrated review of early pancreas development in the mouse. Endocr Rev 28:685–705. doi: 10.1210/er.2007-0016

4. Lin C-LV, Vuguin PM (2012) Determinants of pancreatic islet development in mice and men: a focus on the role of transcription factors. Horm Res Paediatr 77:205–213. doi: 10.1159/000337219

5. Ferrara N, Gerber HP, LeCouter J (2003) The biology of VEGF and its receptors. Nat Med 9:669–676. doi: 10.1038/nm0603-669

6. Hebrok M, Kim SK, Melton DA (1998) Notochord repression of endodermal Sonic hedgehog permits pancreas development. Genes Dev 12:1705–1713.

7. Kim SK, Melton DA (1998) Pancreas development is promoted by cyclopamine, a hedgehog signaling inhibitor. Proc Natl Acad Sci USA 95:13036–13041.

8. Habener JF, Kemp DM, Thomas MK (2005) Minireview: transcriptional regulation in pancreatic development. Endocrinology 146:1025–1034. doi: 10.1210/en.2004-1576

9. Gradwohl G, Dierich A, LeMeur M, Guillemot F (2000) neurogenin3 is required for the development of the four endocrine cell lineages of the pancreas. Proc Natl Acad Sci USA 97:1607–1611.

10. Lammert E, Cleaver O, Melton D (2001) Induction of pancreatic differentiation by signals from blood vessels. Science 294:564–567. doi: 10.1126/science.1064344

11. Yoshitomi H, Zaret KS (2004) Endothelial cell interactions initiate dorsal pancreas development by selectively inducing the transcription factor Ptf1a. Development 131:807–817. doi: 10.1242/dev.00960

12. Jacquemin P, Yoshitomi H, Kashima Y, et al. (2006) An endothelial-mesenchymal relay pathway regulates early phases of pancreas development. Dev Biol 290:189–199. doi: 10.1016/j.ydbio.2005.11.023

13. Henderson JR, Moss MC (1985) A morphometric study of the endocrine and exocrine capillaries of the pancreas. Q J Exp Physiol 70:347–356.

14. Jansson L, Carlsson P-O (2002) Graft vascular function after transplantation of pancreatic islets. Diabetologia 45:749–763. doi: 10.1007/s00125-002-0827-4

15. Lee S, Jilani SM, Nikolova GV, et al. (2005) Processing of VEGF-A by matrix metalloproteinases regulates bioavailability and vascular patterning in tumors. J Cell Biol 169:681–691. doi: 10.1083/jcb.200409115

16. Johansson M, Mattsson G, Andersson A, et al. (2006) Islet endothelial cells and pancreatic beta-cell proliferation: studies in vitro and during pregnancy in adult rats. Endocrinology 147:2315–2324. doi: 10.1210/en.2005-0997

17. Bouwens L, Rooman I (2005) Regulation of pancreatic beta-cell mass. Physiol Rev 85:1255–1270. doi: 10.1152/physrev.00025.2004

18. Bonner-Weir S (2000) Life and death of the pancreatic beta cells. Trends Endocrinol Metab 11:375–378.

19. Orci L, Ravazzola M, Perrelet A (1984) (Pro)insulin associates with Golgi membranes of pancreatic B cells. Proc Natl Acad Sci USA 81:6743–6746.

20. Orci L, Ravazzola M, Amherdt M, et al. (1986) Conversion of proinsulin to insulin occurs coordinately with acidification of maturing secretory vesicles. J Cell Biol 103:2273–2281.

21. Slack JM (1995) Developmental biology of the pancreas. Development 121:1569–1580.

22. Caumo A, Luzi L (2004) First-phase insulin secretion: does it exist in real life? Considerations on shape and function. Am J Physiol Endocrinol Metab 287:E371–85. doi: 10.1152/ajpendo.00139.2003

23. Public Health Agency of Canada (2011) Diabetes in Canada: Facts and figures from a public health perspective.

24. Redondo MJ, Fain PR, Eisenbarth GS (2001) Genetics of type 1A diabetes. Recent Prog Horm Res 56:69–89.

25. Pugliese A, Zeller M, Fernandez A, et al. (1997) The insulin gene is transcribed in the human thymus and transcription levels correlated with allelic variation at the INS VNTR-IDDM2 susceptibility locus for type 1 diabetes. Nat Genet 15:293–297. doi: 10.1038/ng0397-293

26. Nisticò L, Buzzetti R, Pritchard LE, et al. (1996) The CTLA-4 gene region of chromosome 2q33 is linked to, and associated with, type 1 diabetes. Belgian Diabetes Registry. Hum Mol Genet 5:1075–1080.

27. Moore F, Colli ML, Cnop M, et al. (2009) PTPN2, a candidate gene for type 1 diabetes, modulates interferon-gamma-induced pancreatic beta-cell apoptosis. Diabetes 58:1283–1291. doi: 10.2337/db08-1510

28. Thomas HE, McKenzie MD, Angstetra E, et al. (2009) Beta cell apoptosis in diabetes. Apoptosis 14:1389–1404. doi: 10.1007/s10495-009-0339-5

29. Estella E, McKenzie MD, Catterall T, et al. (2006) Granzyme B-mediated death of pancreatic beta-cells requires the proapoptotic BH3-only molecule bid. Diabetes 55:2212–2219. doi: 10.2337/db06-0129

30. Reimers JI (1998) Interleukin-1 beta induced transient diabetes mellitus in rats. A model of the initial events in the pathogenesis of insulin-dependent diabetes mellitus? Dan Med Bull 45:157–180.

31. Thomas HE, Irawaty W, Darwiche R, et al. (2004) IL-1 receptor deficiency slows progression to diabetes in the NOD mouse. Diabetes 53:113–121.

32. Hanis CL, Boerwinkle E, Chakraborty R, et al. (1996) A genome-wide search for human non-insulin-dependent (type 2) diabetes genes reveals a major susceptibility locus on chromosome 2. Nat Genet 13:161–166. doi: 10.1038/ng0696-161

33. Butler AE, Janson J, Bonner-Weir S, et al. (2003) Beta-cell deficit and increased beta-cell apoptosis in humans with type 2 diabetes. Diabetes 52:102–110.

34. Maedler K, Donath MY (2004) Beta-cells in type 2 diabetes: a loss of function and mass. Horm Res 62 Suppl 3:67–73. doi: 10.1159/000080503

35. Kaneto H, Kawamori D, Matsuoka T-A, et al. (2005) Oxidative stress and pancreatic beta-cell dysfunction. Am J Ther 12:529–533.

36. Chen J, Saxena G, Mungrue IN, et al. (2008) Thioredoxin-interacting protein: a critical link between glucose toxicity and beta-cell apoptosis. Diabetes 57:938–944. doi: 10.2337/db07-0715

37. Federici M, Hribal M, Perego L, et al. (2001) High glucose causes apoptosis in cultured human pancreatic islets of Langerhans: a potential role for regulation of specific Bcl family genes toward an apoptotic cell death program. Diabetes 50:1290–1301.

38. Jeffrey KD, Alejandro EU, Luciani DS, et al. (2008) Carboxypeptidase E mediates palmitate-induced beta-cell ER stress and apoptosis. Proceedings of the National Academy of Sciences 105:8452–8457. doi: 10.1073/pnas.0711232105

39. Gwiazda KS, Yang T-LB, Lin Y, Johnson JD (2009) Effects of palmitate on ER and cytosolic Ca2+ homeostasis in beta-cells. Am J Physiol Endocrinol Metab 296:E690–701. doi: 10.1152/ajpendo.90525.2008

40. Ehses JA, Perren A, Eppler E, et al. (2007) Increased number of islet-associated macrophages in type 2 diabetes. Diabetes 56:2356–2370. doi: 10.2337/db06-1650

41. Cardozo AK, Ortis F, Størling J, et al. (2005) Cytokines downregulate the sarcoendoplasmic reticulum pump Ca2+ ATPase 2b and deplete endoplasmic reticulum

Ca2+, leading to induction of endoplasmic reticulum stress in pancreatic beta-cells. Diabetes 54:452–461.

42. Collins S, Martin TL, Surwit RS, Robidoux J (2004) Genetic vulnerability to diet-induced obesity in the C57BL/6J mouse: physiological and molecular characteristics. Physiol Behav 81:243–248. doi: 10.1016/j.physbeh.2004.02.006

43. Sato A, Kawano H, Notsu T, et al. (2010) Antiobesity effect of eicosapentaenoic acid in high-fat/high-sucrose diet-induced obesity: importance of hepatic lipogenesis. Diabetes 59:2495–2504. doi: 10.2337/db09-1554

44. Alejandro R, Barton FB, Hering BJ, et al. (2008) 2008 Update from the Collaborative Islet Transplant Registry. Transplantation 86:1783–1788. doi: 10.1097/TP.0b013e3181913f6a

45. Shapiro AM, Lakey JR, Ryan EA, et al. (2000) Islet transplantation in seven patients with type 1 diabetes mellitus using a glucocorticoid-free immunosuppressive regimen. N Engl J Med 343:230–238. doi: 10.1056/NEJM200007273430401

46. Ryan EA, Paty BW, Senior PA, et al. (2005) Five-year follow-up after clinical islet transplantation. Diabetes 54:2060–2069.

47. Yarden Y, Kuang WJ, Yang-Feng T, et al. (1987) Human proto-oncogene c-kit: a new cell surface receptor tyrosine kinase for an unidentified ligand. EMBO J 6:3341–3351.

48. Chabot B, Stephenson DA, Chapman VM, et al. (1988) The proto-oncogene c-kit encoding a transmembrane tyrosine kinase receptor maps to the mouse W locus. Nature 335:88–89. doi: 10.1038/335088a0

49. Qiu FH, Ray P, Brown K, et al. (1988) Primary structure of c-kit: relationship with the CSF-1/PDGF receptor kinase family--oncogenic activation of v-kit involves deletion of extracellular domain and C terminus. EMBO J 7:1003–1011.

50. Coussens L, Van Beveren C, Smith D, et al. (1986) Structural alteration of viral homologue of receptor proto-oncogene fms at carboxyl terminus. Nature 320:277–280. doi: 10.1038/320277a0

51. Matthews W, Jordan CT, Wiegand GW, et al. (1991) A receptor tyrosine kinase specific to hematopoietic stem and progenitor cell-enriched populations. Cell 65:1143–1152.

52. Yuzawa S, Opatowsky Y, Zhang Z, et al. (2007) Structural basis for activation of the receptor tyrosine kinase KIT by stem cell factor. Cell 130:323–334. doi: 10.1016/j.cell.2007.05.055

53. Crosier PS, Ricciardi ST, Hall LR, et al. (1993) Expression of isoforms of the human receptor tyrosine kinase c-kit in leukemic cell lines and acute myeloid leukemia. Blood 82:1151–1158.

54. Reith AD, Ellis C, Lyman SD, et al. (1991) Signal transduction by normal isoforms and W mutant variants of the Kit receptor tyrosine kinase. EMBO J 10:2451–2459.

55. Zhu WM, Dong WF, Minden M (1994) Alternate splicing creates two forms of the human kit protein. Leuk Lymphoma 12:441–447. doi: 10.3109/10428199409073786

56. Piao X, Curtis JE, Minkin S, et al. (1994) Expression of the Kit and KitA receptor isoforms in human acute myelogenous leukemia. Blood 83:476–481.

57. Voytyuk O (2003) Src Family Kinases Are Involved in the Differential Signaling from Two Splice Forms of c-Kit. Journal of Biological Chemistry 278:9159–9166. doi: 10.1074/jbc.M211726200

58. Sun J, Pedersen M, Rönnstrand L (2008) Gab2 is involved in differential phosphoinositide 3-kinase signaling by two splice forms of c-Kit. J Biol Chem 283:27444–27451. doi: 10.1074/jbc.M709703200

59. Ropers HH, Craig IW (1989) Report of the committee on the genetic constitution of chromosomes 12 and 13. Cytogenet Cell Genet 51:259–279.

60. Majumdar MK, Feng L, Medlock E, et al. (1994) Identification and mutation of primary and secondary proteolytic cleavage sites in murine stem cell factor cDNA yields biologically active, cell-associated protein. J Biol Chem 269:1237–1242.

61. Pandiella A, Bosenberg MW, Huang EJ, et al. (1992) Cleavage of membrane-anchored growth factors involves distinct protease activities regulated through common mechanisms. J Biol Chem 267:24028–24033.

62. Hsu YR, Wu GM, Mendiaz EA, et al. (1997) The majority of stem cell factor exists as monomer under physiological conditions. Implications for dimerization mediating biological activity. J Biol Chem 272:6406–6415.

63. Shull RM, Suggs SV, Langley KE, et al. (1992) Canine stem cell factor (c-kit ligand) supports the survival of hematopoietic progenitors in long-term canine marrow culture. Exp Hematol 20:1118–1124.

64. Langley KE, Bennett LG, Wypych J, et al. (1993) Soluble stem cell factor in human serum. Blood 81:656–660.

65. Reber L, Da Silva CA, Frossard N (2006) Stem cell factor and its receptor c-Kit as targets for inflammatory diseases. Eur J Pharmacol 533:327–340. doi: 10.1016/j.ejphar.2005.12.067

66. Blechman JM, Lev S, Barg J, et al. (1995) The fourth immunoglobulin domain of the stem cell factor receptor couples ligand binding to signal transduction. Cell 80:103–113.

67. Philo JS, Wen J, Wypych J, et al. (1996) Human stem cell factor dimer forms a complex with two molecules of the extracellular domain of its receptor, Kit. J Biol Chem 271:6895–6902.

68. Rottapel R, Reedijk M, Williams DE, et al. (1991) The Steel/W transduction pathway: kit autophosphorylation and its association with a unique subset of cytoplasmic signaling proteins is induced by the Steel factor.

69. Chan PM, Ilangumaran S, La Rose J, et al. (2003) Autoinhibition of the kit receptor tyrosine kinase by the cytosolic juxtamembrane region. Mol Cell Biol 23:3067–3078.

70. Mol CD, Lim KB, Sridhar V, et al. (2003) Structure of a c-kit product complex reveals the basis for kinase transactivation. J Biol Chem 278:31461–31464. doi: 10.1074/jbc.C300186200

71. Mol CD, Dougan DR, Schneider TR, et al. (2004) Structural basis for the autoinhibition and STI-571 inhibition of c-Kit tyrosine kinase. J Biol Chem 279:31655–31663. doi: 10.1074/jbc.M403319200

72. Serve H, Hsu YC, Besmer P (1994) Tyrosine residue 719 of the c-kit receptor is essential for binding of the P85 subunit of phosphatidylinositol (PI) 3-kinase and for c-kit-associated PI 3-kinase activity in COS-1 cells. J Biol Chem 269:6026–6030.

73. Hashimoto K (2002) Necessity of tyrosine 719 and phosphatidylinositol 3'-kinase-mediated signal pathway in constitutive activation and oncogenic potential of c-kit receptor tyrosine kinase with the Asp814Val mutation. Blood 101:1094–1102. doi: 10.1182/blood-2002-01-0177

74. Blume-Jensen P, Jiang G, Hyman R, et al. (2000) Kit/stem cell factor receptor-induced activation of phosphatidylinositol 3′-kinase is essential for male fertility. Nat Genet 24:157–162. doi: 10.1038/72814

75. Thömmes K, Lennartsson J, Carlberg M, Rönnstrand L (1999) Identification of Tyr-703 and Tyr-936 as the primary association sites for Grb2 and Grb7 in the c-Kit/stem cell factor receptor. Biochem J 341 (Pt 1):211–216.

76. Wollberg P, Lennartsson J, Gottfridsson E, et al. (2003) The adapter protein APS associates with the multifunctional docking sites Tyr-568 and Tyr-936 in c-Kit. Biochem J 370:1033–1038. doi: 10.1042/BJ20020716

77. Price DJ, Rivnay B, Fu Y, et al. (1997) Direct association of Csk homologous kinase (CHK) with the diphosphorylated site Tyr568/570 of the activated c-Kit in megakaryocytes. J Biol Chem 272:5915–5920.

78. Timokhina I, Kissel H, Stella G, Besmer P (1998) Kit signaling through PI 3-kinase and Src kinase pathways: an essential role for Rac1 and JNK activation in mast cell proliferation. EMBO J 17:6250–6262. doi: 10.1093/emboj/17.21.6250

79. Bondzi C, Litz J, Dent P, Krystal GW (2000) Src family kinase activity is required for Kit-mediated mitogen-activated protein (MAP) kinase activation, however loss of functional retinoblastoma protein makes MAP kinase activation unnecessary for growth of small cell lung cancer cells. Cell Growth Differ 11:305–314.

80. Gommerman JL, Sittaro D, Klebasz NZ, et al. (2000) Differential stimulation of c-Kit mutants by membrane-bound and soluble Steel Factor correlates with leukemic potential. Blood 96:3734–3742.

81. Maddens S, Charruyer A, Plo I (2002) Kit signaling inhibits the sphingomyelin-ceramide pathway through PLCγ1: implication in stem cell factor radioprotective effect.

82. Plo I, Lautier D, Casteran N, et al. (2001) Kit signaling and negative regulation of daunorubicin-induced apoptosis: role of phospholipase Cgamma. Oncogene 20:6752–6763. doi: 10.1038/sj.onc.1204877

83. Liu L, Cutler RL, Mui AL, Krystal G (1994) Steel factor stimulates the serine/threonine phosphorylation of the interleukin-3 receptor. J Biol Chem 269:16774–16779.

84. Wu H, Klingmüller U, Besmer P, Lodish HF (1995) Interaction of the erythropoietin and stem-cell-factor receptors. Nature 377:242–246. doi: 10.1038/377242a0

85. Ye Z-J, Gulcicek E, Stone K, et al. (2011) Complex interactions in EML cell stimulation by stem cell factor and IL-3. Proc Natl Acad Sci USA 108:4882–4887. doi: 10.1073/pnas.1018002108

86. Drube S, Heink S, Walter S, et al. (2010) The receptor tyrosine kinase c-Kit controls IL-33 receptor signaling in mast cells. Blood 115:3899–3906. doi: 10.1182/blood-2009-10-247411

87. Jahn T, Sindhu S, Gooch S, et al. (2007) Direct interaction between Kit and the interleukin-7 receptor. Blood 110:1840–1847. doi: 10.1182/blood-2005-12-028019

88. Bandi SR, Brandts C, Rensinghoff M, et al. (2009) E3 ligase-defective Cbl mutants lead to a generalized mastocytosis and myeloproliferative disease. Blood 114:4197–4208. doi: 10.1182/blood-2008-12-190934

89. Masson K, Heiss E, Band H, Rönnstrand L (2006) Direct binding of Cbl to Tyr568 and Tyr936 of the stem cell factor receptor/c-Kit is required for ligand-induced ubiquitination, internalization and degradation. Biochem J 399:59–67. doi: 10.1042/BJ20060464

90. De Sepulveda P, Okkenhaug K, Rose JL, et al. (1999) Socs1 binds to multiple signaling proteins and suppresses steel factor-dependent proliferation. EMBO J 18:904–915. doi: 10.1093/emboj/18.4.904

91. Bayle J, Letard S, Frank R, et al. (2004) Suppressor of cytokine signaling 6 associates with KIT and regulates KIT receptor signaling. J Biol Chem 279:12249–12259. doi: 10.1074/jbc.M313381200

92. Blume-Jensen P, Wernstedt C, Heldin CH, Rönnstrand L (1995) Identification of the major phosphorylation sites for protein kinase C in kit/stem cell factor receptor in vitro and in intact cells. J Biol Chem 270:14192–14200.

93. Edling CE, Pedersen M, Carlsson L, et al. (2007) Haematopoietic progenitor cells utilise conventional PKC to suppress PKB/Akt activity in response to c-Kit stimulation. Br J Haematol 136:260–268. doi: 10.1111/j.1365-2141.2006.06434.x

94. Yee NS, Hsiau CW, Serve H, et al. (1994) Mechanism of down-regulation of c-kit receptor. Roles of receptor tyrosine kinase, phosphatidylinositol 3'-kinase, and protein kinase C. J Biol Chem 269:31991–31998.

95. Blume-Jensen P, Siegbahn A, Stabel S, et al. (1993) Increased Kit/SCF receptor induced mitogenicity but abolished cell motility after inhibition of protein kinase C. EMBO J 12:4199–4209.

96. Simon C, Dondi E, Chaix A, et al. (2008) Lnk adaptor protein down-regulates specific Kit-induced signaling pathways in primary mast cells. Blood 112:4039–4047. doi: 10.1182/blood-2008-05-154849

97. Kozlowski M, Larose L, Lee F, et al. (1998) SHP-1 binds and negatively modulates the c-Kit receptor by interaction with tyrosine 569 in the c-Kit juxtamembrane domain. Mol Cell Biol 18:2089–2099.

98. Okumura N, Tsuji K, Ebihara Y, et al. (1996) Chemotactic and chemokinetic activities of stem cell factor on murine hematopoietic progenitor cells. Blood 87:4100–4108.

99. Bendall LJ, Makrynikola V, Hutchinson A, et al. (1998) Stem cell factor enhances the adhesion of AML cells to fibronectin and augments fibronectin-mediated anti-apoptotic and proliferative signals. Leukemia 12:1375–1382.

100. Kaneko Y, Takenawa J, Yoshida O, et al. (1991) Adhesion of mouse mast cells to fibroblasts: adverse effects of steel (Sl) mutation. J Cell Physiol 147:224–230. doi: 10.1002/jcp.1041470206

101. Kinashi T, Springer TA (1994) Steel factor and c-kit regulate cell-matrix adhesion. Blood 83:1033–1038.

102. Edling CE, Hallberg B (2007) c-Kit--a hematopoietic cell essential receptor tyrosine kinase. Int J Biochem Cell Biol 39:1995–1998. doi: 10.1016/j.biocel.2006.12.005

103. Baxter LL, Hou L, Loftus SK, Pavan WJ (2004) Spotlight on spotted mice: a review of white spotting mouse mutants and associated human pigmentation disorders. Pigment Cell Res 17:215–224. doi: 10.1111/j.1600-0749.2004.00147.x

104. Kunisada T, Lu SZ, Yoshida H, et al. (1998) Murine cutaneous mastocytosis and epidermal melanocytosis induced by keratinocyte expression of transgenic stem cell factor. J Exp Med 187:1565–1573.

105. Kunisada T, Yoshida H, Yamazaki H, et al. (1998) Transgene expression of steel factor in the basal layer of epidermis promotes survival, proliferation, differentiation and migration of melanocyte precursors. Development 125:2915–2923.

106. Cable J, Jackson IJ, Steel KP (1995) Mutations at the W locus affect survival of neural crest-derived melanocytes in the mouse. Mech Dev 50:139–150.

107. Mackenzie MA, Jordan SA, Budd PS, Jackson IJ (1997) Activation of the receptor tyrosine kinase Kit is required for the proliferation of melanoblasts in the mouse embryo. Dev Biol 192:99–107. doi: 10.1006/dbio.1997.8738

108. Wu M, Hemesath TJ, Takemoto CM, et al. (2000) c-Kit triggers dual phosphorylations, which couple activation and degradation of the essential melanocyte factor Mi. Genes Dev 14:301–312.

109. Hemesath TJ, Price ER, Takemoto C, et al. (1998) MAP kinase links the transcription factor Microphthalmia to c-Kit signaling in melanocytes. Nature 391:298–301. doi: 10.1038/34681

110. Galan JJ, De Felici M, Buch B, et al. (2006) Association of genetic markers within the KIT and KITLG genes with human male infertility. Hum Reprod 21:3185–3192. doi: 10.1093/humrep/del313

111. Loveland KL, Schlatt S (1997) Stem cell factor and c-kit in the mammalian testis: lessons originating from Mother Nature's gene knockouts. J Endocrinol 153:337–344.

112. Dolci S, Pellegrini M, Di Agostino S, et al. (2001) Signaling through extracellular signal-regulated kinase is required for spermatogonial proliferative response to stem cell factor. J Biol Chem 276:40225–40233. doi: 10.1074/jbc.M105143200

113. Kissel H, Timokhina I, Hardy MP, et al. (2000) Point mutation in kit receptor tyrosine kinase reveals essential roles for kit signaling in spermatogenesis and oogenesis without affecting other kit responses. EMBO J 19:1312–1326. doi: 10.1093/emboj/19.6.1312

114. Farini D, La Sala G, Tedesco M, De Felici M (2007) Chemoattractant action and molecular signaling pathways of Kit ligand on mouse primordial germ cells. Dev Biol 306:572–583. doi: 10.1016/j.ydbio.2007.03.031

115. Sette C, Bevilacqua A, Geremia R, Rossi P (1998) Involvement of phospholipase Cgamma1 in mouse egg activation induced by a truncated form of the C-kit tyrosine kinase present in spermatozoa. J Cell Biol 142:1063–1074.

116. Sette C, Paronetto MP, Barchi M, et al. (2002) Tr-kit-induced resumption of the cell cycle in mouse eggs requires activation of a Src-like kinase. EMBO J 21:5386–5395.

117. Lennartsson J, Rönnstrand L (2012) Stem cell factor receptor/c-Kit: from basic science to clinical implications. Physiol Rev 92:1619–1649. doi: 10.1152/physrev.00046.2011

118. Oberg C, Waltenberger J, Claesson-Welsh L, Welsh M (1994) Expression of protein tyrosine kinases in islet cells: possible role of the Flk-1 receptor for beta-cell maturation from duct cells. Growth Factors 10:115–126.

119. Oberg-Welsh C, Welsh M (1996) Effects of certain growth factors on in vitro maturation of rat fetal islet-like structures. Pancreas 12:334–339.

120. LeBras S, Czernichow P, Scharfmann R (1998) A search for tyrosine kinase receptors expressed in the rat embryonic pancreas. Diabetologia 41:1474–1481. doi: 10.1007/s001250051094

121. Rachdi L, Ghazi El L, Bernex F, et al. (2001) Expression of the receptor tyrosine kinase KIT in mature beta-cells and in the pancreas in development. Diabetes 50:2021–2028.

122. Yashpal NK, Li J, Wang R (2004) Characterization of c-Kit and nestin expression during islet cell development in the prenatal and postnatal rat pancreas. Dev Dyn 229:813–825. doi: 10.1002/dvdy.10496

123. Ma F, Chen F, Chi Y, et al. (2012) Isolation of pancreatic progenitor cells with the surface marker of hematopoietic stem cells. Int J Endocrinol 2012:948683. doi: 10.1155/2012/948683

124. Bernex F, De Sepulveda P, Kress C, et al. (1996) Spatial and temporal patterns of c-kit-expressing cells in WlacZ/+ and WlacZ/WlacZ mouse embryos. Development 122:3023–3033.

125. Feng ZC, Li J, Turco BA, et al. (2012) Critical role of c-Kit in beta cell function: increased insulin secretion and protection against diabetes in a mouse model. Diabetologia 55:2214–2225. doi: 10.1007/s00125-012-2566-5

126. Feng Z-C, Donnelly L, Li J, et al. (2012) Inhibition of Gsk3β activity improves β-cell function in c-KitWv/+ male mice. Lab Invest 92:543–555. doi: 10.1038/labinvest.2011.200

127. Wu Y, Li J, Saleem S, et al. (2010) c-Kit and stem cell factor regulate PANC-1 cell differentiation into insulin- and glucagon-producing cells. Lab Invest 90:1373–1384. doi: 10.1038/labinvest.2010.106

128. Wang R, Li J, Yashpal N (2004) Phenotypic analysis of c-Kit expression in epithelial monolayers derived from postnatal rat pancreatic islets. J Endocrinol 182:113–122.

129. Mancuso F, Calvitti M, Luca G, et al. (2010) Acceleration of functional maturation and differentiation of neonatal porcine islet cell monolayers shortly in vitro cocultured with microencapsulated sertoli cells. Stem Cells Int 2010:587213. doi: 10.4061/2010/587213

130. Li J, Goodyer CG, Fellows F, Wang R (2006) Stem cell factor/c-Kit interactions regulate human islet-epithelial cluster proliferation and differentiation. Int J Biochem Cell Biol 38:961–972. doi: 10.1016/j.biocel.2005.08.014

131. Li J, Quirt J, Do HQ, et al. (2007) Expression of c-Kit receptor tyrosine kinase and effect on beta-cell development in the human fetal pancreas. Am J Physiol Endocrinol Metab 293:E475–83. doi: 10.1152/ajpendo.00172.2007

132. Wang RN, Klöppel G, Bouwens L (1995) Duct- to islet-cell differentiation and islet growth in the pancreas of duct-ligated adult rats. Diabetologia 38:1405–1411.

133. Peters K, Panienka R, Li J, et al. (2005) Expression of stem cell markers and transcription factors during the remodeling of the rat pancreas after duct ligation. Virchows Arch 446:56–63. doi: 10.1007/s00428-004-1145-7

134. Tiemann K, Panienka R, Klöppel G (2007) Expression of transcription factors and precursor cell markers during regeneration of beta cells in pancreata of rats treated with streptozotocin. Virchows Arch 450:261–266. doi: 10.1007/s00428-006-0349-4

135. Gong J, Zhang G, Tian F, Wang Y (2012) Islet-derived stem cells from adult rats participate in the repair of islet damage. J Mol Histol 43:745–750. doi: 10.1007/s10735-012-9447-6

136. Hess D, Li L, Martin M, et al. (2003) Bone marrow-derived stem cells initiate pancreatic regeneration. Nat Biotechnol 21:763–770. doi: 10.1038/nbt841

137. Bell GI, Meschino MT, Hughes-Large JM, et al. (2012) Combinatorial human progenitor cell transplantation optimizes islet regeneration through secretion of paracrine factors. Stem Cells Dev 21:1863–1876. doi: 10.1089/scd.2011.0634

138. Bell GI, Putman DM, Hughes-Large JM, Hess DA (2012) Intrapancreatic delivery of human umbilical cord blood aldehyde dehydrogenase-producing cells promotes islet regeneration. Diabetologia 55:1755–1760. doi: 10.1007/s00125-012-2520-6

139. Raimondi S, Lowenfels AB, Morselli-Labate AM, et al. (2010) Pancreatic cancer in chronic pancreatitis; aetiology, incidence, and early detection. Best Pract Res Clin Gastroenterol 24:349–358. doi: 10.1016/j.bpg.2010.02.007

140. Liang J, Wu Y-L, Chen B-J, et al. (2013) The C-kit receptor-mediated signal transduction and tumor-related diseases. Int J Biol Sci 9:435–443. doi: 10.7150/ijbs.6087

141. Thrower E, Husain S, Gorelick F (2008) Molecular basis for pancreatitis. Curr Opin Gastroenterol 24:580–585. doi: 10.1097/MOG.0b013e32830b10e6

142. Esposito I, Friess H, Kappeler A, et al. (2001) Mast cell distribution and activation in chronic pancreatitis. Hum Pathol 32:1174–1183.

143. Raimondi S, Maisonneuve P (2009) Epidemiology of pancreatic cancer: an overview. Nature Reviews …

144. Yasuda A, Sawai H, Takahashi H, et al. (2006) The stem cell factor/c-kit receptor pathway enhances proliferation and invasion of pancreatic cancer cells. Mol Cancer 5:46. doi: 10.1186/1476-4598-5-46

145. Zhang M, Ma Q, Hu H, et al. (2011) Stem cell factor/c-kit signaling enhances invasion of pancreatic cancer cells via HIF-1α under normoxic condition. Cancer Lett 303:108–117. doi: 10.1016/j.canlet.2011.01.017

146. Esposito I, Kleeff J, Bischoff SC, et al. (2002) The stem cell factor-c-kit system and mast cells in human pancreatic cancer. Lab Invest 82:1481–1492.

147. Attoub S, Rivat C, Rodrigues S, et al. (2002) The c-kit tyrosine kinase inhibitor STI571 for colorectal cancer therapy. Cancer Res 62:4879–4883.

148. Mehren von M (2006) Beyond imatinib: second generation c-Kit inhibitors for the management of gastrointestinal stromal tumors. Clin Colorectal Cancer 6 Suppl 1:S30–4.

149. Krishnamurthy M, Ayazi F, Li J, et al. (2007) c-Kit in early onset of diabetes: a morphological and functional analysis of pancreatic beta-cells in c-KitW-v mutant mice. Endocrinology 148:5520–5530. doi: 10.1210/en.2007-0387

150. Nocka K, Tan J, Chiu E, et al. (1990) Molecular bases of dominant negative and loss of function mutations at the murine c-Kit/white spotting locus: W^{37}, W^{v}, W^{41} and W. EMBO J. 9:1805–1813.

151. Chervonsky AV, Wang Y, Wong FS, et al. (1997) The Role of Fas in Autoimmune Diabetes. Cell 89:17–24. doi: 10.1016/S0092-8674(00)80178-6

152. Itoh N, Imagawa A, Hanafusa T, et al. (1997) Requirement of Fas for the development of autoimmune diabetes in nonobese diabetic mice. J Exp Med 186:613–618.

153. Su X, Hu Q, Kristan JM, et al. (2000) Significant role for Fas in the pathogenesis of autoimmune diabetes.

154. Savinov AY, Tcherepanov A, Green EA, et al. (2003) Contribution of Fas to diabetes development. Proc Natl Acad Sci USA 100:628–632. doi: 10.1073/pnas.0237359100

155. Nakayama M, Nagata M, Yasuda H, et al. (2002) Fas/Fas ligand interactions play an essential role in the initiation of murine autoimmune diabetes. Diabetes 51:1391–1397.

156. Suarez-Pinzon WL, Power RF, Rabinovitch A (2000) Fas ligand-mediated mechanisms are involved in autoimmune destruction of islet beta cells in non-obese diabetic mice. Diabetologia 43:1149–1156. doi: 10.1007/s001250051506

157. Choi D, Radziszewska A, Schroer SA, et al. (2009) Deletion of Fas in the pancreatic beta-cells leads to enhanced insulin secretion. Am J Physiol Endocrinol Metab 297:E1304–12. doi: 10.1152/ajpendo.00217.2009

158. Sharov AA, Li G-Z, Palkina TN, et al. (2003) Fas and c-kit are involved in the control of hair follicle melanocyte apoptosis and migration in chemotherapy-induced hair loss. J Invest Dermatol 120:27–35. doi: 10.1046/j.1523-1747.2003.12022.x

159. Sakata S, Sakamaki K, Watanabe K, et al. (2003) Involvement of death receptor Fas in germ cell degeneration in gonads of Kit-deficient Wv/Wv mutant mice. Cell Death Differ 10:676–686. doi: 10.1038/sj.cdd.4401215

160. Moniruzzaman M, Sakamaki K, Akazawa Y, Miyano T (2007) Oocyte growth and follicular development in KIT-deficient Fas-knockout mice. Reproduction 133:117–125. doi: 10.1530/REP-06-0161

161. Mori T, Ando K, Tanaka K, et al. (1997) Fas-mediated apoptosis of the hematopoietic progenitor cells in mice infected with murine cytomegalovirus. Blood 89:3565–3573.

162. Lammert E, Gu G, McLaughlin M, et al. (2003) Role of VEGF-A in vascularization of pancreatic islets. Curr Biol 13:1070–1074.

163. Brissova M, Shostak A, Shiota M, et al. (2006) Pancreatic islet production of vascular endothelial growth factor--a is essential for islet vascularization, revascularization, and function. Diabetes 55:2974–2985. doi: 10.2337/db06-0690

164. Iwashita N, Uchida T, Choi JB, et al. (2007) Impaired insulin secretion in vivo but enhanced insulin secretion from isolated islets in pancreatic beta cell-specific vascular

endothelial growth factor-A knock-out mice. Diabetologia 50:380–389. doi: 10.1007/s00125-006-0512-0

165. Litz J, Krystal GW (2006) Imatinib inhibits c-Kit-induced hypoxia-inducible factor-1alpha activity and vascular endothelial growth factor expression in small cell lung cancer cells. Mol Cancer Ther 5:1415–1422. doi: 10.1158/1535-7163.MCT-05-0503

166. Beppu K, Jaboine J, Merchant MS, et al. (2004) Effect of imatinib mesylate on neuroblastoma tumorigenesis and vascular endothelial growth factor expression. J Natl Cancer Inst 96:46–55.

167. Potapova O, Laird AD, Nannini MA, et al. (2006) Contribution of individual targets to the antitumor efficacy of the multitargeted receptor tyrosine kinase inhibitor SU11248. Mol Cancer Ther 5:1280–1289. doi: 10.1158/1535-7163.MCT-03-0156

Chapter 2

2 Summary of materials and methods for Chapters 3, 4, 5 and 6

2.1 Mouse models

The crossbreeding strategies used to generate the mouse models used throughout this thesis are detailed below. Mice were maintained in an environment of constant temperature (20°C) and were exposed to regular 12-hour day, 12-hour night cycles. All mice were fed *ad libitum* with a normal diet (5% vol./vol. fat; Harlan Tekard, Indianapolis, IN, USA), unless specified. Male mice were used in the following studies due to male mice having a more severe diabetic phenotype as compared to females. The animal experimental protocol used in the following studies was approved by the University of Western Ontario Animal Use Subcommittee, in accordance with the guidelines of the Canadian Council of Animal Care (Appendix 1 and 2).

2.1.1 Mouse models used in Chapter 3

Generation of the c-Kit$^{Wv/+}$ mouse model: Paired *c-Kit W^{v}* heterozygous mutant (*c-Kit$^{Wv/+}$*) mice on a C57BL/6J background obtained from the Jackson Laboratory (stock no. 000049, Jackson Laboratory, Bar Harbor, ME, USA) were bred (Figure 2-1). Mice were genotyped by their distinct differences in fur pigmentation as described previously [1]. Homozygous mutant (*c-Kit$^{Wv/Wv}$*) mice are severely anemic and infertile and do not survive for a long time after maturity. Since sufficient *c-Kit$^{Wv/Wv}$* male mice could not be obtained, they were excluded them from this study [1]. Thus, this study focused on *c-Kit$^{+/+}$* and *c-Kit$^{Wv/+}$* male mice at 8 weeks of age.

Treatment with Gsk3β inhibitor: At 6 weeks of age, both *c-Kit$^{+/+}$* and *c-Kit$^{Wv/+}$* male mice were intraperitoneally injected with either 1-Azakenpaullone **(**1-AKP, Calbiochem, Etobicoke, ON, Canada) at 2 mg/kg or with saline, every other day for 2 weeks, to establish four experimental groups including: *c-Kit$^{+/+}$/saline, c-Kit$^{+/+}$/1-AKP, c-Kit$^{Wv/+}$/saline,* and *c-Kit$^{Wv/+}$/1-AKP* mice (Figure 2-2).

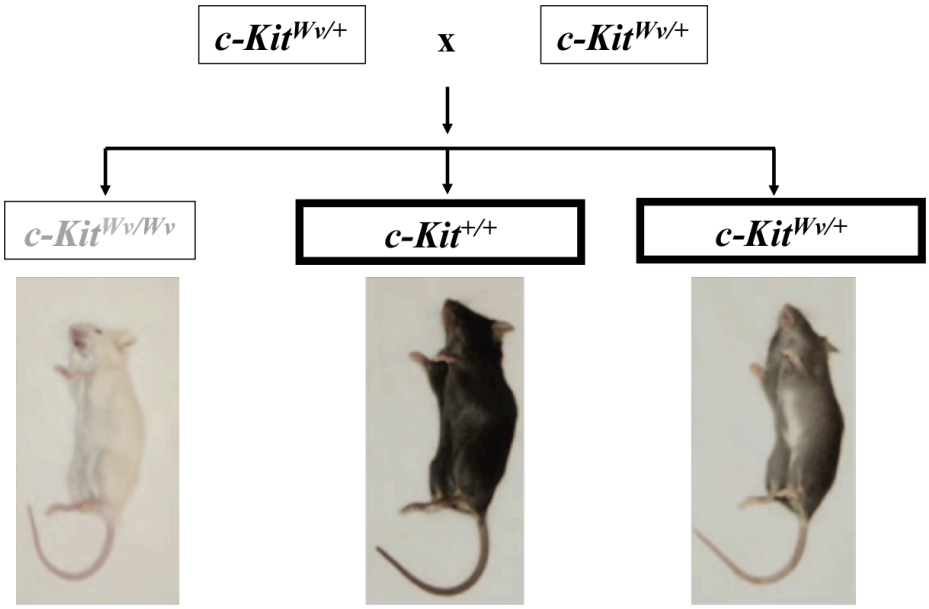
c-Kit^Wv/+
x
c-Kit^Wv/+
c-Kit^Wv/Wv
c-Kit^+/+
c-Kit^Wv/+

Figure 2-1. Breeding schematic for *c-Kit*$^{Wv/+}$ mice.

C57BL/6J/*Kit*$^{Wv/+}$ (stock no. 000049) from the Jackson laboratory were crossed to obtain three mouse genotypes. The study focused on male *c-Kit*$^{+/+}$ and *c-Kit*$^{Wv/+}$ mice as highlighted above.

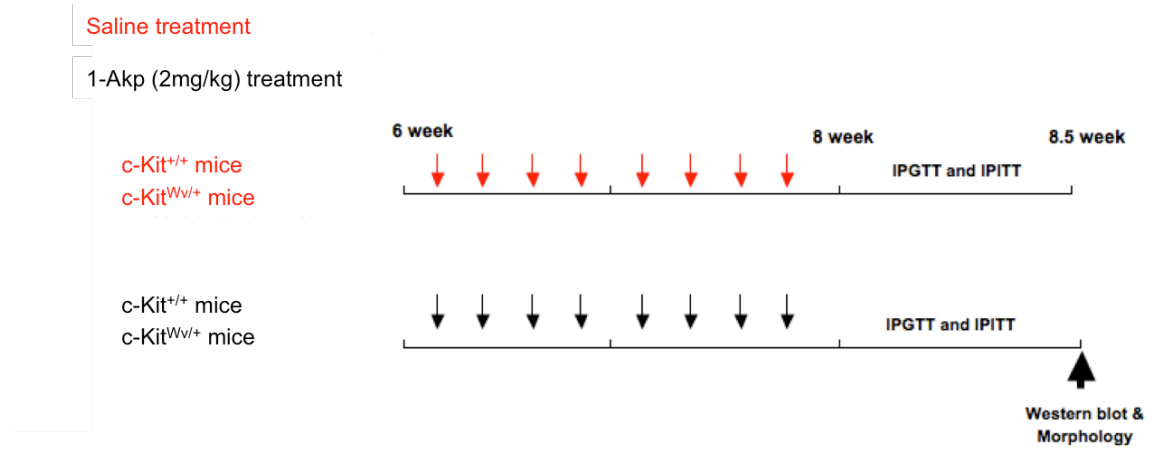
Saline treatment
1-Akp (2mg/kg) treatment
6 week
8 week
8.5 week
c-Kit+/+ mice
c-KitWv/+ mice
IPGTT and IPITT
c-Kit+/+ mice
c-KitWv/+ mice
IPGTT and IPITT
Western blot &
Morphology

Figure 2-2. Experimental design of 1-AKP treatments for *c-Kit*$^{Wv/+}$ mice.

6-week-old male *c-Kit*$^{+/+}$ mice or *c-Kit*$^{Wv/+}$ mice received either i.p. injections of saline or 1-AKP for two weeks. Four experimental groups including, *c-Kit*$^{+/+}$*/saline*, *c-Kit*$^{Wv/+}$*/saline*, *c-Kit*$^{+/+}$*/1-AKP*, and *c-Kit*$^{Wv/+}$*/1-AKP* mice were established.

2.1.2 Mouse models used in Chapter 4

c-Kit$^{Wv/+}$ and *Fas*$^{lpr/lpr}$ mice with a C57BL/6J background were obtained from the Jackson Laboratory (stock no. 000049 for C57BL/6J/*Kit*$^{Wv/+}$; stock no. 000482 for B6.MRL-*Fas*$^{lpr/lpr}$; the Jackson Laboratory) and cross-bred to generate six genotypes including: *c-Kit*$^{+/+}$*;Fas*$^{+/+}$, *c-Kit*$^{Wv/+}$*;Fas*$^{+/+}$, *c-Kit*$^{Wv/+}$*;Fas*$^{lpr/lpr}$, *c-Kit*$^{+/+}$*;Fas*$^{lpr/+}$, *c-Kit*$^{Wv/+}$*;Fas*$^{lpr/+}$, and *c-Kit*$^{+/+}$*;Fas*$^{lpr/lpr}$ mice (Figure 2-3). This study focused on three groups: *c-Kit*$^{+/+}$*;Fas*$^{+/+}$, *c-Kit*$^{Wv/+}$*;Fas*$^{+/+}$, and *c-Kit*$^{Wv/+}$*;Fas*$^{lpr/lpr}$ mice. Male mice at 8 weeks of age were used for this study. The *c-Kit W*^{v} mutation was distinguished by fur pigmentation: black for *c-Kit*$^{+/+}$ and piebaldism for *c-Kit*$^{Wv/+}$ [1]. The *Fas* (*lpr*) mutation was identified by genotyping using PCR with DNA isolated from tails (Appendix 3).

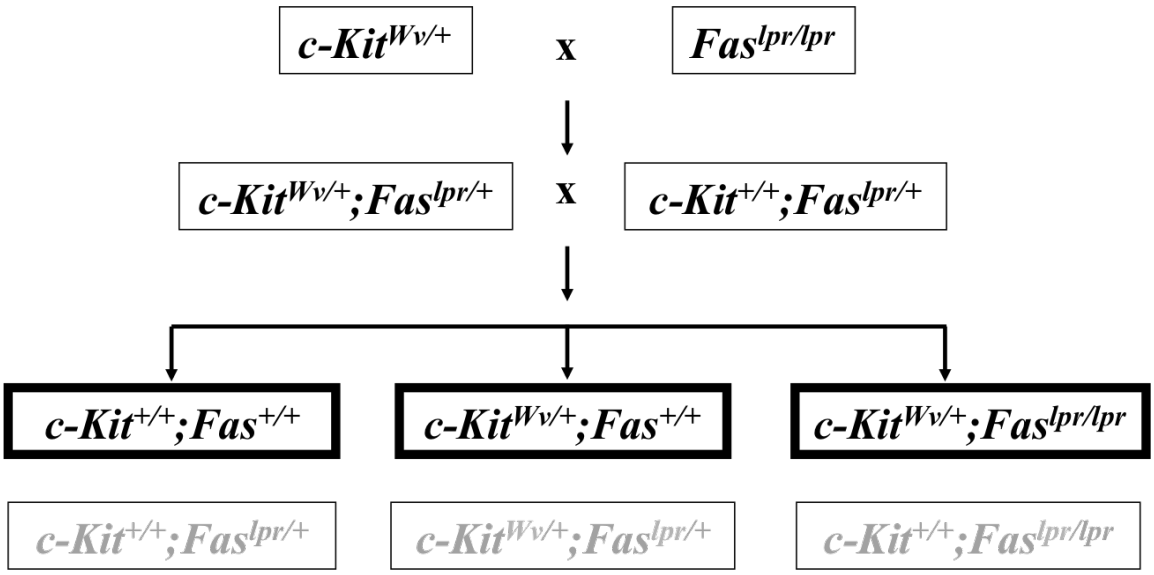
c-Kit^Wv/+
x
Fas^lpr/lpr
c-Kit^Wv/+;Fas^lpr/+
x
c-Kit^+/+;Fas^lpr/+
c-Kit^+/+;Fas^+/+
c-Kit^Wv/+;Fas^+/+
c-Kit^Wv/+;Fas^lpr/lpr
c-Kit^+/+;Fas^lpr/+
c-Kit^Wv/+;Fas^lpr/+
c-Kit^+/+;Fas^lpr/lpr

Figure 2-3. Breeding schematic for *c-Kit$^{Wv/+}$;Fas$^{lpr/lpr}$* double mutant mice.

C57BL/6J/*Kit$^{Wv/+}$* (stock no. 000049) and B6.MRL-*Fas$^{lpr/lpr}$* (stock no. 000482) mice from the Jackson Laboratory were crossed to obtain *c-Kit$^{Wv/+}$;Fas$^{lpr/+}$* and *c-Kit$^{+/+}$;Fas$^{lpr/+}$* mice. Crossbreeding these mice resulted in six mouse genotypes. This study focused on three groups including, *c-Kit$^{+/+}$;Fas$^{+/+}$*, *c-Kit$^{Wv/+}$;Fas$^{+/+}$*, and *c-Kit$^{Wv/+}$;Fas$^{lpr/lpr}$* mice as highlighted above.

2.1.3 Mouse models used in Chapter 5

Generation of the c-KitβTg mouse model: the human *c-KIT* cDNA (2.9 kbp) followed by IRES2 linked with enhanced green fluorescent protein (eGFP) sequence was inserted into the pKS/RIP plasmid to generate the transgene. Transgenic mice (*c-KitβTg*) were generated using C57BL/6J embryos and identified by PCR first using primers globin5 and c-Kit, and further confirmed by a second set of primers eGFP3 and globin3 (Appendix 3) [2, 3]. Five RIP-c-Kit transgenic founders were obtained (Dr. Siu-Pok Yee, University of Connecticut), and bred with C57BL/6J mice (the Jackson Laboratory) to establish the independent mouse lines. Initial characterization revealed that they display a similar, if not identical, pattern of transgene expression and phenotype, which eliminated any positional effects due to the location of transgene integration. We therefore used offspring from two independent transgenic lines for subsequent detailed analyses. Male mice were used in this study.

Generation of HFD-induced diabetes in c-KitβTg and wild type (WT) littermates: the HFD study was conducted starting at 6 weeks of age, and male *c-KitβTg* and *WT* littermates were fed with HFD containing 60 kcal % fat (D12492, Research Diets, New Brunswick, NJ, USA) for 4 weeks.

Generation of the c-KitβTg;Wv mouse model: the *c-KitβTg;Wv* mouse model was generated by crossbreeding *c-KitβTg* with *c-Kit*$^{Wv/+}$ mice, which would yield mice with four different genotypes including: wild type (*WT*); *c-Kit*$^{Wv/+}$; *c-KitβTg*; *c-KitβTg;c-Kit*$^{Wv/+}$ (*c-KitβTg;Wv*) mice (Figure 2-4). The *c-Kit W*^{v} allele was identified by its characteristic fur pigmentation (Figure 2-1) [1], and *c-KitβTg* allele was determined by PCR (Appendix 3). Male mice at 8 weeks of age were used for this study.

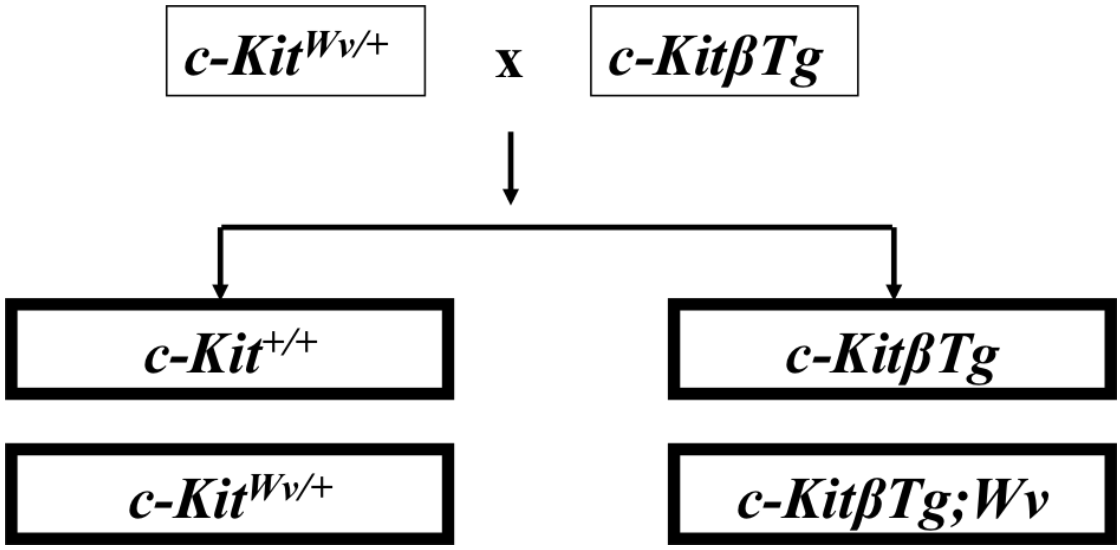
c-Kit^Wv/+
x
c-KitβTg
c-Kit^+/+
c-KitβTg
c-Kit^Wv/+
c-KitβTg;Wv

Figure 2-4. Breeding schematic for *c-KitβTg;Wv* mice.

C57BL/6J/*Kit*$^{Wv/+}$ mice (stock no. 000049) from the Jackson Laboratory and *c-KitβTg* mice were crossed to obtain four experimental groups including: *c-Kit*$^{+/+}$, *c-Kit*$^{Wv/+}$, *c-KitβTg*, and *c-KitβTg;Wv* mice.

2.1.4 Mouse models used in Chapter 6

Generation of the c-KitβTg;Wv mouse model: *c-KitβTg* with *c-Kit*$^{Wv/+}$ mice were crossed to obtain mice with listed all 4 different genotypes including: *WT*, *c-KitβTg*, *c-Kit*$^{Wv/+}$, and *c-KitβTg;Wv* mice, as described in 2.1.3 section (Figure 2-4). Male mice at 8 weeks of age were used for this study.

The long-term HFD treatment for c-KitβTg mice: *c-KitβTg* male mice and their age-matched *WT* littermates were generated as described in section 2.1.3. A HFD study was performed using HFD (D12492, Research Diets) starting at 6 weeks of age in both *c-KitβTg* and *WT* mice for 20-22 weeks (labelled as experimental groups: *c-KitβTg-HFD* and *WT-HFD*). In parallel, age-matched *c-KitβTg* and *WT* mice under normal diet were also examined.

2.2 DNA extraction and PCR genotyping

Genotyping was performed on all mice at weaning (21 days after birth). In brief, 2 mm of tail was obtained and placed into Eppendorf tubes for DNA extraction, with the exception of c-*Kit*$^{Wv/+}$ mice. Each tail sample was digested by 50 µL of base solution (25 mM NaOH; 0.2 mM EDTA), and placed on heat block at 95 ^{o}C for 30 minutes following by an hour cooldown at room temperature. Fifty µL of 40 mM Tris HCl (pH 5.5) was added to each digested sample, and centrifuged at 13,000 rpm x g for 1 minute. One µL of aliquot was taken for PCR. PCR was performed with a mixture of primer sequences listed in Appendix 3 using a thermocycler (Biometra GmbH, Goettingen, Germany) as follows: 94 ^{o}C for 30 seconds (melting temperature), 59 ^{o}C for 1 minute (annealing temperature), and 72 ^{o}C for 1 minute (primer extension phase), for 25-35 cycles depending on the primers. The PCR products were separated on 2% agarose gel, stained with 1 µg/mL ethidium bromide, and visualized under UV light (Appendix 3).

2.3 Body weight, food intake, and *in vivo* metabolic studies

Body weight, blood glucose level, and intraperitoneal glucose (IPGTT) and insulin tolerance tests (IPITT) were performed on the listed mouse models [1]. Food intake was monitored. In brief, a known amount of a diet is given to the animal. After 7 days, the

food was reweighed and the amount consumed was calculated by measuring the difference. Blood glucose levels were examined under the non-fasting, as well as after 4-hour or 16-hour (overnight) fasting with *ad libitum* water access. For IPGTT and IPITT, an intraperitoneal injection of glucose (D-(+)-glucose; dextrose; Sigma, St. Louis, MO, USA) at a dosage of 2 mg/g of body weight or human insulin (Humalin, Eli Lilly, Toronto, ON, Canada) at 1 U/kg of body weight was administrated. Blood glucose levels were examined at 0, 15, 30, 60, and 120 minutes following injection, and area under the curve (AUC) was used to quantify glucose or insulin responsiveness. The data is shown with units of ([mmol/L] x minutes) [1].

2.4 *In vivo* and *ex vivo* glucose stimulated insulin secretion assay

For *in vivo* glucose stimulated insulin secretion (GSIS), mouse blood samples were collected from the tail vein following 4 hours of fasting (0 minute), and at 5 and 35 minutes after glucose loading [1]. Plasma samples were immediately obtained by centrifuging at 3000 rpm x g for 10 minutes and stored at -20^{o}C.

For *ex vivo* GSIS, islets from each experimental group were isolated. In brief, the bile duct was clamped closed to the duodenum. The pancreas was inflated via an intraductal collagenase V (1 mg/mL, Sigma) injection through the common bile duct (3 mL) [4]. The inflated pancreas was carefully excised and moved into a falcon tube with 3 mL of cold dissociation buffer (Hank's balanced salt solution with HEPES, 0.6% g/mL). The excised pancreas was digested at 37 ^{o}C in a water bath for 20-30 minutes. Freshly isolated islets were hand-picked and incubated with an oxygenated Krebs-Ringer bicarbonate HEPES plus 0.5% BSA buffer containing 2.2 mmol/L or 22 mmol/L glucose for 1 hour. Media and islets were collected and stored at –20 ^{o}C for measuring insulin secretion and content by ELISA.

2.5 Insulin ELISA analyses

Insulin secretion and content was measured using an ultrasensitive (mouse) insulin ELISA (ALPCO, Salem, NH, USA) with a sensitivity of 0.15 ng/mL, according to the manufacturer's instruction [1]. Plasma insulin levels were expressed as ng/mL. A static

glucose stimulation index in isolated islets was calculated by dividing the insulin output from the high glucose (22 mM) incubation by the insulin output during the low glucose (2.2 mM) incubation. Insulin content in the islets was expressed as ng/μg of DNA. DNA content of the islets was determined along with insulin content using a Multiskan spectrum microplate spectrophotometer (Thermo Electron Corp., Waltham, MA, USA) [1].

2.6 Cell culture and treatment

2.6.1 Treatment with Gsk3β inhibitor on isolated islets in Chapter 3

Islets were isolated from *c-Kit*$^{+/+}$ and *c-Kit*$^{Wv/+}$ male mice at 8 weeks of age (isolation procedure is described in section 2.4). Isolated islets were cultured in RPMI-1640 medium (Gibco, Burlington, ON, Canada), supplemented with sodium bicarbonate (0.2% g/mL), Soybean trypsin inhibitor (10% mg/mL), fetal bovine serum (10% mL/mL), Penicillin-Streptomycin (1% mL/mL), and Fungizone (1% mL/mL) with or without 1-AKP (10 μM, Calbiochem) for 24 hours [5]. Islets were harvested for protein and quantitative RT-PCR (qRT-PCR) analyses.

2.6.2 INS-1 cell culture in Chapter 4 and 5

Rat insulinoma (INS-1 832/13 cells, a gift from Dr. Christopher Newgard, Duke University Medical Center, USA) were cultured in RPMI-1640 medium (Gibco), containing sodium bicarbonate (0.2% g/mL), fetal bovine serum (10% mL/mL), HEPES (2.5% mL/mL), sodium pyruvate (1% mL/mL), and β-mercaptoethanol (0.4% μL/mL) under a humidified condition of 95% air and 5% carbon dioxide at 37 °C. Medium was replaced every other day until cells reached near 80% confluence.

Treatment with human SCF: INS-1 cells were starved in serum-free RPMI-1640 plus 1% BSA medium (Gibco) for 3 hours. Cell cultures were then treated with either SCF vehicle (10 mM acetic acid) as a control, SCF (50 ng/mL, ID labs, London, ON, Canada), or SCF plus wortmannin (100 nM, Sigma) for 24 hours [6].

c-Kit and Fas siRNA transfection of INS-1 cell lines: INS-1 cells were transfected for 48 hours with either control siRNA (sc-37007, proprietary sequence), *c-Kit* (rat) siRNA (sc-

63363) with or without a p53 inhibitor, pifithrin-alpha (PFT-α, 5 μM, Sigma), or combined *c-Kit* (rat) siRNA and *Fas* (rat) siRNA (sc-270241) (Santa Cruz Biotechnology, Santa Cruz, CA, USA) using an siRNA transfection protocol described by the manufacturer (Santa Cruz Biotechnology) [6]. The sequence for *c-Kit* (rat) and *Fas* (rat) siRNAs are listed (Appendix 4). Transfection efficiency was monitored using fluorescein-conjugated control siRNA (sc-36869, Santa Cruz Biotechnology), with approximately 60-70% of the cells being transfected.

At the end of the culture period, cells were harvested and prepared for qRT-PCR analyses, immunofluorescence staining, and protein extraction for western blot. Cell apoptosis was examined using the Terminal deoxynucleotidyl transferase dUTP nick end labeling (TUNEL) assay. Cell viability was examined using the (3-(4,5-Dimethylthiazol-2-yl)-2,5-diphenyltetrazolium bromide (MTT) assay and cell proliferation was examined using the Ki67 staining [7].

2.7 Immunofluorescence and morphometric analyses

Pancreata from all mouse models used in this thesis were fixed in 4% paraformaldehyde overnight at 4 °C followed by a standard protocol of dehydration and paraffin embedding. Pancreatic tissue sections (4 μm thick) were prepared and double-stained with primary antibodies of appropriate dilutions as listed in Appendix 5. Secondary antibodies, fluorescein isothiocyanate (FITC, anti-mouse; anti-rabbit; or anti-guinea pig) and TexRed (anti mouse; anti-rabbit; or anti-guinea pig) (Jackson ImmunoResearch, West Grove, PA, USA) were used. Nuclei were counterstained with 4'-6'-diamidino-2-phenylindol (DAPI) (Sigma) and were blue in color. To determine the specificity of the antibodies used in this thesis, the pancreatic sections were processed with the omission of primary or secondary antibodies, and tests resulted in a negative staining reaction [8]. Double-immunolabeled images were captured using a Leica DMIRE2 fluorescence microscope with Openlab image (Improvision, Lexington, MA, USA), or with Image Pro Plus (Media Cybernetics, Rockville, MD, USA).

Quantitative evaluation for islet number, islet size, alpha-cell, and beta-cell mass was performed using computer-assisted image analysis [1]. Islet number (density) was

obtained from total islet counts divided by the total area of the pancreas. Islet size was measured and grouped into different size classes, then expressed as a percentage of the total number of islet. Alpha-cell positive areas were identified by glucagon-staining, whereas beta-cell positive areas were identified by insulin-staining on the pancreatic sections. Alpha-cell or beta-cell mass was calculated by multiplying relative glucagon-positive or insulin-positive area over the total pancreas area by pancreas weight and expressed as mg.

The beta-cell proliferation, apoptosis, and expression of different transcription factors were determined by double immunofluorescence staining and cell counting (Appendix 5). $MafA^{+}$ staining on pancreatic islets was determined by immunohistochemical staining using the streptavidin-biotin horseradish peroxidase complex and developed with aminoethyl carbazole substrate kit (Invitrogen, Burlington, ON, Canada). In brief, 12 random islets from the head, middle, and tail of the pancreata per pancreatic section were chosen, with a minimum of 5 pancreata per experimental group was analyzed [1].

In Chapter 6, the pancreatic endocrine and exocrine vasculature was analyzed. The capillaries were labeled by platelet endothelial cell adhesion molecule-1 (PECAM-1) on the pancreatic sections (Appendix 5). Islet capillary density, capillary area per islet, average islet capillary size and diameter, exocrine capillary density, and exocrine capillary area were measured [9-11]. Islet capillary density was calculated by dividing the total number of capillaries over the islet area. Capillary area per islet was determined as a ratio of the total islet capillary area to the islet area. Average islet capillary size was determined by dividing the total islet capillary area over the number of islet capillaries. Average islet capillary diameter was determined by dividing the sum of individual islet capillary diameter (the maximum inner diameter of the capillary lumen) over the number of islet capillaries. Exocrine capillary density was determined by dividing the number of capillaries over the pancreatic exocrine area, and exocrine capillary area was determined as a ratio of the exocrine capillary area to the pancreatic exocrine area. A minimum of 5 pancreata per age per experimental group with at least 12 random islets was analyzed.

2.8 Protein extraction and western blot analyses

Proteins from mouse pancreata and isolated islets were extracted by homogenization in a Nonidet-P40 lysis buffer (Nonidet-P40, phenylmethylsulfonyl fluoride, sodium orthovanadate, Sigma; and complete inhibitor cocktail tablet, Roche) [1]. Samples were then centrifuged at 12,000 rpm x g for 20 minutes at 4 ^{o}C. The resulting supernatant was collected and frozen at -80 ^{o}C until use. The protein concentration was measured by a protein assay using Bradford dye (BioRad Laboratories; Mississauga, ON, Canada), with bovine serum albumin (fraction V) as the standard.

Equal amounts of lysate were separated by 5%, 7.5% or 10% sodium dodecyl sulfate-polyacrylamide gel electrophoresis (SDS-PAGE) and transferred onto a nitrocellulose membrane (Bio-Rad Laboratories). The membrane was then incubated with primary antibodies (Appendix 6), and a goat anti- mouse or rabbit IgG secondary antibody conjugated to horseradish peroxidase (Cell Signaling Technology, Danvers, MA, USA). The blot was probed with antibodies against total proteins or housekeeping proteins for a sample loading control (Appendix 6). The membrane was then incubated with chemiluminescence reagents (Perkin Elmer, Wellesley, MA, USA). The protein bands were visualized on BioMax MR Film (Kodak, Rochester, NY, USA), or were imaged by Versadoc Imaging System (Bio-Rad Laboratories). Densitometric quantification of bands at sub-saturation levels was analyzed by Syngenetool gel analysis software (Syngene, Cambridge, UK) and normalized to the loading controls, or was quantified by Image Lab (Bio-Rad laboratories).

2.9 RNA extraction and real-time RT-PCR analyses

RNA was extracted from isolated islets of mouse pancreata using RNAqueous-4 PCR kit (Ambion, Austin TX, USA), according to the manufacturer's instruction. The extraction procedure includes a DNase I treatment step, which eliminates any potential DNA contamination [1]. The RNA quality was verified by 1% agarose gel electrophoresis using ethidium bromide staining. Sequences of PCR primers are listed in Appendix 7. For each reverse transcription reaction (RT), 2 μg of DNA-free RNA from isolated islets were incubated with random hexamers/oligo-(dT) primers and superscript reverse

transcriptase (Invitrogen) to generate the complementary DNA (cDNA). The qRT-PCR analyses were performed using 0.1 μg of cDNA with iQ SYBR Green Supermix kit on Chromo4 qRT-PCR system (Bio-Rad Laboratories). Controls were performed by omitting reverse transcriptase, cDNA, or DNA polymerase and showed no reaction bands. Relative expression of mRNA were calculated using the arithmetic formula "$2^{-\Delta\Delta CT}$", where ΔCT is the difference between the threshold cycle of a given target cDNA and *18S* rRNA subunit cDNA, with at least five repeats per experimental group. The melting curve was used to indicate if the qRT-PCR assay had any amplified target sequence with an excellent specificity.

2.10 Statistical analyses

Data are expressed as means ± SEM. Statistical significance was determined by unpaired student's *t*-test, if comparing only two groups, or a one-way ANOVA followed by least significant difference (LSD) *post-hoc* test if there was more than two groups. Differences were considered to be statistically significant when $p<0.05$.

2.11 References

1. Krishnamurthy M, Ayazi F, Li J, et al. (2007) c-Kit in early onset of diabetes: a morphological and functional analysis of pancreatic beta-cells in c-KitW-v mutant mice. Endocrinology 148:5520–5530. doi: 10.1210/en.2007-0387

2. Valera A, Solanes G, Fernández-Alvarez J, et al. (1994) Expression of GLUT-2 antisense RNA in beta cells of transgenic mice leads to diabetes. J Biol Chem 269:28543–28546.

3. Nagy A (2003) Manipulating the Mouse Embryo. Firefly Books

4. Ilieva A, Yuan S, Wang RN, et al. (1999) Pancreatic islet cell survival following islet isolation: the role of cellular interactions in the pancreas. J Endocrinol 161:357–364.

5. Liu H, Remedi MS, Pappan KL, et al. (2009) Glycogen synthase kinase-3 and mammalian target of rapamycin pathways contribute to DNA synthesis, cell cycle progression, and proliferation in human islets. Diabetes 58:663–672. doi: 10.2337/db07-1208

6. Wu Y, Li J, Saleem S, et al. (2010) c-Kit and stem cell factor regulate PANC-1 cell differentiation into insulin- and glucagon-producing cells. Lab Invest 90:1373–1384. doi: 10.1038/labinvest.2010.106

7. Li J, Goodyer CG, Fellows F, Wang R (2006) Stem cell factor/c-Kit interactions regulate human islet-epithelial cluster proliferation and differentiation. Int J Biochem Cell Biol 38:961–972. doi: 10.1016/j.biocel.2005.08.014

8. Yashpal NK, Li J, Wang R (2004) Characterization of c-Kit and nestin expression during islet cell development in the prenatal and postnatal rat pancreas. Dev Dyn 229:813–825. doi: 10.1002/dvdy.10496

9. Cai Q, Brissova M, Reinert RB, et al. (2012) Enhanced expression of VEGF-A in β cells increases endothelial cell number but impairs islet morphogenesis and β cell proliferation. Dev Biol 367:40–54. doi: 10.1016/j.ydbio.2012.04.022

10. Brissova M, Shostak A, Shiota M, et al. (2006) Pancreatic islet production of vascular endothelial growth factor--a is essential for islet vascularization, revascularization, and function. Diabetes 55:2974–2985. doi: 10.2337/db06-0690

11. Dai C, Brissova M, Reinert RB, et al. (2013) Pancreatic islet vasculature adapts to insulin resistance through dilation and not angiogenesis. Diabetes 62:4144–4153. doi: 10.2337/db12-1657

Chapter 3

3 Inhibition of Gsk3β activity improves beta-cell function in *c-Kit*$^{Wv/+}$ mice[2]

[2] This chapter has been modified and adapted from the following manuscript:

- **Feng ZC**, Donnelly L, Li J, Krishnamurthy M, Riopel M, Wang R. (2012) Inhibition of Gsk3β activity improves beta-cell function in *c-Kit*$^{Wv/+}$ male mice. *Lab Invest.* 92:543-555.

3.1 Introduction

Recent studies by our lab and others demonstrated that c-Kit and its ligand, SCF, are important in pancreatic beta-cell survival and maturation [1-8]. Stimulation of c-Kit by SCF leads to dimerization of c-Kit and subsequent auto phosphorylation of intrinsic tyrosine kinases. Moreover, c-Kit activation mediates multiple intracellular pathways, including the PI3K pathway for modulation of gene transcription, proliferation, differentiation, metabolic homeostasis and cell survival [9-12]. PI3K is, a common signaling pathway, required for the regulation of glucose and preproinsulin gene expression as well as the nuclear translocation of Pdx-1, a transcription factor to regulate beta-cell function [13]. Our previous *in vitro* studies of human fetal islets demonstrated that increased c-KIT activity leads to enhanced PDX-1 and insulin expression, and cell proliferation via the activation of the PI3K/AKT pathway [14, 15]. Recently, our *in vivo* study using *c-Kit*$^{Wv/+}$ male mice showed that reduced c-Kit activity correlated with reduced beta-cell function and proliferation, which is associated with significantly decreased Pdx-1 expression and glucose intolerance [6]. However, the signaling pathway under c-Kit including PI3K/Akt and downstream targets involved in beta-cell proliferation and function *in vivo* remain unclear.

Gsk3, a serine/threonine kinase, consists of two highly homologous α (Gsk3α) and β (Gsk3β) isoforms that share overlaping physiological functions in terms of regulating a diverse array of cellular processes. Gsk3β is one of the substrates that are directly regulated by the PI3K/Akt pathway. Activation of Akt, which phosphorylates Gsk3β at Serine residue 9, leads to inactivation of Gsk3β [16-18]. Unphosphorylated Gsk3β can directly phosphorylate downstream substrates, and modulate their activity [19]. Apart from the function from which it derives its name (i.e., suppressing glycogen synthesis by phosphorylating glycogen synthase), studies have shown that Gsk3β is involved in mediating cell cycle, motility, and apoptosis [19], and that Gsk3β dysregulation is linked to several prevalent pathological diseases including Alzheimer's disease, cancer, and diabetes [19]. Indeed, mice with beta-cell-specific overexpression of *Gsk3β* displayed glucose intolerence due to reduced beta-cell mass and proliferation [20]. Furthermore, isolated adult human and rat islets incubated with Gsk3β inhibitors demonstrated a

significant increase in islet cell proliferation [21]. This evidence was further confirmed by mice with beta-cell specific ablation of *Gsk3β* [22]. Although the beneficial effect of Gsk3β inhibition has been demonstrated in islet biology, the physiological role of Gsk3β under disrupted c-Kit signaling in beta-cell has yet to be investigated.

In order to understand the intracellular mechanisms that relate c-Kit to physiological changes in beta-cells in c-$Kit^{Wv/+}$ mice [6], we proposed to examine whether beta-cell dysfunction in *c-*$Kit^{Wv/+}$ mice is associated with down-regulation of the phospho-Akt/Gsk3β pathway. Furthermore, 1-AKP, a specific organic inhibitor that prevents Gsk3β phosphorylation of multiple downstream substrates by competitively binding at its ATP-binding site [23], was used to investigate whether inhibition of Gsk3β could improve beta-cell proliferation and function, delaying the onset of diabetes in *c-*$Kit^{Wv/+}$ mice. Here, we report that decreased beta-cell proliferation and function in *c-*$Kit^{Wv/+}$ mice was associated with dysregulated Akt and Gsk3β phosphorylation as well as cyclin D1 protein levels. Treating *c-*$Kit^{Wv/+}$ mice with 1-AKP delayed onset of diabetes, maintained beta-cell mass and enhanced beta-cell function. This study demonstrates a functional role for c-Kit in mediating glucose homeostasis and beta-cell function via the Akt/Gsk3β axis in *c-*$Kit^{Wv/+}$ mice.

3.2 Materials and methods

Mouse model: in this study, *c-*$Kit^{+/+}$ and *c-*$Kit^{Wv/+}$ mice were bred and genotyped by differences in fur pigmentation as detailed in section 2.1.1. Mice were kept until 8 weeks of age with normal diet at which point, metabolic studies, and subsequent islet morphological studies, islet qRT-PCR, and pancreatic and islet protein analyses were performed. Only male mice were used for this study [6].

In vivo and in vitro treatment with Gsk3β inhibitor: to investigate whether inhibition of Gsk3β activity could prevent early onset of diabetes in *c-*$Kit^{Wv/+}$ mice at 8 weeks of age [6], both *c-*$Kit^{+/+}$ and *c-*$Kit^{Wv/+}$ 6-week-old mice were treated with either 1-AKP at 2 mg/kg or saline injections intraperitoneally every other day for 2 weeks to establish four experimental groups: *c-*$Kit^{+/+}$*/saline, c-*$Kit^{+/+}$*/1-AKP, c-*$Kit^{Wv/+}$*/saline* and *c-*$Kit^{Wv/+}$*/1-AKP*, as detailed in section 2.1.1 [24, 25]. To examine whether administrating the Gsk3β

inhibitor to isolated *c-Kit*$^{Wv/+}$ mouse islets could improve islet beta-cell function, islets were isolated from *c-Kit*$^{+/+}$ and *c-Kit*$^{Wv/+}$ mice at 8 weeks of age and cultured with or without 1-AKP (10 μM) for 24 hours, as detailed in section 2.6.1 [21].

Metabolic studies: body weight was measured weekly while fasting (4-hour) blood glucose levels, IPGTT and IPITT analyses were performed on *c-Kit*$^{+/+}$*/saline, c-Kit*$^{+/+}$*/1-AKP, c-Kit*$^{Wv/+}$*/saline* and *c-Kit*$^{Wv/+}$*/1-AKP* mice at 8 weeks of age (after 2 weeks of 1-AKP treatment), as detailed in section 2.3.

In vivo, ex vivo GSIS studies, and insulin ELISA analyses: in vivo GSIS, and *ex vivo* GSIS on isolated islets, were performed on *c-Kit*$^{+/+}$ and *c-Kit*$^{Wv/+}$ mice at 8 weeks of age, as detailed in sections 2.4 and 2.5.

Immunofluorescence and morphometric analyses: pancreatic tissue sections from mice at 8 weeks of age were prepared and double-stained with appropriate antibodies listed in Appendix 5. Islet number, islet size, alpha and beta-cell mass were measured. Cell proliferation (Ki67$^+$ labeling), cyclin D1 and Pdx-1 positive staining in beta-cell nuclear was quantified, and the average percent of Ki67$^+$/insulin$^+$, cyclin D1$^+$/insulin$^+$, and Pdx-1$^+$/insulin$^+$ cells was calculated. MafA$^+$ staining on pancreatic islets was determined by immunohistochemical staining, as detailed in section 2.7.

Protein extraction and western blot analyses: protein levels of phospho-Akt^{S473}, phospho-Akt^{T308} total-Akt, phospho-Gsk3β^{S9}, phospho-Gsk3β^{Y216}, total-Gsk3β, β-catenin, cyclin D1 and Pdx-1 and corresponding housekeeping proteins including calnexin and β-actin in pancreata and isolated islets from *c-Kit*$^{+/+}$ and *c-Kit*$^{Wv/+}$ mice at 8 weeks of age with or without 1-AKP were analyzed (Appendix 6), as detailed in section 2.8.

RNA extraction and real-time RT-PCR analyses: RNA was extracted from isolated islets of *c-Kit*$^{+/+}$ and *c-Kit*$^{Wv/+}$ mice with or without 1-AKP at 8 weeks of age. mRNA expression of *Ccnd1* (cyclin D1*)*, *Ins I* (*Insulin I)*, *Ins II* (*Insulin II)*, *MafA*, *Pdx-1* was measured and normalized to *18S* rRNA (Appendix 7), as detailed in section 2.9.

3.3 Results

3.3.1 Reduction of phospho-Akt, phospho-Gsk3β and cyclin D1 in *c-Kit*$^{Wv/+}$ mice

Our recent study has demonstrated that mice with mutated c-Kit develop early onset of diabetes with a loss of beta-cell mass and proliferation, suggesting that c-Kit plays a critical role in beta-cell proliferation and function [6]. Moreover, experiments in isolated human fetal islet-epithelial cells revealed that the PI3K/Akt pathway is significantly up-regulated upon exogenous SCF stimulation [14, 15]. Here, we showed that both whole pancreatic tissue and isolated islets from *c-Kit*$^{Wv/+}$ mice displayed a significant reduction in phosphorylated Akt at S473 (Figure 3-1A), but not at T308 (Figure 3-2A). In parallel, decreased protein levels of phosphorylated Gsk3β at S9 was observed in *c-Kit*$^{Wv/+}$ mice when compared to *c-Kit*$^{+/+}$ mice (Figure 3-1B), but not at Y216 (Figure 3-2B). No alteration in cyclin D1 protein levels was observed in total pancreatic tissue extract. However, a significant reduction in cyclin D1 protein expression was noted in isolated islets of *c-Kit*$^{Wv/+}$ mice (Figure 3-3A) along with a 60% reduction in the proportion of cyclin D1^{+}/insulin^{+} cells when compared to *c-Kit*$^{+/+}$ mice (Figure 3-3B and C).

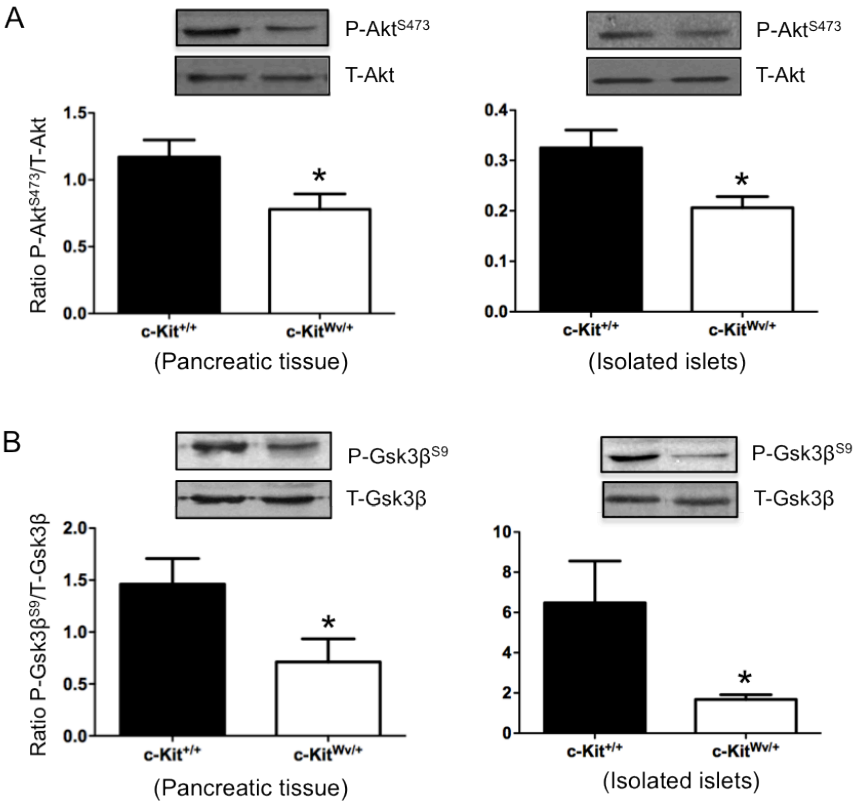
A
P-Akt^{S473}
T-Akt
Ratio P-Akt^{S473}/T-Akt
1.5
1.0
0.5
0.0
*
c-Kit$^{+/+}$
c-Kit$^{Wv/+}$
(Pancreatic tissue)
P-Akt^{S473}
T-Akt
0.4
0.3
0.2
0.1
0.0
*
c-Kit$^{+/+}$
c-Kit$^{Wv/+}$
(Isolated islets)
B
P-Gsk3β^{S9}
T-Gsk3β
Ratio P-Gsk3β^{S9}/T-Gsk3β
2.0
1.5
1.0
0.5
0.0
*
c-Kit$^{+/+}$
c-Kit$^{Wv/+}$
(Pancreatic tissue)
P-Gsk3β^{S9}
T-Gsk3β
10
8
6
4
2
0
*
c-Kit$^{+/+}$
c-Kit$^{Wv/+}$
(Isolated islets)

Figure 3-1. Down-regulation of phospho-Akt/Gsk3β signaling in the pancreata and isolated islets from *c-Kit*$^{Wv/+}$ mice.

Western blot analyses of S473-phosphorylated (P) and total (T) Akt (**A**), S9-(P) and total (T) Gsk3β (**B**) protein levels in the pancreata and isolated islets of *c-Kit*$^{+/+}$ and *c-Kit*$^{Wv/+}$ mice at 8 weeks of age. Representative blots are shown. Data (**A** and **B**) are normalized to total protein and expressed as mean ± SEM (*n=11* pancreata; *n=3* isolated islets), **p*<0.05 analyzed by unpaired student's *t*-test.

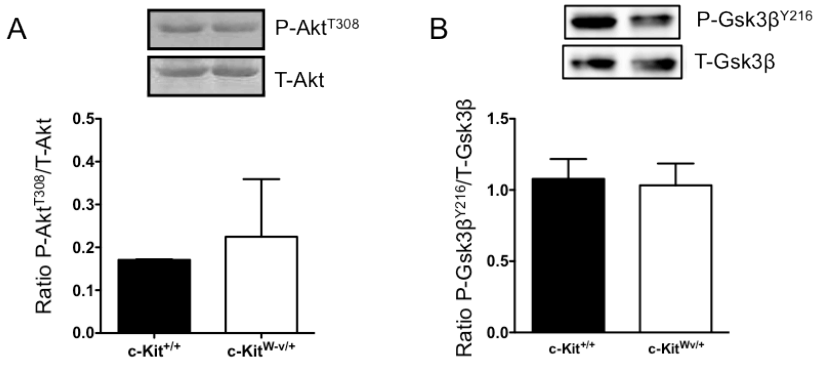
A
P-Akt^{T308}
T-Akt
Ratio P-Akt^{T308}/T-Akt
0.5
0.4
0.3
0.2
0.1
0.0
c-Kit$^{+/+}$
c-Kit$^{W-v/+}$
B
P-Gsk3β^{Y216}
T-Gsk3β
Ratio P-Gsk3β^{Y216}/T-Gsk3β
1.5
1.0
0.5
0.0
c-Kit$^{+/+}$
c-Kit$^{Wv/+}$

Figure 3-2. Western blot analyses of phospho-Akt^{T308}, and phospho-Gsk3β^{Y216} protein levels in isolated islets from *c-Kit*$^{Wv/+}$ mice.

T308-phosphorylated (P) and total (T) Akt (**A**), Y216-(P) and total (T) Gsk3β (**B**) protein levels in isolated islets of *c-Kit*$^{+/+}$ and *c-Kit*$^{Wv/+}$ mice at 8 weeks of age. Representative blots are shown. Data (**A** and **B**) are normalized to total protein and expressed as mean ± SEM (*n=3*), analyzed by unpaired student's *t*-test.

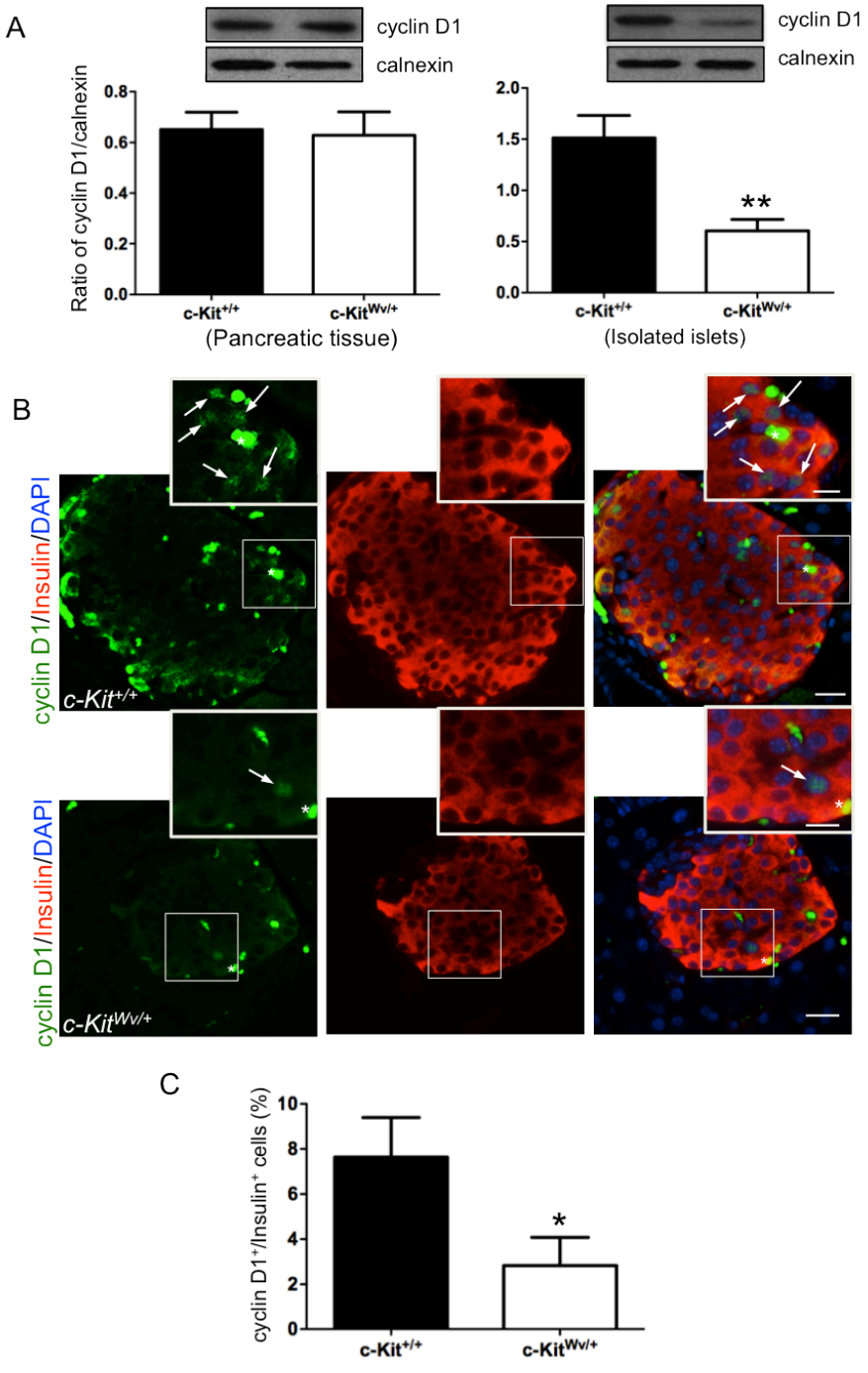
A
cyclin D1
calnexin
Ratio of cyclin D1/calnexin
0.8
0.6
0.4
0.2
0.0
c-Kit+/+
c-KitWv/+
(Pancreatic tissue)
cyclin D1
calnexin
2.0
1.5
1.0
0.5
0.0
**
c-Kit+/+
c-KitWv/+
(Isolated islets)
B
cyclin D1/Insulin/DAPI
c-Kit+/+
cyclin D1/Insulin/DAPI
c-KitWv/+
C
cyclin D1+/Insulin+ cells (%)
10
8
6
4
2
0
*
c-Kit+/+
c-KitWv/+

Figure 3-3. Decreased cyclin D1 protein levels in isolated islets of *c-Kit*$^{Wv/+}$ mice.

(**A**) Western blot analysis of cyclin D1 in the pancreata and isolated islets of *c-Kit*$^{+/+}$ and *c-Kit*$^{Wv/+}$ mice at 8 weeks of age. Representative blots are shown. Data are normalized to loading control calnexin and expressed as mean ± SEM (*n=4* pancreas; *n=6* isolated islets), $^{**}p<0.01$ analyzed by unpaired student's *t*-test. (**B**) Double immunofluorescence staining for cyclin D1 (green), insulin (red) of *c-Kit*$^{+/+}$ and *c-Kit*$^{Wv/+}$ mice pancreatic section at 8 weeks of age. Nuclear counter stained by DAPI (blue). Scale bar 20 μm (inset: 10 μm). Arrows indicate cyclin D1/insulin double-positive cells. (**C**) The percentage of cyclin D1^{+} cells in beta-cells of *c-Kit*$^{+/+}$ and *c-Kit*$^{Wv/+}$ mice at 8 weeks of age. Data are expressed as mean percent positive cells over insulin^{+} cells ± SEM (*n=6*), $^{*}p<0.05$ analyzed by unpaired student's *t*-test.

3.3.2 Inhibition of Gsk3β activity prevents early onset of diabetes in *c-Kit$^{Wv/+}$* mice

c-Kit$^{+/+}$ and *c-Kit$^{Wv/+}$* mice that received saline or 1-AKP treatment revealed no significant change in body weight at 8 weeks of age (Figure 3-4A). However, fasting blood glucose levels in *c-Kit$^{Wv/+}$/1-AKP* mice showed a significant improvement when compared to *c-Kit$^{Wv/+}$/saline* group (Figure 3-4B) and reached similar fasting blood glucose levels of *c-Kit$^{+/+}$/saline* and *c-Kit$^{+/+}$/1-AKP* groups (Figure 3-4B). These improvements in glucose metabolism were further confirmed by glucose tolerance tests (Figure 3-4C). *c-Kit$^{Wv/+}$/1-AKP* mice showed similar glucose tolerance capacity to both *c-Kit$^{+/+}$/saline* and *c-Kit$^{+/+}$/1-AKP* groups, along with significant decreases in AUC when the IPGTT was performed (Figure 3-4C). Insulin tolerance tests revealed no significant differences between the four experimental groups (Figure 3-4D).

Furthermore, the effects of Gsk3β inhibition on insulin secretion were examined by the GSIS assay *in vivo* and on isolated islets. No significant differences were found in basal plasma insulin levels between the four experimental groups. However, 5 minutes after glucose stimulation, an increase in plasma insulin release was noted in *c-Kit$^{Wv/+}$/1-AKP* mice when compared to *c-Kit$^{Wv/+}$/saline* and *c-Kit$^{+/+}$/saline* groups (Figure 3-5A). There was a further increase in plasma insulin secretion at 35 minutes following stimulation in both 1-AKP treated groups (Figure 3-5A). To further confirm if these changes in insulin secretion upon glucose stimulation are observed in isolated islets, *in vitro* GSIS was performed using isolated islets from all experimental groups. Insulin secretion in response to 22 mM glucose was significantly increased in the islets of *c-Kit$^{Wv/+}$/1-AKP* mice, showing a 2-fold increase in insulin secretion compared to *c-Kit$^{Wv/+}$/saline* group (Figure 3-5B).

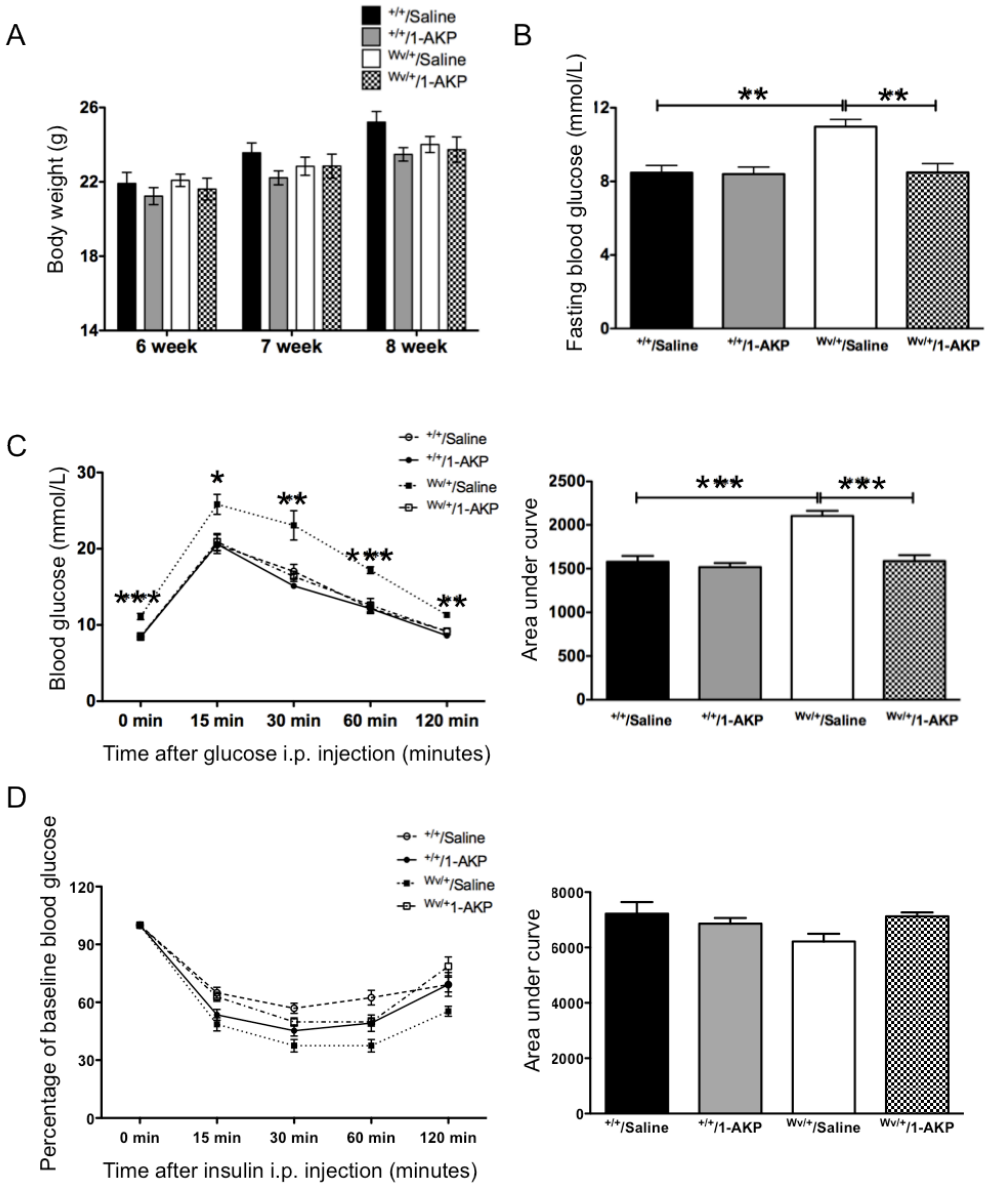
A
+/+/Saline
+/+/1-AKP
Wv/+/Saline
Wv/+/1-AKP
Body weight (g)
26
22
18
14
6 week
7 week
8 week
B
Fasting blood glucose (mmol/L)
12
8
4
0
**
**
+/+/Saline
+/+/1-AKP
Wv/+/Saline
Wv/+/1-AKP
C
+/+/Saline
+/+/1-AKP
Wv/+/Saline
Wv/+/1-AKP
Blood glucose (mmol/L)
30
20
10
0
*
**
***
***
**
0 min
15 min
30 min
60 min
120 min
Time after glucose i.p. injection (minutes)
Area under curve
2500
2000
1500
1000
500
0
***
***
+/+/Saline
+/+/1-AKP
Wv/+/Saline
Wv/+/1-AKP
D
+/+/Saline
+/+/1-AKP
Wv/+/Saline
Wv/+1-AKP
Percentage of baseline blood glucose
120
90
60
30
0
0 min
15 min
30 min
60 min
120 min
Time after insulin i.p. injection (minutes)
Area under curve
8000
6000
4000
2000
0
+/+/Saline
+/+/1-AKP
Wv/+/Saline
Wv/+/1-AKP

Figure 3-4. Effect of Gsk3β inhibitor on glucose homeostasis of *c-Kit$^{Wv/+}$/1-AKP* mice.

Body weight (**A**) and fasting blood glucose (**B**) of *c-Kit$^{+/+}$/saline*, *c-Kit$^{+/+}$/1-AKP*, *c-Kit$^{Wv/+}$/saline* and *c-Kit$^{Wv/+}$/1-AKP* groups. IPGTT (**C**), and IPITT (**D**) in *c-Kit$^{+/+}$/saline*, *c-Kit$^{+/+}$/1-AKP*, *c-Kit$^{Wv/+}$/saline*, and *c-Kit$^{Wv/+}$/1-AKP* groups. Glucose responsiveness of the corresponding experimental groups is shown as a measurement of AUC of the IPGTT or IPITT graphs with units of (mmol/L x minutes). Data (**A**-**D**) are expressed as mean ± SEM (*n=6–8*), **p*<0.05, ***p*<0.01, ****p*<0.001 analyzed by one-way ANOVA followed by LSD *post-hoc* test.

A

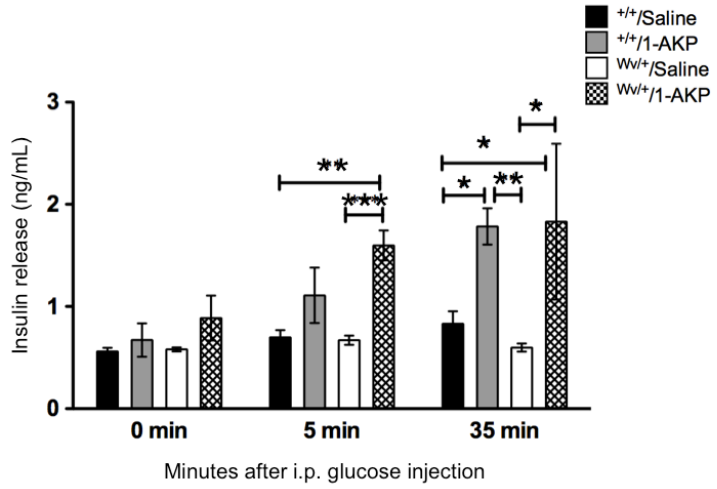
+/+/Saline
+/+/1-AKP
Wv/+/Saline
Wv/+/1-AKP
Insulin release (ng/mL)
0
1
2
3
**
***
*
*
**
*
0 min
5 min
35 min
Minutes after i.p. glucose injection

B

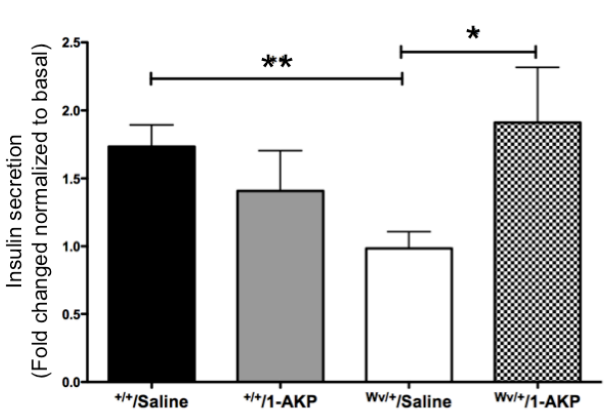
Insulin secretion
(Fold changed normalized to basal)
0.0
0.5
1.0
1.5
2.0
2.5
**
*
+/+/Saline
+/+/1-AKP
Wv/+/Saline
Wv/+/1-AKP

Figure 3-5. Effect of Gsk3β inhibitor on beta-cell function of *c-Kit$^{Wv/+}$/1-AKP* mice.

(**A**) *In vivo* GSIS of *c-Kit$^{+/+}$/saline*, *c-Kit$^{+/+}$/1-AKP*, *c-Kit$^{Wv/+}$/saline* and *c-Kit$^{Wv/+}$/1-AKP* groups. *c-Kit$^{Wv/+}$/1-AKP* group demonstrated an increase in plasma insulin release after glucose loading (*n=3–8*), **p*<0.05, ***p*<0.01, ****p*< 0.001 analyzed by one-way ANOVA followed by LSD *post-hoc* test. (**B**) Insulin secretion is improved in isolated islets from *c-Kit$^{Wv/+}$/1-AKP* mice in response to 22 mM glucose challenge; data are expressed as fold change normalized to basal (2.2 mM glucose) secretion as mean ± SEM (*n=4–5*), **p*<0.05, ***p*<0.01 analyzed by one-way ANOVA followed by LSD *post-hoc* test.

3.3.3 Inhibition of Gsk3β activity preserves beta-cell mass in *c-Kit*$^{Wv/+}$ mice

Our *in vivo* metabolic data suggests that inhibition of Gsk3β activity in *c-Kit*$^{Wv/+}$ mice could prevent early onset of diabetes. There was no observed difference in pancreatic weight between all experimental groups (data not shown). Morphometric analyses were performed to examine the effects of the Gsk3β inhibitor on islet number and size as well as alpha and beta-cell mass in *c-Kit*$^{+/+}$ and *c-Kit*$^{Wv/+}$ mice with or without 1-AKP treatments. A significant increase in the number of pancreatic islets was noted in *c-Kit*$^{Wv/+}$*/1-AKP* mice (Figure 3-6A), with a significant increase in the number of small islets (<500 μm^2) when compared to *c-Kit*$^{Wv/+}$*/saline* group (Figure 3-6B). Moreover, the number of large islets (>10000 μm^2) was only slightly increased in *c-Kit*$^{Wv/+}$*/1-AKP* mice when compared to *c-Kit*$^{Wv/+}$*/saline* group, while both *c-Kit*$^{+/+}$*/saline* and *c-Kit*$^{+/+}$*/1-AKP* groups had the most number of large islets (Figure 3-6B). Furthermore, beta-cell mass in *c-Kit*$^{Wv/+}$*/1-AKP* mice also increased by 24% when compared to *c-Kit*$^{Wv/+}$*/saline* group (Figure 3-6D), however it only reached 80-90% of the beta-cell mass of *c-Kit*$^{+/+}$*/saline* and *c-Kit*$^{+/+}$*/1-AKP* groups (Figure 3-6D). Increased beta-cell mass was also correlated with increased expression of *Insulin I* and *II* genes in the islets of 1-AKP treated *c-Kit*$^{+/+}$*and c-Kit*$^{Wv/+}$ mice (Figure 3-6E). No alterations were detected in alpha-cell mass among any of the four experimental groups (Figure 3-6C).

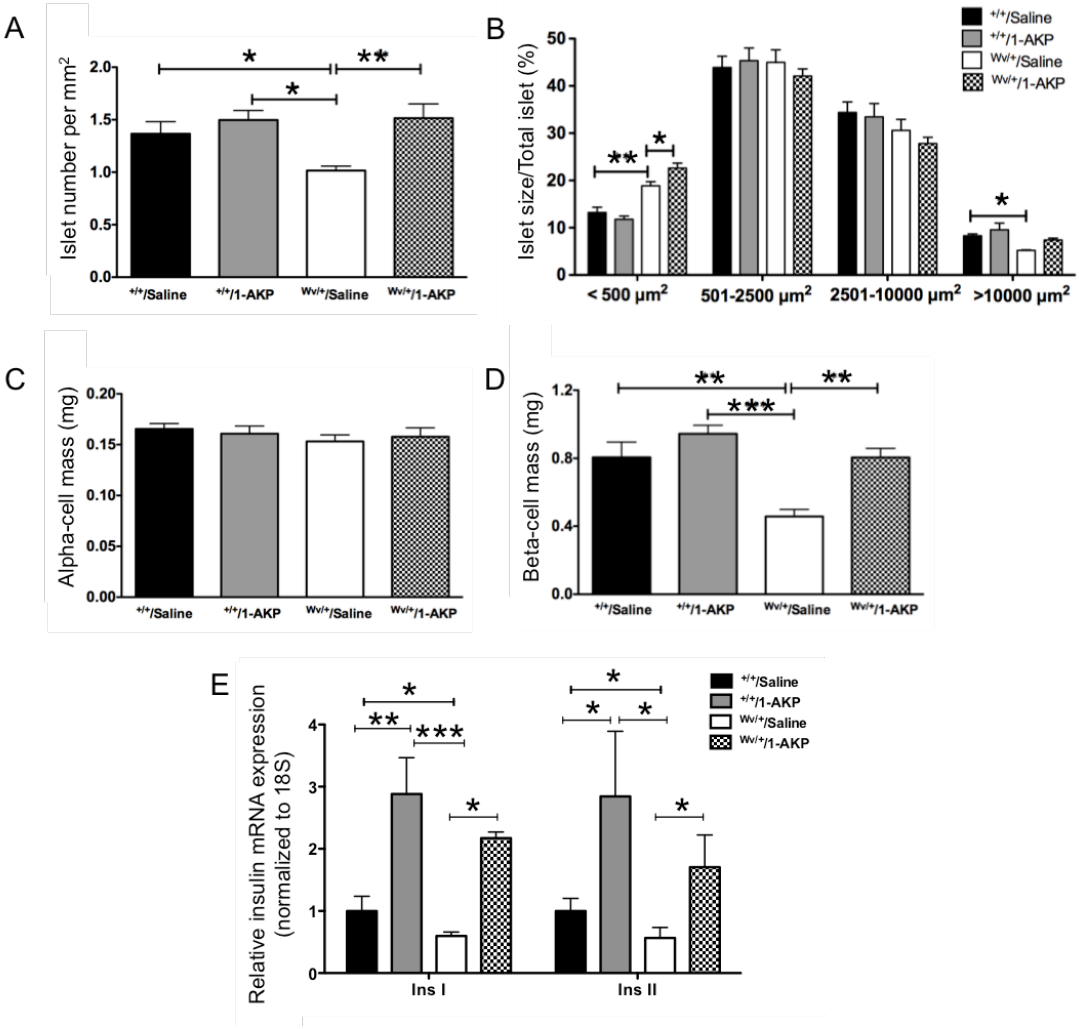
A
Islet number per mm2
2.0
1.5
1.0
0.5
0.0
*
**
*
+/+/Saline
+/+/1-AKP
Wv/+/Saline
Wv/+/1-AKP
B
Islet size/Total islet (%)
50
40
30
20
10
0
**
*
*
< 500 µm2
501-2500 µm2
2501-10000 µm2
>10000 µm2
+/+/Saline
+/+/1-AKP
Wv/+/Saline
Wv/+/1-AKP
C
Alpha-cell mass (mg)
0.20
0.15
0.10
0.05
0.00
+/+/Saline
+/+/1-AKP
Wv/+/Saline
Wv/+/1-AKP
D
Beta-cell mass (mg)
1.2
0.8
0.4
0.0
**
***
**
+/+/Saline
+/+/1-AKP
Wv/+/Saline
Wv/+/1-AKP
E
Relative insulin mRNA expression (normalized to 18S)
4
3
2
1
0
*
**
***
*
*
*
*
Ins I
Ins II
+/+/Saline
+/+/1-AKP
Wv/+/Saline
Wv/+/1-AKP

Figure 3-6. Effect of Gsk3β inhibitor on pancreatic morphology of *c-Kit$^{Wv/+}$/1-AKP* mice.

Morphometric analyses of islet number (**A**), islet size (**B**), alpha-cell mass (**C**) and beta-cell mass (**D**) in *c-Kit$^{+/+}$/saline*, *c-Kit$^{+/+}$/1-AKP*, *c-Kit$^{Wv/+}$/saline*, and *c-Kit$^{Wv/+}$/1-AKP* groups. (**E**) qRT-PCR analyses of *insulin I* and *II* mRNA in isolated islets of *c-Kit$^{+/+}$/saline*, *c-Kit$^{+/+}$/1-AKP*, *c-Kit$^{Wv/+}$/saline* and *c-Kit$^{Wv/+}$/1-AKP* mice. Data (**A**-**E**) are expressed as mean ± SEM (n=*5-8*), *p<0.05, **p<0.01, ***p<0.001 analyzed by one-way ANOVA followed by LSD *post-hoc* test.

3.3.4 Inhibition of Gsk3β activity preserves β-catenin, cyclin D1, Pdx-1, and MafA expression and increases the proliferative capacity of beta-cells of *c-Kit*$^{Wv/+}$ mice

The effect of Gsk3β inhibition on downstream signaling mediators of β-catenin protein levels in the islets of *c-Kit*$^{Wv/+}$*/1-AKP* mice was significantly higher when compared to *c-Kit*$^{Wv/+}$*/saline* group (Figure 3-7A). However, this protein levels only reached 78% of both *c-Kit*$^{+/+}$*/saline* and *c-Kit*$^{+/+}$*/1-AKP* groups (Figure 3-7A). *c-Kit*$^{Wv/+}$*/saline* group showed a significantly lower level of islet β-catenin protein than that of *c-Kit*$^{+/+}$*/1-AKP* and *c-Kit*$^{+/+}$*/saline* groups (Figure 3-7A). In addition, *c-Kit*$^{+/+}$*/1-AKP* mice showed slightly increased β-catenin protein levels in islet protein extracts but did not reach statistical significance when compared to *c-Kit*$^{+/+}$*/saline* group (Figure 3-7A). The protein levels of β-catenin were also significantly higher in isolated islets from *c-Kit*$^{Wv/+}$ mice, when treated with 1-AKP for 24 hours, compared to non-treated *c-Kit*$^{+/+}$ and *c-Kit*$^{Wv/+}$ islets (Figure 3-7A). These increases in islet β-catenin corresponded with significantly elevated islet cyclin D1 protein levels in *c-Kit*$^{Wv/+}$*/1-AKP* mice and *c-Kit*$^{Wv/+}$ islets cultured with 1-AKP when compared to *c-Kit*$^{Wv/+}$*/saline* mice and untreated isolated *c-Kit*$^{Wv/+}$ islets, respectively (Figure 3-7B). These findings were further corroborated using qRT-PCR and double immunofluorescence, which revealed a significantly increased *Ccnd1* mRNA (Figure 3-7C) and a higher number of cyclin D1^{+}/insulin^{+} cells in *c-Kit*$^{Wv/+}$*/1-AKP* mice (*vs. c-Kit*$^{Wv/+}$*/saline* group, Figure 3-7D). Quantitative RT-PCR analyses of *Pdx-1 and MafA* showed significantly increased mRNA levels in the islets of both 1-AKP treated *c-Kit*$^{+/+}$and *c-Kit*$^{Wv/+}$ mice (Figure 3-8A). Double immunofluorescence demonstrated a significant increase in the number of Pdx-1^{+} cells in beta-cells of *c-Kit*$^{Wv/+}$*/1-AKP* mice (*vs. c-Kit*$^{Wv/+}$*/saline* group, Figure 3-8B). Increased MafA staining intensity was also observed in *c-Kit*$^{Wv/+}$*/1-AKP* mouse beta-cells (Figure 3-8D). These results were further supported by western blot analysis and showed significantly higher Pdx-1 protein levels in *c-Kit*$^{Wv/+}$ islets from either 1-AKP injected mice or 1-AKP incubation when compared to *c-Kit*$^{Wv/+}$*/saline* mice and *c-Kit*$^{Wv/+}$ islets without 1-AKP treatment, respectively (Figure 3-8C). Furthermore, increased cyclin D1 expression (Figure 3-7B and C and D) was correlated with a significant increase in Ki67

immunoreactivity in beta-cells of *c-Kit$^{Wv/+}$/1-AKP* mice (*vs. c-Kit$^{Wv/+}$/saline* group, Figure 3-9).

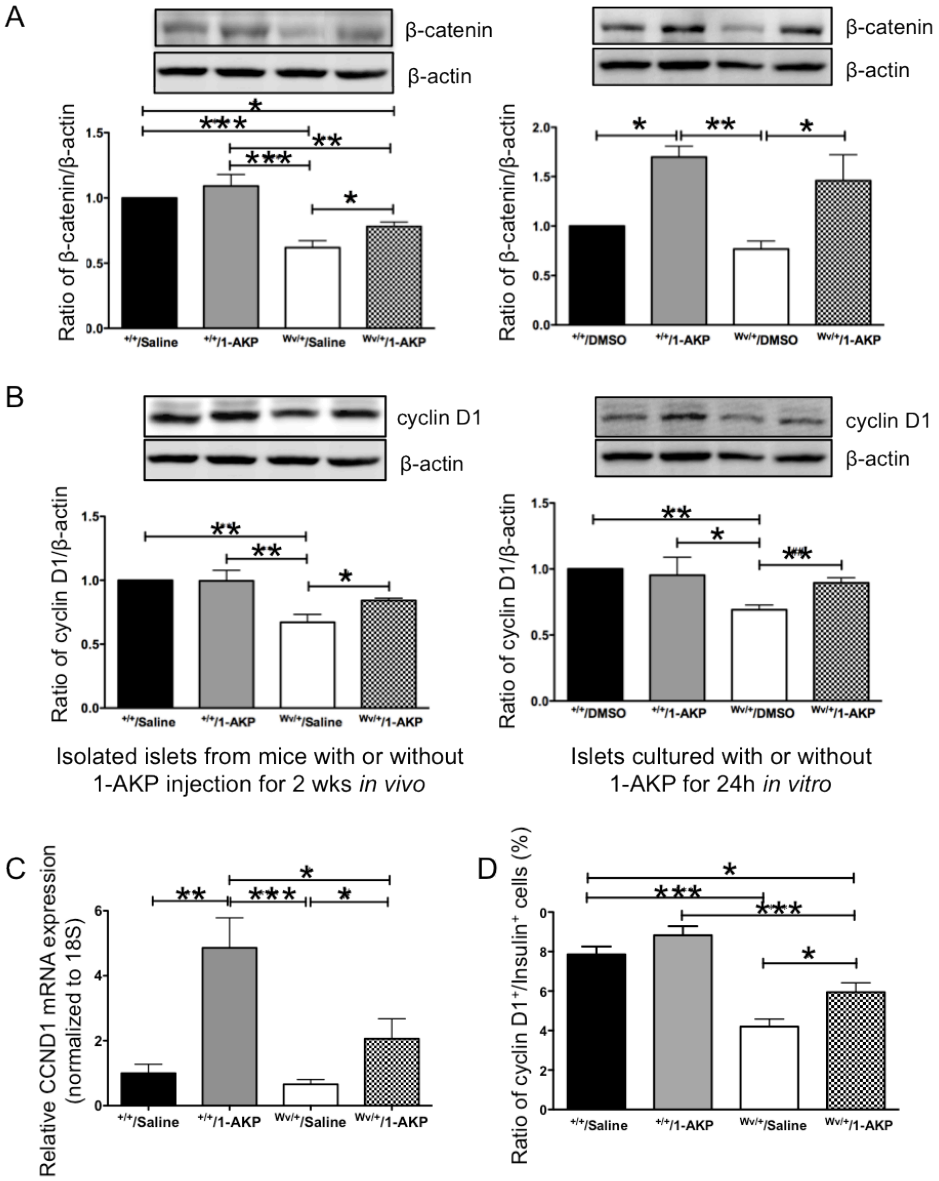
A
β-catenin
β-actin
Ratio of β-catenin/β-actin
+/+/Saline
+/+/1-AKP
Wv/+/Saline
Wv/+/1-AKP
β-catenin
β-actin
Ratio of β-catenin/β-actin
+/+/DMSO
+/+/1-AKP
Wv/+/DMSO
Wv/+/1-AKP
B
cyclin D1
β-actin
Ratio of cyclin D1/β-actin
+/+/Saline
+/+/1-AKP
Wv/+/Saline
Wv/+/1-AKP
cyclin D1
β-actin
Ratio of cyclin D1/β-actin
+/+/DMSO
+/+/1-AKP
Wv/+/DMSO
Wv/+/1-AKP
Isolated islets from mice with or without 1-AKP injection for 2 wks *in vivo*
Islets cultured with or without 1-AKP for 24h *in vitro*
C
Relative CCND1 mRNA expression (normalized to 18S)
+/+/Saline
+/+/1-AKP
Wv/+/Saline
Wv/+/1-AKP
D
Ratio of cyclin D1+/Insulin+ cells (%)
+/+/Saline
+/+/1-AKP
Wv/+/Saline
Wv/+/1-AKP

Figure 3-7. Inhibition of Gsk3β maintains β-catenin and cyclin D1 level in *c-Kit$^{Wv/+}$/1-AKP* mouse islets.

Western blot analyses of β-catenin (**A**) and cyclin D1 (**B**) protein levels in isolated islets from 8-week-old *c-Kit$^{+/+}$/saline*, *c-Kit$^{+/+}$/1-AKP*, *c-Kit$^{Wv/+}$/saline* and *c-Kit$^{Wv/+}$/1-AKP* mice (left column) and isolated islets from 8-week-old *c-Kit$^{+/+}$* and *c-Kit$^{Wv/+}$* mice cultured with or without 1-AKP treatment for 24 hours (right column). Representative blots are shown. Data (**A** and **B**) are normalized to β-actin. qRT-PCR analysis of *Ccnd1* mRNA in isolated islets (**C**) and the number of nuclear cyclin D1^{+} cells in beta-cells (**D**) of *c-Kit$^{+/+}$/saline*, *c-Kit$^{+/+}$/1-AKP*, *c-Kit$^{Wv/+}$/saline*, and *c-Kit$^{Wv/+}$/1-AKP* mice. Data (**A**-**D**) are expressed as mean ± SEM (*n=5–8*), **p*<0.05, ***p*<0.01, ****p*<0.001 analyzed by one-way ANOVA followed by LSD *post-hoc* test.

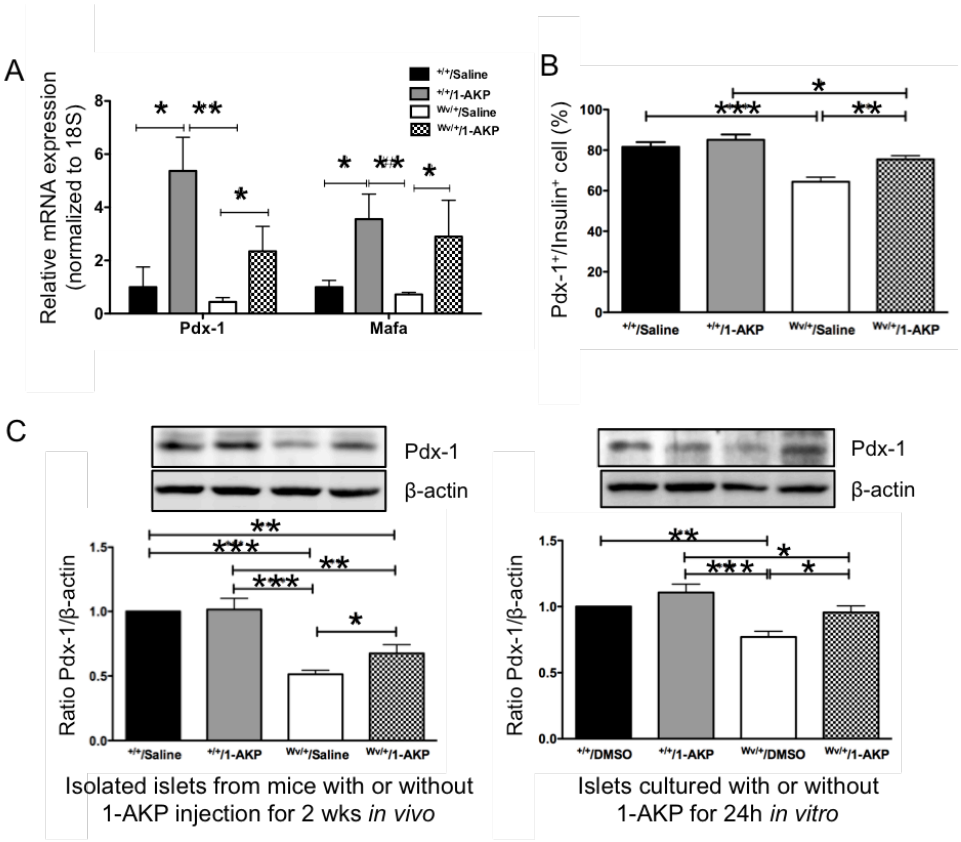
A
Relative mRNA expression (normalized to 18S)
+/+/Saline
+/+/1-AKP
Wv/+/Saline
Wv/+/1-AKP
Pdx-1
Mafa
B
Pdx-1+/Insulin+ cell (%)
+/+/Saline
+/+/1-AKP
Wv/+/Saline
Wv/+/1-AKP
C
Pdx-1
β-actin
Ratio Pdx-1/β-actin
+/+/Saline
+/+/1-AKP
Wv/+/Saline
Wv/+/1-AKP
Isolated islets from mice with or without 1-AKP injection for 2 wks in vivo
+/+/DMSO
Wv/+/DMSO
Islets cultured with or without 1-AKP for 24h in vitro
D
MafA
+/+/Saline
+/+/1-AKP
Wv/+/Saline
Wv/+/1-AKP

Figure 3-8. Inhibition of Gsk3β results in increased Pdx-1 and MafA expression in *c-Kit$^{Wv/+}$/1-AKP* mice.

qRT-PCR analyses of *Pdx-1* and *MafA* mRNA in isolated islets (**A**) and the number of Pdx-1^{+} cells (**B**) in beta-cells of *c-Kit$^{+/+}$/saline*, *c-Kit$^{+/+}$/1-AKP*, *c-Kit$^{Wv/+}$/saline* and *c-Kit$^{Wv/+}$/1-AKP* mice. (**C**) Western blot analysis of Pdx-1 protein levels in isolated islets from 8-week-old *c-Kit$^{+/+}$/saline*, *c-Kit$^{+/+}$/1-AKP*, *c-Kit$^{Wv/+}$/saline* and *c-Kit$^{Wv/+}$/1-AKP* mice (left column) and isolated islets from 8-week-old *c-Kit$^{+/+}$* and *c-Kit$^{Wv/+}$* mice cultured with or without 1-AKP treatment for 24 hours (right column). (**D**) An increased MafA staining intensity was observed in the islet of *c-Kit$^{Wv/+}$/1-AKP* mice when compared to *c-Kit$^{Wv/+}$/saline* treated mice. No counterstaining was applied and nuclei are white transparent. Scale bar 25 μm. Data (**A**-**C**) are expressed mean ± SEM (n=5–8) *p<0.05, **p<0.01, ***p<0.001 analyzed by one-way ANOVA followed by LSD *post-hoc* test.

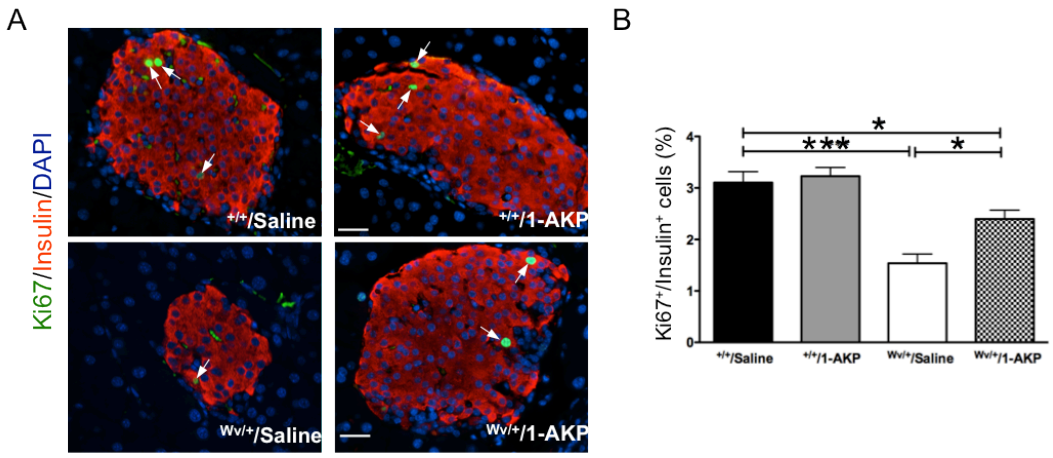
A
Ki67/Insulin/DAPI
+/+/Saline
+/+/1-AKP
Wv/+/Saline
Wv/+/1-AKP
B
Ki67+/Insulin+ cells (%)
0
1
2
3
4
*
***
*
+/+/Saline
+/+/1-AKP
Wv/+/Saline
Wv/+/1-AKP

Figure 3-9. Inhibition of Gsk3β results in increased beta-cell proliferation in *c-Kit$^{Wv/+}$/1-AKP* mice.

(**A**) Double immunofluorescence staining of Ki67 (green) with insulin (red) and nuclear stained with DAPI (blue). Arrows indicate Ki67/insulin double-positive cells. Scale bar 20 μm. (**B**) Percentage of Ki67^{+} cells in beta-cells of *c-Kit$^{+/+}$/saline*, *c-Kit$^{+/+}$/1-AKP*, *c-Kit$^{Wv/+}$/saline* and *c-Kit$^{Wv/+}$/1-AKP* mice. Data are expressed mean ± SEM (*n=5–8*) **p*<0.05, ***p*<0.01, ****p*<0.001 analyzed by one-way ANOVA followed by LSD *post-hoc* test.

A

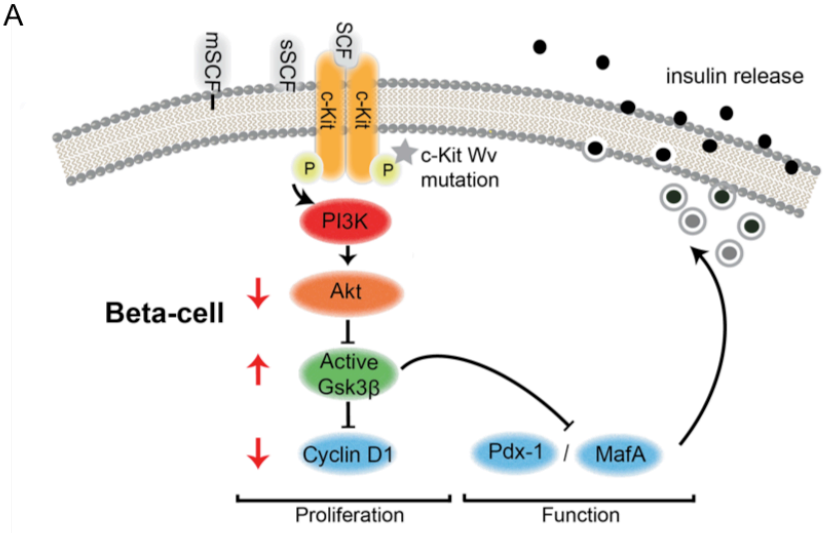
mSCF
sSCF
SCF
c-Kit
c-Kit
P
P
c-Kit Wv
mutation
insulin release
PI3K
Akt
Beta-cell
Active
Gsk3β
Cyclin D1
Pdx-1
/
MafA
Proliferation
Function

B

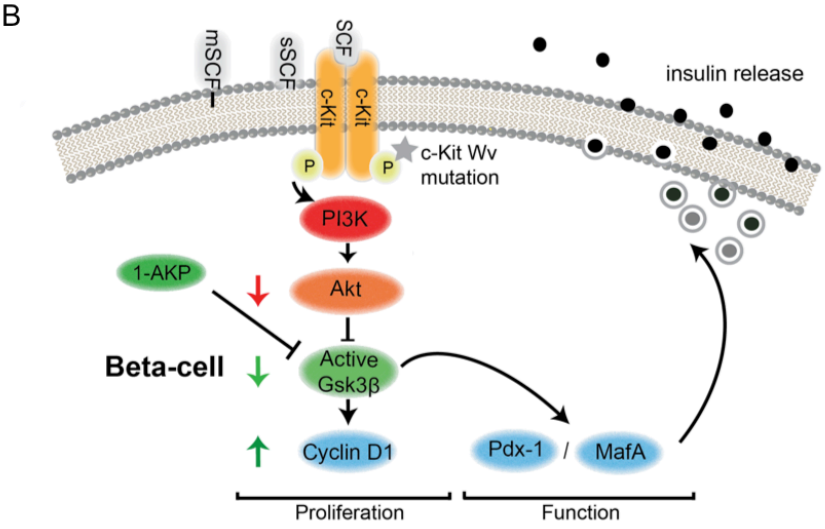
mSCF
sSCF
SCF
c-Kit
c-Kit
P
P
c-Kit Wv
mutation
insulin release
PI3K
1-AKP
Akt
Beta-cell
Active
Gsk3β
Cyclin D1
Pdx-1
/
MafA
Proliferation
Function

Figure 3-10. A proposed model involving c-Kit/Akt/Gsk3β signaling pathways in beta-cell survival and function in *c-Kit*$^{Wv/+}$ mice.

(**A**) Mutating the c-Kit receptor (grey star) at the W^v locus lead to a down-regulation of the PI3K/Akt pathway via reduced phosphorylation of Akt at S473, which resulted in enhanced active Gsk3 β and increased inhibition of Pdx-1 and cyclin D1 expression. (**B**) Direct inhibition of active Gsk3 β with 1-AKP preserved β-catenin protein levels, along with maintained cyclin D1 and Pdx-1 expression that allowed improvement of beta-cell proliferation and function and prevented the onset of diabetes in *c-Kit*$^{Wv/+}$ mice. sSCF: soluble Stem Cell Factor; mSCF: membrane-bound Stem Cell Factor. Green arrow: positive signaling; red arrow: negative signaling.

3.4 Discussion

The present study demonstrates that diabetic *c-Kit*$^{Wv/+}$ mice displayed reduced levels of phospho-Akt at residue S473 and phospho-Gsk3β at residue S9 in both pancreatic and isolated islet protein extracts. These mice also possess decreased cyclin D1 expression in their beta-cells. When treated with 1-AKP, *c-Kit*$^{Wv/+}$ mice demonstrated significant improvements in fasting glucose, glucose tolerance and insulin secretion along with increased beta-cell mass and proliferation. These results indicate that the Akt/Gsk3β pathway downstream of c-Kit is predominantly involved in regulating beta-cell proliferation and function in *c-Kit*$^{Wv/+}$ mice and that inhibition of Gsk3β activation can significantly improve glucose tolerance and beta-cell function (Figure 3-10).

The PI3K pathway is one of the major downstream pathways of c-Kit that triggers a variety of pro-survival signaling events, such as cell survival, cell growth, and cell cycle entry via Akt phosphorylation [14, 26]. Akt, a serine/threonine protein kinase, exerts its effects after being phosphorylated by PI3K at two regulatory residues: T308 in the activation segment, and S473 in the hydrophobic motif of the kinase domain [27]. In this study, we showed decreased protein levels of phospho-Akt at S473, but not at T308 in *c-Kit*$^{Wv/+}$ mice when compared to controls. *c-Kit*$^{Wv/+}$ mice are heterozygous for the *c-Kit W*^{v} mutation caused by substitution of a threonine to methionine at amino acid 660 in the kinase domains of the c-Kit gene [28], and this loss-of-function mutation leads to down-regulation, but not abolition of c-Kit activity. Previous research has demonstrated that Akt monophosphorylation on T308 showed only 10% kinase activity compared to 100% when Akt was doubly phosphorylated on S473 and T308 [27], suggesting that S473 phosphorylation is required for maximal kinase activity of Akt [27]. Therefore, our results demonstrate that *c-Kit*$^{Wv/+}$ mice showed significant down-regulation of the primary Akt phosphorylation site required conferring maximal activity, S473.

It is well documented that Gsk3β is the target of many important signaling molecules [29]. In particular, Akt blocks the catalytic activity of the kinase, and activates downstream signals repressed by active Gsk3β [26]. In this study, we observed reduced Gsk3β phosphorylation and cyclin D1 protein levels in islets of *c-Kit*$^{Wv/+}$ mice, which is

consistent with the role of cyclin D1 as essential for postnatal beta-cell growth [30]. Active Gsk3β promotes destabilization of cyclin D1 and thus cell cycle arrest, which is associated with Akt inactivation [31]. Taken together, our results suggest that Akt/Gsk3β axis dysregulation from the *c-Kit* W^v mutation contributed to loss of beta-cell mass and function, which may have been responsible for the early onset of diabetes observed in *c-Kit*$^{Wv/+}$ mice reported previously [6].

It has been previously shown that Gsk3β is involved in differentiation and proliferation of numerous tissue types including beta-cells [21, 22]. Tanabe *et al.* showed that genetic ablation of *Gsk3β* in *Irs*$^{-/-}$ mice preserved beta-cell function and prevented the onset of diabetes [32]. Moreover, mice with beta-cell-specific ablation of *Gsk3β* were resistant to HFD-induced diabetes [22]. These studies suggest that endogenous Gsk3β activity is involved in a highly specialized feedback inhibition mechanism with the insulin receptor, which primarily signals via the PI3K/Akt pathway. In this study, *c-Kit*$^{Wv/+}$ mice received treatment of a Gsk3β inhibitor for 2 weeks and showed significant improvements in glucose tolerance and beta-cell function when compared to saline-treated *c-Kit*$^{Wv/+}$ controls, which showed diabetic symptoms. In addition, no significant differences in insulin tolerance were observed between the experimental groups suggesting that this improvement in glucose tolerance and beta-cell function was not due to enhanced peripheral insulin sensitivity, but primarily to improved beta-cell proliferation and function in *c-Kit*$^{Wv/+}$ mice received 1-AKP treatment.

Our morphological analyses revealed that improved glucose tolerance and insulin secretion was associated with preservation of beta-cell mass and an increase in islet number in *c-Kit*$^{Wv/+}$*/1-AKP* mice. The most notable change was a significant increase in the percentage of small islets (<500 μm^2), with a relative increase in the number of large islets (>10000 μm^2), suggesting that inhibition of Gsk3β activity is associated with an increase in beta-cell neogenesis and proliferation. β-catenin and cyclin D1 are two potential targets of Gsk3β, and have been implicated in beta-cell growth [30, 33]. Preserved beta-cell mass in *c-Kit*$^{Wv/+}$*/1-AKP* group was accompanied by increased beta-cell proliferation (Ki67), and maintained β-catenin and cyclin D1 protein levels, which closely matched those in *c-Kit*$^{+/+}$ group. This is in agreement with the role of β-catenin in

up-regulating cyclin D1 expression to promote beta-cell expansion [33, 34]. These results suggest that Akt/Gsk3β axis-mediated β-catenin activation in islets may regulate beta-cell growth and function in *c-Kit*$^{Wv/+}$ mice [1-8, 35].

The critically important pancreatic transcription factor, Pdx-1 has been shown to regulate beta-cell survival, function and pancreatic development [9-12, 36, 37]. Previous studies have also demonstrated that reduction of Pdx-1 impairs islet insulin secretion [13, 38, 39], while, a partial reduction in Pdx-1 has a major effect on beta-cell survival with reductions in Bcl_{XL} and Bcl2 expression [14, 37, 40]. Using *c-Kit*$^{Wv/+}$ mice, we observed a significant reduction in Pdx-1 expression (~50% of *c-Kit*$^{+/+}$ controls) along with impaired beta-cell function [6], and an up-regulation in the Fas associated cell death pathway (see Chapter 4). In this study, *Pdx-1* mRNA and protein levels were maintained upon Gsk3β inhibition. Previous studies in isolated mouse islets have shown that Pdx-1 is negatively regulated in a Gsk3β-dependent manner [16-18, 41]. In addition, inhibition of Gsk3β by activated Akt could ameliorate Pdx-1 phosphorylation leading to a consequential delay of its degradation, which suggests that Pdx-1 accumulation in beta-cells may be regulated by the Akt/Gsk3β axis [19, 42]. Further *in vivo* studies have demonstrated that Gsk3β ablation in mouse beta-cells lead to increased Pdx-1 protein levels [19, 22, 32]. In addition, a significant up-regulation of *MafA* mRNA expression in *c-Kit*$^{Wv/+}$*/1-AKP* mouse islets was observed. Overexpression of *MafA* in neonatal rat beta-cells led to enhanced glucose-responsive insulin secretion and beta-cell maturation [19, 43]. Taken together, the findings of the present study showed that Akt/Gsk3β signaling, downstream of c-Kit, is not only required for beta-cell proliferation. By modulating Pdx-1 and MafA expression, this signalling pathway is likely essential for beta-cell function and differentiation.

This study demonstrates that the Gsk3β inhibitor, 1-AKP, predominantly improved beta-cell proliferation and function, and had no significant effects in peripheral tissues, like muscle or liver insulin sensitivity. However, previous studies have shown that treatment of Gsk3β inhibitors improved glucose homeostasis by ameliorating muscle and liver insulin resistance in non-insulin dependent obese animal models [20, 44-46]. The *c-Kit* *W*^{v} point mutation primarily causes defect in melanocytic, hematopoietic, and endocrine

cell lineages, with no apparent muscle and liver dysfunction [6, 21, 28, 47]. This is in contrast to non-insulin dependent diabetic animal models, such as ZDF rat and ob mice that have primary defects in muscle and liver insulin stimulated peripheral glucose transport activity [22, 44-46]. Thus, we speculate that the effect of Gsk3β inhibition is highly tissue-specific depends on functional defects in specific cell types among different mouse models.

In summary, this study elucidates a novel link between c-Kit and the Akt/Gsk3β/cyclin D1 signaling pathways and their effects on beta-cell proliferation and function *in vivo*. Our results suggest that dysregulated Akt/Gsk3β/cyclin D1 downstream from the *c-Kit* W^{v} mutation is the possible signaling mechanism that contributes to the loss of beta-cell mass and function in *c-Kit*$^{Wv/+}$ mice reported in our previous publication [6]. Furthermore, chronic inhibition of Gsk3β in *c-Kit*$^{Wv/+}$ mice resulted in increased β-catenin, cyclin D1, and Pdx-1 protein levels, suggesting that regulation of downstream signaling increased beta-cell proliferative capacity, mass, as well as later improved glucose tolerance, and helped prevent early onset of diabetes. Taken together, the findings of present study emphasizes that understanding the complex intracellular pathways that affect beta-cell proliferation and function *in vivo,* which c-Kit regulates, will enable the development of more successful treatment protocols for diabetes.

3.5 References

1. Oberg-Welsh C, Welsh M (1996) Effects of certain growth factors on in vitro maturation of rat fetal islet-like structures. Pancreas 12:334–339.

2. LeBras S, Czernichow P, Scharfmann R (1998) A search for tyrosine kinase receptors expressed in the rat embryonic pancreas. Diabetologia 41:1474–1481. doi: 10.1007/s001250051094

3. Rachdi L, Ghazi El L, Bernex F, et al. (2001) Expression of the receptor tyrosine kinase KIT in mature beta-cells and in the pancreas in development. Diabetes 50:2021–2028.

4. Yashpal NK, Li J, Wang R (2004) Characterization of c-Kit and nestin expression during islet cell development in the prenatal and postnatal rat pancreas. Dev Dyn 229:813–825. doi: 10.1002/dvdy.10496

5. Wang R, Li J, Yashpal N (2004) Phenotypic analysis of c-Kit expression in epithelial monolayers derived from postnatal rat pancreatic islets. J Endocrinol 182:113–122.

6. Krishnamurthy M, Ayazi F, Li J, et al. (2007) c-Kit in early onset of diabetes: a morphological and functional analysis of pancreatic beta-cells in c-KitW-v mutant mice. Endocrinology 148:5520–5530. doi: 10.1210/en.2007-0387

7. Peters K, Panienka R, Li J, et al. (2005) Expression of stem cell markers and transcription factors during the remodeling of the rat pancreas after duct ligation. Virchows Arch 446:56–63. doi: 10.1007/s00428-004-1145-7

8. Tiemann K, Panienka R, Klöppel G (2007) Expression of transcription factors and precursor cell markers during regeneration of beta cells in pancreata of rats treated with streptozotocin. Virchows Arch 450:261–266. doi: 10.1007/s00428-006-0349-4

9. Blume-Jensen P, Janknecht R, Hunter T (1998) The kit receptor promotes cell survival via activation of PI 3-kinase and subsequent Akt-mediated phosphorylation of Bad on Ser136. Curr Biol 8:779–782.

10. Timokhina I, Kissel H, Stella G, Besmer P (1998) Kit signaling through PI 3-kinase and Src kinase pathways: an essential role for Rac1 and JNK activation in mast cell proliferation. EMBO J 17:6250–6262. doi: 10.1093/emboj/17.21.6250

11. Linnekin D (1999) Early signaling pathways activated by c-Kit in hematopoietic cells. Int J Biochem Cell Biol 31:1053–1074.

12. van Dijk TB, van Den Akker E, Amelsvoort MP, et al. (2000) Stem cell factor induces phosphatidylinositol 3'-kinase-dependent Lyn/Tec/Dok-1 complex formation in hematopoietic cells. Blood 96:3406–3413.

13. Rafiq I, da Silva Xavier G, Hooper S, Rutter GA (2000) Glucose-stimulated preproinsulin gene expression and nuclear trans-location of pancreatic duodenum homeobox-1 require activation of phosphatidylinositol 3-kinase but not p38 MAPK/SAPK2. J Biol Chem 275:15977–15984.

14. Li J, Goodyer CG, Fellows F, Wang R (2006) Stem cell factor/c-Kit interactions regulate human islet-epithelial cluster proliferation and differentiation. Int J Biochem Cell Biol 38:961–972. doi: 10.1016/j.biocel.2005.08.014

15. Li J, Quirt J, Do HQ, et al. (2007) Expression of c-Kit receptor tyrosine kinase and effect on beta-cell development in the human fetal pancreas. Am J Physiol Endocrinol Metab 293:E475–83. doi: 10.1152/ajpendo.00172.2007

16. Cross DA, Alessi DR, Cohen P, et al. (1995) Inhibition of glycogen synthase kinase-3 by insulin mediated by protein kinase B. Nature 378:785–789. doi: 10.1038/378785a0

17. Hajduch E, Litherland GJ, Hundal HS (2001) Protein kinase B (PKB/Akt)--a key regulator of glucose transport? FEBS Lett 492:199–203.

18. Roberts MS, Woods AJ, Dale TC, et al. (2004) Protein kinase B/Akt acts via glycogen synthase kinase 3 to regulate recycling of alpha v beta 3 and alpha 5 beta 1 integrins. Mol Cell Biol 24:1505–1515.

19. Jope RS, Johnson GVW (2004) The glamour and gloom of glycogen synthase kinase-3. Trends Biochem Sci 29:95–102. doi: 10.1016/j.tibs.2003.12.004

20. Liu Z, Tanabe K, Bernal-Mizrachi E, Permutt MA (2008) Mice with beta cell overexpression of glycogen synthase kinase-3beta have reduced beta cell mass and proliferation. Diabetologia 51:623–631. doi: 10.1007/s00125-007-0914-7

21. Liu H, Remedi MS, Pappan KL, et al. (2009) Glycogen synthase kinase-3 and mammalian target of rapamycin pathways contribute to DNA synthesis, cell cycle progression, and proliferation in human islets. Diabetes 58:663–672. doi: 10.2337/db07-1208

22. Liu Y, Tanabe K, Baronnier D, et al. (2010) Conditional ablation of Gsk-3β in islet beta cells results in expanded mass and resistance to fat feeding-induced diabetes in mice. Diabetologia 53:2600–2610. doi: 10.1007/s00125-010-1882-x

23. Kunick C, Lauenroth K, Leost M, et al. (2004) 1-Azakenpaullone is a selective inhibitor of glycogen synthase kinase-3 beta. Bioorg Med Chem Lett 14:413–416.

24. Mao Y, Ge X, Frank CL, et al. (2009) Disrupted in schizophrenia 1 regulates neuronal progenitor proliferation via modulation of GSK3beta/beta-catenin signaling. Cell 136:1017–1031. doi: 10.1016/j.cell.2008.12.044

25. Le Bacquer O, Shu L, Marchand M, et al. (2011) TCF7L2 splice variants have distinct effects on beta-cell turnover and function. Hum Mol Genet 20:1906–1915. doi: 10.1093/hmg/ddr072

26. Cantley LC (2002) The phosphoinositide 3-kinase pathway. Science 296:1655–1657. doi: 10.1126/science.296.5573.1655

27. Yang J, Cron P, Good VM, et al. (2002) Crystal structure of an activated Akt/protein kinase B ternary complex with GSK3-peptide and AMP-PNP. Nat Struct Biol 9:940–944. doi: 10.1038/nsb870

28. Nocka K, Tan JC, Chiu E, et al. (1990) Molecular bases of dominant negative and loss of function mutations at the murine c-kit/white spotting locus: W37, Wv, W41 and W. EMBO J 9:1805–1813.

29. Doble BW, Woodgett JR (2003) GSK-3: tricks of the trade for a multi-tasking kinase. J Cell Sci 116:1175–1186.

30. Kushner JA, Ciemerych MA, Sicinska E, et al. (2005) Cyclins D2 and D1 are essential for postnatal pancreatic beta-cell growth. Mol Cell Biol 25:3752–3762. doi: 10.1128/MCB.25.9.3752-3762.2005

31. Mukherji A, Janbandhu VC, Kumar V (2008) GSK-3beta-dependent destabilization of cyclin D1 mediates replicational stress-induced arrest of cell cycle. FEBS Lett 582:1111–1116. doi: 10.1016/j.febslet.2008.02.068

32. Tanabe K, Liu Z, Patel S, et al. (2008) Genetic deficiency of glycogen synthase kinase-3beta corrects diabetes in mouse models of insulin resistance. PLoS Biol 6:e37. doi: 10.1371/journal.pbio.0060037

33. Rulifson IC, Karnik SK, Heiser PW, et al. (2007) Wnt signaling regulates pancreatic beta cell proliferation. Proc Natl Acad Sci USA 104:6247–6252. doi: 10.1073/pnas.0701509104

34. Figeac F, Uzan B, Faro M, et al. (2010) Neonatal growth and regeneration of beta-cells are regulated by the Wnt/beta-catenin signaling in normal and diabetic rats. Am J Physiol Endocrinol Metab 298:E245–56. doi: 10.1152/ajpendo.00538.2009

35. Lee G, Goretsky T, Managlia E, et al. (2010) Phosphoinositide 3-kinase signaling mediates beta-catenin activation in intestinal epithelial stem and progenitor cells in colitis. Gastroenterology 139:869–81– 881.e1–9. doi: 10.1053/j.gastro.2010.05.037

36. Offield MF, Jetton TL, Labosky PA, et al. (1996) PDX-1 is required for pancreatic outgrowth and differentiation of the rostral duodenum. Development 122:983–995.

37. Johnson JD, Ahmed NT, Luciani DS, et al. (2003) Increased islet apoptosis in Pdx1+/- mice. J Clin Invest 111:1147–1160. doi: 10.1172/JCI16537

38. Brissova M, Shiota M, Nicholson WE, et al. (2002) Reduction in pancreatic transcription factor PDX-1 impairs glucose-stimulated insulin secretion. J Biol Chem 277:11225–11232. doi: 10.1074/jbc.M111272200

39. Gauthier BR, Wiederkehr A, Baquié M, et al. (2009) PDX1 deficiency causes mitochondrial dysfunction and defective insulin secretion through TFAM suppression. Cell Metab 10:110–118. doi: 10.1016/j.cmet.2009.07.002

40. Li T-S, Hamano K, Nishida M, et al. (2003) CD117+ stem cells play a key role in therapeutic angiogenesis induced by bone marrow cell implantation. Am J Physiol Heart Circ Physiol 285:H931–7. doi: 10.1152/ajpheart.01146.2002

41. Boucher M-J, Selander L, Carlsson L, Edlund H (2006) Phosphorylation marks IPF1/PDX1 protein for degradation by glycogen synthase kinase 3-dependent mechanisms. J Biol Chem 281:6395–6403. doi: 10.1074/jbc.M511597200

42. Humphrey RK, Yu S-M, Flores LE, Jhala US (2010) Glucose regulates steady-state levels of PDX1 via the reciprocal actions of GSK3 and AKT kinases. J Biol Chem 285:3406–3416. doi: 10.1074/jbc.M109.006734

43. Aguayo-Mazzucato C, Koh A, Khattabi El I, et al. (2011) Mafa expression enhances glucose-responsive insulin secretion in neonatal rat beta cells. Diabetologia 54:583–593. doi: 10.1007/s00125-010-2026-z

44. Henriksen EJ, Kinnick TR, Teachey MK, et al. (2003) Modulation of muscle insulin resistance by selective inhibition of GSK-3 in Zucker diabetic fatty rats. Am J Physiol Endocrinol Metab 284:E892–900. doi: 10.1152/ajpendo.00346.2002

45. Cline GW, Johnson K, Regittnig W, et al. (2002) Effects of a novel glycogen synthase kinase-3 inhibitor on insulin-stimulated glucose metabolism in Zucker diabetic fatty (fa/fa) rats. Diabetes 51:2903–2910.

46. Kaidanovich-Beilin O, Eldar-Finkelman H (2006) Long-term treatment with novel glycogen synthase kinase-3 inhibitor improves glucose homeostasis in ob/ob mice: molecular characterization in liver and muscle. J Pharmacol Exp Ther 316:17–24. doi: 10.1124/jpet.105.090266

47. Reith AD, Rottapel R, Giddens E, et al. (1990) W mutant mice with mild or severe developmental defects contain distinct point mutations in the kinase domain of the c-kit receptor. Genes Dev 4:390–400.

Chapter 4

4 Down-regulation of Fas activity rescues early onset of diabetes in *c-Kit*$^{Wv/+}$ mice[3]

[3] This chapter has been modified and adapted from the following manuscript:

- **Feng ZC**, Riopel M, Li J, Donnelly L, Wang R. **(**2013) Improved beta-cell proliferation and function in *c-Kit*$^{Wv/+}$*;Fas*$^{lpr/lpr}$ double mutant mice. *Am J Physiol Endocrinol Metab.* 304:E557-E565.

4.1 Introduction

The prevalence of diabetes has been increasing at an alarming rate. During the progression of diabetes, pancreatic beta-cells are often lost because the delicate balance between beta-cell proliferation and death is disrupted [1-4]. Our previous studies showed that *c-Kit*$^{Wv/+}$ mice, which contain a point mutation in the kinase region (*W*^{v}) of c-Kit, exhibit severe beta-cell mass loss that was associated with a significant down-regulation of the PI3K/Gsk3β/cyclin D1 signaling [5, 6] and this affects beta-cell proliferation. However, the underlying mechanisms involved in c-Kit-mediated effects on beta-cell apoptosis have yet to be determined in *c-Kit*$^{Wv/+}$ mice.

Fas belongs to the tumor necrosis factor family and requires the FasL for activation. Fas/FasL interactions result in activation of Fas-associated death domains and cleavage of caspase 8, which triggers apoptotic pathway. In diabetes, beta-cells constitutively express Fas [7-11]. Fas/FasL interactions were suggested to be one of the major mechanisms leading to beta-cell apoptosis in T cell-mediated autoimmune diabetes [12-14]. In addition, cytokine-induced up-regulation of the Fas apoptotic pathway is also involved in glucotoxicity and subsequent increases in beta-cell death [15]; meanwhile, deletion of *FAS* protects human islet amyloid polypeptide deposition-mediated beta-cell apoptosis [16]. *In vivo* studies have demonstrated that non-obese diabetic mice with non-functional *Fas* (global *lpr/lpr* mutation) show protection against diabetes [13, 14], and transgenic mice with beta-cell specific knockout of *Fas* exhibit increased beta-cell insulin secretion function [2].

There have been numerous studies in hematopoietic cells, melanocytes and germ cells indicating that Fas-mediated cell apoptosis can be prevented by up-regulation of SCF/c-Kit interactions [17, 18]. Conversely, in cells with deficient c-Kit signaling, down-regulation of Fas can rescue cell death and dysfunction [19-23]. In this study, we generated *c-Kit*$^{Wv/+}$*;Fas*$^{lpr/lpr}$ (*Wv;-/-*) double mutant mice to understand the inter-relationship between c-Kit and Fas with respect to beta-cell survival and function.

4.2 Materials and methods

Mouse model: In this study, two mouse models were used: 1) *c-Kit*$^{Wv/+}$ mice (see detail in section 2.1.1, and same mouse model used in Chapter 3), and 2) *c-Kit*$^{Wv/+}$*;Fas*$^{lpr/lpr}$ double mutant mice (see detail in section 2.1.2). *c-Kit*$^{Wv/+}$, *c-Kit*$^{Wv/+}$*;Fas*$^{+/+}$(*Wv;+/+*), and *c-Kit*$^{Wv/+}$*;Fas*$^{lpr/lpr}$(*Wv;-/-*) mice were the experimental groups, while *c-Kit*$^{+/+}$ and *c-Kit*$^{+/+}$*;Fas*$^{+/+}$(*WT*) were designated as the control groups. Genotyping was detailed in section 2.2. Mice were kept until 8 weeks of age with normal diet at which point, metabolic studies, islet morphological studies, and islet qRT-PCR, islet protein analyses were performed. Only male mice were used for this study.

Metabolic studies: Body weight, fasting (4-hour) blood glucose levels, IPGTT and IPITT analyses were performed on *Wv;-/-* mice and compared to *WT* and *Wv;+/+* littermates at 8 weeks of age, as detailed in section 2.3.

In vivo, ex vivo GSIS studies, and insulin ELISA analyses: in vivo GSIS, and *ex vivo* GSIS on isolated islets, were performed from *WT*, *Wv;+/+* and *Wv;-/-* mice at 8 weeks of age, as detailed in sections 2.4 and 2.5.

INS-1 cell culture studies: To study the inter-balance relationship between c-Kit and Fas signaling on cell apoptosis, INS-1 cells were treated with SCF for 24 hours, or cultured for 48 hours with control siRNA, *c-Kit* siRNA with or without PFT-α (p53 inhibitor), or combined *c-Kit* siRNA and *Fas* siRNA, as detailed in section 2.6.2.

Immunofluorescence and morphometric analyses: Pancreatic tissue sections from mice at 8 weeks of age were prepared and double-stained with appropriate antibodies listed in Appendix 5. Islet number, islet size, alpha and beta-cell mass were measured. Cell proliferation (Ki67$^+$ labeling), and apoptosis (TUNEL$^+$ labeling), Fas positive staining in beta-cell nuclei was quantified, and the average percent of Ki67$^+$/insulin$^+$, TUNEL$^+$/insulin$^+$, and Fas$^+$/insulin$^+$ cells was calculated, as detailed in section 2.7.

Protein extraction and western blot analyses: protein levels of Fas, FasL, c-Kit, cleaved caspase 3^{D175}, total caspase 3, cleaved caspase 8^{D391}, total caspase 8, p53, and corresponding housekeeping proteins including calnexin and β-actin in isolated islets

from mice at 8 weeks of age or in INS-1 cells were analyzed (Appendix 6), as detailed in section 2.8.

RNA extraction and real-time RT-PCR analyses: RNA was extracted from isolated islets of *WT*, *Wv;+/+*, *Wv;-/-* mice at 8 weeks of age. mRNA expression of *Bax*, *Bcl2*, *Cflar* (c-Flip), *Kit* (c-Kit), *Fas*, *FasL*, *Glucagon*, *Insulin*, *MafA*, *NFkb1* (Nfκb1), *NFkb2* (Nfκb2), *Pdx-1*, *RelA*, *RelB*, *Trp53* (p53) was measured and normalized to *18S* rRNA (Appendix 7), as detailed in section 2.9.

4.3 Results

4.3.1 *c-Kit*$^{Wv/+}$ mice show increased beta-cell apoptosis due to increased p53 signaling and resulting up-regulated Fas activity

c-Kit$^{Wv/+}$ mice had severe beta-cell loss and dysfunction, which was associated with Akt/Gsk3β/cyclin D1 pathway down-regulation[6]. Significantly elevated *p53* mRNA expression and protein levels were observed in the islets of *c-Kit*$^{Wv/+}$ mice when compared to *c-Kit*$^{+/+}$ mice (Figure 4-1A). *Fas* mRNA expression was significantly elevated in *c-Kit*$^{Wv/+}$ islets (Figure 4-1B), which was corroborated with increased Fas protein levels (Figure 4-1B) and Fas-expressing insulin positive cells (Figure 4-1D) relative to *c-Kit*$^{+/+}$ group. However, there was no significant alteration of FasL among all groups (Figure 4-1C). A significant increase in beta-cell apoptosis, as indicated by elevated TUNEL staining in insulin-positive cells, was observed in *c-Kit*$^{Wv/+}$ mice (Figure 4-1E).

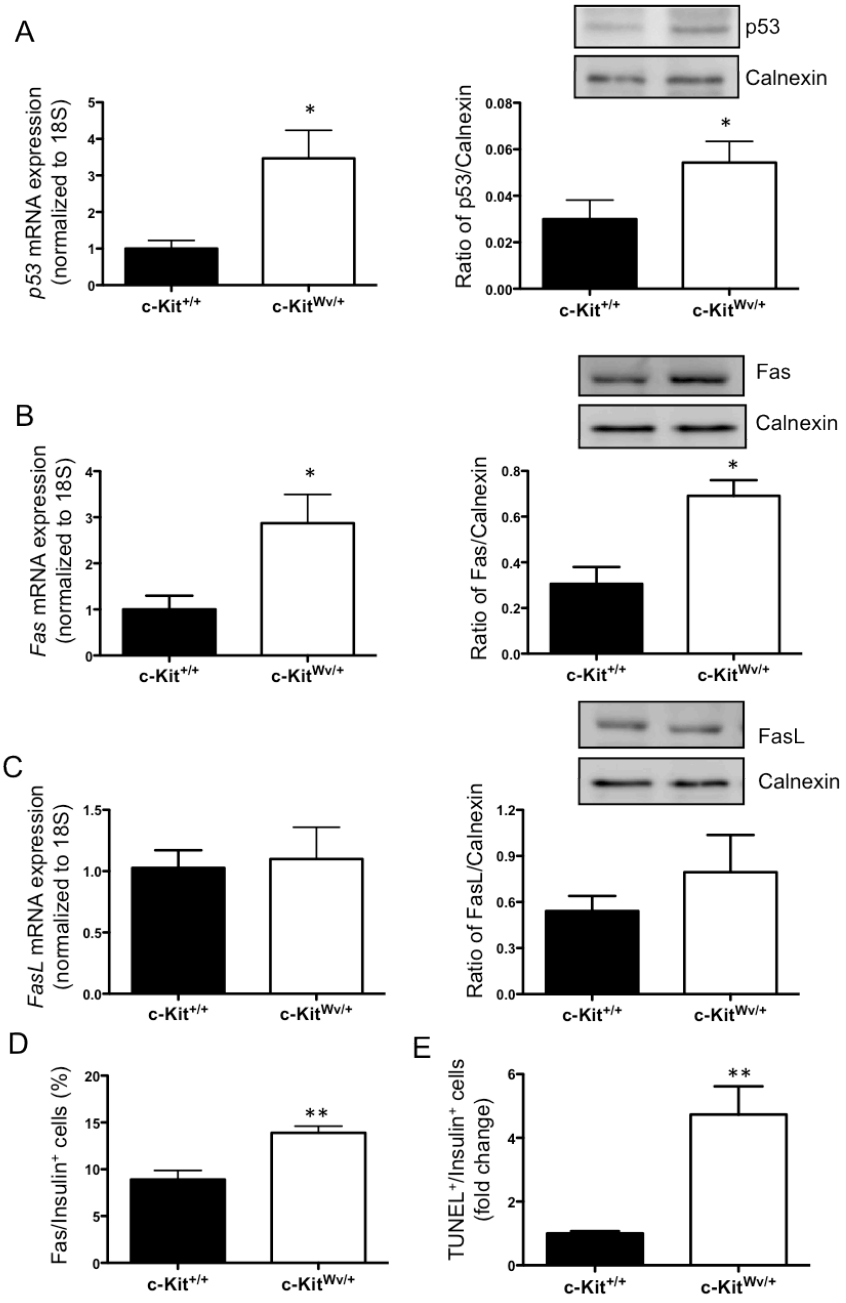
A
p53 mRNA expression (normalized to 18S)
c-Kit+/+
c-KitWv/+
p53
Calnexin
Ratio of p53/Calnexin
B
Fas mRNA expression (normalized to 18S)
Fas
Calnexin
Ratio of Fas/Calnexin
C
FasL mRNA expression (normalized to 18S)
FasL
Calnexin
Ratio of FasL/Calnexin
D
Fas/Insulin+ cells (%)
E
TUNEL+/Insulin+ cells (fold change)

Figure 4-1. Up-regulation of p53 and Fas signaling in isolated islets from *c-Kit*$^{Wv/+}$ mice.

qRT-PCR and western blot analyses of p53 (**A**), Fas (**B**), and FasL levels (**C**) in isolated islets of *c-Kit*$^{+/+}$ and *c-Kit*$^{Wv/+}$ mice at 8 weeks of age. Representative blots are shown. Data are normalized to loading control (calnexin). Percentage of Fas^{+} (**D**) and TUNEL^{+} (**E**) beta-cells in *c-Kit*$^{+/+}$ and *c-Kit*$^{Wv/+}$ mice at 8 weeks of age. Data (**A-E**) are expressed as mean ± SEM (*n=3-10*), **p*<0.05, ***p*<0.01 analyzed by unpaired student's *t*-test.

In vitro studies on INS-1 cells were used to further understand the relationship between c-Kit, p53, and Fas in the regulation of beta-cell survival. The expression of *c-Kit* and *Fas* mRNA in INS-1 cells was measured by qRT-PCR and showed relatively higher *c-Kit* and lower *Fas* expression in INS-1 cells when compared to normal mouse islets (Figure 4-2A). INS-1 cells treated with exogenous SCF showed a slight reduction in p53 and a significant decrease in Fas protein levels, which was attenuated by the addition of a PI3K inhibitor, wortmannin (Figure 4-2B). However, when INS-1 cells were transfected with *c-Kit* siRNA, the protein levels of p53, Fas and cleaved caspase 3 was significantly elevated compared to the controls (Figure 4-3). Interestingly, cells transfected with *c-Kit* siRNA and treated with PFT-α (p53 inhibitor) or co-transfected with *Fas* siRNA displayed significantly abated protein levels of p53, Fas and cleaved caspase 3 when compared to *c-Kit* siRNA-transfected INS-1 cells (Figure 4-3). Fas protein levels were significantly reduced in the *Fas* siRNA group when compared to the control siRNA group (Figure 4-4A). Furthermore, INS-1 cell apoptosis was measured by TUNEL staining, which demonstrated a significant increase in the *c-Kit* siRNA group as compared to other experimental conditions (Figure 4-4B).

A

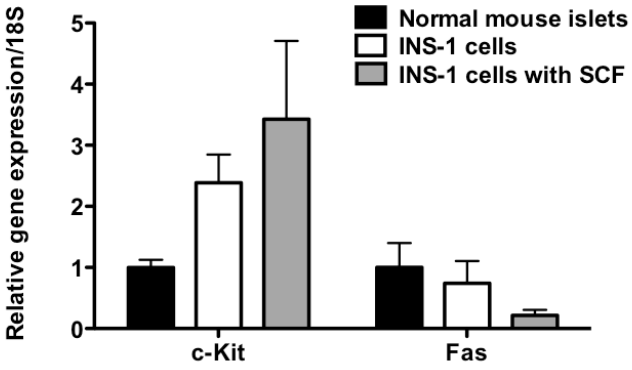
Normal mouse islets
INS-1 cells
INS-1 cells with SCF
Relative gene expression/18S
0
1
2
3
4
5
c-Kit
Fas

B

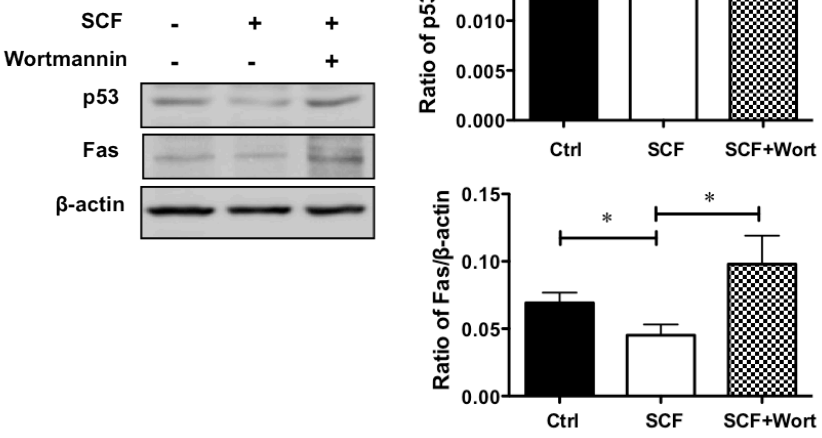
SCF - + +
Wortmannin - - +
p53
Fas
β-actin
Ratio of p53/β-actin
0.000
0.005
0.010
0.015
0.020
*
Ctrl
SCF
SCF+Wort
Ratio of Fas/β-actin
0.00
0.05
0.10
0.15
*
*
Ctrl
SCF
SCF+Wort

Figure 4-2. Increased SCF/c-Kit interaction in INS-1 cells results in decrease of p53 and Fas expression via the PI3K pathway.

(A) qRT-PCR analyses of *c-Kit* and *Fas* mRNA levels, in 8-week-old *c-Kit*$^{+/+}$ mouse islets, INS-1 cells, and INS-1 cells with SCF treatment cultured for 24 hours. (**B**) Western blot analyses of p53 and Fas protein levels in INS-1 cells cultured with serum-free medium plus 50 ng/mL SCF with and without wortmannin (Wort, PI3K inhibitor) for 24 hours. Representative blots are shown. Data are normalized to loading control (β-actin). Data (**A** and **B**) are expressed as mean ± SEM ($n=3$), *$p<0.05$ analyzed by one-way ANOVA followed by LSD *post-hoc* test.

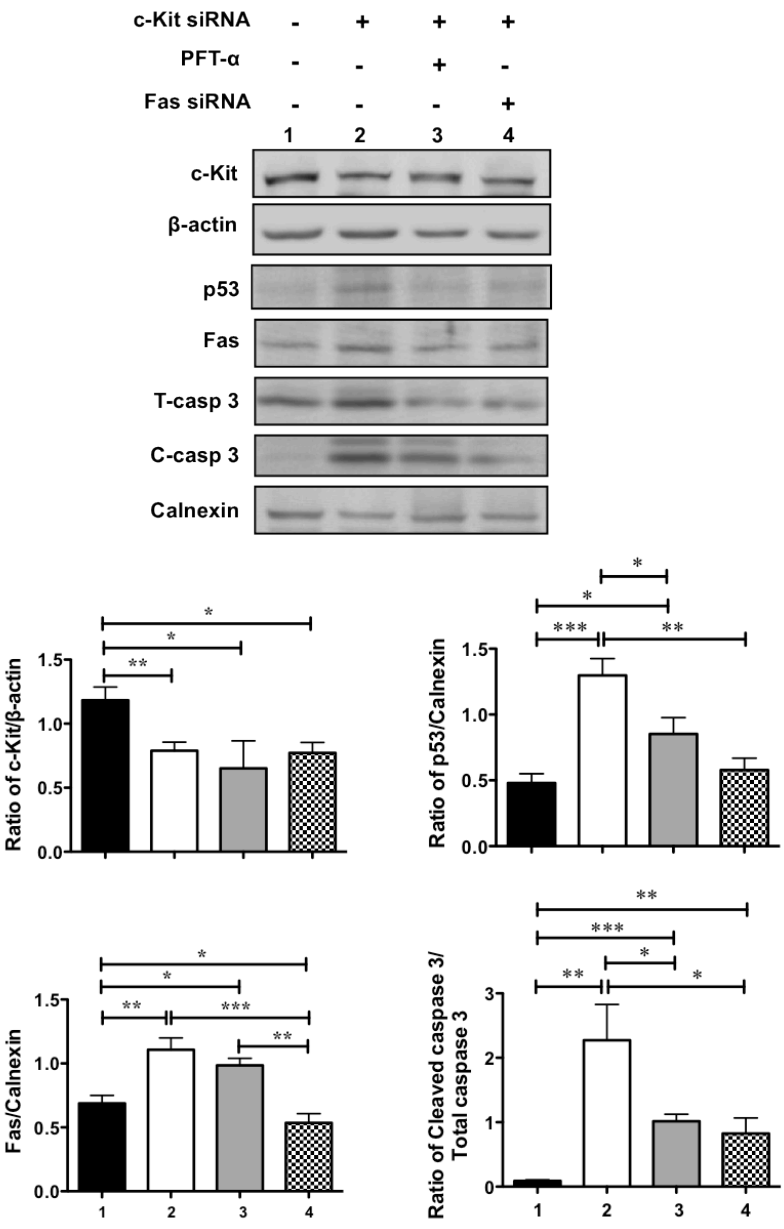
c-Kit siRNA - + + +
PFT-α - - + -
Fas siRNA - - - +
1 2 3 4
c-Kit
β-actin
p53
Fas
T-casp 3
C-casp 3
Calnexin
Ratio of c-Kit/β-actin
Ratio of p53/Calnexin
Fas/Calnexin
Ratio of Cleaved caspase 3/ Total caspase 3

Figure 4-3. Absence of c-Kit signaling induces the p53/Fas-mediated caspase-dependent apoptotic signaling.

Western blot analyses of c-Kit, p53, Fas, and D175-cleaved (C) and total (T) caspase 3 protein levels in INS-1 cells transfected with *c-Kit* siRNA and cotreated with PFT-α (p53 inhibitor) or *Fas* siRNA for 48 hours. Representative blots are shown. Data are normalized to total protein or loading control (calnexin or β-actin) and expressed as mean ± SEM ($n=3–4$), *$p<0.05$, **$p<0.01$, ***$p<0.001$ analyzed by one-way ANOVA followed by LSD *post-hoc* test.

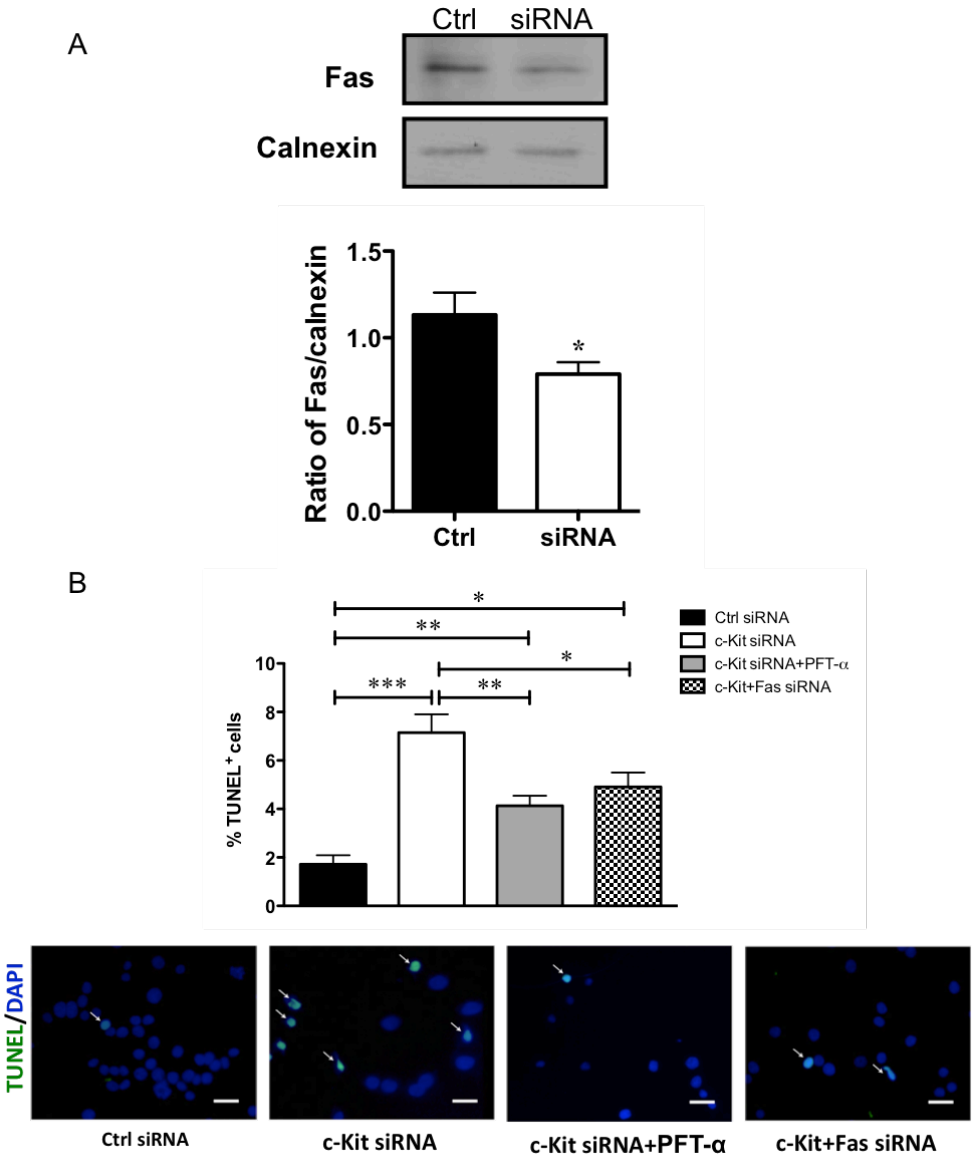
A
Ctrl
siRNA
Fas
Calnexin
Ratio of Fas/calnexin
1.5
1.0
0.5
0.0
*
Ctrl
siRNA
B
*
**
*
***
**
Ctrl siRNA
c-Kit siRNA
c-Kit siRNA+PFT-α
c-Kit+Fas siRNA
% TUNEL+ cells
10
8
6
4
2
0
TUNEL/DAPI
Ctrl siRNA
c-Kit siRNA
c-Kit siRNA+PFT-α
c-Kit+Fas siRNA

Figure 4-4. Knockdown of Fas decreases cell apoptosis.

(**A**) Fas protein levels in INS-1 cells cultured with control or *Fas* siRNA for 48 hours. Representative blots are shown. Data is normalized to loading control (calnexin) and expressed as mean ± SEM (*n=4*), **p*<0.05 analyzed by unpaired student's *t*-test, (**B**) Percentage of TUNEL positivity in INS-1 cells under all experimental conditions (control siRNA, *c-Kit* siRNA, *c-Kit* siRNA with PFT-α, *c-Kit* siRNA with *Fas* siRNA). Data are expressed as mean ± SEM (*n=4*), **p*<0.05, ***p*<0.01, ****p*<0.001 analyzed by one-way ANOVA followed by LSD *post-hoc* test. Representative images of TUNEL staining (green) and DAPI (blue). Scale bar, 10 μm.

4.3.2 Down-regulation of Fas in *c-Kit*$^{Wv/+}$ mice leads to improved beta-cell function

At 8 weeks of age, there was no difference in body weight (Figure 4-5A), but fasting blood glucose levels were significantly lower in *Wv;-/-* mice compared to *Wv;+/+* mice (Figure 4-5B), while significantly higher than their *WT* littermates (Figure 4-5B). *Wv;-/-* mice had significantly improved glucose tolerance demonstrated by decreased AUC relative to *Wv;+/+* mice (Figure 4-5C). There were no significant changes observed in insulin tolerance among the three different groups (Figure 4-5D). *In vivo* GSIS analyses demonstrated that insulin secretion in *Wv;-/-* mice was significantly higher at all three time points (0, 5 and 35 minutes after glucose challenge) when compared to *Wv;+/+* mice (Figure 4-6A). This was further corroborated with our observations from the *ex vivo* GSIS assay, which showed a significant increase in insulin secretion from *Wv;-/-* mouse islets after incubation in 22 mM glucose, as compared to *Wv;+/+* mouse islets (Figure 4-6B). However, the ability of *Wv;-/-* mice islets to respond to a 22 mM glucose challenge was significantly lower compared to islets from *WT* mice (Figure 4-6B). Insulin secretion from the *ex vivo* GSIS assay was comparable to measured insulin content, which was significantly higher in islets from *Wv;-/-* mice relative to *Wv;+/+* mice (Figure 4-6C), but not significantly lower than *WT* mice (Figure 4-6C). It was noted that the effect of glucose on islet insulin secretion was smaller in all groups when compared to previous reports, which may be associated with increased sensitivity when islets are freshly isolated.

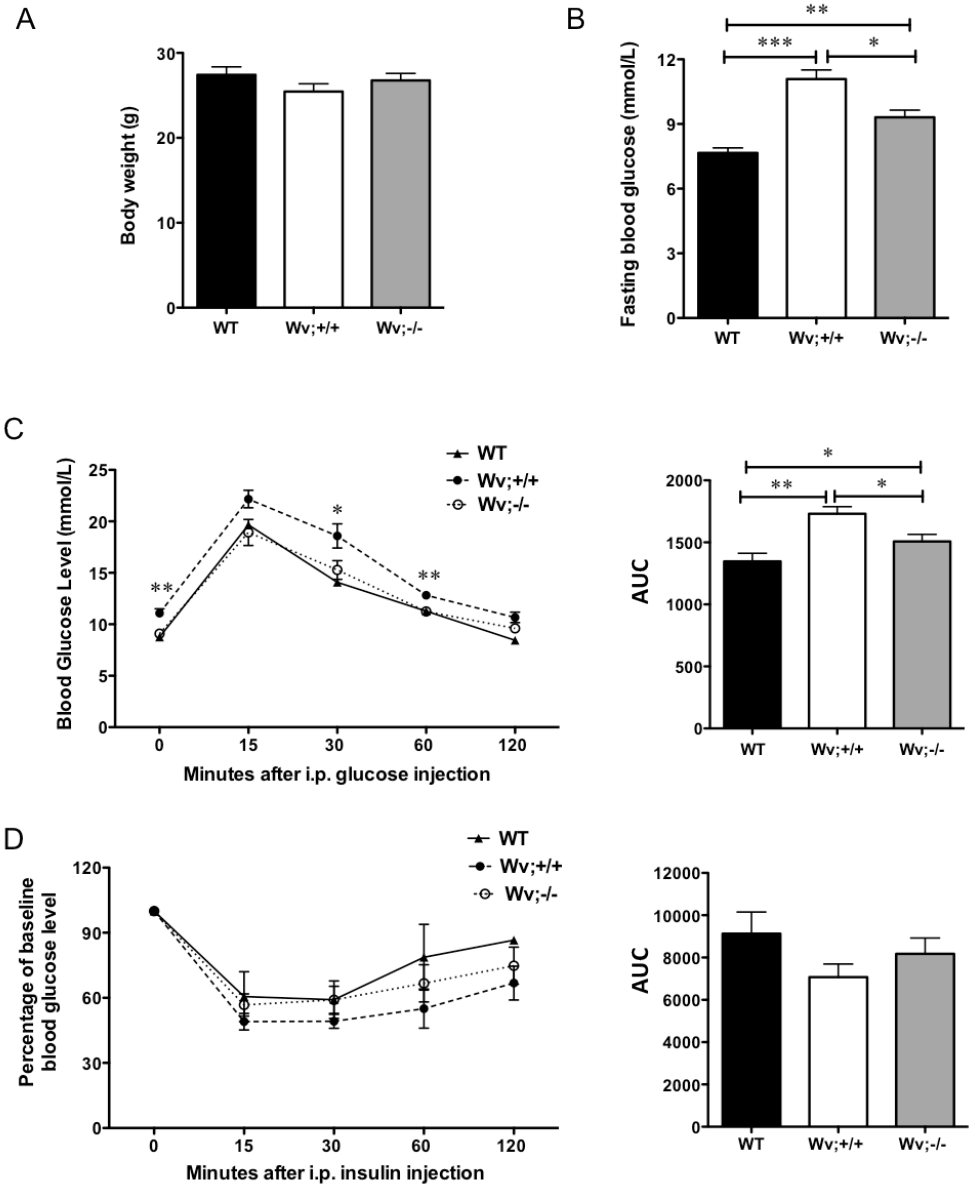
A
Body weight (g)
30
20
10
0
WT
Wv;+/+
Wv;-/-
B
**
***
*
Fasting blood glucose (mmol/L)
12
9
6
3
0
WT
Wv;+/+
Wv;-/-
C
WT
Wv;+/+
Wv;-/-
Blood Glucose Level (mmol/L)
25
20
15
10
5
0
**
*
**
0
15
30
60
120
Minutes after i.p. glucose injection
*
**
*
AUC
2000
1500
1000
500
0
WT
Wv;+/+
Wv;-/-
D
WT
Wv;+/+
Wv;-/-
Percentage of baseline blood glucose level
120
90
60
30
0
0
15
30
60
120
Minutes after i.p. insulin injection
AUC
12000
10000
8000
6000
4000
2000
0
WT
Wv;+/+
Wv;-/-

Figure 4-5. Fasting blood glucose and glucose tolerance on *c-Kit$^{Wv/+}$;Fas$^{lpr/lpr}$ (Wv;-/-)* mice at 8 weeks of age.

Body weight (**A**), fasting blood glucose (**B**), IPGTT (**C**), and IPITT (**D**) of *WT*, *Wv;+/+*, and *Wv;−/−* mice at 8 weeks of age. Glucose responsiveness of the corresponding experimental groups is shown as a measurement of AUC of the IPGTT or IPITT graphs with units of (mmol/L x minutes). Data (**A**-**D**) are expressed as mean ± SEM (*n=5-8*), **p*<0.05, ***p*<0.01, ****p*<0.001 analyzed by one-way ANOVA followed by LSD *post-hoc* test.

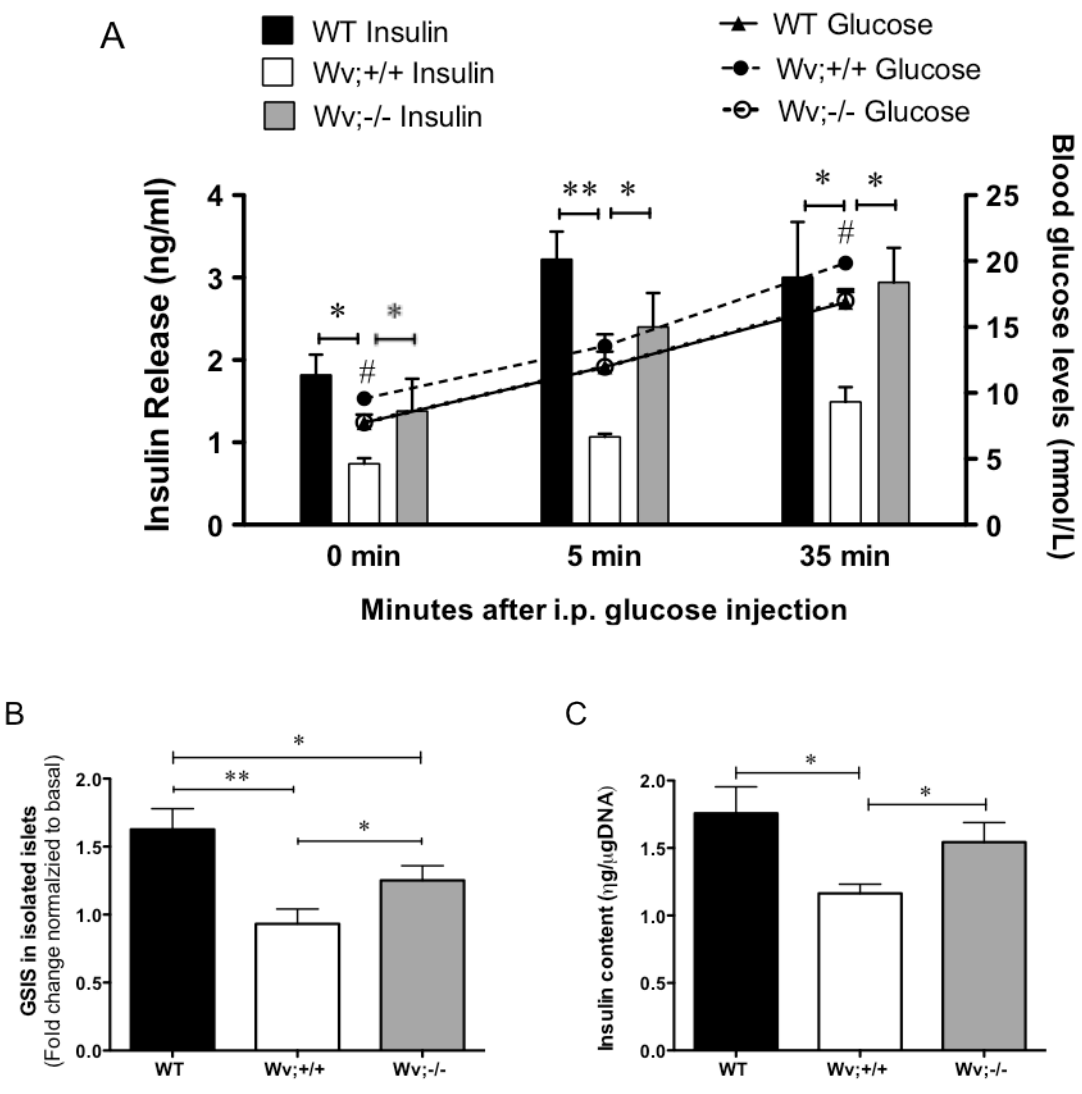
A
WT Insulin
Wv;+/+ Insulin
Wv;-/- Insulin
WT Glucose
Wv;+/+ Glucose
Wv;-/- Glucose
Insulin Release (ng/ml)
Blood glucose levels (mmol/L)
0 min
5 min
35 min
Minutes after i.p. glucose injection
B
GSIS in isolated islets
(Fold change normalzied to basal)
WT
Wv;+/+
Wv;-/-
C
Insulin content (ηg/μgDNA)
WT
Wv;+/+
Wv;-/-

Figure 4-6. GSIS and insulin content in *c-Kit$^{Wv/+}$;Fas$^{lpr/lpr}$(Wv;-/-)* mice at 8 weeks of age.

(**A**) *In vivo* GSIS of *WT*, *Wv;+/+*, and *Wv;−/−* mice at 8 weeks of age, (**B**) *Ex vivo* GSIS on isolated islets from *WT*, *Wv;+/+*, and *Wv;−/−* mice at 8 weeks of age. Data are expressed as fold change normalized to basal (2.2 mM glucose) secretion, (**C**) Insulin content in isolated islets from *WT*, *Wv;+/+*, and *Wv;−/−* mice at 8 weeks of age where data are normalized to DNA content. Data (**A**-**C**) are expressed as mean ± SEM (*n=3-7*), **p*<0.05, ***p*<0.01 analyzed by one-way ANOVA followed by LSD *post-hoc* test.

4.3.3 Increased beta-cell mass and proliferation, and decreased beta-cell apoptosis observed in c-*Kit*$^{Wv/+}$;*Fas*$^{lpr/lpr}$ double mutant mice

Islet morphology was analyzed by immunostaining (Figure 4-7A). Pancreatic weight was unchanged between experimental groups at 8 weeks of age (data not shown). However, *Wv;-/-* mice displayed a significant increase in islet number when compared to *Wv;+/+* mice (Figure 4-7B), and no difference when compared to *WT* mice (Figure 4-7B). Alpha-cell mass was unchanged among the experimental groups (data no shown), but *Wv;-/-* mice exhibited a doubling of beta-cell mass compared to *Wv;+/+* mice (Figure 4-7C). Furthermore, *Wv;-/-* mice showed a significant increase in beta-cell proliferation, determined by Ki67 labeling (Figure 4-7D and F), with a 2-fold decreased in TUNEL positive beta-cells when compared to *Wv;+/+* mice (Figure 4-7E and G).

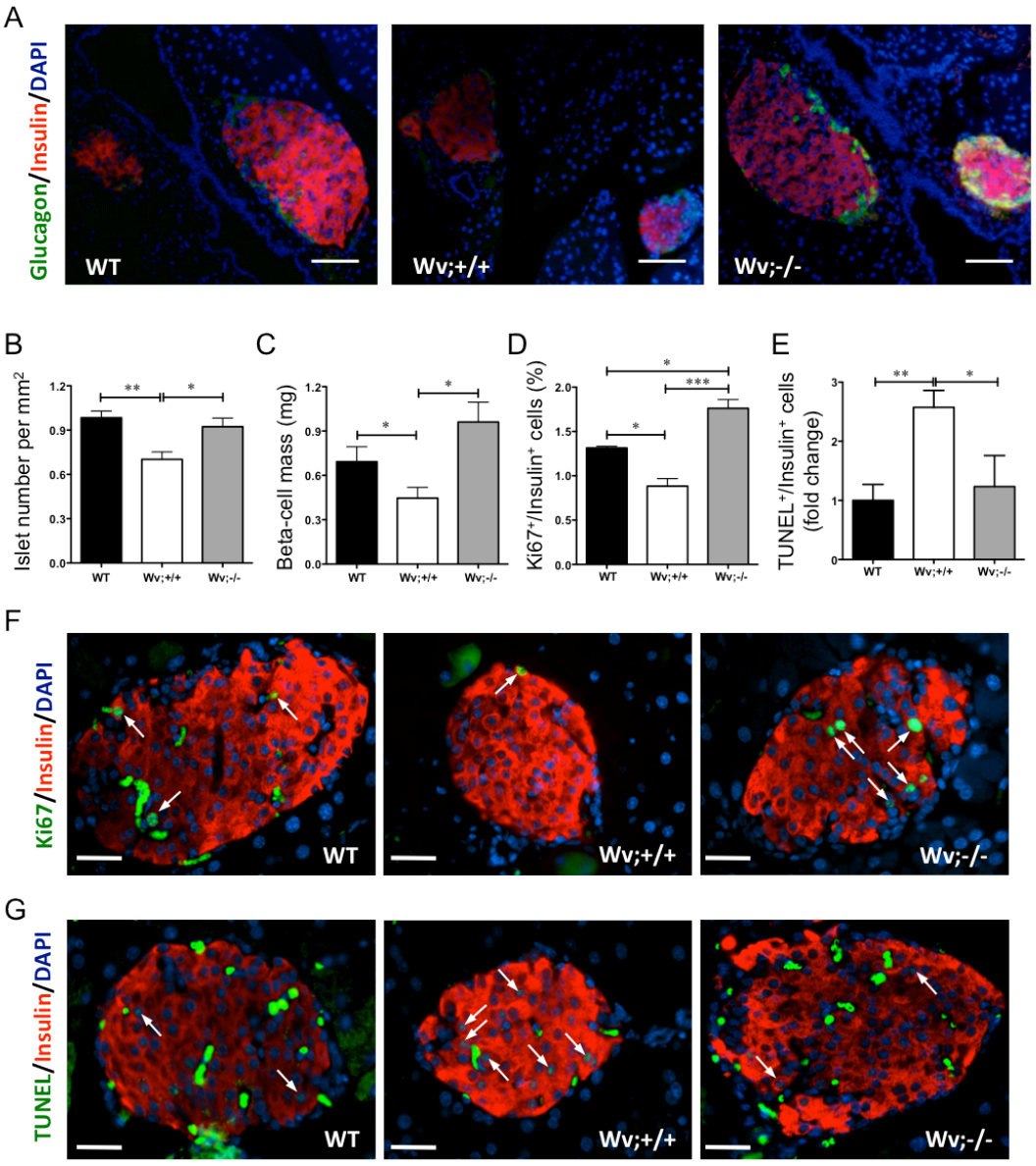
A
Glucagon/Insulin/DAPI
WT
Wv;+/+
Wv;-/-
B
Islet number per mm2
C
Beta-cell mass (mg)
D
Ki67+/Insulin+ cells (%)
E
TUNEL+/Insulin+ cells (fold change)
F
Ki67/Insulin/DAPI
G
TUNEL/Insulin/DAPI

Figure 4-7. Islet morphology and immunohistochemical analysis of endocrine cell mass, cell proliferation, and cell death in *c-Kit$^{Wv/+}$;Fas$^{lpr/lpr}$(Wv;-/-)* mice at 8 weeks of age.

(**A**) Representative images of islet morphology by double immunofluorescence staining for insulin (red) and glucagon (green), and nuclei stained with DAPI (blue). Scale bar, 50 μm. Islet number (**B**), beta-cell mass (**C**), percentage of Ki67^{+} (**D**) and TUNEL^{+} beta-cells (**E**) in *WT*, *Wv;*+/+, and *Wv;*−/− mice at 8 weeks of age. Data (**B**-**E**) are expressed as mean ± SEM (*n=3-6*), **p*<0.05, ***p*<0.01, ****p*<0.001 analyzed by one-way ANOVA. Representative double immunofluorescence staining images for Ki67 (**F**) and TUNEL (**G**) (green) with insulin (red) in islets of *WT*, *Wv;*+/+, and *Wv;*−/− mice at 8 weeks of age. Nuclei are stained with DAPI (blue). Arrows indicate double-labeled cells. Scale bar, 20 μm.

4.3.4 Down-regulation of Fas in the absence of c-Kit signaling activates the cFlip/NF-κB pathway, and increases islet transcription factor expression

To further investigate the underlying mechanisms in *Wv;-/-* mice, gene expression was assessed in isolated islets by qRT-PCR. Analyses of *insulin*, *glucagon*, *Pdx-1,* and *MafA* showed significantly increased mRNA expression in *Wv;-/-* mice when compared to *Wv;+/+* and *WT* mice (Figure 4-8A). Furthermore, the mRNA expression of *cFlip, RelA, RelB*, and *NFkb2* in isolated islets of *Wv;-/-* mice were significantly increased as compared to *Wv;+/+* mice (Figure 4-8B). However, no significant changes were found in the mRNA expression of *Bax* and a ratio of *Bcl-2* over *Bax* between *Wv;+/+* and *Wv;-/-* mouse islets (Figure 4-8C). Furthermore, western blot analyses showed down-regulation of Fas signaling, as indicated by a significant reduction of cleaved caspase 8 and 3 protein levels in *Wv;-/-* mouse islets (Figure 4-9) and this was correlated with reduced beta-cell apoptosis in *Wv;-/-* mice compared to *Wv;+/+* group (Figure 4-7E and G).

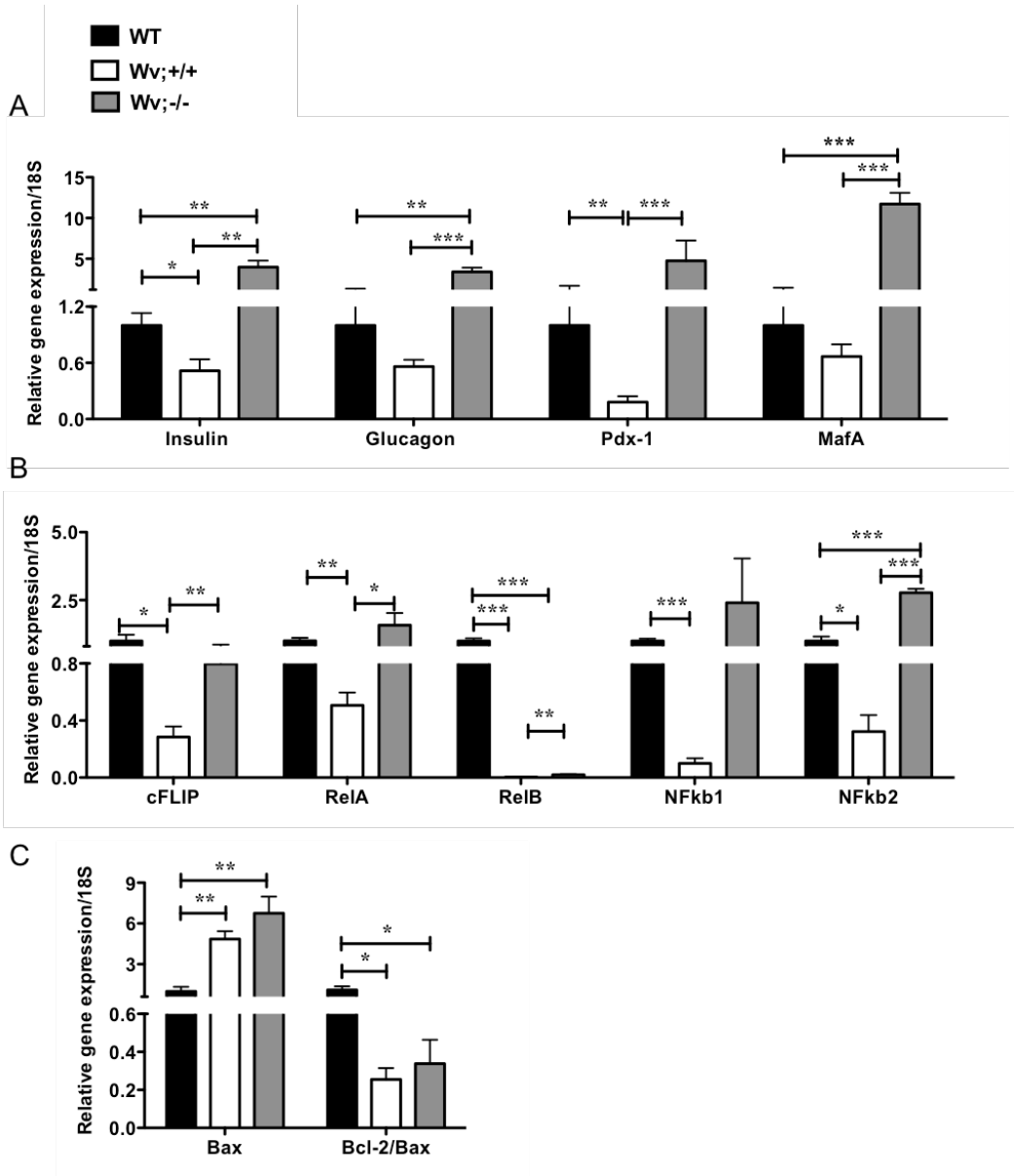
A
WT
Wv;+/+
Wv;-/-
Relative gene expression/18S
Insulin
Glucagon
Pdx-1
MafA
B
Relative gene expression/18S
cFLIP
RelA
RelB
NFkb1
NFkb2
C
Relative gene expression/18S
Bax
Bcl-2/Bax

Figure 4-8. Expression of transcription factors, endocrine genes, and signaling molecules in *c-Kit$^{Wv/+}$;Fas$^{lpr/lpr}$(Wv;-/-)* mice.

(**A**) qRT-PCR analyses of *insulin* (*I* and *II*), *glucagon, Pdx-1*, and *MafA*. Fas-mediated signaling molecules (**B**), and *Bax* and *Bcl2/Bax* ratio (**C**) in isolated islets of *WT*, *Wv;+/+*, and *Wv;−/−* mice at 8 weeks of age. Data (**A**-**C**) are expressed as mean ± SEM (*n=4*). **p*<0.05, ***p*<0.01, ****p*<0.001 analyzed by one-way ANOVA followed by LSD *post-hoc* test.

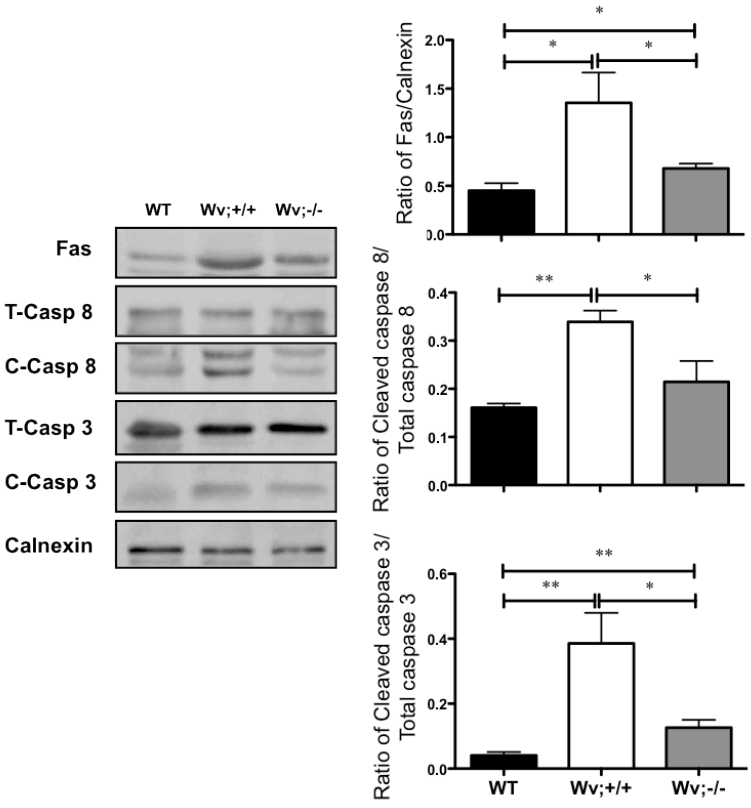
WT
Wv;+/+
Wv;-/-
Fas
T-Casp 8
C-Casp 8
T-Casp 3
C-Casp 3
Calnexin
Ratio of Fas/Calnexin
Ratio of Cleaved caspase 8/ Total caspase 8
Ratio of Cleaved caspase 3/ Total caspase 3
WT
Wv;+/+
Wv;-/-

Figure 4-9. Expression of cleaved caspase 8 and 3 in *c-Kit$^{Wv/+}$;Fas$^{lpr/lpr}$* (*Wv;-/-*) mice at 8 weeks of age.

Western blot analyses of Fas levels along with cleaved (C) and total (T) caspase 8 and 3 levels in isolated islets of *WT*, *Wv;+/+*, and *Wv;−/−* mice at 8 weeks of age. Representative blots are shown. Data are normalized to total protein or loading control (calnexin) and expressed as mean ± SEM ($n=4$). *$p<0.05$, **$p<0.01$ analyzed analyzed by one-way ANOVA followed by LSD *post-hoc* test.

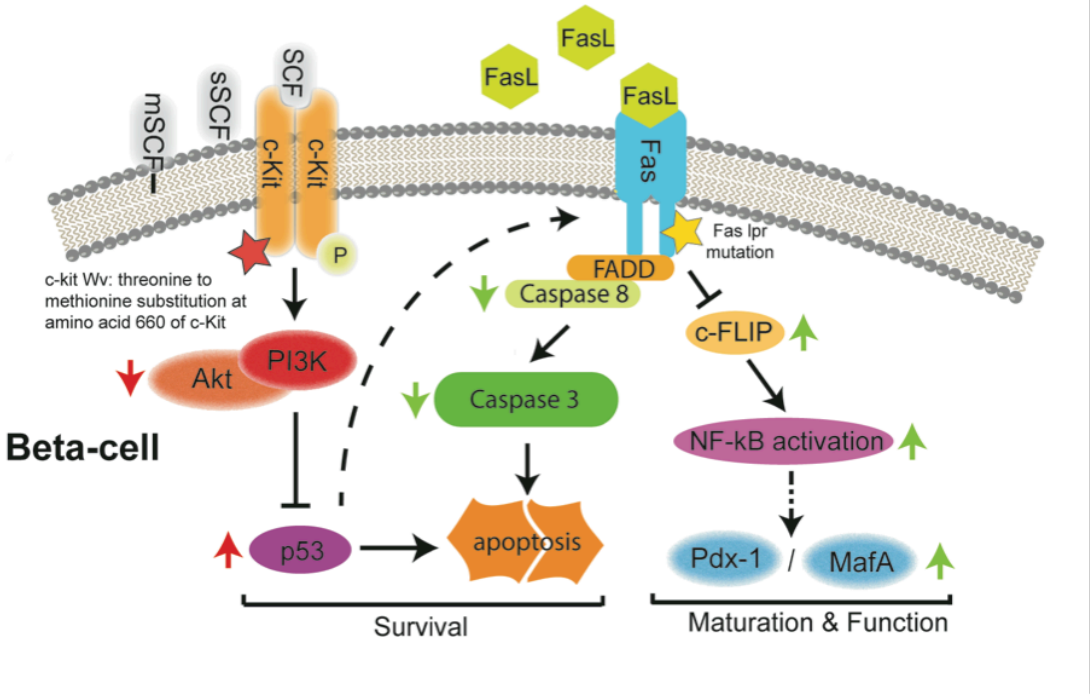
FasL
FasL
FasL
mSCF
sSCF
SCF
c-Kit
c-Kit
Fas
P
Fas lpr
mutation
c-kit Wv: threonine to
methionine substitution at
amino acid 660 of c-Kit
FADD
Caspase 8
c-FLIP
PI3K
Akt
Caspase 3
NF-kB activation
Beta-cell
p53
apoptosis
Pdx-1
/
MafA
Survival
Maturation & Function

Figure 4-10. Proposed model of c-Kit and Fas signaling that mediates beta-cell proliferation, function, and survival.

The W^v mutation of c-Kit (red star) causes down-regulation of Akt phosphorylation with increased p53 levels and subsequent induction of Fas-mediated beta-cell apoptosis. Down-regulation of the Fas pathway (yellow star) by the *lpr* mutation in *c-Kit*$^{Wv/+}$ mice rescues early onset of diabetes by down-regulating caspase 8 and 3 cleavage, up-regualting beta-cell proliferation, and key islet transcription factors, suggesting that the interrelationship between c-Kit and Fas signaling is critical for the maintenance of beta-cell mass and function. sSCF: soluble Stem Cell Factor; mSCF: membrane-bound Stem Cell Factor; FasL: Fas ligand. Red arrow: negative signaling; green arrow: positive signaling. Solid line: direct regulation; Dotted line: indirect regulation.

4.4 Discussion

In this study, we demonstrated that the loss of beta-cell mass in *c-Kit*$^{Wv/+}$ mice is due to increased p53 and Fas levels, along with associated downstream caspase-mediated beta-cell death in *c-Kit*$^{Wv/+}$ mouse islets (Figure 4-10). Mutation of *Fas* (*lpr*) rescued early onset of diabetes in *c-Kit*$^{Wv/+}$ mice by enhancing insulin secretory function and increasing beta-cell survival. This improvement was associated with down-regulation of the Fas-mediated extrinsic apoptotic pathway, and up-regulation of the cFLIP/NF-κB pathway, as well as the key islet transcription factors (Pdx-1 and MafA). Therefore, the present findings suggest that a balance between c-Kit and Fas signaling pathway is required to maintain beta-cell mass and function.

Both p53 and Fas levels were up-regulated in the islets of *c-Kit*$^{Wv/+}$ mice, which was correlated with increased beta-cell apoptosis. It has been documented that p53 is an important checkpoint protein that regulates cyclin D1 expression during cell cycle progression in many cell types [24, 25]. Although the cellular mechanism by which c-Kit regulates p53 is unclear, we have previously demonstrated that decreased cyclin D1 levels are observed in *c-Kit*$^{Wv/+}$ mouse islets [6], suggesting that inhibition of cell cycle progression by c-Kit deficiency may be p53-dependent. Not only is p53 involved in cell cycle arrest, it also plays a pivotal role in cell apoptosis. Several apoptotic genes are up regulated by p53 [26-29], in particular, p53 induces *Fas* mRNA expression by binding to elements that are found in the promoter and first intron regions of the *Fas* gene [27]. Also, overexpression of p53 may promote trafficking of the Fas to the cell surface via the Golgi apparatus [30]. Thus, the elevated p53 levels observed in *c-Kit*$^{Wv/+}$ mouse islets suggest that p53 serves as a mediator in cell cycle arrest and may induce Fas-mediated apoptosis in the absence of c-Kit signaling, *in vivo*. However, FasL levels were slightly increased in *c-Kit*$^{Wv/+}$ mouse islets, suggesting that FasL was already present at sufficiently high levels, and that beta-cell apoptosis is dependent upon Fas expression in islets. The inter-relation between c-Kit, p53 and Fas was further examined by stimulation of c-Kit via up- and down-regulation assays in INS-1 cells. Activation of c-Kit by exogenous SCF reduced both p53 and Fas protein levels in a PI3K-dependent manner. When cells were transfected with *c-Kit* siRNA, there was up-regulation of p53 and Fas

protein levels, which was reversed by the addition of a p53 inhibitor or *Fas* siRNA transfection and led to reduced apoptosis. These data suggest that c-Kit plays a key role in regulating p53-induced Fas-mediated cell death. p53-mediated Fas up-regulation has been proposed by several *in vitro* [27, 30, 31] and rodent studies [32, 33], and is likely responsible for increasing beta-cell apoptosis in *c-Kit*$^{Wv/+}$ mice.

To further elucidate the physiological role of Fas in the absence of c-Kit signaling, *in vivo*, we generated *Wv;-/-* mice bearing both *c-Kit W*^{v} and *Fas lpr* mutations, and found that anti-apoptotic genes such as *cFlip*, *NFκB2*, and both *RelA* and *RelB* were significantly up-regulated in *Wv;-/-* mouse islets. It is well-established that Fas-mediated apoptosis occurs through activation of procaspase-8, the most upstream caspase in the Fas apoptotic pathway, while cFlip, a protease-deficient caspase homolog to caspase-8, is able to modulate activation of procaspase-8, and trigger pro-survival signaling [34]. Although previous studies have documented that caspase 8 may be involved in the activation of NF-κB [35], the present study suggests that the up-regulation of NF-κB is independent of caspase-8 activity. Our data indicate that cFlip exerts its physiological function by triggering the NF-κB signaling pathway, which plays an important role in regulating cell survival and proliferation [36]. Therefore, in *Wv;-/-* mouse islets, an up-regulation of cFlip could have enhanced NF-κB activity by increasing NF-κB-inducing kinases, leading to improved beta-cell function and survival.

We further investigated the signaling pathway downstream of Fas that regulates beta-cell apoptosis and dysfunction in *c-Kit*$^{Wv/+}$ mice. Cleaved caspase 8 and 3 levels were significantly increased in *c-Kit* siRNA-transfected INS-1 cells and *c-Kit*$^{Wv/+}$ mouse islets. However, down-regulation of *Fas* in c-Kit-deficient islets resulted in significantly decreased cleaved caspase 8 and 3 levels when compared to controls. Previous *ex vivo* studies with human pancreatic beta-cells have shown that glucotoxicity-induced beta-cell apoptosis occurs via up-regulation of the Fas-mediated apoptotic pathway, which could be rescued by down-regulation of *Fas* [15, 16]. Furthermore, deletion of *Fas* in rodent pancreatic beta-cells has showed protection against FasL-induced apoptosis, and increased *in vivo* insulin secretion [2]. While much evidence has pointed to Fas as an important mediator of beta-cell apoptosis, downstream caspase 8 and 3 are also well

known for their roles as the principle executioners of beta-cells. *In vivo*, deletion of either caspase 8 or 3 in mouse beta-cells has shown to be protective against low doses of streptozotocin-induced cell death [37, 38]. Taken together, these results suggest that a loss of c-Kit signaling promotes beta-cell apoptosis and dysfunction, in part, by activation of the Fas-dependent apoptotic pathway.

In this study, we demonstrated that c-Kit deficiency led to an increase in Fas expression, and a mutation in *Fas* rescued defects associated with the *c-Kit*$^{Wv/+}$ mutation. The correlation between c-Kit and Fas signaling coincides well with previous studies, which suggest that PI3K/Akt signaling via c-Kit suppresses Fas-mediated extrinsic apoptotic signaling. However, several lines of evidence have also demonstrated that SCF-induced PI3K/Akt pathway signaling can inactivate proapoptotic transcriptional factor, FKHRL-1 [8], as well as Bim, a proapoptotic member of the Bcl-2 family [10]. Therefore, our findings suggest that Fas-mediated apoptotic signaling is directly involved in beta-cell dysfunction, especially when Fas is up-regulated due to the *c-Kit* W^v mutation, but we also cannot exclude the participation of other apoptotic factors that may be regulated by the disrupted c-Kit/PI3K/Akt pathway.

The biological role of Fas signaling is becoming increasingly complex. Controversial findings have reported both apoptotic and anti-apoptotic roles for Fas in the beta-cell *in vivo*. A previous study has reported that Fas is essential for beta-cell insulin secretory function, but not in the regulation of beta-cell mass [7]. Other studies have showed that islet-specific *Fas* deletion is protective against FasL- and ceramide-induced apoptosis *ex vivo*, and enhances beta-cell insulin secretion *in vivo* [2]. These discrepancies may be linked to differences in genetic backgrounds of the mouse strains used in these two studies. In this study, *Wv;-/-* mice were obtained by crossbreeding *c-Kit*$^{Wv/+}$ and *Fas*$^{lpr/lpr}$ mice both from a C57BL/6J background. Using the same mutant mouse model, previous studies have reported that loss of Fas function led to reduced apoptosis and improved function in granulosa cells, oocytes and germ cells of *c-Kit*$^{Wv/+}$ mice [21, 22]. In agreement with these findings, we propose that a balance between c-Kit and Fas signaling is important for beta-cell survival and function.

Through analyses of INS-1 cells and c-*Kit*$^{Wv/+}$;*Fas*$^{lpr/lpr}$ mice, our results suggest that SCF/c-Kit interactions prevent Fas-mediated beta-cell apoptosis and dysfunction. This study advances the understanding of the relationship between c-Kit-mediated survival signals and Fas-mediated death signals in beta-cells, which will assist in the development of protocols that maintain beta-cell survival and function essential for cell-based therapies in the treatment of diabetes.

4.5 References

1. Bernard-Kargar C, Ktorza A (2001) Endocrine pancreas plasticity under physiological and pathological conditions. Diabetes 50 Suppl 1:S30–5.

2. Choi D, Radziszewska A, Schroer SA, et al. (2009) Deletion of Fas in the pancreatic beta-cells leads to enhanced insulin secretion. Am J Physiol Endocrinol Metab 297:E1304–12. doi: 10.1152/ajpendo.00217.2009

3. Bonner-Weir S (2000) Life and death of the pancreatic beta cells. Trends Endocrinol Metab 11:375–378.

4. Weir GC, Bonner-Weir S (2004) Five stages of evolving beta-cell dysfunction during progression to diabetes. Diabetes 53 Suppl 3:S16–21.

5. Krishnamurthy M, Ayazi F, Li J, et al. (2007) c-Kit in early onset of diabetes: a morphological and functional analysis of pancreatic beta-cells in c-KitW-v mutant mice. Endocrinology 148:5520–5530. doi: 10.1210/en.2007-0387

6. Feng Z-C, Donnelly L, Li J, et al. (2012) Inhibition of Gsk3β activity improves β-cell function in c-KitWv/+ male mice. Lab Invest 92:543–555. doi: 10.1038/labinvest.2011.200

7. Schumann DM, Maedler K, Franklin I, et al. (2007) The Fas pathway is involved in pancreatic beta cell secretory function. Proc Natl Acad Sci USA 104:2861–2866. doi: 10.1073/pnas.0611487104

8. Möller C, Alfredsson J, Engström M, et al. (2005) Stem cell factor promotes mast cell survival via inactivation of FOXO3a-mediated transcriptional induction and MEK-regulated phosphorylation of the proapoptotic protein Bim. Blood 106:1330–1336. doi: 10.1182/blood-2004-12-4792

9. Loweth AC, Williams GT, James RF, et al. (1998) Human islets of Langerhans express Fas ligand and undergo apoptosis in response to interleukin-1beta and Fas ligation. Diabetes 47:727–732.

10. Bakker WJ, van Dijk TB, Parren-van Amelsvoort M, et al. (2007) Differential regulation of Foxo3a target genes in erythropoiesis. Mol Cell Biol 27:3839–3854. doi: 10.1128/MCB.01662-06

11. Mathis D, Vence L, Benoist C (2001) beta-Cell death during progression to diabetes. Nature 414:792–798. doi: 10.1038/414792a

12. Chervonsky AV, Wang Y, Wong FS, et al. (1997) The Role of Fas in Autoimmune Diabetes. Cell 89:17–24. doi: 10.1016/S0092-8674(00)80178-6

13. Itoh N, Imagawa A, Hanafusa T, et al. (1997) Requirement of Fas for the development of autoimmune diabetes in nonobese diabetic mice. J Exp Med 186:613–618.

14. Savinov AY, Tcherepanov A, Green EA, et al. (2003) Contribution of Fas to diabetes development. Proc Natl Acad Sci USA 100:628–632. doi: 10.1073/pnas.0237359100

15. Maedler K, Sergeev P, Ris F, et al. (2002) Glucose-induced beta cell production of IL-1beta contributes to glucotoxicity in human pancreatic islets. J Clin Invest 110:851–860. doi: 10.1172/JCI15318

16. Park YJ, Lee S, Kieffer TJ, et al. (2012) Deletion of Fas protects islet beta cells from cytotoxic effects of human islet amyloid polypeptide. Diabetologia. doi: 10.1007/s00125-012-2451-2

17. Lee JW, Gersuk GM, Kiener PA, et al. (1997) HLA-DR-triggered inhibition of hemopoiesis involves Fas/Fas ligand interactions and is prevented by c-kit ligand. J Immunol 159:3211–3219.

18. Nishio M, Oda A, Koizumi K, et al. (2001) Stem cell factor prevents Fas-mediated apoptosis of human erythroid precursor cells with Src-family kinase dependency. Exp Hematol 29:19–29.

19. Ito M, Kawa Y, Ono H, et al. (1999) Removal of stem cell factor or addition of monoclonal anti-c-Kit antibody induces apoptosis in murine melanocyte precursors. J Invest Dermatol 112:796–801. doi: 10.1046/j.1523-1747.1999.00552.x

20. Kimura S, Kawakami T, Kawa Y, et al. (2005) Bcl-2 reduced and fas activated by the inhibition of stem cell factor/KIT signaling in murine melanocyte precursors. J Invest Dermatol 124:229–234. doi: 10.1111/j.0022-202X.2004.23540.x

21. Moniruzzaman M, Sakamaki K, Akazawa Y, Miyano T (2007) Oocyte growth and follicular development in KIT-deficient Fas-knockout mice. Reproduction 133:117–125. doi: 10.1530/REP-06-0161

22. Sakata S, Sakamaki K, Watanabe K, et al. (2003) Involvement of death receptor Fas in germ cell degeneration in gonads of Kit-deficient Wv/Wv mutant mice. Cell Death Differ 10:676–686. doi: 10.1038/sj.cdd.4401215

23. Sharov AA, Li G-Z, Palkina TN, et al. (2003) Fas and c-kit are involved in the control of hair follicle melanocyte apoptosis and migration in chemotherapy-induced hair loss. J Invest Dermatol 120:27–35. doi: 10.1046/j.1523-1747.2003.12022.x

24. Rocha S, Martin AM, Meek DW, Perkins ND (2003) p53 represses cyclin D1 transcription through down regulation of Bcl-3 and inducing increased association of the p52 NF-kappaB subunit with histone deacetylase 1. Mol Cell Biol 23:4713–4727.

25. Schreiber M, Kolbus A, Piu F, et al. (1999) Control of cell cycle progression by c-Jun is p53 dependent. Genes Dev 13:607–619.

26. Miyashita T, Reed JC (1995) Tumor suppressor p53 is a direct transcriptional activator of the human bax gene. Cell 80:293–299.

27. Müller M, Wilder S, Bannasch D, et al. (1998) p53 activates the CD95 (APO-1/Fas) gene in response to DNA damage by anticancer drugs. J Exp Med 188:2033–2045.

28. Nakano K, Vousden KH (2001) PUMA, a novel proapoptotic gene, is induced by p53. Mol Cell 7:683–694.

29. Wu GS, Burns TF, McDonald ER, et al. (1997) KILLER/DR5 is a DNA damage-inducible p53-regulated death receptor gene. Nat Genet 17:141–143. doi: 10.1038/ng1097-141

30. Bennett M, Macdonald K, Chan SW, et al. (1998) Cell surface trafficking of Fas: a rapid mechanism of p53-mediated apoptosis. Science 282:290–293.

31. Semont A, Nowak EB, Silva Lages C, et al. (2004) Involvement of p53 and Fas/CD95 in murine neural progenitor cell response to ionizing irradiation. Oncogene 23:8497–8508. doi: 10.1038/sj.onc.1207821

32. Bouvard V, Zaitchouk T, Vacher M, et al. (2000) Tissue and cell-specific expression of the p53-target genes: bax, fas, mdm2 and waf1/p21, before and following ionising irradiation in mice. Oncogene 19:649–660. doi: 10.1038/sj.onc.1203366

33. Kim JM, Yoon YD, Tsang BK (1999) Involvement of the Fas/Fas ligand system in p53-mediated granulosa cell apoptosis during follicular development and atresia. Endocrinology 140:2307–2317. doi: 10.1210/endo.140.5.6726

34. Krueger A, Schmitz I, Baumann S, et al. (2001) Cellular FLICE-inhibitory protein splice variants inhibit different steps of caspase-8 activation at the CD95 death-inducing signaling complex. J Biol Chem 276:20633–20640. doi: 10.1074/jbc.M101780200

35. Chaudhary PM, Eby MT, Jasmin A, et al. (2000) Activation of the Nf-kappaB pathway by caspase 8 and its homologs. Oncogene 19:4451-4460.

36. Kataoka T, Budd RC, Holler N, et al. (2000) The caspase-8 inhibitor FLIP promotes activation of NF-kappaB and Erk signaling pathways. Curr Biol 10:640–648.

37. Liadis N, Murakami K, Eweida M, et al. (2005) Caspase-3-dependent beta-cell apoptosis in the initiation of autoimmune diabetes mellitus. Mol Cell Biol 25:3620–3629. doi: 10.1128/MCB.25.9.3620-3629.2005

38. Liadis N, Salmena L, Kwan E, et al. (2007) Distinct in vivo roles of caspase-8 in beta-cells in physiological and diabetes models. Diabetes 56:2302–2311. doi: 10.2337/db06-1771

Chapter 5

5 Critical role of c-Kit in beta-cell function: *increased insulin secretion and protection against diabetes*[4]

[4] This chapter has been modified and adapted from the following manuscript:

- **Feng ZC***, Li J*, Turco B, Riopel M, Yee SP, Wang R. (2012) Critical role of c-Kit in beta-cell function: increased insulin secretion and protection against diabetes in a mouse model. *Diabetologia* 55:2214-2225. *Equal contribution

5.1 Introduction

c-Kit is expressed in fetal and adult rodent pancreatic islets [1-4]. Our previous studies demonstrated that human and rat fetal pancreatic ductal cells expressing c-Kit display high proliferation and SCF expression [5-7]. Fetal rat islets treated with SCF demonstrates to a significant increase in insulin and DNA content [1]. Manipulation of islets in cell culture has further revealed that c-Kit-enriched cells can give rise to new beta-cells that secrete insulin in a glucose-responsive fashion [8]. However, down-regulation of *c-KIT* expression in the human islet-epithelial clusters using siRNA leads to significantly reduced mRNA and protein levels of PDX-1 and insulin in conjunction with decreased cell proliferation and increased cell death [6]. These studies reveal a remarkable correlation between c-Kit function and enhanced beta-cell development and function. After pancreatic duct ligation in the rat, c-Kit is activated in ductal cells during islet cell neogenesis, along with increased of Pdx-1 expression [9]. Furthermore, increased c-Kit and Pdx-1 expression is observed in islets of streptozotocin-induced diabetic rat pancreata, suggesting that c-Kit is involved in beta-cell regeneration [10].

Homozygous c-Kit null mutant mice display relatively normal islet morphology, but they die shortly after birth and are not available for further functional studies [11]. We have previously characterized *c-Kit*$^{Wv/+}$ mice, which have a point mutation in *c-Kit*, disrupting its receptor function. These mice exhibit a loss of beta-cell mass and proliferation, resulting in early onset of diabetes [12]. However, the global *c-Kit*$^{Wv/+}$ mice model may not be sufficient to reveal whether c-Kit plays a primary or secondary role in beta-cell survival and function. In this study, we describe a novel mouse model, *c-KitβTg*, with specific *c-KIT* overexpression in beta-cells to further delineate the physiological role of c-Kit in normal, HFD-induced diabetic and *c-Kit*$^{Wv/+}$ mice.

5.2 Materials and methods

Mouse model: transgenic mice (*c-KitβTg*) with the human *c-KIT* gene insertion specifically in beta-cells was the experimental group, while the wild type (*WT*) littermates without the human *c-KIT* gene were designated as the control group. Both *c-KitβTg* and *WT* mice were kept for 4 to 40 weeks of age with normal diet at which point,

metabolic studies, and subsequent islet morphological studies, islet qRT-PCR, and islet protein analyses were performed. For the HFD study, *c-KitβTg* and *WT* mice at 6 weeks of age were fed HFD for 4 weeks, at which point metabolic studies, and islet morphological studies were performed. For a rescue study in *c-Kit*$^{Wv/+}$ mice, the c-*KitβTg;Wv* mouse model was generated by crossbreeding *c-KitβTg* with *c-Kit*$^{Wv/+}$ mice, yielding mice with four different genotypes including: wild type (*WT*), *c-KitβTg*, *c-Kit*$^{Wv/+}$ *(Wv)*, and *c-KitβTg;c-Kit*$^{Wv/+}$ (*c-KitβTg;Wv*), that were kept until 8 weeks of age, at which point metabolic studies were performed. Only male mice were used for this study. Generation of animal models was detailed in section 2.1.3, and genotyping was detailed in section 2.2.

Metabolic studies, in vivo, and ex vivo GSIS analyses: Body weight, blood glucose levels (non-fasting, 4-hour and overnight fasting (16-hour)), IPGTT and IPITT analyses were performed throughout the study. *In vivo* GSIS, and *ex vivo* GSIS on isolated islets, were performed on mice in the normal diet, the HFD, and the rescued study. Food intake was monitored at 6 weeks of age for a 2-week period in the HFD study. See description in sections 2.3, 2.4 and 2.5.

Immunofluorescence and morphometric analyses: Pancreatic tissue sections from mice were prepared and double-stained with appropriate antibodies listed in Appendix 5. Islet number, islet size, alpha and beta-cell mass were measured. Proliferation (Ki67^{+} labeling), Pdx-1, Pax6, Nkx2.2, Nkx.6.1, c-Kit, SCF, eGFP, Glut2, Glp1R (Glucagon-like peptide 1 receptor) positive staining in beta-cell nuclear was determined by double immunofluorescence staining. MafA^{+} staining on pancreatic islets was determined by immunohistochemical, as detailed in section 2.7.

Protein extraction and western blot analyses: protein levels of Pdx-1, c-Kit, SCF, eGFP, phospho-Akt^{S473}, total Akt, phospho-Gsk3β^{S9}, total Gsk3β, cyclin D1, and correspond housekeeping proteins including calnexin and β-actin from isolated mouse islets was analyzed (Appendix 6), as detailed in section 2.8.

RNA extraction and real-time RT-PCR analyses: RNA was extracted from isolated mouse islets. mRNA expression of c-*Kit*, *Glp1r* (Glucagon-like peptide 1 receptor), *Gcg*

(Glucagon), *Slc2a2* (Glut2), *Insulin*, *MafA*, *Neurod1*, *Nkx2.2*, *Nkx6.1*, *Pax4*, *Pax6*, *Pdx-1*, *Kitl* (SCF) was measured and normalized to *18S* rRNA (Appendix 7), as detailed in section 2.9.

5.3 Results

5.3.1 Generation of transgenic mouse model with *c-KIT* overexpression specifically in beta-cells

We generated *c-KitβTg* mice on a C57BL/6J background using the RIP to direct overexpression of the human *c-KIT* gene specifically in beta-cells. Human *c-KIT* was also linked with an IRES-eGFP to facilitate monitoring of transgene expression. Immunoblot analysis of eGFP in pancreas, liver, muscle, brain and isolated islet protein lysates showed positive signals in the pancreas and islets of *c-KitβTg* mice (Figure 5-1A). The RIP did not lead to any aberrant transgene expression. Fluorescence microscopy showed that eGFP was present in islets freshly isolated from *c-KitβTg*, but not in those from *WT* littermates (Figure 5-1B). This was further confirmed by immunofluorescence staining for eGFP and insulin (Figure 5-1B). The human *c-KIT* mRNA was only detected in *c-KitβTg* mouse islets (Figure 5-1C), a finding corroborated by elevated islet c-Kit levels (Figure 5-1D) and c-Kit immunofluorescence staining (Figure 5-1E). We also examined the abundance of SCF, a ligand of c-Kit, in *c-KitβTg* mouse islets (Figure 5-2A). A significant increase of *SCF* (also known as *Kitl*) mRNA was noted in *c-KitβTg* islets compared with *WT* islets (Figure 5-2A); however, protein levels of SCF were not statistically different between *c-KitβTg* and *WT* islets (Figure 5-2B). Taken together, these results indicate that overexpression of human *c-KIT* under the transcriptional control of the RIP in *c-KitβTg* mice is specific to beta-cells.

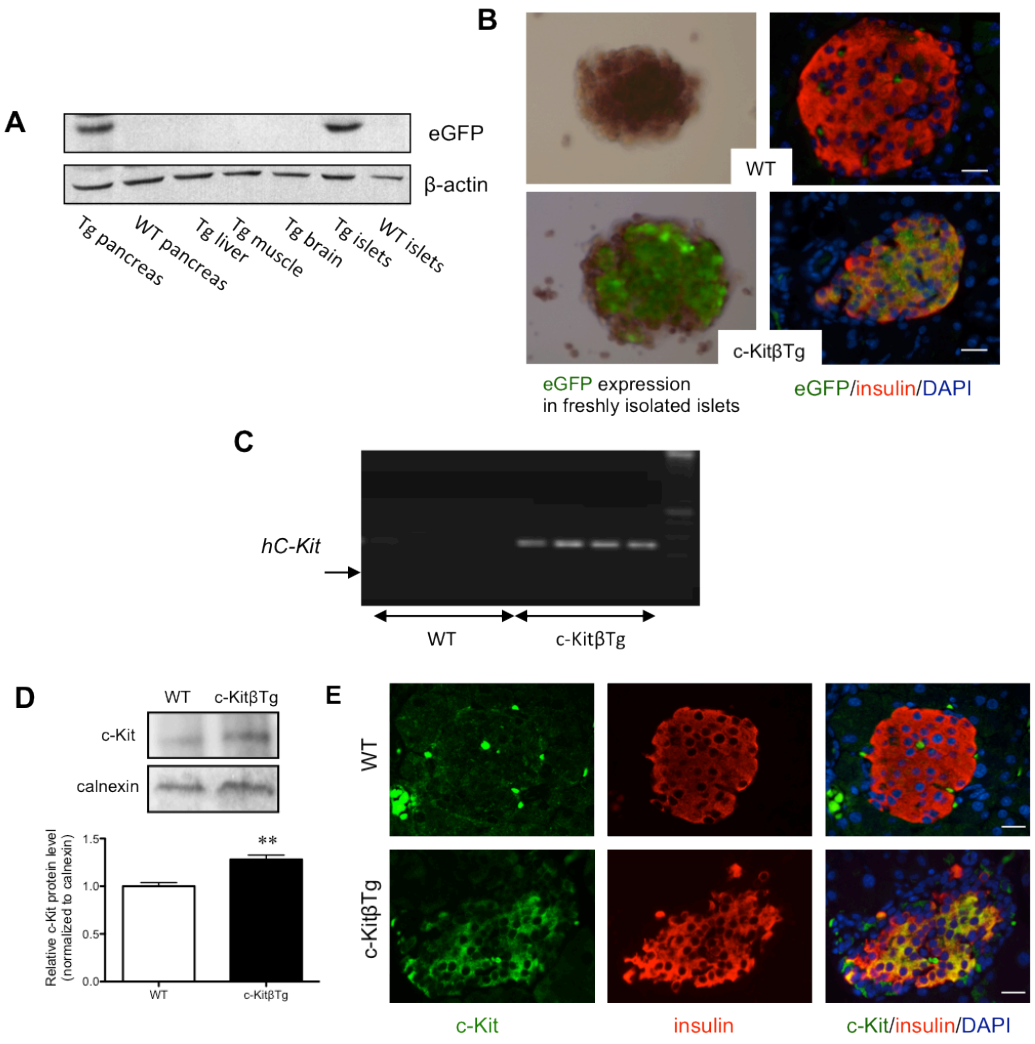
A
eGFP
β-actin
Tg pancreas
WT pancreas
Tg liver
Tg muscle
Tg brain
Tg islets
WT islets
B
WT
c-KitβTg
eGFP expression
in freshly isolated islets
eGFP/insulin/DAPI
C
hC-Kit
WT
c-KitβTg
D
WT
c-KitβTg
c-Kit
calnexin
Relative c-Kit protein level
(normalized to calnexin)
1.5
1.0
0.5
0.0
**
WT
c-KitβTg
E
WT
c-KitβTg
c-Kit
insulin
c-Kit/insulin/DAPI

Figure 5-1. Generation of C57BL/6J transgenic mice with *c-KIT* overexpression specifically in beta-cells (*c-KitβTg*).

A) Western blot analysis of eGFP abundance in tissues as indicated and isolated islets. Representative blots are shown. (**B)** Abundance of eGFP on freshly isolated islets and pancreatic sections of 4-week-old *WT* and *c-KitβTg* mice by double immunofluorescence staining for eGFP (green) with insulin (red). (**C)** qRT-PCR analysis of the human *c-KIT* mRNA in isolated islets of *WT* and *c-KitβTg* mice at 4 weeks of age. (**D)** Western blot analysis of c-Kit levels in isolated islets of *WT* and *c-KitβTg* mice at 8 weeks of age. Data are expressed as mean ± SEM (*n=3*), $^{**}p<0.01$ analyzed by unpaired student's *t*-test. (**E)** Immunofluorescence staining for c-Kit (green) and insulin (red) on pancreatic sections from 4-week-old *WT* and *c-KitβTg* mice. Nuclei were stained with DAPI (blue). Representative images are shown. Scale bars (**B**, **E**), 25 μm. eGFP: enhanced green fluorescent protein.

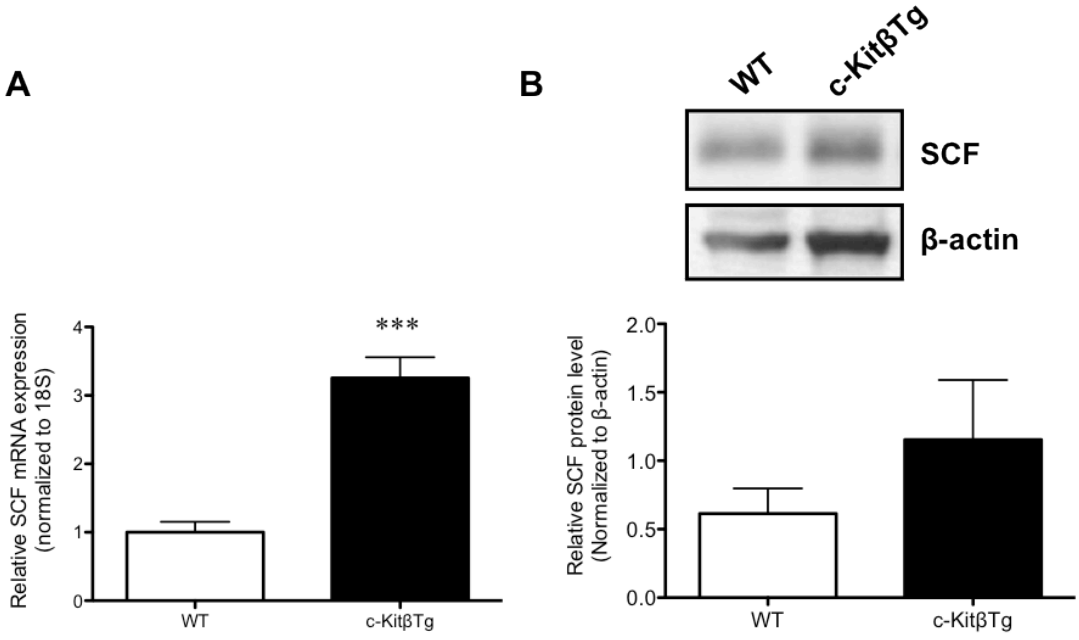
A
B
WT
c-KitβTg
SCF
β-actin
Relative SCF mRNA expression
(normalized to 18S)
***
0
1
2
3
4
WT
c-KitβTg
Relative SCF protein level
(Normalized to β-actin)
0.0
0.5
1.0
1.5
2.0
WT
c-KitβTg

Figure 5-2. Expression of SCF levels in C57BL/6J transgenic mice with *c-KIT* overexpression specifically in beta-cells (*c-KitβTg*).

(**A**) qRT-PCR and (**B**) western blot analysis of SCF in isolated islets of *WT* and *c-KitβTg* mice at 8 weeks of age. Representative blots are shown. Data are normalized to loading control (β-actin). Data (**A** and **B**) are expressed as mean ± SEM (*n =4*), ***$p<0.001$ analyzed by unpaired student's *t*-test.

5.3.2 Improved glucose tolerance and insulin secretion in *c-KitβTg* mice

There were no significant differences in body weight during the 40 weeks of observation (Figure 5-3A), with no changes in food intake at 8 weeks of age, between *c-KitβTg* and *WT* mice (Figure 5-3B). No significant differences in 4-hour fasting plasma insulin and blood glucose levels (Figure 5-3C and D) were detected between *c-KitβTg* and *WT* mice at 8 weeks of age; however, the overnight fasting blood glucose levels were significantly lower in *c-KitβTg* mice than in *WT* littermates (Figure 5-3D). The IPGTT showed a relatively similar response capacity in *c-KitβTg* and *WT* mice at 4 weeks of age (Figure 5-4A). However, significantly improved glucose tolerance was observed in *c-KitβTg* mice at 8 and 20 weeks of age, along with significant decreases in the AUC during the IPGTT (Figure 5-4B and C). No changes were observed in insulin tolerance between the experimental groups (Figure 5-4D). Furthermore, the effect of *c-KIT* overexpression on beta-cell insulin secretion was significant, with isolated islets from *c-KitβTg* mice releasing significantly more insulin than *WT* littermates in response to 22 mmol/L glucose (Figure 5-4E). This was associated with higher insulin content in *c-KitβTg* islets (Figure 5-4F).

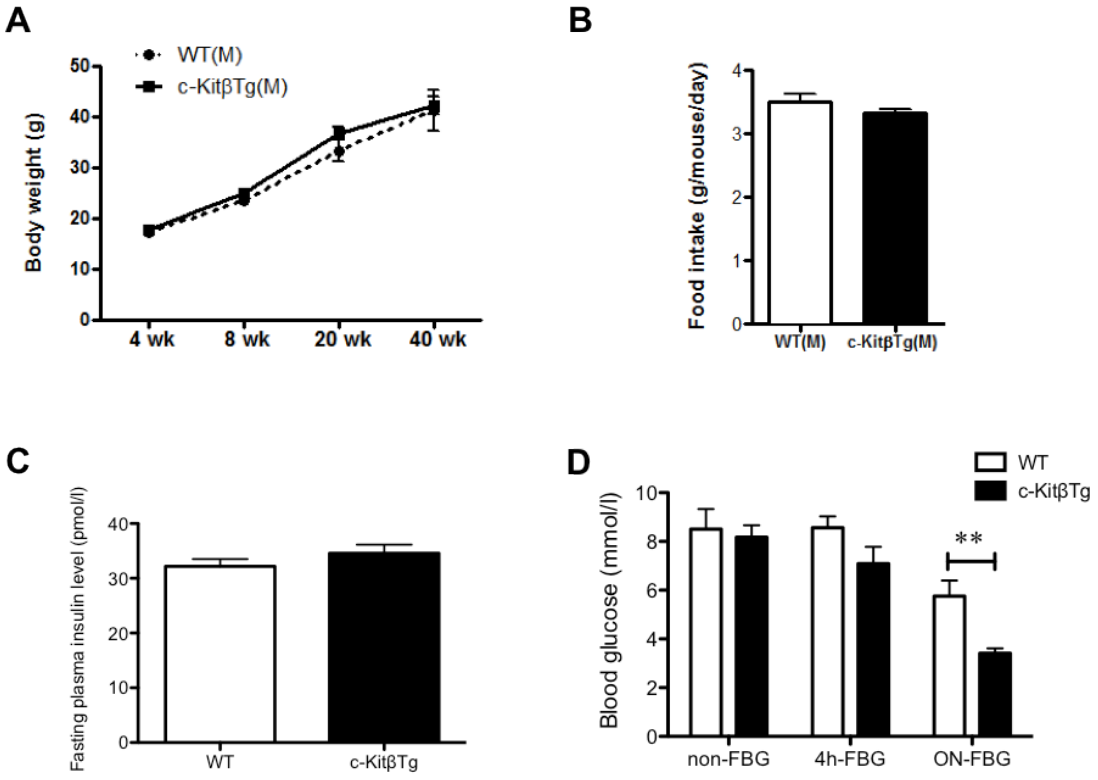
A
WT(M)
c-KitβTg(M)
Body weight (g)
50
40
30
20
10
0
4 wk
8 wk
20 wk
40 wk
B
Food intake (g/mouse/day)
4
3
2
1
0
WT(M)
c-KitβTg(M)
C
Fasting plasma insulin level (pmol/l)
40
30
20
10
0
WT
c-KitβTg
D
WT
c-KitβTg
Blood glucose (mmol/l)
10
8
6
4
2
0
**
non-FBG
4h-FBG
ON-FBG

Figure 5-3. Body weight, food intake and blood glucose level in *c-KitβTg* mice.

(**A**) Body weight of *c-KitβTg* and *WT* mice from 4 to 40 weeks of age. (**B**) Food intake, (**C**) Fasting (4-hour) plasma insulin and **(D)** blood glucose levels in *c-KitβTg* and *WT* mice at 8 weeks of age. Data (**A**-**D**) are expressed as mean ± SEM (*n=5-18*). ***p*<0.01 analyzed by unpaired student's *t*-test. FBG: fasting blood glucose; ON: overnight

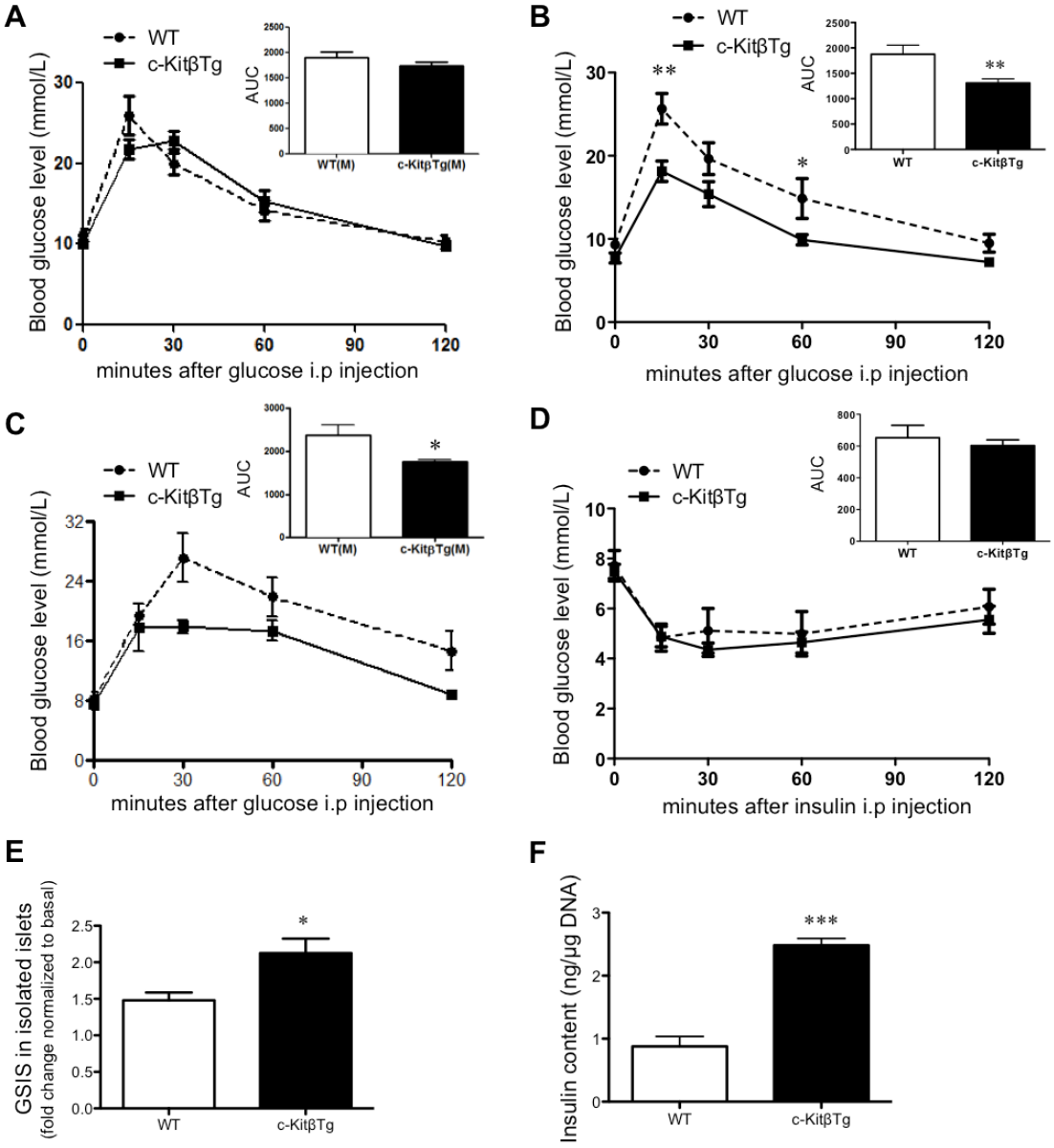
A
WT
c-KitβTg
Blood glucose level (mmol/L)
minutes after glucose i.p injection
AUC
WT(M)
c-KitβTg(M)
B
**
*
WT
c-KitβTg
C
WT
c-KitβTg
D
WT
c-KitβTg
minutes after insulin i.p injection
E
GSIS in isolated islets
(fold change normalized to basal)
WT
c-KitβTg
F
Insulin content (ng/μg DNA)
***

Figure 5-4. Glucose tolerance, GSIS, and insulin content in *c-KitβTg* mice.

IPGTT at 4 (**A**), 8 (**B**), and 20 (**C**) weeks of age, and (**D**) IPITT at 8 weeks of age on *c-KitβTg* and *WT* mice. Glucose responsiveness of the corresponding experimental groups is shown as a measurement of AUC of the IPGTT or IPITT graphs expressed as (mmol/L x minutes). (**E)** *Ex vivo* GSIS on isolated islets from *c-KitβTg* and *WT* mice at 8 weeks of age. Data are expressed as fold change normalized to basal (2.2 mM glucose) secretion. (**F**) Insulin content in isolated islets from *c-KitβTg* and *WT* mice at 8 weeks of age where data are normalized to DNA content. Data (**A-F**) are expressed as mean ± SEM (*n=3-18*). **p*<0.05, ***p*<0.01, ****p*<0.001 analyzed by unpaired student's *t*-test.

5.3.3 Increased islet transcription factors, beta-cell mass and proliferation in *c-KitβTg* mice

To further characterize the functional role of c-Kit in beta-cells, we examined levels of transcription factors essential for islet growth, function and morphology in *c-KitβTg* and *WT* mice. At 8 weeks of age, we observed a slightly increased islet number (Figure 5-5A), with a significant increase in the number of small (<500 μm^2) and large islets (>10,000 μm^2; Figure 5-5B) in *c-KitβTg* mice. No significant alterations in alpha-cell mass were detected between *c-KitβTg* and *WT* mice (Figure 5-5C). However, beta-cell mass in *c-KitβTg* mice was increased by 1.6-fold compared with *WT* (Figure 5-5D). Increased beta-cell mass was associated with an increase in beta-cell proliferation in *c-KitβTg* mice (Figure 5-5E and F). qRT-PCR analyses of *Pdx-1*, *Neurod1*, *MafA*, *Pax6*, *Nkx2.2* and *Nkx6.1* showed significantly increased mRNA levels in *c-KitβTg* mice (Figure 5-6A), with elevated intensity of the corresponding signals in the islets of *c-KitβTg* mice (Figure 5-6B). The expression of *Glut2*, *Ins1* and *Ins2*, *Gcg* and *Glp1r* mRNA in isolated *c-KitβTg* islets was also significantly increased (Figure 5-7A) with relatively enhanced Glut2 and Glp1R staining (Figure 5-7B).

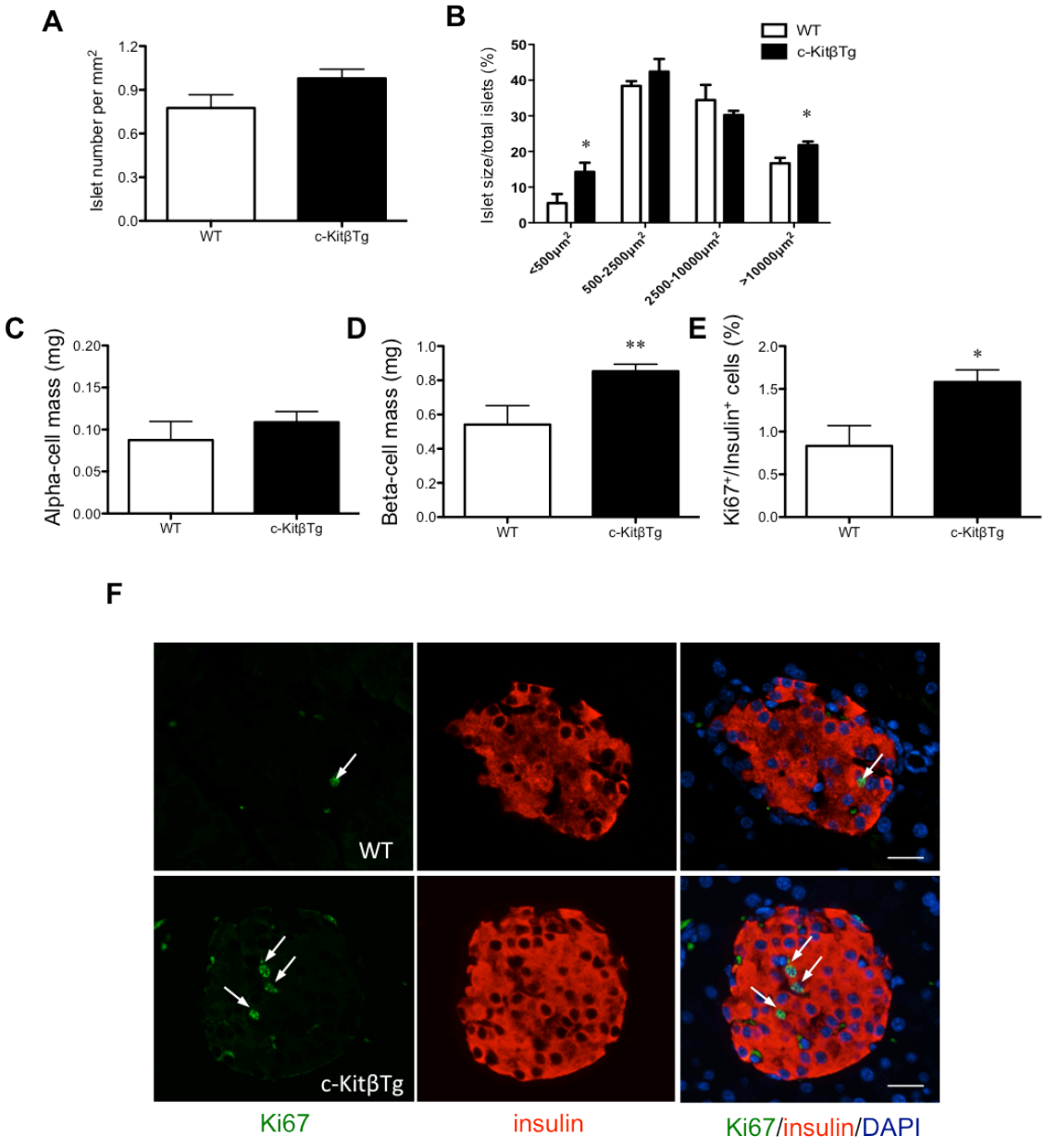
A
Islet number per mm2
1.2
0.9
0.6
0.3
0.0
WT
c-KitβTg
B
WT
c-KitβTg
Islet size/total islets (%)
50
40
30
20
10
0
*
*
<500μm2
500-2500μm2
2500-10000μm2
>10000μm2
C
Alpha-cell mass (mg)
0.20
0.15
0.10
0.05
0.00
WT
c-KitβTg
D
Beta-cell mass (mg)
1.0
0.8
0.6
0.4
0.2
0.0
**
WT
c-KitβTg
E
Ki67+/Insulin+ cells (%)
2.0
1.5
1.0
0.5
0.0
*
WT
c-KitβTg
F
WT
c-KitβTg
Ki67
insulin
Ki67/insulin/DAPI

Figure 5-5. Islet morphology in *c-KitβTg* mice at 8 weeks of age.

Morphometric analyses of islet number (**A**), islet size (**B**), alpha-cell mass (**C**), beta-cell mass (**D**), and percentage of $Ki67^+$ beta-cells (**E**) in *c-KitβTg* and *WT* mice at 8 weeks of age. Data (**A**-**E**) are expressed as mean ± SEM (*n=4–8*), **p*<0.05, ***p*<0.01 analyzed by unpaired student's *t*-test. (**F**) Double immunofluorescence staining of Ki67 (green), with insulin (red) on pancreatic sections from 8-week-old *c-KitβTg* and *WT* mice. Nuclei were stained with DAPI (blue). Arrows indicate $Ki67^+$/$insulin^+$ cells. Representative images are shown. Scale bar, 25 μm.

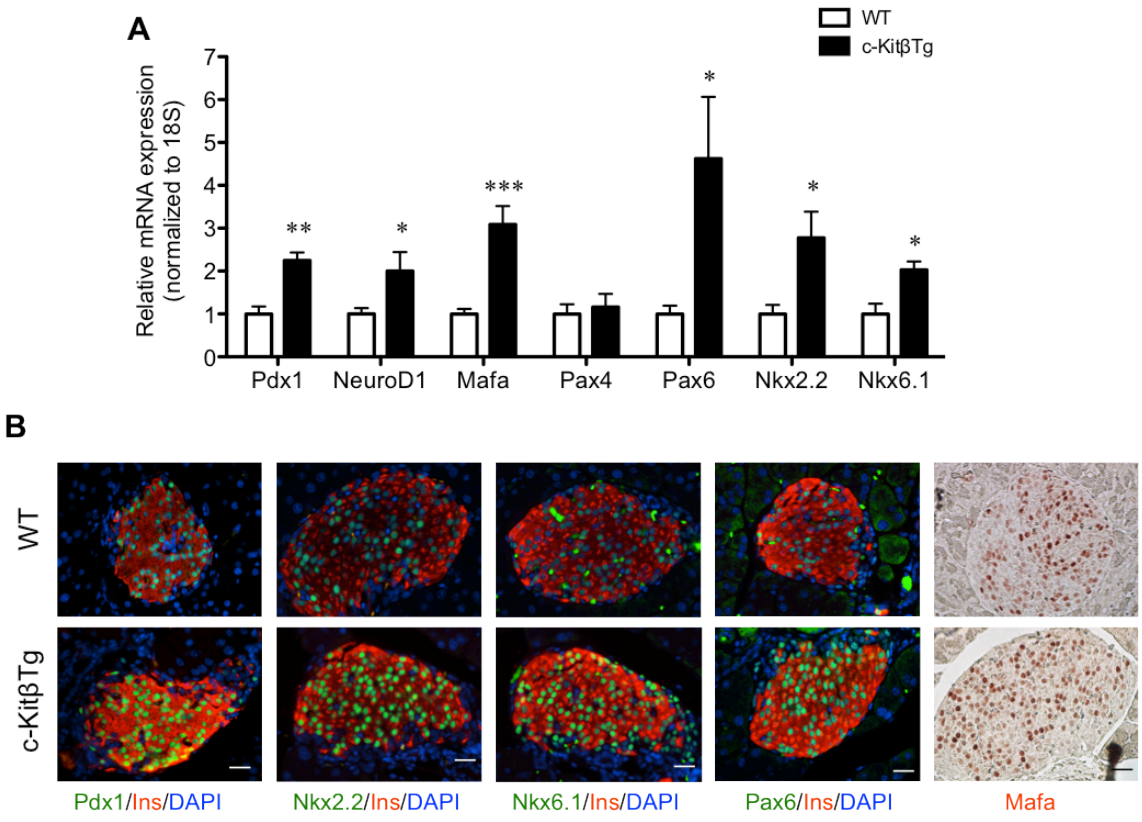
A
WT
c-KitβTg
Relative mRNA expression
(normalized to 18S)
0
1
2
3
4
5
6
7
**
*
***
*
*
*
Pdx1
NeuroD1
Mafa
Pax4
Pax6
Nkx2.2
Nkx6.1
B
WT
c-KitβTg
Pdx1/Ins/DAPI
Nkx2.2/Ins/DAPI
Nkx6.1/Ins/DAPI
Pax6/Ins/DAPI
Mafa

Figure 5-6. Expression of islet transcription factors in *c-KitβTg* mice at 8 weeks of age.

(**A**) Islet transcription factors in *c-KitβTg* and *WT* mice at 8 weeks of age, as analyzed by qRT-PCR. Data are expressed as mean ± SEM (*n=4–8*), **p*<0.05, ***p*<0.01, and ****p*<0.001 analyzed by unpaired student's *t*-test. (**B**) Double immunofluorescence staining for transcription factors (green) with insulin (red), with nuclei stained with DAPI (blue), with immunohistochemistry staining for MafA (red in nuclei) on pancreatic sections from 8-week-old *c-KitβTg* and *WT* mice. Representative images are shown. Scale bar, 50 μm.

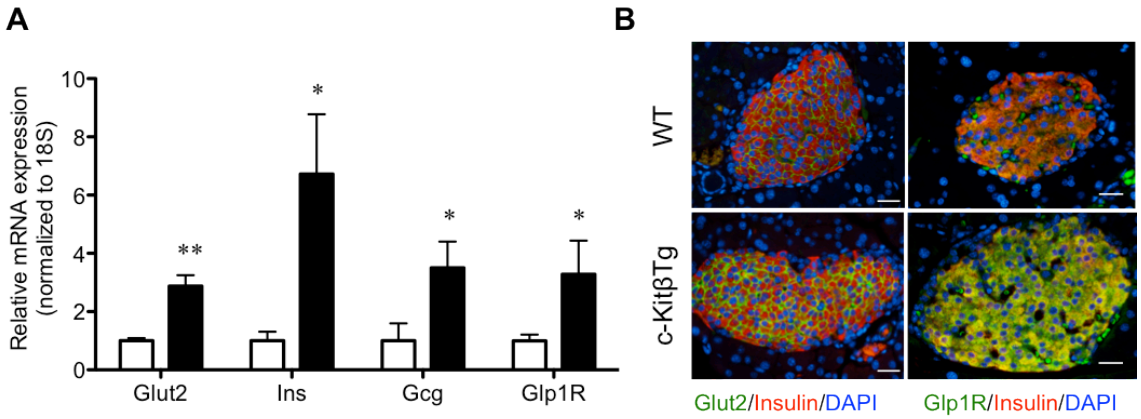
A
B
Relative mRNA expression (normalized to 18S)
10
8
6
4
2
0
**
*
*
*
Glut2
Ins
Gcg
Glp1R
WT
c-KitβTg
Glut2/Insulin/DAPI
Glp1R/Insulin/DAPI

Figure 5-7. Expression of islet endocrine genes, Glut2, and Glp1 receptors in *c-KitβTg* mice at 8 weeks of age.

(**A**) Islet gene expression in *c-KitβTg* and *WT* mice at 8 weeks of age, as analyzed by qRT-PCR. Data are expressed as mean ± SEM (*n=4–8*), **p*<0.05, ***p*<0.01 analyzed by unpaired student's *t*-test, (**B**) double immunofluorescence staining for Glut2 and Glp1R (green) with insulin (red), with nuclei stained with DAPI (blue) on pancreatic sections from 8-week-old *c-KitβTg* and *WT* mice. Representative images are shown. Scale bar, 50 μm.

5.3.4 Increased PI3K/Gsk3β/cyclin D1 signaling pathway in *c-KitβTg* mouse islets

Our previous study showed that the *c-Kit W*^{v} mutation caused beta-cell dysfunction [12], and that this mutation was associated with down-regulation of the Akt/Gsk3β/cyclin D1 pathway [13]. We therefore examined whether signaling molecules up- and downstream of the PI3K/Akt pathway or cell survival signals are altered in *c-KitβTg* islets. We found that protein levels of S473 phospho-Akt (Figure 5-8A), S9 phospho-Gsk3β (Figure 5-8B), cyclin D1 (Figure 5-8C) and Pdx-1 (Figure 5-8D) were significantly increased in *c-KitβTg* islets compared with islets isolated from *WT* littermates.

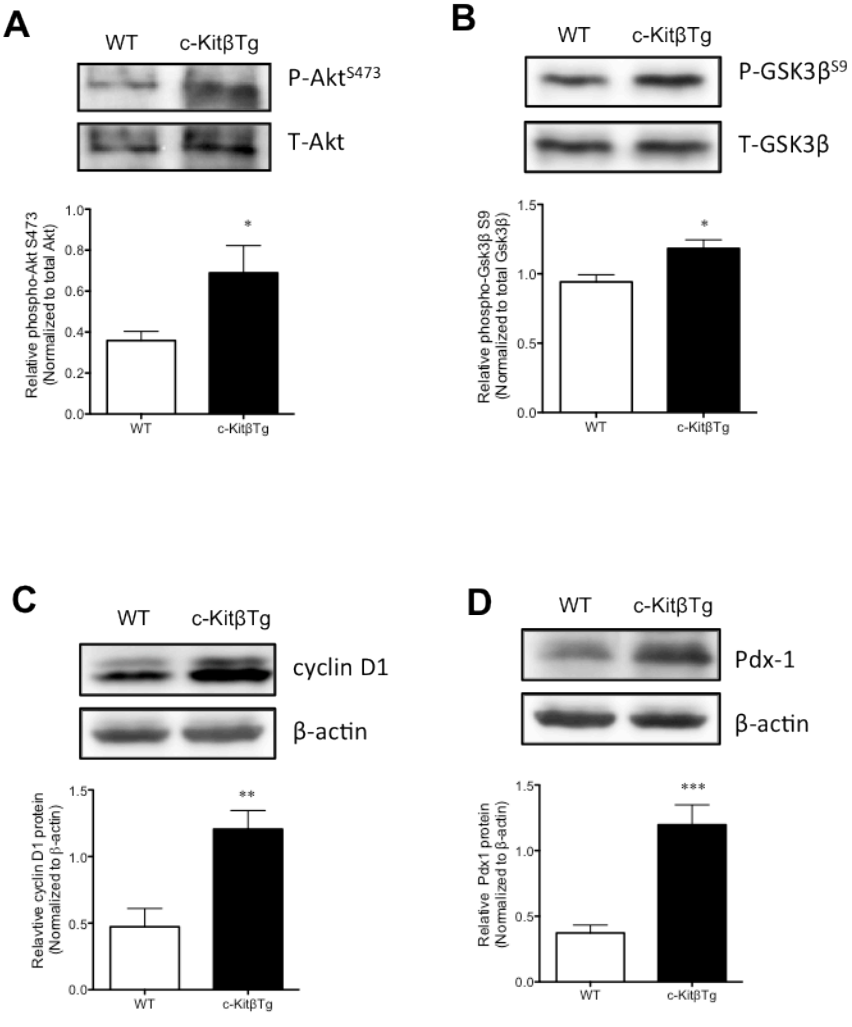
A
WT
c-KitβTg
P-Akt^{S473}
T-Akt
Relative phospho-Akt S473 (Normalized to total Akt)
1.0
0.8
0.6
0.4
0.2
0.0
*
WT
c-KitβTg
B
WT
c-KitβTg
P-GSK3β^{S9}
T-GSK3β
Relative phospho-Gsk3β S9 (Normalized to total Gsk3β)
1.5
1.0
0.5
0.0
*
WT
c-KitβTg
C
WT
c-KitβTg
cyclin D1
β-actin
Relavtive cyclin D1 protein (Normalized to β-actin)
1.5
1.0
0.5
0.0
**
WT
c-KitβTg
D
WT
c-KitβTg
Pdx-1
β-actin
Relative Pdx1 protein (Normalized to β-actin)
1.5
1.0
0.5
0.0
***
WT
c-KitβTg

Figure 5-8. Levels of phosphorylated Akt/Gsk3β/cyclin D1 signaling and downstream signaling molecules in *c-KitβTg* mice at 8 weeks of age.

Western blot analyses of (**A**) S473-phosphorylated (P) and total (T) Akt, (**B**) Ser9 P-Gsk3β and T-Gsk3β, (**C**) cyclin D1 and (**D**) Pdx-1 abundance in isolated islets of *c-KitβTg* and *WT* mice at 8 weeks of age. Representative blots are shown. Data (**A**-**D**) are normalized to total protein or loading control (β-actin) and expressed as mean ± SEM (*n=4-5*), **p*<0.05, ***p*<0.01 and ****p*<0.001 analyzed by unpaired student's *t*-test.

5.3.5 *c-KitβTg* mice tolerate HFD-induced diabetes

To investigate how beta-cell-specific *c-KIT* overexpression would affect glucose homeostasis of mice under diabetic conditions, *c-KitβTg* and *WT* littermates were subjected to a HFD. Similar body weight gains were observed in both experimental groups (Figure 5-9A). Interestingly, after 4 weeks of HFD, the 4-hour fasting glucose level was lower in *c-KitβTg-HFD* mice than in *WT-HFD* mice (Figure 5-9B). Glucose intolerance was noted in *WT-HFD* littermates, but was significantly improved in *c-KitβTg-HFD* mice (Figure 5-9C), with similar results for insulin response in *WT-HFD* as determined by the IPITT (Figure 5-9D). *In vivo* GSIS assays revealed slightly higher basal and 5-minute plasma insulin levels in *c-KitβTg-HFD* mice (Figure 5-9E); moreover, at 35 minutes after glucose stimulation, the plasma insulin release was significantly reduced in *WT-HFD* compared with *c-KitβTg-HFD* mice (Figure 5-9E). GSIS on isolated islets further demonstrated that *c-KitβTg-HFD* islet insulin secretion was significantly increased in response to 22 mmol/L glucose compared with *WT-HFD* islets (Figure 5-9F). The insulin content was also significantly increased in *c-KitβTg-HFD* islets (Figure 5-9G). The improved metabolic phenotype of *c-KitβTg-HFD* mice was associated with a significant increase in the number of pancreatic islets and beta-cell mass compared with *WT-HFD* mice (Figure 5-10A and C). A slightly increased alpha-cell mass was observed in *c-KitβTg-HFD* mice; however, the increase was not statistically significant (Figure 5-10B). Nevertheless, a significant increase in beta-cell mass was detected, with increased beta-cell proliferation in *c-KitβTg-HFD* mice compared with *WT-HFD* group (Figure 5-10D).

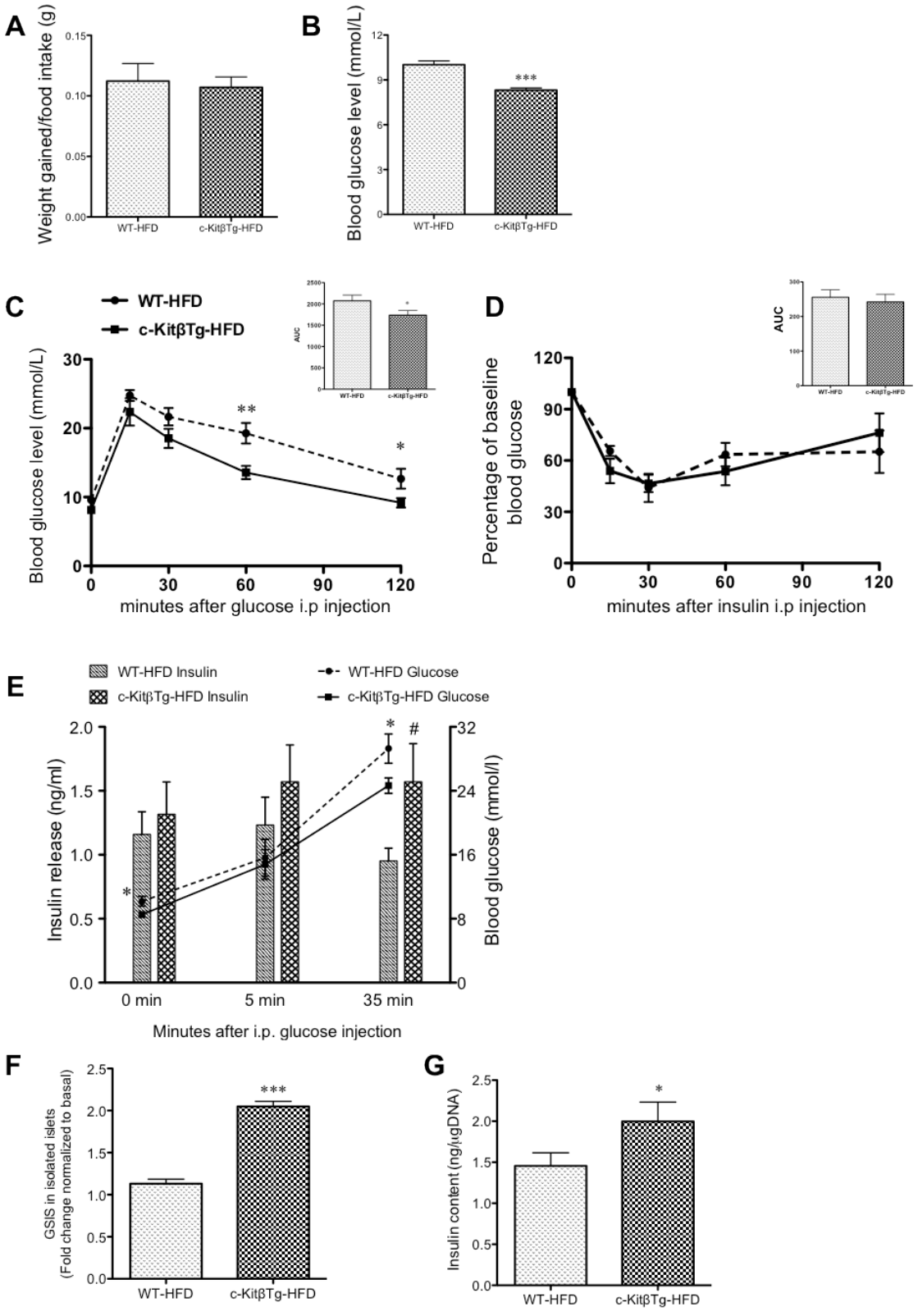
A
Weight gained/food intake (g)
0.15
0.10
0.05
0.00
WT-HFD
c-KitβTg-HFD
B
Blood glucose level (mmol/L)
12
9
6
3
0
***
WT-HFD
c-KitβTg-HFD
C
WT-HFD
c-KitβTg-HFD
Blood glucose level (mmol/L)
30
20
10
0
**
*
0
30
60
90
120
minutes after glucose i.p injection
AUC
WT-HFD
c-KitβTg-HFD
D
Percentage of baseline blood glucose
120
90
60
30
0
0
30
60
90
120
minutes after insulin i.p injection
AUC
WT-HFD
c-KitβTg-HFD
E
WT-HFD Insulin
c-KitβTg-HFD Insulin
WT-HFD Glucose
c-KitβTg-HFD Glucose
Insulin release (ng/ml)
2.0
1.5
1.0
0.5
0.0
Blood glucose (mmol/l)
32
24
16
8
0
*
*
#
0 min
5 min
35 min
Minutes after i.p. glucose injection
F
GSIS in isolated islets
(Fold change normalized to basal)
2.5
2.0
1.5
1.0
0.5
0.0
***
WT-HFD
c-KitβTg-HFD
G
Insulin content (ng/μgDNA)
2.5
2.0
1.5
1.0
0.5
0.0
*
WT-HFD
c-KitβTg-HFD

Figure 5-9. Effect of a HFD on *c-KitβTg* mice.

(**A**) Weight gained per food intake, and (**B**) 4-hour fasting blood glucose levels in *WT-HFD* and *c-KitβTg-HFD* mice. (**C**) IPGTT and (**D**) IPITT in *WT-HFD* and *c-KitβTg-HFD* mice. Glucose responsiveness of the corresponding experimental groups is shown as the AUC of the IPGTT (**C**, insert) or IPITT (**D**, insert) graphs with units of (mmol/L x minutes). (**E**) *In vivo* GSIS of *WT-HFD* and c-*KitβTg-HFD* mice (Lighted bars, *WT-HFD* insulin; darken bars, *c-KitβTg-HFD* insulin; black circles, *WT-HFD* glucose; black squares, *c-KitβTg-HFD* glucose). (**F**) *Ex vivo* GSIS on isolated islets from *WT-HFD* and *c-KitβTg-HFD* mice. Data are expressed as fold change normalized to basal (2.2 mM glucose) secretion as mean ± SEM. (**G**) Insulin content in isolated islets from *WT-HFD* and *c-KitβTg-HFD* mice where data are normalized to DNA content and expressed as mean ± SEM. Data (**A**-**G**) are expressed as mean ± SEM (*n =5-10*), **p*<0.05 and ****p*<0.001 analyzed by unpaired student's *t*-test.

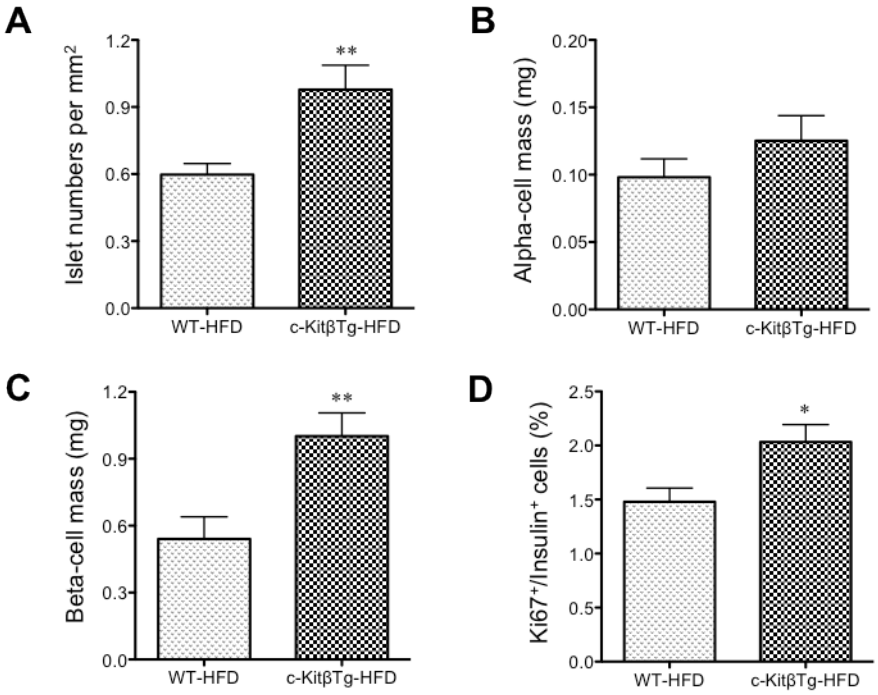
A
Islet numbers per mm2
1.2
0.9
0.6
0.3
0.0
**
WT-HFD
c-KitβTg-HFD
B
Alpha-cell mass (mg)
0.20
0.15
0.10
0.05
0.00
WT-HFD
c-KitβTg-HFD
C
Beta-cell mass (mg)
1.2
0.9
0.6
0.3
0.0
**
WT-HFD
c-KitβTg-HFD
D
Ki67+/Insulin+ cells (%)
2.5
2.0
1.5
1.0
0.5
0.0
*
WT-HFD
c-KitβTg-HFD

Figure 5-10. Effect of a HFD on islet morphology of *c-KitβTg* mice.

Morphometric analyses of islet number (**A**), alpha-cell mass (**B**), beta-cell mass (**C**), and percentage of $Ki67^{+}$ beta-cells (**D**) in *WT-HFD* and *c-KitβTg-HFD* mice. Data (**A-D**) are expressed as mean ± SEM (*n=6-7*), **p*<0.05, ***p*<0.01 analyzed by unpaired student's *t*-test.

5.3.6 *c-Kit*$^{Wv/+}$ mice with specific overexpression of *c-KIT* in beta-cells display normal glucose metabolism

c-Kit$^{Wv/+}$ mice were bred with *c-KitβTg* mice to determine whether *c-KIT* overexpression in beta-cells could rescue animals with the *c-Kit* W^v mutation from early onset of diabetes. *WT*, *c-KitβTg* and *c-KitβTg;Wv* mice exhibited similar fasting blood glucose levels, with a significant improvement in fasting blood glucose levels being noted in *c-KitβTg;Wv* compared with *c-Kit*$^{Wv/+}$ mice (Figure 5-11A). *c-KitβTg;Wv* mice also had a similar glucose tolerance capacity to that of *WT* and *c-KitβTg* groups, and also displayed significant decreases in the AUC (Figure 5-11B). The IPITT revealed no differences between the experimental groups (Figure 5-11C). Significantly improved GSIS was observed at 5 and 35 minutes in *c-KitβTg;Wv* mice compared with *c-Kit*$^{Wv/+}$ mice (Figure 5-11D). To further confirm islet function, an *ex vivo* GSIS study was conducted. Insulin secretion in response to a 22 mmol/L glucose challenge in *c-KitβTg;Wv* islets was similar to that in *WT* and *c-KitβTg* islets (Figure 5-11E), but significantly higher than that of *c-Kit*$^{Wv/+}$ islets (Figure 5-11E). These results indicate that the *c-Kit* point mutation is directly responsible for defective beta-cell function in *c-Kit*$^{Wv/+}$ mice and that *c-KIT* overexpression was able to preserve beta-cell function in *c-Kit*$^{Wv/+}$ mice.

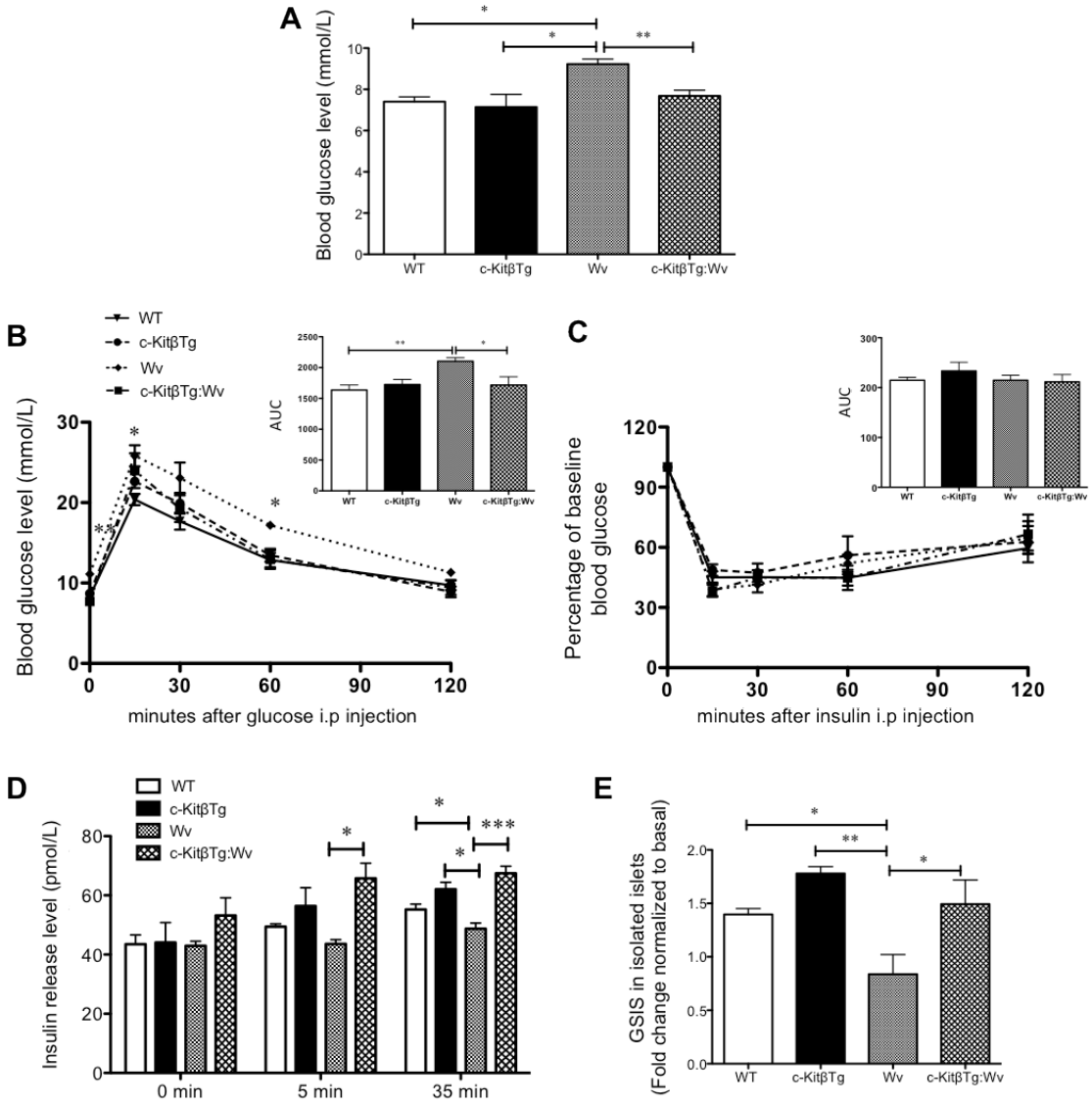
A
Blood glucose level (mmol/L)
WT
c-KitβTg
Wv
c-KitβTg:Wv
B
WT
c-KitβTg
Wv
c-KitβTg:Wv
Blood glucose level (mmol/L)
minutes after glucose i.p injection
AUC
C
Percentage of baseline blood glucose
minutes after insulin i.p injection
AUC
D
Insulin release level (pmol/L)
0 min
5 min
35 min
E
GSIS in isolated islets
(Fold change normalized to basal)

Figure 5-11. Glucose tolerance and insulin secretion in *c-KitβTg;Wv* mice.

(**A**) 4-hour fasting blood glucose levels, (**B**) IPGTT, and (**C**) IPITT in *WT*, *c-KitβTg*, *c-Kit*$^{Wv/+}$ and *c-KitβTg;Wv* mice at 8 weeks of age. Glucose responsiveness of the corresponding experimental groups is shown as the AUC of the IPGTT (**B**, insert) or IPITT (**C**, insert) graphs with units of (mmol/L x minutes). (**D**) *In vivo* GSIS of *WT* (white bars), *c-KitβTg* (black bars), *c-Kit*$^{Wv/+}$ (grey bars) and *c-KitβTg;Wv* (dotted bars) mice. (**E**) *Ex vivo* GSIS on isolated islets from *c-KitβTg;Wv* mice are improved in response to a 22 mmol/L glucose challenge. Data are expressed as fold change normalized to basal (2.2 mM glucose) secretion. Data (**A-E**) are expressed as mean ± SEM (*n=3-8*), **p*<0.05, ***p*<0.01, and ****p*<0.001 analyzed by one-way ANOVA followed by LSD *post-hoc* test.

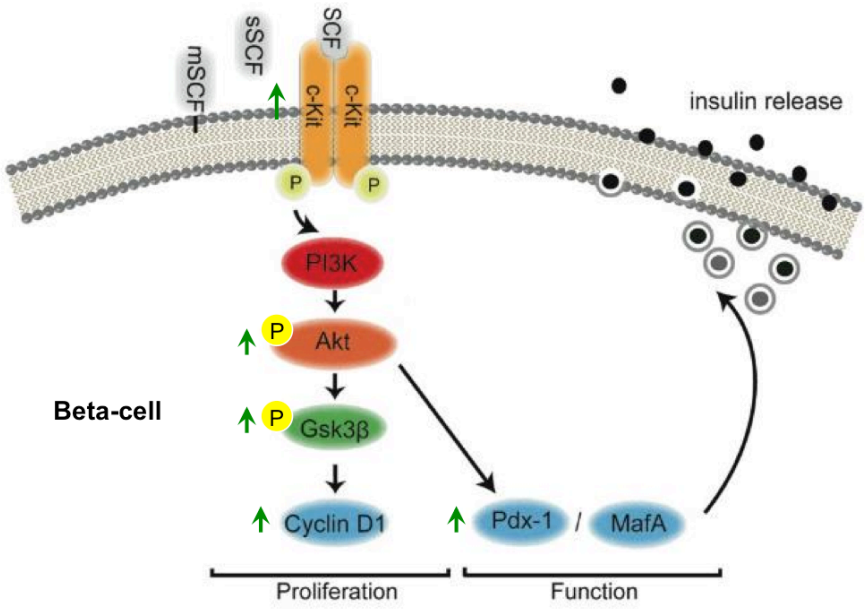
sSCF
SCF
mSCF
c-Kit
c-Kit
P
P
insulin release
PI3K
P
Akt
Beta-cell
P
Gsk3β
Cyclin D1
Pdx-1
/
MafA
Proliferation
Function

Figure 5-12. A proposed model of SCF/c-Kit signaling to mediate beta-cell proliferation and function.

SCF/c-Kit interaction activates the PI3K/Akt/Gskβ pathway. This leads to increased cyclin D1, Pdx-1 and MafA expressions which are important to beta-cell proliferation, and function. sSCF: soluble SCF; mSCF: membrane-bound SCF. Green arrow: positive signaling.

5.4 Discussion

Here, we demonstrated that *c-KIT* overexpression in beta-cells confers improved glucose metabolism by enhancing insulin secretion, and increasing beta-cell mass and proliferation, probably through activation of the PI3K/Akt signaling pathway. When *c-KitβTg* mice were subjected to a HFD, they displayed resistance to HFD-induced glucose intolerance and preserved beta-cell function relative to *WT* littermates. Moreover, *c-KitβTg* mice were protected against early onset of diabetes. These results clearly indicate that c-Kit is intrinsic to beta-cell function and proliferation. This effect is mediated by the regulation of key beta-cell transcription factors (e.g. Pdx-1 and MafA) and possibly through activation of downstream PI3K/Akt signaling (Figure 5-12).

Compared with *WT* mice, *c-KitβTg* mice had significantly lower overnight fasting blood glucose levels, improved glucose tolerance and enhanced GSIS. The improvement in glucose metabolism of *c-KitβTg* mice was associated with an increase in beta-cell mass and proliferation, as well as in *Glut2* and *Glp1r* expression. These results corroborate our previous finding of glucose intolerance in *c-Kit*$^{Wv/+}$ mice [12]. We monitored *c-KitβTg* mice up to 40 weeks of age and did not detect any abnormal cell growth or islet tumors (data not shown), indicating that beta-cell specific *c-KIT* overexpression does not lead to malignancy. We detected a significant increase in *SCF* mRNA, but only a modest increase in the corresponding protein. This is likely to be due to our western blotting technique, which could only detect membrane-associated, not soluble, SCF. Nevertheless, the concentration of SCF may be in excess and is sufficient to interact with the increased number of c-Kit (~25%) to transduce markedly enhanced intracellular signals in *c-KitβTg* mice. Our data indicate that c-Kit overabundance in beta-cells enhances glucose tolerance and beta-cell function in males. These sex-related differences in glucose metabolism are consistent with our previous results using *c-Kit*$^{Wv/+}$ mice and conditional β1 integrin knockout mice [12, 14], and have also been described in other mouse models indicating that the sex-related differences may involve other pathways, such as the contribution of estrogen to glucose homeostasis in female rodents [15, 16].

Significantly increased *Pdx-1* mRNA and protein abundance was observed in *c-KitβTg* mice. We previously reported that SCF-stimulated c-KIT activity leads to increased *PDX-1* mRNA expression in human fetal islet-epithelial clusters [7], while *c-Kit*$^{Wv/+}$ mice showed a significant reduction in *Pdx-1* expression in islets [12]. It is well documented that Pdx-1 is integral to normal pancreas development and beta-cell function [17]. In addition to beta-cell proliferation [18], *Pdx-1* expression is also required for modulation of *insulin* gene expression and glucose metabolism [19]. Our results showed that *c-KitβTg* islets exhibited high Pdx-1 levels and had increased beta-cell proliferation and mass, confirming a correlation between Pdx-1 and islet beta-cell replication. Indeed, the enhanced islet insulin secretion in response to a high glucose challenge and the improved glucose tolerance observed in *c-KitβTg* mice may also be due to increased islet Pdx-1 abundance. Interestingly, significant up-regulation of *MafA* mRNA was observed in *c-KitβTg* mice. MafA binds to the C1 element of the *insulin* gene to modulate *insulin* gene transcription and enhance beta-cell maturation [20]. *MafA*-null mice had a defect only in adult islet architecture and beta-cell activity, while MafA overproduction enhanced beta-cell insulin biosynthesis and secretion through up-regulation of important beta-cell genes, including *Pdx1*, *Neurod1*, *Nkx6.1* and *Glp1r* [21]. Moreover, overexpression of *MafA* in neonatal rat beta-cells led to enhanced glucose-responsive insulin secretion and beta-cell maturation [22]. Thus, improved glucose metabolism and insulin secretion in *c-KitβTg* mice may be due to increased c-Kit stimulation of islet *Pdx-1* and *MafA* expression.

The molecular mechanisms associated with the phenotypic changes observed in *c-KitβTg* mice include significant up-regulation of phospho-Akt and phospho-Gsk3β in beta-cells. Our previous *in vitro* study on human fetal islet-epithelial clusters demonstrated that increased SCF/c-KIT interactions resulted in up-regulation of PI3K/AKT, but not of ERK pathway signaling [7]. In this study, we also observed significant increases in Akt and Gsk3β phosphorylation together with up-regulation of cyclin D1 in islets isolated from *c-KitβTg* mice. These results suggest that c-Kit might stimulate beta-cell function and proliferation via direct activation of the Akt/Gsk3β/cyclin D1 pathways [7, 23], in association with Pdx-1 and MafA-induced insulin secretion. Islets of beta-cell specific *Gsk3β* ablated mice had increased beta-cell mass with lower fasting blood glucose,

along with improved glucose tolerance and GSIS [24]. In contrast, the Akt/Gsk3β signaling pathway is significantly down-regulated in *c-Kit*$^{Wv/+}$ mouse islets [13]. Taken together, these results suggest that Akt/Gsk3β/cyclin D1 signaling downstream of c-Kit is essential for beta-cell function.

HFD treatment is detrimental to beta-cell function and insulin sensitivity in mice [25, 26], and leads to impaired glucose tolerance due to insulin resistance and insufficient beta-cell insulin secretion [25-28]. *c-KitβTg* and *WT* mice maintained on a HFD showed similar food intake and weight gain. Importantly, *c-KitβTg-HFD* mice exhibited significantly improved glucose tolerance and GSIS, supporting the notion that c-Kit has a direct effect on beta-cell function via up-regulation the PI3K/Akt signaling pathway, which enables *c-KitβTg-HFD* mice to tolerate HFD-induced diabetes.

Finally, we bred *c-KitβTg* with *c-Kit*$^{Wv/+}$ mice to determine whether *c-KIT* overexpression could prevent beta-cell dysfunction in *c-Kit*$^{Wv/+}$ mice. Our results showed that *c-KitβTg;Wv* mice displayed normal fasting glycaemia and glucose tolerance, as well as enhanced glucose-induced insulin secretion. This marked improvement in glucose metabolism in *c-KitβTg;Wv* mice provided direct evidence of a primary effect of c-Kit on beta-cell function.

In summary, we showed that *c-KIT* overexpression in beta-cells led to improved beta-cell proliferation and function, and protected mice from HFD-induced diabetes. Furthermore, beta-cell specific overexpression of *c-KIT* was able to prevent beta-cell defects in *c-Kit*$^{Wv/+}$ mice. This study provides direct evidence to support the notion that c-Kit plays a primary physiological role in beta-cells, and thus may help efforts to develop gene and cell therapeutic schemes for patients with diabetes.

5.5 References

1. Oberg-Welsh C, Welsh M (1996) Effects of certain growth factors on in vitro maturation of rat fetal islet-like structures. Pancreas 12:334–339.

2. Oberg C, Waltenberger J, Claesson-Welsh L, Welsh M (1994) Expression of protein tyrosine kinases in islet cells: possible role of the Flk-1 receptor for beta-cell maturation from duct cells. Growth Factors 10:115–126.

3. LeBras S, Czernichow P, Scharfmann R (1998) A search for tyrosine kinase receptors expressed in the rat embryonic pancreas. Diabetologia 41:1474–1481. doi: 10.1007/s001250051094

4. Rachdi L, Ghazi El L, Bernex F, et al. (2001) Expression of the receptor tyrosine kinase KIT in mature beta-cells and in the pancreas in development. Diabetes 50:2021–2028.

5. Yashpal NK, Li J, Wang R (2004) Characterization of c-Kit and nestin expression during islet cell development in the prenatal and postnatal rat pancreas. Dev Dyn 229:813–825. doi: 10.1002/dvdy.10496

6. Li J, Quirt J, Do HQ, et al. (2007) Expression of c-Kit receptor tyrosine kinase and effect on beta-cell development in the human fetal pancreas. Am J Physiol Endocrinol Metab 293:E475–83. doi: 10.1152/ajpendo.00172.2007

7. Li J, Goodyer CG, Fellows F, Wang R (2006) Stem cell factor/c-Kit interactions regulate human islet-epithelial cluster proliferation and differentiation. Int J Biochem Cell Biol 38:961–972. doi: 10.1016/j.biocel.2005.08.014

8. Wang R, Li J, Yashpal N (2004) Phenotypic analysis of c-Kit expression in epithelial monolayers derived from postnatal rat pancreatic islets. J Endocrinol 182:113–122.

9. Peters K, Panienka R, Li J, et al. (2005) Expression of stem cell markers and transcription factors during the remodeling of the rat pancreas after duct ligation. Virchows Arch 446:56–63. doi: 10.1007/s00428-004-1145-7

10. Tiemann K, Panienka R, Klöppel G (2007) Expression of transcription factors and precursor cell markers during regeneration of beta cells in pancreata of rats treated with streptozotocin. Virchows Arch 450:261–266. doi: 10.1007/s00428-006-0349-4

11. Bernex F, De Sepulveda P, Kress C, et al. (1996) Spatial and temporal patterns of c-kit-expressing cells in WlacZ/+ and WlacZ/WlacZ mouse embryos. Development 122:3023–3033.

12. Krishnamurthy M, Ayazi F, Li J, et al. (2007) c-Kit in early onset of diabetes: a morphological and functional analysis of pancreatic beta-cells in c-KitW-v mutant mice. Endocrinology 148:5520–5530. doi: 10.1210/en.2007-0387

13. Feng Z-C, Donnelly L, Li J, et al. (2012) Inhibition of Gsk3β activity improves β-cell function in c-KitWv/+ male mice. Lab Invest 92:543–555. doi: 10.1038/labinvest.2011.200

14. Riopel M, Krishnamurthy M, Li J, et al. (2011) Conditional β1-integrin-deficient mice display impaired pancreatic β cell function. J Pathol 224:45–55. doi: 10.1002/path.2849

15. Liu S, Mauvais-Jarvis F (2010) Minireview: Estrogenic protection of beta-cell failure in metabolic diseases. Endocrinology 151:859–864. doi: 10.1210/en.2009-1107

16. Geisler JG, Zawalich W, Zawalich K, et al. (2002) Estrogen can prevent or reverse obesity and diabetes in mice expressing human islet amyloid polypeptide. Diabetes 51:2158–2169.

17. Ahlgren U, Jonsson J, Jonsson L, et al. (1998) beta-cell-specific inactivation of the mouse Ipf1/Pdx1 gene results in loss of the beta-cell phenotype and maturity onset diabetes. Genes Dev 12:1763–1768.

18. Dutta S, Gannon M, Peers B, et al. (2001) PDX:PBX complexes are required for normal proliferation of pancreatic cells during development. Proc Natl Acad Sci USA 98:1065–1070. doi: 10.1073/pnas.031561298

19. Brissova M, Shiota M, Nicholson WE, et al. (2002) Reduction in pancreatic transcription factor PDX-1 impairs glucose-stimulated insulin secretion. J Biol Chem 277:11225–11232. doi: 10.1074/jbc.M111272200

20. Nishimura W, Bonner-Weir S, Sharma A (2009) Expression of MafA in pancreatic progenitors is detrimental for pancreatic development. Dev Biol 333:108–120. doi: 10.1016/j.ydbio.2009.06.029

21. Wang H, Brun T, Kataoka K, et al. (2007) MAFA controls genes implicated in insulin biosynthesis and secretion. Diabetologia 50:348–358. doi: 10.1007/s00125-006-0490-2

22. Aguayo-Mazzucato C, Koh A, Khattabi El I, et al. (2011) Mafa expression enhances glucose-responsive insulin secretion in neonatal rat beta cells. Diabetologia 54:583–593. doi: 10.1007/s00125-010-2026-z

23. Kushner JA, Ciemerych MA, Sicinska E, et al. (2005) Cyclins D2 and D1 are essential for postnatal pancreatic beta-cell growth. Mol Cell Biol 25:3752–3762. doi: 10.1128/MCB.25.9.3752-3762.2005

24. Liu Y, Tanabe K, Baronnier D, et al. (2010) Conditional ablation of Gsk-3β in islet beta cells results in expanded mass and resistance to fat feeding-induced diabetes in mice. Diabetologia 53:2600–2610. doi: 10.1007/s00125-010-1882-x

25. Qiu L, List EO, Kopchick JJ (2005) Differentially expressed proteins in the pancreas of diet-induced diabetic mice. Mol Cell Proteomics 4:1311–1318. doi: 10.1074/mcp.M500016-MCP200

26. Lewis GF, Carpentier A, Adeli K, Giacca A (2002) Disordered fat storage and mobilization in the pathogenesis of insulin resistance and type 2 diabetes. Endocr Rev 23:201–229. doi: 10.1210/edrv.23.2.0461

27. Ahrén B, Simonsson E, Scheurink AJ, et al. (1997) Dissociated insulinotropic sensitivity to glucose and carbachol in high-fat diet-induced insulin resistance in C57BL/6J mice. Metab Clin Exp 46:97–106.

28. Ahrén B, Pacini G (2002) Insufficient islet compensation to insulin resistance vs. reduced glucose effectiveness in glucose-intolerant mice. Am J Physiol Endocrinol Metab 283:E738–44. doi: 10.1152/ajpendo.00199.2002

Chapter 6

6 c-Kit-mediated VEGF-A production regulates islet microvasculature, beta-cell survival, and function *in vivo*[5]

[5] This chapter has been modified and adapted from the following manuscript:

- **Feng ZC**, Popell A, Li J, Silverstein J, Yee SP, Wang R. c-Kit receptor tyrosine regulates islet microvasculature, beta-cell survival and function *in vivo*. Manuscript in submission 2014.

6.1 Introduction

Islet angiogenesis and innervation are required for proper endocrine pancreatic organogenesis and function [1-3]. The vascular niche that provides oxygen, exchanges nutrients and metabolites to support beta-cell survival [4], also exposes islets to inflammatory cytokines in the setting of diabetes [5, 6]. Hence, the precise regulation of islet angiogenesis plays a prominent role in the modulation of beta-cell survival and insulin production. One pro-angiogenic factor, vascular endothelial growth factor (VEGF), is produced by the beta-cell and plays a critical role in promoting and maintaining islet vascularization [4, 7, 8].

SCF/c-Kit interactions are implicated in the regulation of angiogenesis. Past studies showed that the high co-expression of c-Kit and SCF is associated with increased microvessel density and VEGF expression in multiple neoplasms [9-11]. SCF treatment of multiple c-Kit-expressing cancer cell lines revealed a significant stimulatory effect on VEGF secretion and, conversely, inhibition of c-Kit signaling by imatinib led to reduced VEGF expression [12-14]. Previous studies reported that bone marrow stem/progenitor cells expressing c-Kit established a proangiogenic milieu by releasing VEGF [15, 16]; however, a mutation in *c-Kit* prevents angiogenesis, interfering with myocardial repair tissue formation [16]. Furthermore, c-Kit activity was implicated in mobilization of endothelial progenitor cells required for angiogenesis, and SCF was able to enhance the neovascularization of human endothelial progenitor cells [17, 18]. Transplantation of c-Kit-expressing vascular endothelial progenitor cells could generate functional blood vessels *in vivo*, but inactivation of c-Kit resulted in impaired endothelial cell proliferation and angiogenesis [19]. Taken together, these studies reveal a remarkable correlation between c-Kit and VEGF-driven angiogenesis.

Although c-Kit has been studied in human and murine pancreatic cells, its involvement in the regulation of VEGF production in islets has not been evaluated. Of the six identified members in the VEGF family, the pancreatic beta-cell produces significant levels of VEGF-A, primarily the VEGF-A 120 and VEGF-A 164 isoforms. Prior studies using the genetic mouse model with *VEGF-A* deficit in beta-cells have demonstrated that there is causal effect between VEGF-A production and proper islet vascular development: the

functional vascular niche is not only required for the assembly of complex coordinated islet architecture, but also for normal islet cell function [2, 4, 8]. In this study, we hypothesized that c-Kit-dependent regulation of VEGF-A is critical for islet vasculature, maintaining islet function and survival. Using the *c-Kit W*^{v} mutant (*c-Kit*$^{Wv/+}$) and beta-cell-specific *c-KIT* overexpressing (*c-KitβTg)* mouse models, we aimed to characterize the functional role of SCF/c-Kit interactions in mediating VEGF-A production, islet angiogenesis, as well as beta-cell function and survival under normal diet, and long-term HFD conditions.

6.2 Materials and methods

Mouse model: 1) cross-breeding *c-Kit*$^{Wv/+}$ with *c-KitβTg* mice generated wild-type (*WT*), *c-Kit*$^{Wv/+}$, *c-KitβTg*, and *c-KitβTg;c-Kit*$^{Wv/+}$ (*c-KitβTg;Wv*), and these four experimental groups under normal diet were maintained until 8 weeks of age at which point, islet vascular morphological studies, and islet protein analyses were performed. 2) *WT* and *c-KitβTg* mice were subjected to either normal diet, or HFD for 20 weeks starting at 6 weeks of age at which point, metabolic studies, islet morphological studies, pancreatic vascular morphological studies, and islet protein analyses were performed. Only male mice were used for this study. Generation of animal models was detailed in section 2.1.4, and genotyping was detailed in section 2.2.

Metabolic studies: Body weight, blood glucose levels (non-fasting, 4-hour and overnight fasting (16-hour)), IPGTT and IPITT analyses were performed on mice in the normal diet study, and the HFD study, as detailed in section 2.3.

Immunofluorescence and morphometric analyses: Pancreatic tissue sections from mice were prepared and double-stained with appropriate antibodies listed in Appendix 5. Islet number, islet size, alpha and beta-cell mass was measured. Islet capillary density, capillary area per islet, average islet capillary size and diameter, and pancreatic exocrine vasculature including exocrine capillary density, and exocrine capillary area were quantified. Proliferation (Ki67^{+} labeling), apoptosis (TUNEL^{+} labeling), Pdx-1, Nkx6.1, E-cad (E-cadherin), PECAM-1 positive staining in beta-cell nuclei was determined by

double immunofluorescence staining. $MafA^{+}$ staining in pancreatic islets was determined by immunohistochemical staining, as detailed in section 2.7.

Protein extraction and western blot analyses: protein levels of phospho-Akt^{S473}, total Akt, phospho-$P70S6K^{T389}$, total P70S6K, phospho-$NF\kappa Bp65^{S536}$, total NFκBp65, Pdx-1, VEGF-A, PECAM-1, E-cad, cleaved-$PARP^{D214}$ (cleaved-Poly ADP ribose polymerase), total PARP, Mac-2 (Galectin-3), IL-1β, TNF-α (Tumor necrosis factor-α), and corresponding housekeeping protein GAPDH (Glyceraldehyde 3-phosphate dehydrogenase) from isolated mouse islets was analyzed (Appendix 6), as detailed in section 2.8.

6.3 Results

6.3.1 c-Kit function is required for maintaining the normal islet microvasculature *in vivo*

To investigate the role of c-Kit in islet microvasculature *in vivo*, we examined endothelial cells in 8-week-old mouse pancreatic sections using an immunostaining approach. We observed a reduced staining for $PECAM\text{-}1^{+}$ (specific label for endothelial cells) (Figure 6-1A) but no substantial change in islet capillary number (Figure 6-1B) in *c-Kit*$^{Wv/+}$ mouse islets compared to *WT* group. However, significantly decreased blood vessel area over islet area was found in *c-Kit*$^{Wv/+}$ mouse islets, compared to *WT* by 8 weeks of age (Figure 6-1C). Intra-islet vessels were also significantly smaller in *c-Kit*$^{Wv/+}$ mouse islets, as reflected by a 50% reduction in the average islet capillary size (*vs. WT* islets, Figure 6-1D). This was confirmed by measurement of the internal capillary diameter that showed ~30% reduction in *c-Kit*$^{Wv/+}$ mouse islets when compared to *WT* (Figure 6-1E). In contrast to *c-Kit*$^{Wv/+}$ mice, there was a significant improvement in islet capillary density and area in *c-KitβTg;Wv* mouse islets (*vs. c-Kit*$^{Wv/+}$ islets, Figure 6-1B and C). Furthermore, there was ~30% relative increase in average islet capillary size in *c-KitβTg;Wv* mouse islets (*vs. c-Kit*$^{Wv/+}$ islet, Figure 6-1D) along with significantly increased capillary diameter (*vs. c-Kit*$^{Wv/+}$ islet, Figure 6-1E). No signficiant changes in islet vasculature were observed in *c-KitβTg* mice. These data indicate that c-Kit function is required for maintaining the normal islet vasculature.

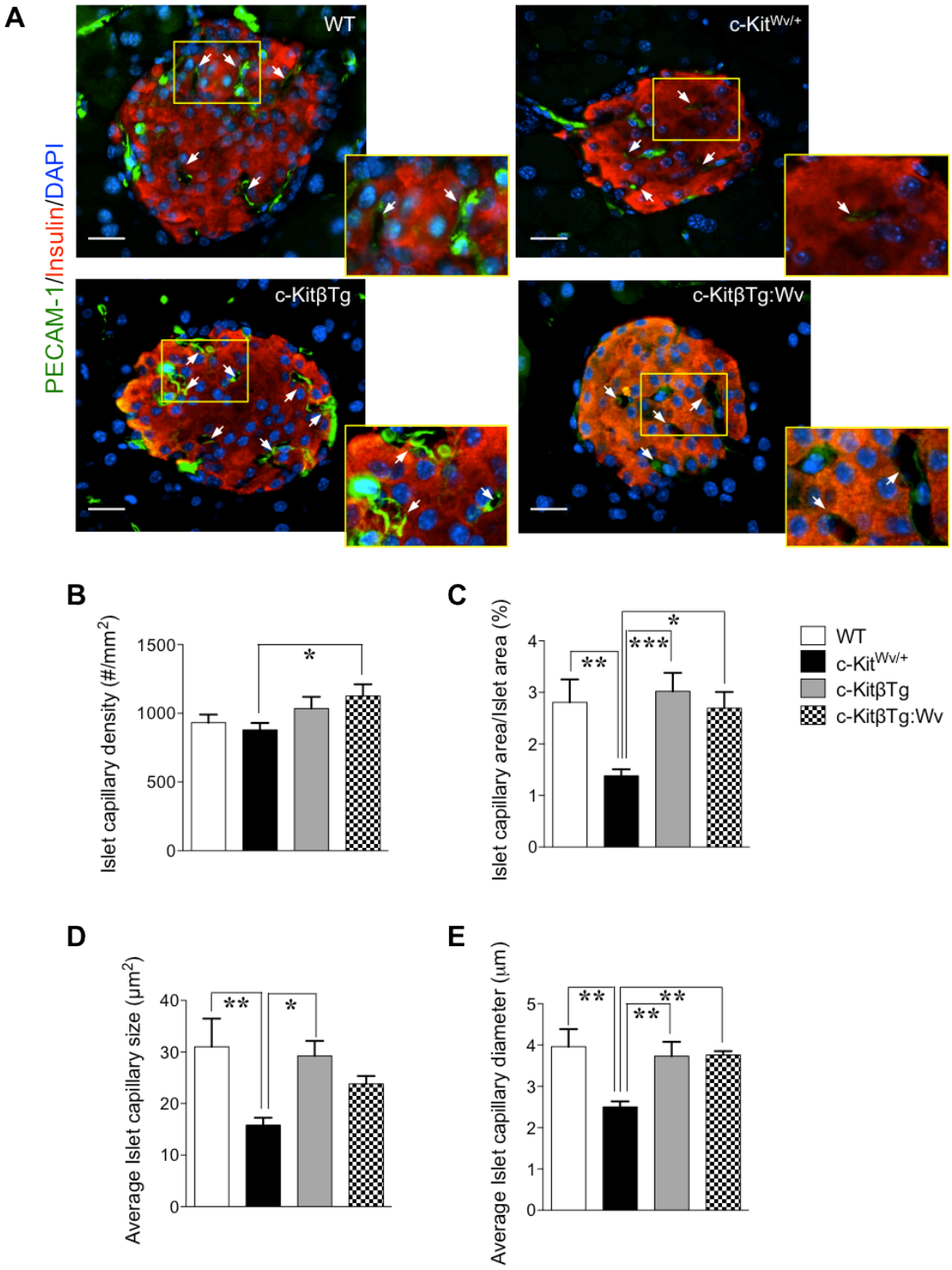
A
WT
c-Kit^Wv/+
c-KitβTg
c-KitβTg:Wv
PECAM-1/Insulin/DAPI
B
Islet capillary density (#/mm2)
1500
1000
500
0
*
C
Islet capillary area/Islet area (%)
4
3
2
1
0
**
***
*
WT
c-Kit^Wv/+
c-KitβTg
c-KitβTg:Wv
D
Average Islet capillary size (μm2)
40
30
20
10
0
**
*
E
Average Islet capillary diameter (μm)
5
4
3
2
1
0
**
**

Figure 6-1. Overexpressing *c-KIT* in beta-cells rescues loss of islet microvasculature in *c-Kit*$^{Wv/+}$ mice.

(**A**) Representative images of PECAM-1 (green) co-stained with insulin (red), and nuclei stain DAPI (blue) of 8-week-old *WT*, *c-Kit*$^{Wv/+}$, *c-KitβTg*, and *c-KitβTg;Wv* pancreatic sections. Scale bar, 25 μm. Magnified images are shown in insets. Arrows: PECAM-1^{+} cells in the islets. Quantitative analyses between all experimental groups of islet capillary density (**B**), capillary area per islet (**C**), average islet capillary size (**D**), and average islet capillary diameter (**E**). Data (**B**-**E**) are expressed as mean ± SEM ($n=5$), *$p<0.05$, **$p<0.01$ and ***$p<0.001$ analyzed by one-way ANOVA followed by LSD *post-hoc* test.

6.3.2 Beta-cell specific c-Kit maintains islet microvasculature via the PI3K/Akt/mTOR pathway and VEGF-A production *in vivo*

We next sought to determine the underlying mechanisms by which c-Kit regulates islet microvasculature *in vivo*. Using isolated islets from pancreata of 8-week-old *WT*, *c-Kit*$^{Wv/+}$, *c-KitβTg*, and *c-KitβTg;Wv* mice, we found a significant decrease in phosphorylation of Akt, P70S6K, and p65NF-κB in *c-Kit*$^{Wv/+}$ mouse islets (Figure 6-2A), which were associated with a reduced level of Pdx-1 protein (Figure 6-2B). However, when c-Kit function was restored in *c-Kit*$^{Wv/+}$ beta-cells, the Akt/mTOR/p65NF-κB pathway was restored in parallel with increased Pdx-1 protein levels (Figure 6-2B). These findings were supported by immunostaining demonstrating that Pdx-1^{+}, Nkx6.1^{+} and MafA^{+} staining was lower in *c-Kit*$^{Wv/+}$ islets when compared to *WT* and *c-KitβTg,* as well as c-*KitβTg;Wv* groups (Figure 6-3). VEGF-A protein levels were also lower in *c-Kit*$^{Wv/+}$ islets than in *WT*, *c-KitβTg* or *c-KitβTg;Wv* islets, but this only reached significance for *c-KitβTg* mice (Figure 6-2B).

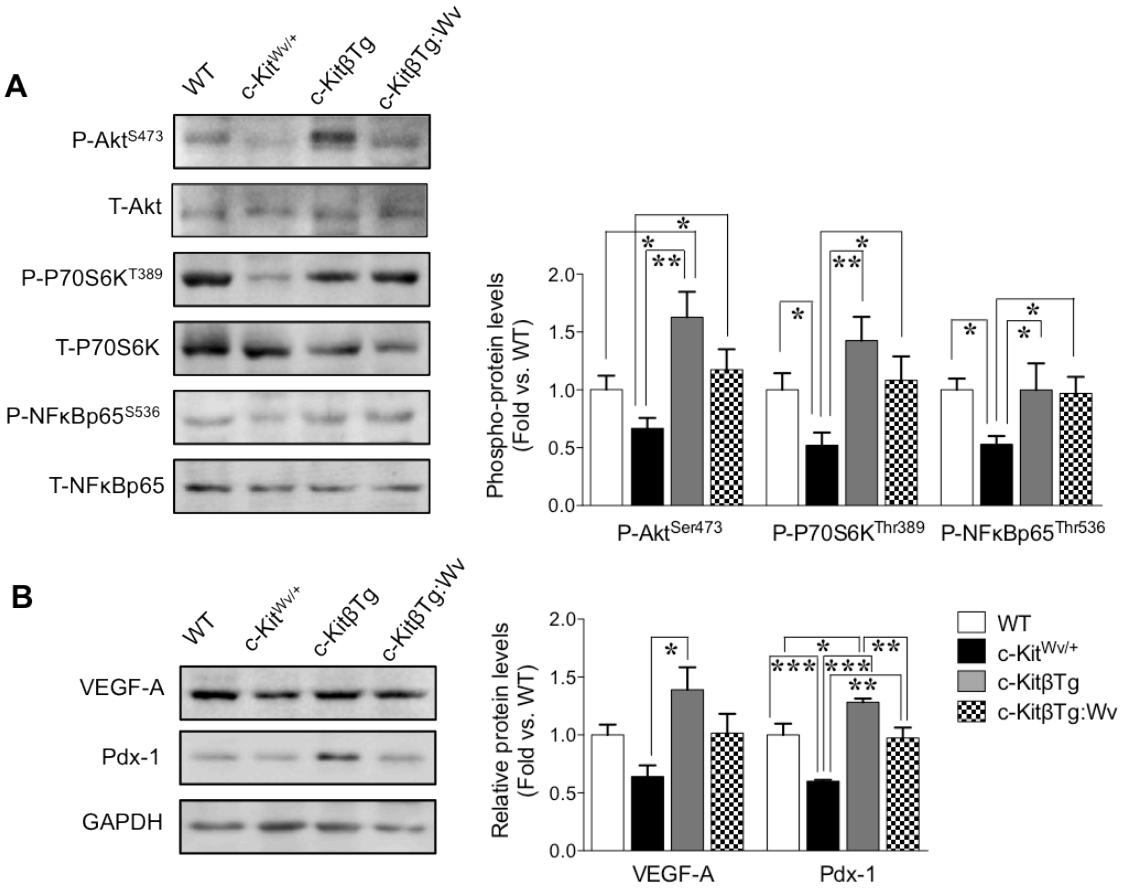
A
WT
c-Kit^Wv/+
c-KitβTg
c-KitβTg:Wv
P-Akt^S473
T-Akt
P-P70S6K^T389
T-P70S6K
P-NFκBp65^S536
T-NFκBp65
Phospho-protein levels (Fold vs. WT)
2.0
1.5
1.0
0.5
0.0
P-Akt^Ser473
P-P70S6K^Thr389
P-NFκBp65^Thr536
B
VEGF-A
Pdx-1
GAPDH
Relative protein levels (Fold vs. WT)
WT
c-Kit^Wv/+
c-KitβTg
c-KitβTg:Wv

Figure 6-2. Rescued islet microvasculature is associated with increased c-Kit-mediated VEGF-A production via the PI3K/mTOR pathway in *c-KitβTg;Wv* mice.

(**A**) Western blot analyses of S473-phosphorylated (P) and total (T) Akt, T389 P-P70S6K and T-P70S6K, S536 P-NFκBp65 and T-NFκBp65, and (**B**) VEGF-A and Pdx-1 abundance in islets isolated from 8-week-old *WT*, *c-Kit*$^{Wv/+}$, *c-KitβTg*, and *c-KitβTg;Wv* mice. Representative blots are shown. Data (**A** and **B**) are expressed as mean ± SEM (*n=4-5*), **p*<0.05, ***p*<0.01 and ****p*<0.001 analyzed by one-way ANOVA followed by LSD *post-hoc* test.

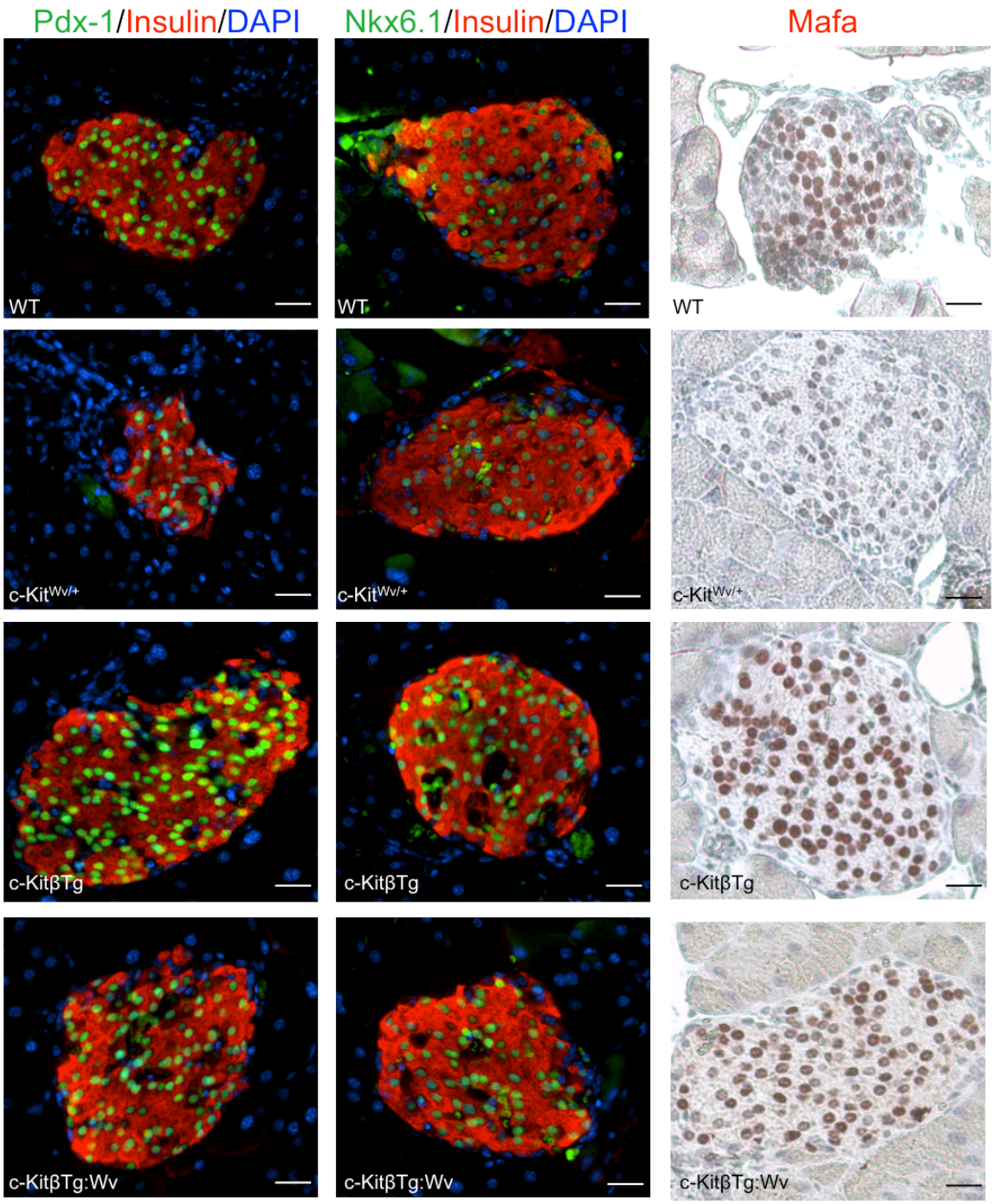
Pdx-1/Insulin/DAPI
Nkx6.1/Insulin/DAPI
Mafa
WT
WT
WT
c-Kit^Wv/+
c-Kit^Wv/+
c-Kit^Wv/+
c-KitβTg
c-KitβTg
c-KitβTg
c-KitβTg:Wv
c-KitβTg:Wv
c-KitβTg:Wv

Figure 6-3. Expression of islet transcription factors in *c-KitβTg;Wv* mice.

Double immunofluorescence staining of 8-week-old *WT*, *c-Kit*$^{Wv/+}$, *c-KitβTg* and *c-KitβTg;Wv* pancreatic sections for transcription factors Pdx-1 or Nkx6.1 (green) with insulin (red) and nuclei stained with DAPI (blue). Immunohistochemistry staining for MafA (red in nuclei). Representative images are shown. Scale bar 25 μm.

6.3.3 *c-KIT* overexpression in beta-cell promotes islet angiogenesis *in vivo*

We further examined the role of c-Kit in islet vasculature in aged (28-week-old) *WT* and *c-KitβTg* mice. Double immunofluorescence for PECAM-1 and insulin showed an increased number of PECAM-1^+ cells in *c-KitβTg* mouse islets (Figure 6-4A), which was correlated with an increase in capillary density and vessel area-to-islet area ratio (Figure 6-4B and C) when compared to *WT* mouse islets. However, no changes in average islet capillary size or diameter (Figure 6-4D and E), and no differences in the vasculature of pancreatic exocrine tissue were observed in *c-KitβTg* mice as compared to *WT* group (Figure 6-4F and G). The observed changes in islet vasculature were supported by western blot analyses showing ~40% increase in islet VEGF-A content, with a similar increase in PECAM-1 protein levels (Figure 6-4H).

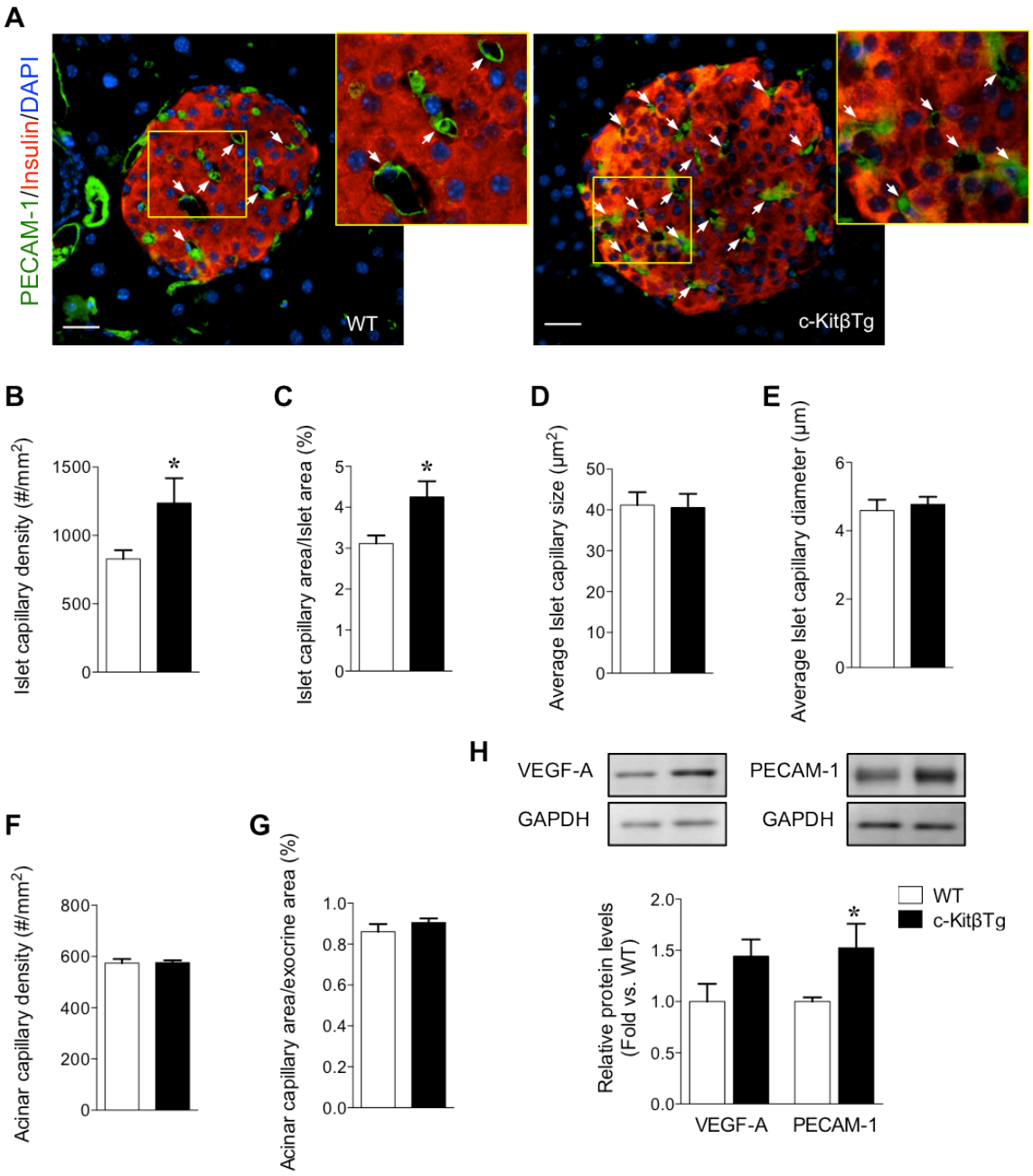
A
PECAM-1/Insulin/DAPI
WT
c-KitβTg
B
Islet capillary density (#/mm2)
1500
1000
500
0
*
C
Islet capillary area/Islet area (%)
5
4
3
2
1
0
*
D
Average Islet capillary size (μm2)
50
40
30
20
10
0
E
Average Islet capillary diameter (μm)
6
4
2
0
F
Acinar capillary density (#/mm2)
800
600
400
200
0
G
Acinar capillary area/exocrine area (%)
1.0
0.8
0.6
0.4
0.2
0.0
H
VEGF-A
GAPDH
PECAM-1
GAPDH
WT
c-KitβTg
Relative protein levels (Fold vs. WT)
2.0
1.5
1.0
0.5
0.0
*
VEGF-A
PECAM-1

Figure 6-4. Beta-cell specific *c-KIT* overexpression promotes islet angiogenesis *in vivo*.

Islet microvasculature morphology was analyzed in 28-week-old *WT* and *c-KitβTg* mice. (**A**) Representative images of PECAM-1 (green) co-stained with insulin (red). Nuclei were stained with DAPI (blue). Scale bar 25μm. Magnified images are shown in insets. Arrows: PECAM-1^+ cells in the islets. Quantitative analyses of islet capillary density (**B**), islet capillary area per islet (**C**), average islet capillary size (**D**), average islet capillary diameter (**E**), exocrine capillary density (**F**), and exocrine capillary area (**G**), and western blot analyses of VEGF-A, and PECAM-1 protein expression in aged *c-KitβTg* mouse islets (**H**). Representative blots are shown. Data (**B**-**H**) are expressed as mean ± SEM ($n=3$-5), *$p<0.05$ analyzed by unpaired student's *t*-test.

6.3.4 *c-KIT* overexpression exaggerates islet hyper-vasculature in 28-week-old *c-KitβTg* mice under long-term HFD.

To determine whether the enhanced islet microvasculature resulting from overexpression of *c-KIT* in beta-cell could preserve beta-cell function and survival under long-term (20-22 week) HFD, we first assessed the islet vasculature changes in *WT-HFD* and *c-KitβTg-HFD* mice. Immunostaining for PECAM-1 and insulin showed more dilated capillaries with accumulated red blood cells in *c-KitβTg-HFD* islets (Figure 6-5A). There were no observed differences in islet capillary density between the two experimental groups (Figure 6-5B). However, there was a significant increase in the overall blood vessel area-to-islet area ratio (Figure 6-5C), average islet capillary size (Figure 6-5D) and intra-islet capillary diameter found in *c-KitβTg-HFD* islets (Figure 6-5E). These results clearly demonstrated that there was an intra-islet capillary enlargement in *c-KitβTg-HFD* islets as compared to *WT-HFD* group. In contrast to the endocrine compartments, the vasculature of pancreatic exocrine tissue was unchanged (Figure 6-5F and G).

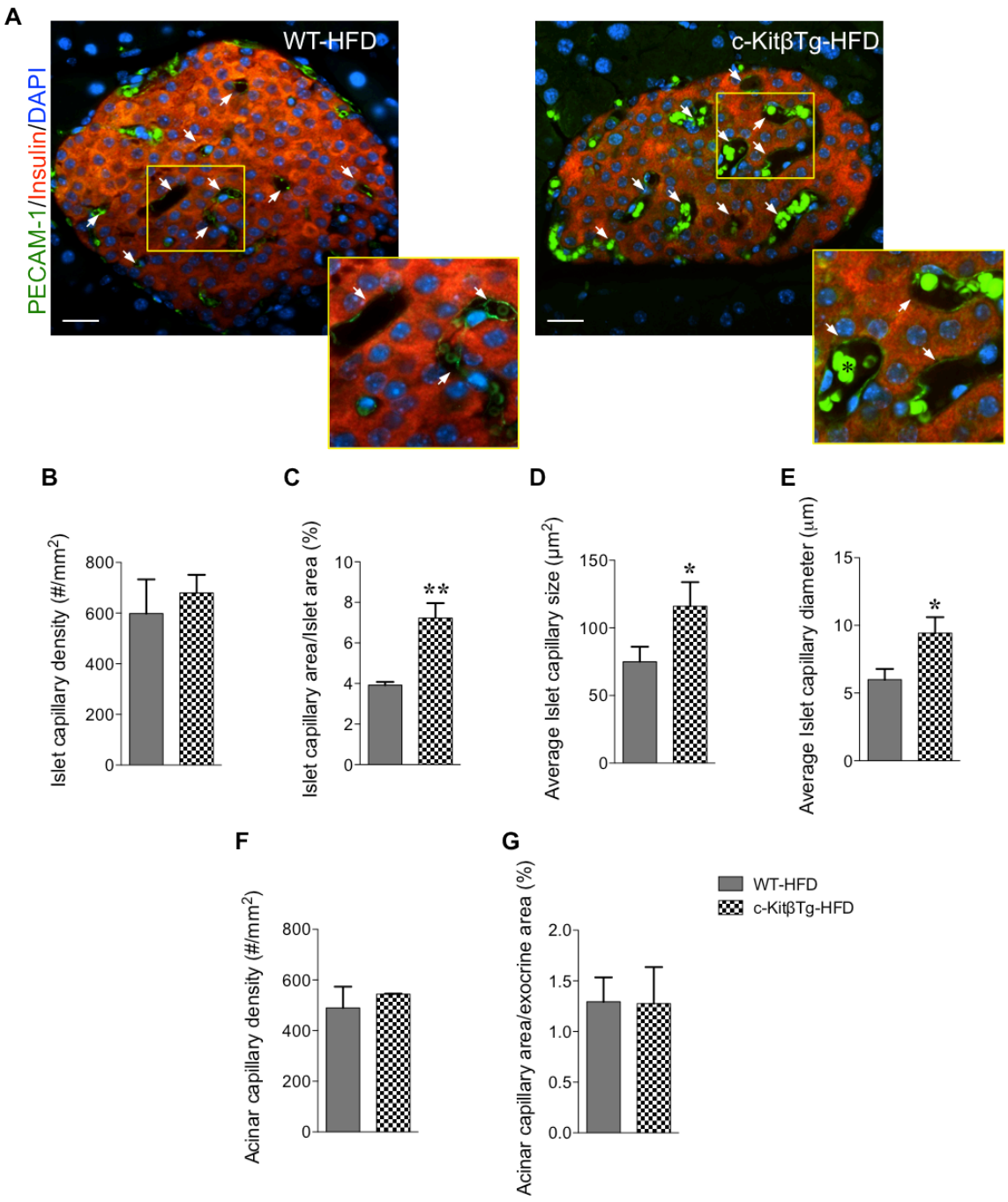
A
WT-HFD
c-KitβTg-HFD
PECAM-1/Insulin/DAPI
B
Islet capillary density (#/mm2)
800
600
400
200
0
C
Islet capillary area/Islet area (%)
10
8
6
4
2
0
**
D
Average Islet capillary size (μm2)
150
100
50
0
*
E
Average Islet capillary diameter (μm)
15
10
5
0
*
F
Acinar capillary density (#/mm2)
800
600
400
200
0
G
Acinar capillary area/exocrine area (%)
2.0
1.5
1.0
0.5
0.0
WT-HFD
c-KitβTg-HFD

Figure 6-5. Increased vessel dilation in 28-week-old *c-KitβTg* mice under long-term HFD.

(**A**) Representative images of PECAM-1 (green) co-stained with insulin (red) in 28-week-old *WT-HFD* and *c-KitβTg-HFD* pancreatic sections. Scale bar 25 μm. Magnified images are shown in insets. Arrows: PECAM-1^+ cells in islets; asterisk: red blood cells. Quantitative analyses of vasculature in endocrine (**B-E**), and exocrine compartment (**F-G**) in 28-week-old *WT-HFD* and *c-KitβTg-HFD* mice. Data (**B-G**) are expressed as mean ± SEM ($n=5$), *$p<0.05$, **$p<0.01$ analyzed by unpaired student's *t*-test.

6.3.5 *c-KIT* overexpression-induced hyper-vasculature impairs beta-cell function in 28-week-old *c-KitβTg* mice under long-term HFD

It was noted that 28-week-old *c-KitβTg* mice displayed persistently lower overnight fasting blood glucose, improved glucose tolerance and significant decreases in AUC when IPGTT was performed (Figure 6-6A and B), with no changes in insulin tolerance (Figure 6-6C). In addition, morphological analysis revealed significantly increased islet number (Figure 6-6D) with increased beta-cell proliferative activity (Figure 6-6E) in *c-KitβTg* mice. An increase in Pdx-1 and Nkx6.1 staining intensity was also noted in *c-KitβTg* mouse islets as compared to *WT* group (Figure 6-7).

However, these protective effects were diminished after long-term HFD challenge. There were no significant differences in body, pancreatic or fat pad weights between *c-KitβTg-HFD* and *WT-HFD* groups (Figure 6-8A-C). In contrast, the overnight fasting blood glucose was significantly higher in *c-KitβTg-HFD* mice as compared to *WT-HFD* group (Figure 6-8D). Glucose tolerance was progressively impaired and there were significant increases in AUC when IPGTT was performed after 20-22 weeks (Figure 6-8E and F). Although *c-KitβTg-HFD* mice showed a slight insulin resistance, no significant changes in the IPITT AUC were observed between groups (Figure 6-8G). *In vivo* GSIS assays showed significantly decreased plasma insulin levels at 35 minutes following glucose stimulation in *c-KitβTg-HFD* mice as compared to *WT-HFD* mice (Figure 6-8H). The impaired glucose tolerance of *c-KitβTg-HFD* mice was associated with a significant decrease in islet density (Figure 6-9A), alpha and beta-cell mass (Figure 6-9B and C). Loss of E-cadherin expression on the beta-cell surface (Figure 6-9D) and reduced total E-cadherin protein levels were observed in *c-KitβTg-HFD* islets when compared to *WT-HFD* group (Figure 6-9E).

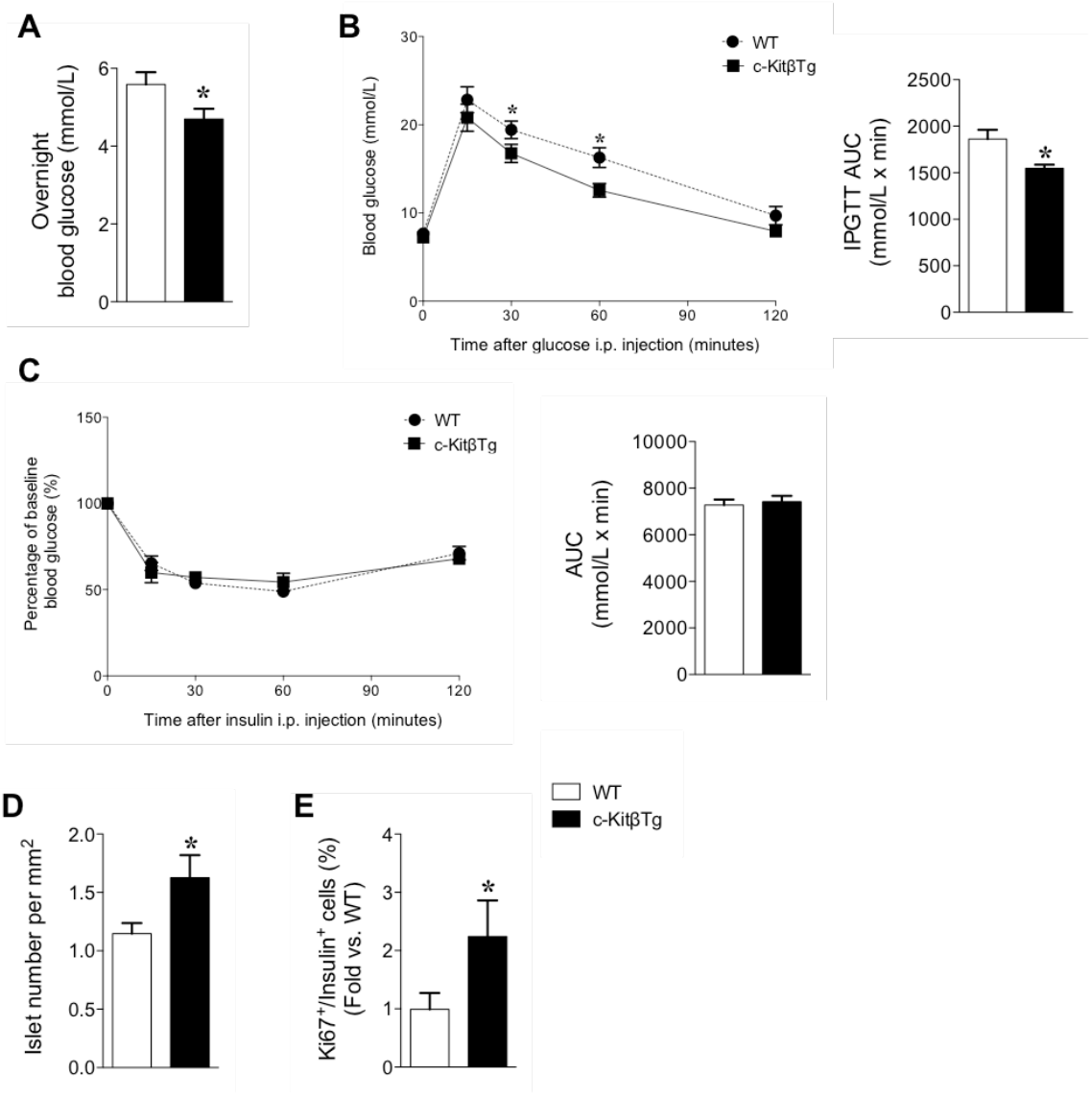
A
Overnight blood glucose (mmol/L)
6
4
2
0
*
B
Blood glucose (mmol/L)
30
20
10
0
0
30
60
90
120
Time after glucose i.p. injection (minutes)
WT
c-KitβTg
*
*
IPGTT AUC (mmol/L x min)
2500
2000
1500
1000
500
0
*
C
Percentage of baseline blood glucose (%)
150
100
50
0
0
30
60
90
120
Time after insulin i.p. injection (minutes)
WT
c-KitβTg
AUC (mmol/L x min)
10000
8000
6000
4000
2000
0
WT
c-KitβTg
D
Islet number per mm2
2.0
1.5
1.0
0.5
0.0
*
E
Ki67+/Insulin+ cells (%) (Fold vs. WT)
4
3
2
1
0
*

Figure 6-6. Glucose tolerance and islet morphology in 28-week-old *c-KitβTg* mice.

Overnight fasting blood glucose levels (**A**), IPGTT (**B**), and IPITT (**C**) in *WT* and *c-KitβTg* mice at 28 weeks of age. Glucose responsiveness of the corresponding experimental groups is shown as a measurement of AUC of the graphs with units of (mmol/L x minutes). Morphometric analyses of islet number (**D**), and quantification of $Ki67^+$ beta-cells (**E**) in *WT* and *c-KitβTg* mice at 28 weeks of age. Data (**A**-**E**) are expressed as mean ± SEM ($n=5$-9), $*p<0.05$ analyzed by unpaired student's *t*-test.

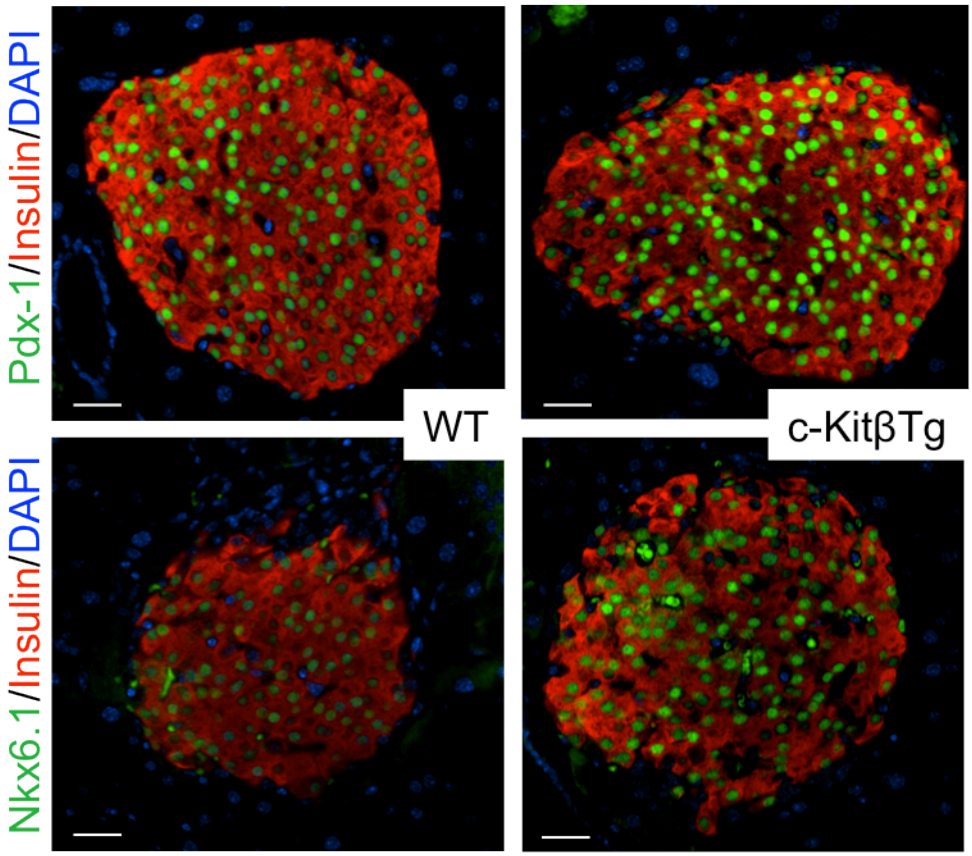
Pdx-1/Insulin/DAPI
WT
c-KitβTg
Nkx6.1/Insulin/DAPI

Figure 6-7. Expression of islet transcription factors in 28-week-old *c-KitβTg* mice.

Double immunofluorescence staining for Pdx-1 or Nkx6.1 (green) and insulin (red), and nuclei stained with DAPI (blue) in 28-week-old *WT* and *c-KitβTg* pancreatic sections. Representative images are shown. Scale bar 25 μm.

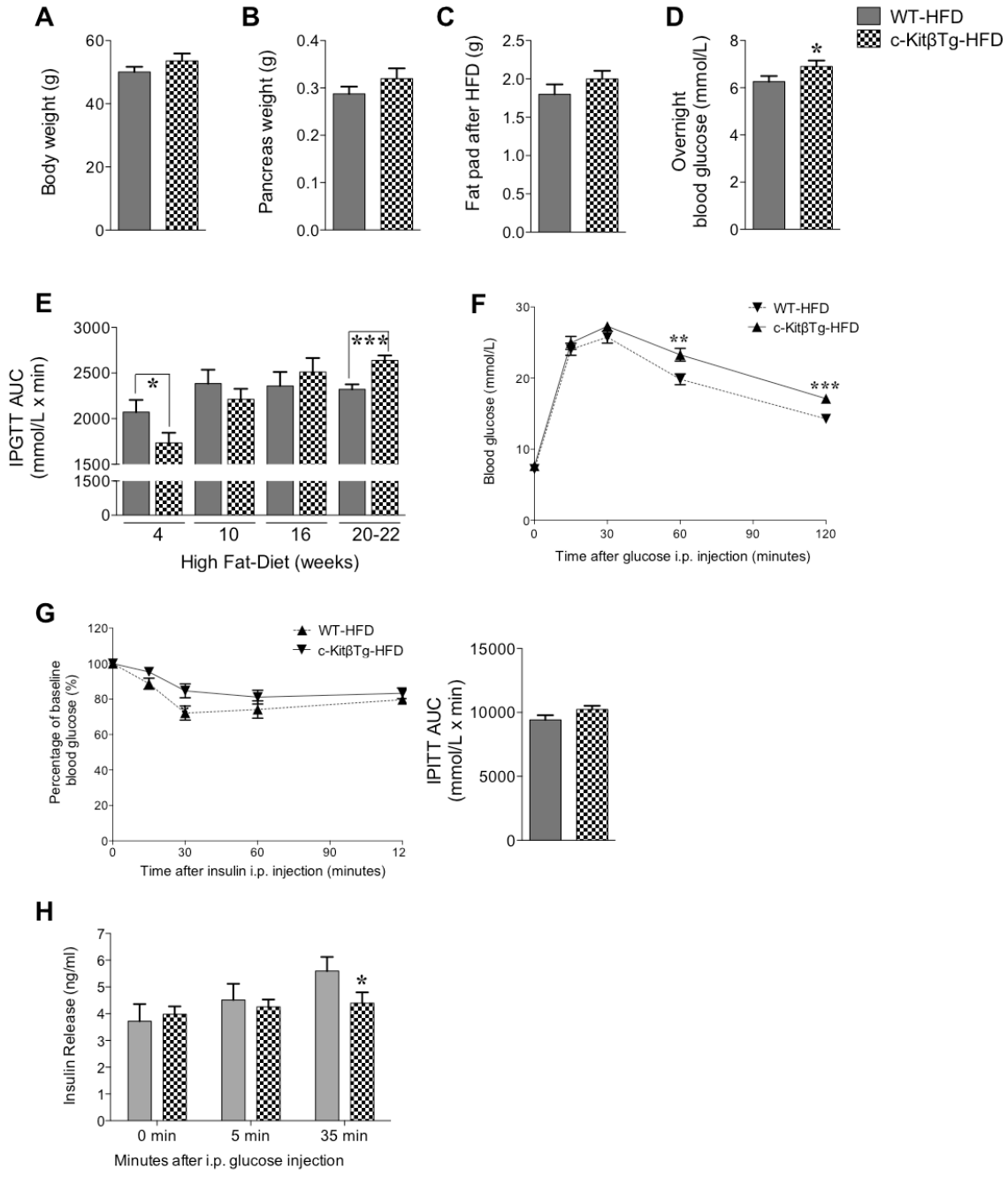
A
Body weight (g)
B
Pancreas weight (g)
C
Fat pad after HFD (g)
D
Overnight blood glucose (mmol/L)
WT-HFD
c-KitβTg-HFD
E
IPGTT AUC (mmol/L x min)
High Fat-Diet (weeks)
4
10
16
20-22
F
Blood glucose (mmol/L)
Time after glucose i.p. injection (minutes)
G
Percentage of baseline blood glucose (%)
Time after insulin i.p. injection (minutes)
IPITT AUC (mmol/L x min)
H
Insulin Release (ng/ml)
0 min
5 min
35 min
Minutes after i.p. glucose injection

Figure 6-8. Islet hypervascularization results in impaired glucose tolerance in 28-week-old *c-KitβTg* mice under long-term HFD.

Body (**A**), pancreatic (**B**), and fat pad weight (**C**), overnight fasting blood glucose levels (**D**); measurement of IPGTT AUC after 4, 10, 16 and 20-22 weeks of HFD (**E**); IPGTT (**F**), IPITT (**G**) and *in vivo* GSIS (**H**) at 20 weeks of HFD performed on *WT-HFD* and *c-KitβTg-HFD* mice. Data (**A-H**) are expressed as mean ± SEM (*n=7-12*). **p*<0.05, ***p*<0.01, ****p*<0.001 analyzed by unpaired student's *t*-test.

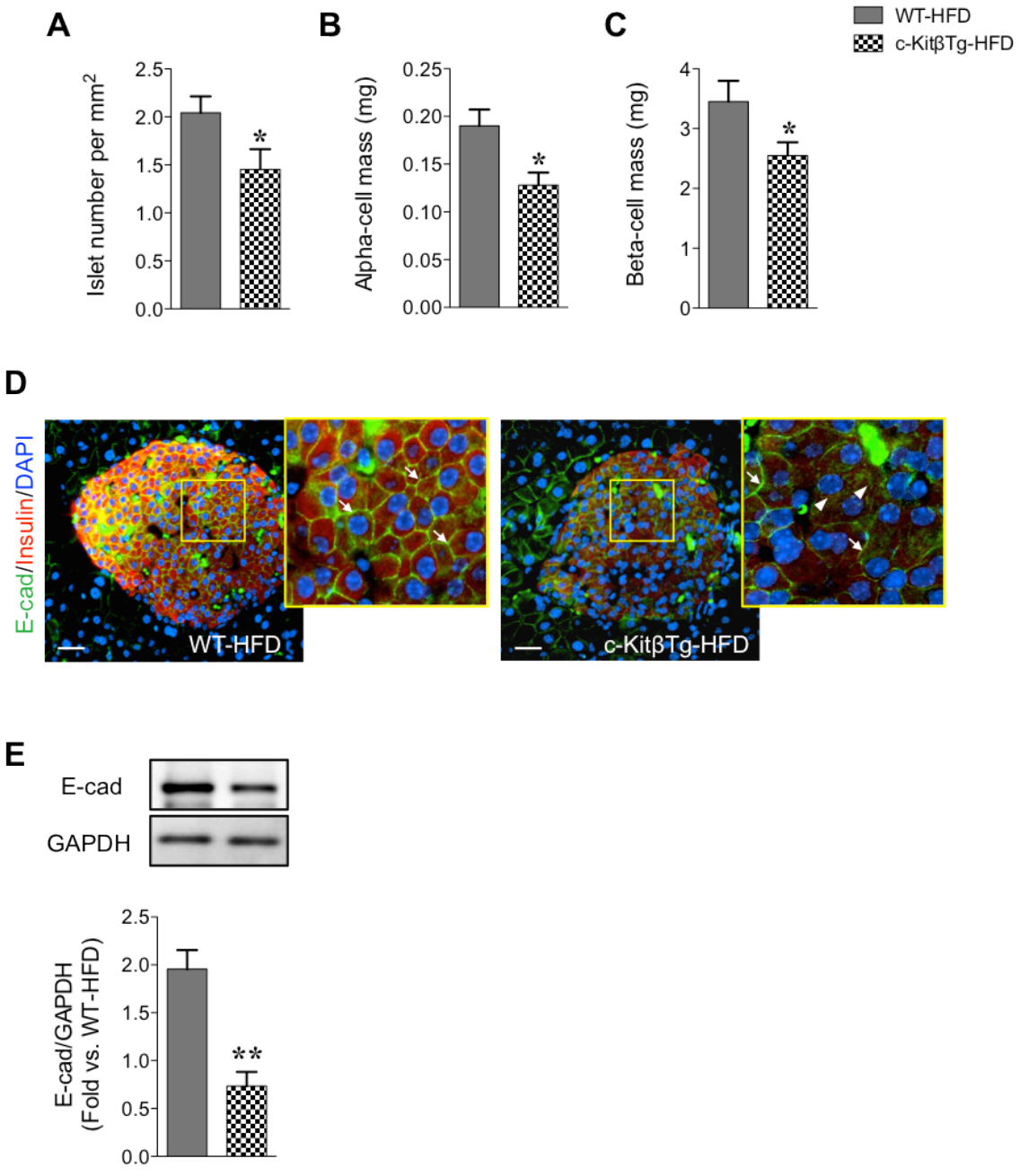
A
Islet number per mm2
2.5
2.0
1.5
1.0
0.5
0.0
*
B
Alpha-cell mass (mg)
0.25
0.20
0.15
0.10
0.05
0.00
*
C
Beta-cell mass (mg)
4
3
2
1
0
*
WT-HFD
c-KitβTg-HFD
D
E-cad/Insulin/DAPI
WT-HFD
c-KitβTg-HFD
E
E-cad
GAPDH
E-cad/GAPDH
(Fold vs. WT-HFD)
2.5
2.0
1.5
1.0
0.5
0.0
**

Figure 6-9. Altered islet morphology is observed in 28-week-old *c-KitβTg* mice under long-term HFD.

Quantitative analyses of islet number (**A**), alpha-cell (**B**), and beta-cell mass (**C**) in 28-week-old *WT-HFD* and *c-KitβTg-HFD* mice. (**D)** Representative images of E-cadherin (green) co-stained with insulin (red), and nuclei stained with DAPI (blue) in *WT-HFD* and *c-KitβTg-HFD* pancreatic sections. Scale bar 25 μm. (**E**) Western blot analysis of E-cadherin in isolated *WT-HFD* and *c-KitβTg-HFD* islets. Representative blots are shown. Data are normalized to loading control (GAPDH). Data (**A**-**C**, and **E**) are expressed as mean ± SEM (*n=4-8*), **p*<0.05, ***p*<0.01 analyzed by unpaired student's *t*-test.

6.3.6 *c-KIT* overexpression-induced hyper-vasculature is associated with islet inflammatory response and cytokine production in 28-week-old *c-KitβTg* mice under long-term HFD

We further investigated the mechanisms of beta-cell dysfunction in *c-KitβTg-HFD* mouse islets. Total VEGF-A protein levels were significantly higher in *c-KitβTg-HFD* mouse islets (*vs. WT-HFD*, Figure 6-10A). Cleaved PARP protein levels (associated with cell apoptosis) were increased (~45%, Figure 6-10B) in parallel with a significant increase in the number of beta-cells positive for TUNEL staining (*vs. WT-HFD*, Figure 6-10C). Western blot analyses showed that levels of MAC-2, TNF-α and IL-1β were significantly elevated in *c-KitβTg-HFD* islets (Figure 6-10D), indicating increased inflammatory response was observed in *c-KitβTg-HFD* islets.

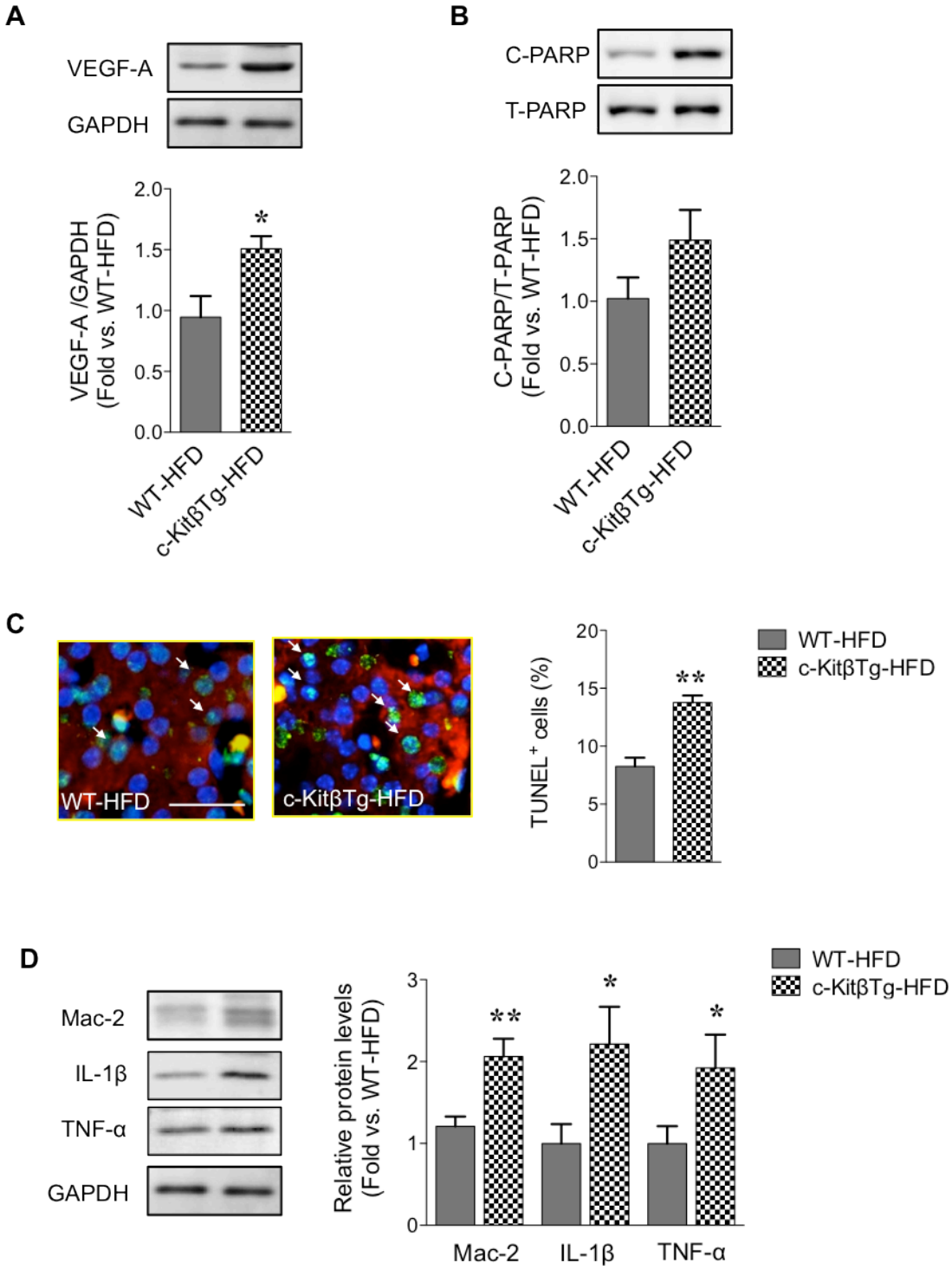
A
VEGF-A
GAPDH
VEGF-A /GAPDH
(Fold vs. WT-HFD)
2.0
1.5
1.0
0.5
0.0
*
WT-HFD
c-KitβTg-HFD
B
C-PARP
T-PARP
C-PARP/T-PARP
(Fold vs. WT-HFD)
2.0
1.5
1.0
0.5
0.0
WT-HFD
c-KitβTg-HFD
C
WT-HFD
c-KitβTg-HFD
TUNEL+ cells (%)
20
15
10
5
0
**
WT-HFD
c-KitβTg-HFD
D
Mac-2
IL-1β
TNF-α
GAPDH
Relative protein levels
(Fold vs. WT-HFD)
3
2
1
0
**
*
*
Mac-2
IL-1β
TNF-α
WT-HFD
c-KitβTg-HFD

Figure 6-10. Increased islet inflammation and cytokine production is induced by islet hypervascularization in 28-week-old *c-KitβTg* mice under long-term HFD.

Western blot analyses of VEGF-A (**A**) and cleaved-PARP (**B**) in islets isolated from *WT-HFD* and *c-KitβTg-HFD* mice. (**C**) Representative images of TUNEL (green) co-stained with insulin (red) and quantitative analysis of $TUNEL^{+}$/$insulin^{+}$ cells in *WT-HFD* and *c-KitβTg-HFD* pancreatic sections. Protein levels of MAC-2, TNF-α, and IL-1β (**D**) in islets isolated from *WT-HFD* and *c-KitβTg-HFD* mice. Representative blots are shown. Data (**A**-**B**, and **D**) are expressed as mean ± SEM ($n=4$-5), *$p<0.05$, **$p<0.01$ analyzed by unpaired student's *t*-test.

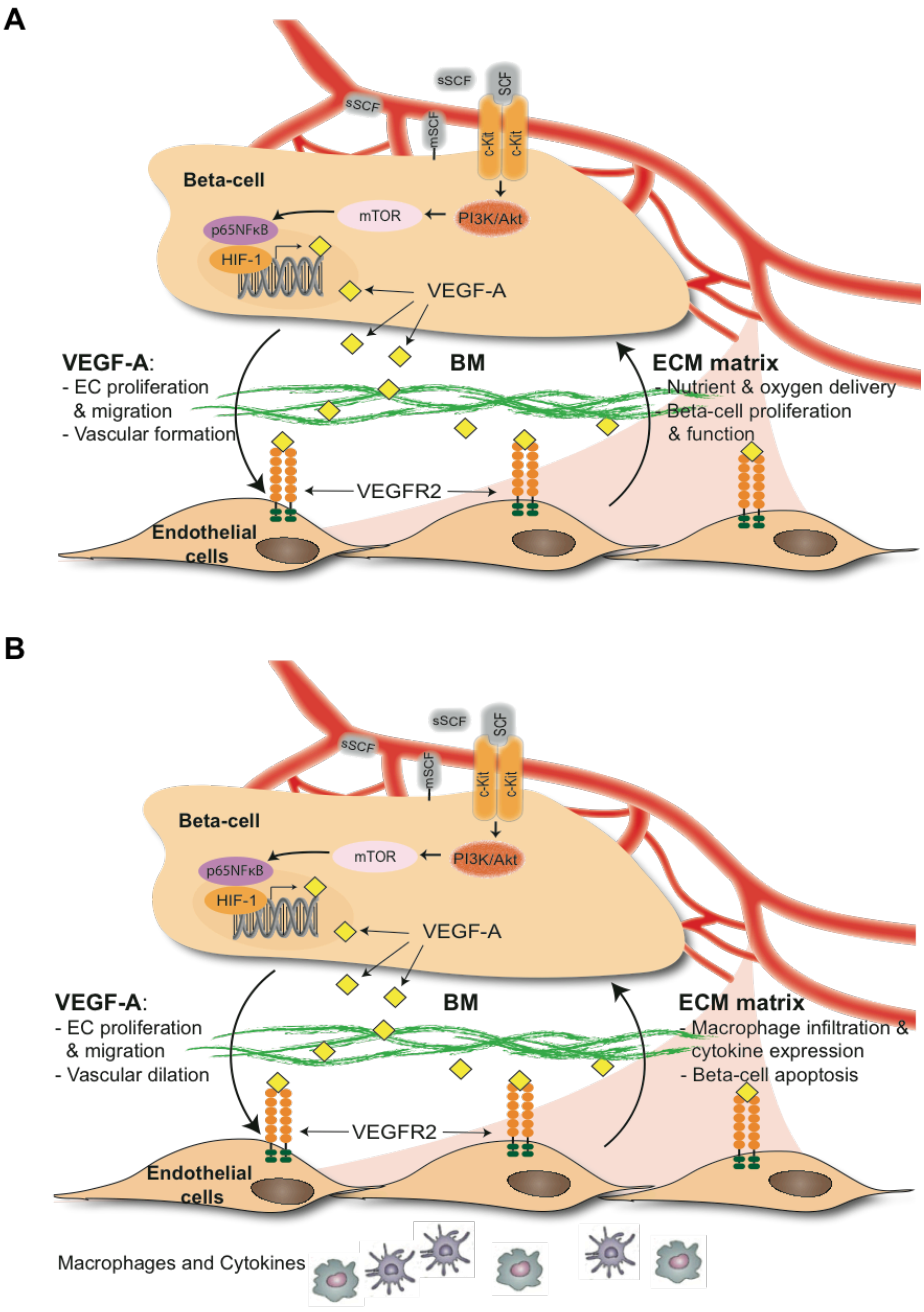
A
sSCF
SCF
sSCF
mSCF
c-Kit
c-Kit
Beta-cell
mTOR
PI3K/Akt
p65NFκB
HIF-1
VEGF-A
VEGF-A:
- EC proliferation
& migration
- Vascular formation
BM
ECM matrix
- Nutrient & oxygen delivery
- Beta-cell proliferation
& function
VEGFR2
Endothelial
cells
B
sSCF
SCF
sSCF
mSCF
c-Kit
c-Kit
Beta-cell
mTOR
PI3K/Akt
p65NFκB
HIF-1
VEGF-A
VEGF-A:
- EC proliferation
& migration
- Vascular dilation
BM
ECM matrix
- Macrophage infiltration &
cytokine expression
- Beta-cell apoptosis
VEGFR2
Endothelial
cells
Macrophages and Cytokines

Figure 6-11. Proposed model of c-Kit signaling that mediates VEGF-A production and modulates islet vasculature, affecting beta-cell function and survival.

(**A**) c-Kit mediates VEGF-A production via the PI3K/Akt/mTOR signaling, which is essential for islet vascular formation. Subsequently, proper islet vasculature facilitates nutrient and oxygen exchange maintaining beta-cell survival and function. (**B**) Constitutive c-Kit-mediated VEGF-A overproduction results in increased islet vasculature. Under HFD-induced diabetic conditions, islet hypervascularization attracts macrophage infiltration and cytokine production leading to beta-cell dysfunction and apoptosis.

6.4 Discussion

The present study demonstrated that c-Kit receptor tyrosine kinase activity regulates VEGF-A production to promote islet vascular formation. At age of 8 weeks, mice bearing a loss of c-Kit function showed severe developmental defects in islet vasculature, which was rescued by *c-KIT* overexpression in beta-cells. *c-KIT* overexpression improved VEGF-A production through activation of the PI3K/Akt/mTOR signaling pathway, which maintained the vascular formation in *c-KitβTg:Wv* mice (Figure 6-11A). At age of 28 weeks, mice with beta-cell specific *c-KIT* overexpression displayed an increase in VEGF-A expression and islet vascularization with persistently improved glucose tolerance compared to *WT* mice. Interestingly, enhanced vasculature may expose islets to HFD-induced macrophage infiltration leading to increased inflammatory responses and elevated beta-cell apoptosis, which subsequently contributed to the development of hyperglycemia (Figure 6-11B).

The relationship between c-Kit and VEGF-A was observed in the mouse models with a loss or gain of c-Kit function in beta-cells. A substantial loss of islet vascularization was observed in *c-Kit*$^{Wv/+}$ mice, while improved islet vascular formation was found in *c-KitβTg;Wv* mice. We previously reported that the severe loss of beta-cell mass and function were associated with glucose intolerance in *c-Kit*$^{Wv/+}$ mice [20, 21], but *c-KitβTg;Wv* mice showed a significant improvement in glucose homeostasis [22]. It is well documented that the vascular niche serves as an inductive signal in pancreatic bud branching and islet maturation. In return, islets release VEGF-A to promote islet endothelium growth and ultimately increase islet vascularization, and this was essential for maintaining beta-cell function and survival [2, 8, 23, 24]. Islet capillaries were not only increased in quantity, but also underwent several changes at the ultrastructural level, including increased capillary diameter and size in *c-KitβTg;Wv* mice likely due to c-Kit-stimulated VEGF-A production. The improved islet capillary structure caused a reversal of the nutrient flow into islets, leading to improved beta-cell function, and increased insulin exocytosis into the bloodstream [25, 26]. At the cellular level, molecular mechanisms associated with the loss of islet vasculature in *c-Kit*$^{Wv/+}$ mice include a significant down-regulation in the PI3K/Akt/mTOR pathway. Conversely, *c-KIT*

overexpression stimulates this signaling pathway including an increase in NFκB phosphorylation and VEGF-A expression. These findings were not only in agreement with previous findings [27-31], but also corroborated by our previous studies showing that the Akt-dependent pathway is a key player to mediate mitogenic signaling in human fetal islet-epithelial clusters *in vitro* [32, 33], and beta-cell proliferation and survival in genetic mouse models [20, 22]. Taken together, this study suggests that c-Kit-mediates VEGF-A production likely via the PI3K/Akt/mTOR pathway, and plays a critical role in proper islet vascular formation in maintaining beta-cell health and euglycemia.

The observation that c-Kit promotes islet vascularization has implications not only in maintaining islet function, but could also be considered as a therapeutic target for promoting revascularization of transplanted islets. Following islet isolation, the survival of transplanted islets depends on the degrees of effective revascularization [25]. Given that the endothelial cells residing within isolated islets retained limited angiogenic capacity, it is postulated that their proliferative potential can, in part, be stimulated by VEGF-A production mediated by c-Kit in the beta-cell [1, 4, 34]. At 28 weeks of age, *c-KitβTg* mice showed significantly increased VEGF-A and PECAM-1 expression with increase of islet vascular formation when compared to *WT* mice, suggesting a chronic causal relationship between *c-KIT* overexpression, and increased islet VEGF-A secretion, which in turn leads to increased islet angiogenesis in mice. These *in vivo* observations further demonstrated that c-Kit-mediated VEGF-A production has a primary role in regulating islet angiogenesis via promoting endothelial cell proliferation and fenestration, and may help to create better methods for revascularization of transplanted islets in the treatment of diabetes.

Previous studies using prediabetic Zucker diabetic fatty rats and HFD-fed mice suggested that islet vessel dilation is an adaptive biological response in the setting of insulin resistance [5, 6, 35]. The fact that intra-islet endothelial cells were in a quiescent state in these insulin resistant animals suggested that such vascular change was independent of angiogenic processes [4, 6]. Indeed, an islet compensatory mechanism characterized by dilation of pre-existing vessels to increased insulin demand was observed in the current chronic HFD studies, in contrast to increased angiogenesis observed in 28-week-old *c-*

KitβTg mice under normal diet. Interestingly, significantly increased intra-islet capillary size with noticeable red blood cell extravasation were observed in *c-KitβTg* islets, as compared to *WT* mice, under chronic HFD treatment. We noticed that the previously reported protective effect against a HFD (4 weeks) in *c-KitβTg* mice [22], was progressively diminished preceding the development of hyperglycaemia after 22 weeks of HFD consumption. The observed glucose intolerance was associated with severe loss of beta-cell mass, reduced *in vivo* insulin release and, in particular, loss of E-cadherin expression in beta-cells. E-cadherin, an adhesion molecule of the cadherin family, was found to be down-regulated in secretory defective beta-cells [36, 37]. Treatment of beta-cells with an anti-E-cadherin blocking antibody affected intracellular Ca^{2+} levels and insulin secretion [38]. Our data suggested that such pronounced islet vasculature remodeling during chronic HFD could be stimulated by severe islet disorganization and beta-cell dysfunction while attempting, but failing, to maintain adequate insulin fenestration and euglycemia. On the other hand, increased islet apoptosis was probably the cause of islet failure in *c-KitβTg* mice during chronic HFD. Previous studies demonstrated that VEGF-A is a potent chemoattractant for inflammatory cytokines and macrophages [5]. In a HFD-induced diabetes mouse model, excessive amounts of circulating fatty acids and cytokines derived from adipose tissue were able to induce beta-cell apoptosis [39], which was consistent with our findings showing that higher levels of inflammatory cytokines and macrophage infiltration were observed in *c-KitβTg-HFD* islets. Taken together, our results suggested that c-Kit-mediated VEGF-A production during a HFD-induced diabetic status lead to undesirable hypervascularization, allowing for cytokine and macrophage infiltration, which may contribute to beta-cell loss and dysfunction, as is a major hallmark in the development and progression of T2D [40].

In summary, this study demonstrated that *c-KIT* overexpression mediated VEGF-A production and secretion via the PI3K/Akt/mTOR pathway, which subsequently modulated islet vascular formation *in vivo*. We noted that increased c-Kit, specifically in beta-cells, enhanced islet vascular recovery on fibrin culture after an invasive isolation procedure (data not shown), and promoted islet angiogenesis in 28-week-old *c-KitβTg*

mice without disturbing glucose homeostasis. Interestingly, 28-week-old *c-Kitβ*Tg mice under chronic HFD displayed dysregulated vascular dilation due to overproduction of VEGF-A, and such vascular changes were associated with beta-cell failure exacerbated by recruitment of inflammatory cytokines, leading to the development of hyperglycemia. This study represents a unique and integrated *in vivo* approach to unraveling the cellular mechanisms by which SCF/c-Kit interactions mediate VEGF-A production to regulate beta-cell function in both positive and negative ways. The finely turned and tightly regulated c-Kit activity is critical for the control of the microenvironmental VEGF-A concentration in islets, maintaining a normal and stable islet vascular network for proper beta-cell function and survival.

6.5 References

1. Brissova M, Powers AC (2008) Revascularization of transplanted islets: can it be improved? Diabetes 57:2269–2271. doi: 10.2337/db08-0814

2. Lammert E, Cleaver O, Melton D (2001) Induction of pancreatic differentiation by signals from blood vessels. Science 294:564–567. doi: 10.1126/science.1064344

3. Pierreux CE, Cordi S, Hick A-C, et al. (2010) Epithelial: Endothelial cross-talk regulates exocrine differentiation in developing pancreas. Dev Biol 347:216–227. doi: 10.1016/j.ydbio.2010.08.024

4. Brissova M, Shostak A, Shiota M, et al. (2006) Pancreatic islet production of vascular endothelial growth factor--a is essential for islet vascularization, revascularization, and function. Diabetes 55:2974–2985. doi: 10.2337/db06-0690

5. Agudo J, Ayuso E, Jimenez V, et al. (2012) Vascular endothelial growth factor-mediated islet hypervascularization and inflammation contribute to progressive reduction of β-cell mass. Diabetes 61:2851–2861. doi: 10.2337/db12-0134

6. Dai C, Brissova M, Reinert RB, et al. (2013) Pancreatic islet vasculature adapts to insulin resistance through dilation and not angiogenesis. Diabetes 62:4144–4153. doi: 10.2337/db12-1657

7. Lai Y, Schneider D, Kidszun A, et al. (2005) Vascular endothelial growth factor increases functional beta-cell mass by improvement of angiogenesis of isolated human and murine pancreatic islets. Transplantation 79:1530–1536.

8. Lammert E, Gu G, McLaughlin M, et al. (2003) Role of VEGF-A in vascularization of pancreatic islets. Curr Biol 13:1070–1074.

9. Puputti M, Tynninen O, Pernilä P, et al. (2010) Expression of KIT receptor tyrosine kinase in endothelial cells of juvenile brain tumors. Brain Pathol 20:763–770. doi: 10.1111/j.1750-3639.2009.00357.x

10. Heinke T, Espiríto Santo KSD, Longatto Filho A, Stavale JN (2013) Vascular endothelial growth factor and KIT expression in relation with microvascular density and tumor grade in supratentorial astrocytic tumors. Acta Cir Bras 28:48–54.

11. Amin MM, El-Hawary AK, Farouk O (2012) Relation of CD117 immunoreactivity and microvascular density in invasive breast carcinoma. Indian J Pathol Microbiol 55:456–460. doi: 10.4103/0377-4929.107780

12. Beppu K, Jaboine J, Merchant MS, et al. (2004) Effect of imatinib mesylate on neuroblastoma tumorigenesis and vascular endothelial growth factor expression. J Natl Cancer Inst 96:46–55.

13. Litz J, Sakuntala Warshamana-Greene G, Sulanke G, et al. (2004) The multi-targeted kinase inhibitor SU5416 inhibits small cell lung cancer growth and angiogenesis, in part by blocking Kit-mediated VEGF expression. Lung Cancer 46:283–291. doi: 10.1016/j.lungcan.2004.05.005

14. Litz J, Krystal GW (2006) Imatinib inhibits c-Kit-induced hypoxia-inducible factor-1alpha activity and vascular endothelial growth factor expression in small cell lung cancer cells. Mol Cancer Ther 5:1415–1422. doi: 10.1158/1535-7163.MCT-05-0503

15. Li T-S, Hamano K, Nishida M, et al. (2003) CD117+ stem cells play a key role in therapeutic angiogenesis induced by bone marrow cell implantation. Am J Physiol Heart Circ Physiol 285:H931–7. doi: 10.1152/ajpheart.01146.2002

16. Fazel S, Cimini M, Chen L, et al. (2006) Cardioprotective c-kit+ cells are from the bone marrow and regulate the myocardial balance of angiogenic cytokines. J Clin Invest 116:1865–1877. doi: 10.1172/JCI27019

17. Dentelli P, Rosso A, Balsamo A, et al. (2007) C-KIT, by interacting with the membrane-bound ligand, recruits endothelial progenitor cells to inflamed endothelium. Blood 109:4264–4271. doi: 10.1182/blood-2006-06-029603

18. Kim KL, Meng Y, Kim JY, et al. (2011) Direct and differential effects of stem cell factor on the neovascularization activity of endothelial progenitor cells. Cardiovasc Res 92:132–140. doi: 10.1093/cvr/cvr161

19. Fang S, Wei J, Pentinmikko N, et al. (2012) Generation of functional blood vessels from a single c-kit+ adult vascular endothelial stem cell. PLoS Biol 10:e1001407. doi: 10.1371/journal.pbio.1001407

20. Feng Z-C, Donnelly L, Li J, et al. (2012) Inhibition of Gsk3β activity improves β-cell function in c-KitWv/+ male mice. Lab Invest 92:543–555. doi: 10.1038/labinvest.2011.200

21. Krishnamurthy M, Ayazi F, Li J, et al. (2007) c-Kit in early onset of diabetes: a morphological and functional analysis of pancreatic beta-cells in c-KitW-v mutant mice. Endocrinology 148:5520–5530. doi: 10.1210/en.2007-0387

22. Feng ZC, Li J, Turco BA, et al. (2012) Critical role of c-Kit in beta cell function: increased insulin secretion and protection against diabetes in a mouse model. Diabetologia 55:2214–2225. doi: 10.1007/s00125-012-2566-5

23. Cleaver O, Melton DA (2003) Endothelial signaling during development. Nat Med 9:661–668. doi: 10.1038/nm0603-661

24. Cleaver O, Dor Y (2012) Vascular instruction of pancreas development. Development 139:2833–2843. doi: 10.1242/dev.065953

25. Konstantinova I, Lammert E (2004) Microvascular development: learning from pancreatic islets. Bioessays 26:1069–1075. doi: 10.1002/bies.20105

26. Richards OC, Raines SM, Attie AD (2010) The role of blood vessels, endothelial cells, and vascular pericytes in insulin secretion and peripheral insulin action. Endocr Rev 31:343–363. doi: 10.1210/er.2009-0035

27. Dan HC, Cooper MJ, Cogswell PC, et al. (2008) Akt-dependent regulation of NF-{kappa}B is controlled by mTOR and Raptor in association with IKK. Genes Dev 22:1490–1500. doi: 10.1101/gad.1662308

28. Ahmed M, Kundu GC (2010) Osteopontin selectively regulates p70S6K/mTOR phosphorylation leading to NF-kappaB dependent AP-1-mediated ICAM-1 expression in breast cancer cells. Mol Cancer 9:101. doi: 10.1186/1476-4598-9-101

29. Jung Y-J, Isaacs JS, Lee S, et al. (2003) IL-1beta-mediated up-regulation of HIF-1alpha via an NFkappaB/COX-2 pathway identifies HIF-1 as a critical link between inflammation and oncogenesis. FASEB J 17:2115–2117. doi: 10.1096/fj.03-0329fje

30. Figueroa YG, Chan AK, Ibrahim R, et al. (2002) NF-kappaB plays a key role in hypoxia-inducible factor-1-regulated erythropoietin gene expression. Exp Hematol 30:1419–1427.

31. Ramanathan M, Pinhal-Enfield G, Hao I, Leibovich SJ (2007) Synergistic up-regulation of vascular endothelial growth factor (VEGF) expression in macrophages by adenosine A2A receptor agonists and endotoxin involves transcriptional regulation via the hypoxia response element in the VEGF promoter. Mol Biol Cell 18:14–23. doi: 10.1091/mbc.E06-07-0596

32. Li J, Goodyer CG, Fellows F, Wang R (2006) Stem cell factor/c-Kit interactions regulate human islet-epithelial cluster proliferation and differentiation. Int J Biochem Cell Biol 38:961–972. doi: 10.1016/j.biocel.2005.08.014

33. Wu Y, Li J, Saleem S, et al. (2010) c-Kit and stem cell factor regulate PANC-1 cell differentiation into insulin- and glucagon-producing cells. Lab Invest 90:1373–1384. doi: 10.1038/labinvest.2010.106

34. Wang X, Meloche M, Verchere CB, et al. (2011) Improving islet engraftment by gene therapy. J Transplant 2011:594851. doi: 10.1155/2011/594851

35. Li X, Zhang L, Meshinchi S, et al. (2006) Islet microvasculature in islet hyperplasia and failure in a model of type 2 diabetes. Diabetes 55:2965–2973. doi: 10.2337/db06-0733

36. Yamagata K, Nammo T, Moriwaki M, et al. (2002) Overexpression of dominant-negative mutant hepatocyte nuclear fctor-1 alpha in pancreatic beta-cells causes abnormal islet architecture with decreased expression of E-cadherin, reduced beta-cell proliferation, and diabetes. Diabetes 51:114–123.

37. Jaques F, Jousset H, Tomas A, et al. (2008) Dual effect of cell-cell contact disruption on cytosolic calcium and insulin secretion. Endocrinology 149:2494–2505. doi: 10.1210/en.2007-0974

38. Rogers GJ, Hodgkin MN, Squires PE (2007) E-cadherin and cell adhesion: a role in architecture and function in the pancreatic islet. Cell Physiol Biochem 20:987–994. doi: 10.1159/000110459

39. Xu H, Barnes GT, Yang Q, et al. (2003) Chronic inflammation in fat plays a crucial role in the development of obesity-related insulin resistance. J Clin Invest 112:1821–1830. doi: 10.1172/JCI19451

40. Olefsky JM, Glass CK (2010) Macrophages, inflammation, and insulin resistance. Annu Rev Physiol 72:219–246. doi: 10.1146/annurev-physiol-021909-135846

Chapter 7

7 Summary, limitations and future directions

7.1 Summary

7.1.1 Overall rationale and main objective

In the previous study using the *c-Kit* W^v mutant mouse model, our lab showed that deficiency of c-Kit signaling resulted in decreased beta-cell mass and proliferation, leading to the onset of diabetes in *c-Kit*$^{Wv/+}$ mice. [1]. However, the mechanisms by which c-Kit regulates beta-cell function and survival, and specifically, how c-Kit activity is coordinated in beta-cells *in vivo,* has not been determined. Thus, the main **objective** of this work was to dissect the intracellular signaling pathways by which c-Kit regulates beta-cell proliferation, survival and function. The central hypothesis of this work was that activation of c-Kit downstream PI3K/Akt signaling pathway plays a critical role in determining beta-cell growth and beta-cell insulin releasing function under normal and diabetic pathophysiological conditions (Figure 7-1).

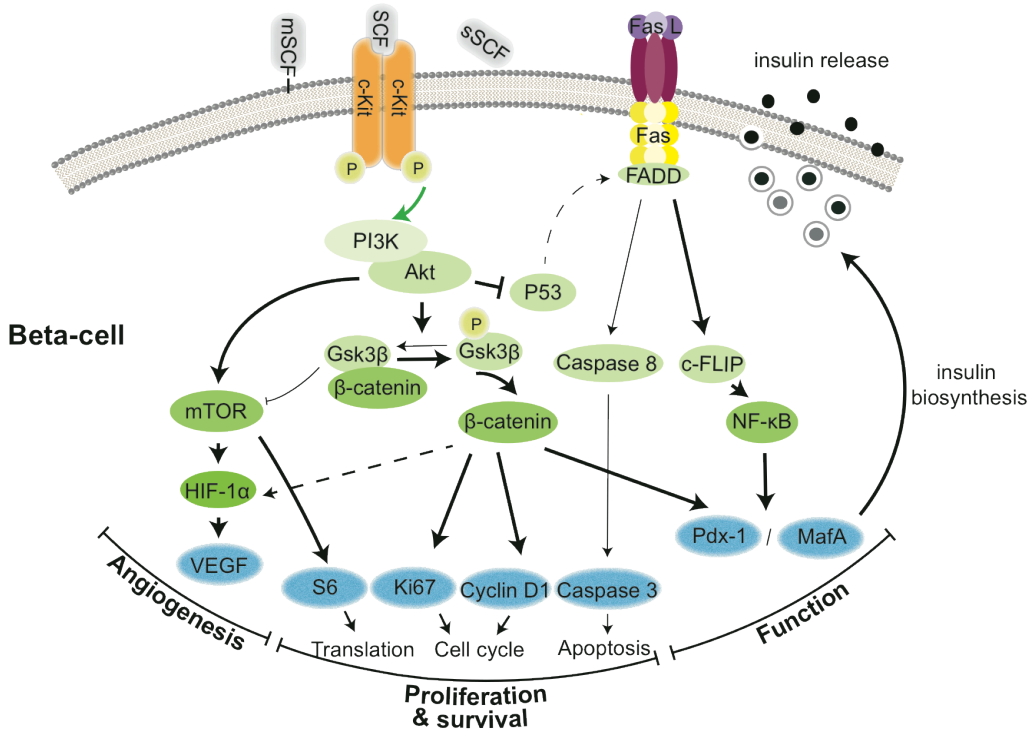
mSCF
SCF
sSCF
c-Kit
c-Kit
P
P
Fas L
Fas
FADD
insulin release
PI3K
Akt
P53
Beta-cell
P
Gsk3β
Gsk3β
β-catenin
Caspase 8
c-FLIP
mTOR
β-catenin
NF-κB
insulin
biosynthesis
HIF-1α
Pdx-1
/
MafA
VEGF
S6
Ki67
Cyclin D1
Caspase 3
Angiogenesis
Translation
Cell cycle
Apoptosis
Function
Proliferation
& survival

Figure 7-1. Summary of c-Kit signaling in the beta-cell.

c-Kit downstream signaling pathways in beta-cells. c-Kit regulates beta-cell proliferation, survival and function through: 1) via the Akt/Gsk3β pathway, 2) by indirectly suppressing the Fas-mediated caspase dependent apoptotic signalling, 3) by modulating islet vascular formation through VEGF-A production via the Akt/mTOR pathway.

7.1.2 The *c-Kit W*^{v} mutation causes beta-cell loss and dysfunction via the dysregulated Akt/Gsk3β pathway and up-regulated Fas-mediated apoptotic signaling in *c-Kit*$^{Wv/+}$ mouse model

We hypothesized that the dysregulated Akt/Gsk3β pathway contributes to a severe loss of beta-cell mass and impaired beta-cell function in *c-Kit*$^{Wv/+}$ mice (**Chapter 3**). We found that reduced c-Kit activity led to a reduction of Akt and Gsk3β phosphorylation, resulting in down-regulation of *cyclin D1* gene and protein expression [2, 3] in *c-Kit*$^{Wv/+}$ mouse islets [4]. Our results suggested that Gsk3β activity plays a key role in affecting beta-cell proliferation and function. When given the exogenous Gsk3β inhibitor, 1-AKP, *c-Kit*$^{Wv/+}$ mice demonstrated significantly enhanced *cyclin D1* and *Pdx-1* gene and protein expression [4]. This was associated with enhanced beta-cell proliferation and improved glucose tolerance in *c-Kit*$^{Wv/+}$ mice that received 1-AKP injections. Overall, the c-Kit mutation triggers beta-cell failure via the impaired Akt/Gsk3β pathway in *c-Kit*$^{Wv/+}$ mice [4]. While c-Kit positively regulates beta-cell proliferation, c-Kit signalling is also involved in the regulation of beta-cell apoptosis. We hypothesized that the balance between c-Kit and Fas signaling is essential for maintaining beta-cell mass and function in *c-Kit*$^{Wv/+}$ mice (**Chapter 4**). Deficient c-Kit signaling led to increased beta-cell death in *c-Kit*$^{Wv/+}$ mice, which was associated with an up-regulation of both *p53* and *Fas* gene and protein expression in *c-Kit*$^{Wv/+}$ islets at 8 weeks of age [5]. p53 is an important checkpoint protein that inhibits cyclin D1 expression in multiple cellular contexts [6, 7]. p53 was not only involved in cell cycle arrest in the absence of c-Kit signaling in beta-cells, but our *in vitro* INS-1 cell study further determined that the up-regulation of p53 by *c-Kit* siRNA contributed to increased cell apoptosis via induction of Fas activity. p53/Fas-mediated cell apoptosis was reversed by the treatment of PFT-α or *Fas* siRNA [5]. Furthermore, the functional role of Fas was further studied by introducing the *lpr* mutation in *c-Kit*$^{Wv/+}$ mice (a double mutation of *c-Kit*$^{Wv/+}$*;Fas*$^{lpr/lpr}$ mouse model). Lack of functional Fas expression in *c-Kit*$^{Wv/+}$ mice prevented beta-cell death via down-regulation of the caspase 8-mediated extrinsic apoptotic pathway. An increase in beta-cell mass and improved insulin releasing function was associated with increased c-FLIP/NF-κB pro-survival signaling in *c-Kit*$^{Wv/+}$*;Fas*$^{lpr/lpr}$ mice [5]. Taken together, these findings

suggested that c-Kit signaling regulates beta-cell turnover and beta-cell insulin secretory function.

7.1.3 *c-KIT* overexpression positively regulates beta-cell proliferation and function via an up-regulation of the Akt/Gsk3β/cyclin D1 pathway in *c-KitβTg* mice

Although the *c-Kit*$^{Wv/+}$ mouse model is an excellent system to study the functional impact of c-Kit signaling deficiency in any tissue, the non-specific tissue mutation in this mouse model does not allow us to determine whether c-Kit has a primary role in beta-cell function and survival. To this end, we generated a transgenic mouse model with beta-cell specific *c-KIT* overexpression (*c-KitβTg*), which has a 30% increase in c-Kit expression on beta-cells (**Chapter 5**) [5]. *c-KitβTg* mice displayed improved glucose tolerance without showing differences in peripheral insulin sensitivity. Expansion of beta-cell mass was due to increased islet number and enhanced beta-cell proliferation. Overexpression of *c-KIT* also led to a profound effect *in vivo* on insulin secretion in response to glucose challenge, and exposure of these islets to an elevated glucose concentration resulted in increased insulin release and insulin content in beta-cells compared to controls [8]. *c-KIT* overexpression increased the expression of islet transcriptional factors, including *Pdx-1*, *MafA*, *insulin* and *glucagon* genes in parallel with significantly elevated *Glp1r* and *Glut2* mRNA levels. The changes in gene expression in *c-KitβTg* islets revealed that c-Kit regulates islet gene transcription via the Akt/Gsk3β/cyclin D1 signalling cascade [8]. Interestingly, *c-KitβTg* mice were able to resist HFD-induced diabetes, and maintained beta-cell function and mass. Furthermore, overexpressing *c-KIT* in beta-cells could partially reverse the diabetic phenotype in *c-Kit*$^{Wv/+}$ mice, demonstrating that c-Kit has a beneficial effect on beta-cell growth and function [8].

7.1.4 c-Kit signaling positively regulates islet vascular formation via the Akt/mTOR/VEGF-A pathway

The relationship between c-Kit signaling and VEGF-A synthesis has been implicated in the regulation of tumor angiogenesis in multiple neoplasms [9-11]; however, c-Kit's role function in the regulation of VEGF-A production from islets has not been evaluated. In **Chapter 6**, we hypothesized that c-Kit-dependent regulation of VEGF-A is critical for

islet vascular formation and beta-cell survival. Our initial study using INS-1 cell cultures (presented by MSc candidate Alexei Popell) demonstrated that the Akt/mTOR pathway downstream of c-Kit, *in vitro*, regulated VEGF-A production. Using the mouse models created in Chapter 3 and 5, we observed a substantial loss of islet vasculature in *c-Kit*$^{Wv/+}$ mice, which was reversed by beta-cell-specific *c-KIT* overexpression via an upregulation of the Akt/mTOR signaling pathway. These results suggested that c-Kit-mediated VEGF-A production is critical for normal islet microvasculature. However, endothelial-to-beta-cell interactions may not always result in a positive outcome: islet endothelial cells have been shown to contribute to islet destruction in an inflammatory environment. After prolonged exposure to a HFD, *c-KitβTg* mice exhibited drastic islet hypervascularization and beta-cell dysfunction and increased beta-cell apoptosis. This observation was explained by the chemoattractant effect that resulted in increased inflammatory factor recruitment via hypervasculature in the islets. These experiments demonstrated that c-Kit is a potential therapeutic target in promoting revascularization during islet cell replacement procedures. However, c-Kit activity must be tightly regulated in order to control the microenvironmental VEGF-A concentration, as this is essential for maintaining a normal and stable islet vascular network for proper beta-cell function and survival.

7.2 Limitations

7.2.1 Chapter 3

Mice homozygous for the c-Kit null mutation (*W* mutation) die late in gestation or shortly after birth, presumably because of the embryo being severely anemic and dying at or near parturition. Compared to *W* mutant mice, the *W*^{v} mutation on *c-Kit* leads to a relatively mild anemia in both heterozygotes and homozygotes in rodents. Although fertility is affected in *W*^{v} homozygotes, heterozygous viable *W*^{v} mutants (*c-Kit*$^{Wv/+}$) have normal reproductive capabilities. The molecular basis of the *W* phenotype is different from the *W*^{v} phenotype as well. The *W* mutation affects *c-Kit* gene transcription, resulting in an absence of c-Kit in tissues. In contrast, the *W*^{v} mutation results in reduced intracellular kinase activity of c-Kit due to a point mutation that resides in a highly conserved region of the c-Kit intracellular region. Therefore, the nature of the *W*^{v} phenotype correlates with

the severity of c-Kit signaling deficiency, whereas the mRNA level, protein size, cell surface expression, and binding affinity of c-Kit to SCF is not altered. Although the *c-Kit*$^{Wv/+}$ mouse model is suitable for examining the functional role of c-Kit signaling on tissue, there are limitations. The *c-Kit*$^{Wv/+}$ model is a global mutation model wherein multiple cell types are affected by the c-Kit mutation. For instance, the *W*^{v} mutation causes a loss of coat pigmentation due to mast cell defects. Moreover, an extensive loss of gastrointestinal cells of Cajal vagal intramuscular arrays results in increased sensitivity to exogenous cholecystokinin in *c-Kit W*^{v} mutant mice. Previous studies demonstrated that cholecystokinin acts on the afferent vagal nerve leading back to the nucleus tractus solitarii in the brain, which decreases appetite, and subsequently lowers glucose production from the liver [12, 13]. Whether such metabolic changes may affect the interpretation of our findings in *c-Kit W*^{v} mutant mice remains to be studied. Thus, a mouse model with beta-cell specific c-Kit manipulation would be useful to dissect the primary functional role of c-Kit in the beta-cell.

c-Kit$^{Wv/+}$ male mice displayed glucose intolerance at 8 weeks of age, whereas such symptoms were not observed in *c-Kit*$^{Wv/+}$ females until 40 weeks of age [1]. In accordance with our findings, a higher incidence of diabetes in males is also found in other diabetic models [14-16]. The reason for this sexual dimorphism remains to be investigated, but multiple underlying mechanisms have been proposed. First, the male gonadectomy with additional estradiol treatment showed a protective effect against diabetes in mice [17]. Second, the rise of androgens at puberty is associated with a more severe diabetic state in male rats than in females, since during the neonatal period the effect of streptozotocin was not influenced by gender [18, 19]. Third, the genetic susceptibility represented by inbred mouse strains could be another contributing factor. For example, the inbred cohen diabetic rat males have a more severe glucose intolerance pattern compared to females [20], and spontaneous onset of diabetes with a high cumulative incidence is observed in male inbred insectivore musk shrews compared to females [21]. In addition, gender differences could be related to mitochondrial function [22] or the redox state of beta-cells [23]. More interestingly, sexual dimorphism exists in counter-regulatory responses to different stressors including fasting, hypoglycemia, and exercise [24]. Therefore, underlying mechanisms contributing to the gender bias in *c-*

Kit$^{Wv/+}$ mice remain to be elucidated. For furture studies, gonadectomy and estradiol treatment may be performed to examine whether the onset of diabetes is delayed in *c-Kit*$^{Wv/+}$ males. Furthermore, genes involved in mitochondrial dysfunction and oxidative stress, as well as the responses of neural systems to hunger and satiety, deserve additional study between genders.

Phylogenetically, Gsk3 is closely related to cyclin dependent kinases. Therefore, it is not surprising that Gsk3 inhibitors not only inhibit both α and β forms, but also act on selective cyclin dependent kinases. Compared to previously used Gsk3 inhibitors, 1-AKP has a high potency and selectivity to Gsk3β over the α form and other cyclin dependent kinases [25]. The difference in charge distribution throughout the molecule confers the ability to distinguish between the ATP cavities of Gsk3β and others on 1-AKP [25]. This warrants the use of 1-AKP to inhibit Gsk3β in our studies. However, Gsk3β is a ubiquitously expressed, highly conserved serine/threonine protein kinase found in all eukaryotes. Therefore, the 1-AKP injection that globally inhibits Gsk3β, and may have unknown effects in other tissue. A *c-Kit*$^{Wv/+}$ mouse model with beta-cell specific Gsk3β ablation will be useful to circumvent this challenge. Nevertheless, since we combined *in vitro* and *in vivo* approaches to assess the effect of Gsk3β inhibition on beta-cell function and survival, we are confident that active Gsk3β is the molecular switch leading to beta-cell failure in *c-Kit*$^{Wv/+}$ mice. Gsk3β and Gsk3α share almost identical sequence homology, they overlap in function and compensate for each other, but also have distinct roles and pathways that they regulate in different tissue [26-28]. The role of Gsk3α has largely been ignored, therefore the role of Gsk3α in beta-cells warrants substantial attention in future diabetes research.

7.2.2 Chapter 4

A *c-Kit*$^{Wv/+}$*;Fas*$^{lpr/lpr}$ mouse model was used to study the relationship between c-Kit and Fas in beta-cell turnover and function. The gene coding Fas is located near the *lpr* locus of chromosome 19 in rodents [29]. The *lpr* mutation leads to the production of non-functional truncated *Fas* mRNA due to an early transposable element, similar to an endogenous retrovirus inserted into intron 2. Thus, the *Fas*$^{lpr/lpr}$ mouse is an excellent system to study the effect of a Fas signaling deficiency in any given tissue. A concern is

raised by the global mutation in Fas, which leads to additional effects in the *Fas*$^{lpr/lpr}$ mouse model, whereby these mice develop lymphadenopathy and splenomegaly due to the accumulation of lymphocytes. In contrast to the apoptotic role of Fas signaling in some tissues, Fas also triggers pro-survival cellular processes in other cell types under specific conditions. Thus, any phenotype observed in *c-Kit*$^{Wv/+}$*;Fas*$^{lpr/lpr}$ mice cannot be attributed with complete certainty to the *Fas lpr* mutation in beta-cells. However, given that the percentage of the Fas-expressing beta-cell population was increased, and was correlated with the onset of diabetes in *c-Kit*$^{Wv/+}$ mice at 8 weeks of age, we are confident that the improved beta-cell mass and function was at least partly due to the beneficial effect from the *Fas lpr* mutation in beta-cells of *c-Kit*$^{Wv/+}$*;Fas*$^{lpr/lpr}$ mice. Furthermore, our findings showed that the *Fas lpr* mutation only partially restored beta-cell survival and function in *c-Kit*$^{Wv/+}$*;Fas*$^{lpr/lpr}$ mice, indicating that there are other potential mechanisms underlying beta-cell destruction that may be triggered by the c-Kit mutation. These findings open new avenues for research directed at other apoptotic mediators of cell death, such as tumor necrosis factor receptor and tumor necrosis factor-related apoptosis-inducing ligand receptor. In addition, further research may examine whether beta-cell specific *c-KIT* overexpression is able to block these apoptotic receptors signaling in beta-cells.

7.2.3 Chapter 5

A particular concern is the use of transgene constructs to generate beta-cell-specific gene overexpression *in vivo*. Multiple transgenic lines indicate that the gene directed by RIP is not only expressed in beta-cells, but also in regions of the brain, as revealed by the presence of fluorescent reporters [30-32]. The brain and islets are linked through the neural-entero-islet axis. The brain regulates insulin production from beta-cells, while circulating insulin may influence energy balance and metabolism due to its action in the hypothalamus. Therefore, targeting gene expression via RIP may yield overlapping metabolic phenotypes. In this study, the human *c-KIT* gene followed by IRES2eGFP sequence was inserted into the pKS/RIP plasmid, therefore tissue specificity is achieved through the use of RIP allowing for de novo induction of the human *c-KIT* gene in beta-cells of *c-KitβTg* mice. No eGFP signal in the brain was detected using western blot and

fluorescence microscopy, but we cannot ignore the potential limitations these methods may have. That being said, given that *c-KitβTg* mice had no changes in body weight, food intake or peripheral insulin sensitivity compared to controls, we are confident that improved glucose tolerance is associated with the specific overexpression of human *c-KIT* genes in beta-cells of *c-KitβTg* mice.

Human c-KIT is not structurally identical to mouse c-Kit. Although the C-terminal intracellular signaling domain of mouse c-Kit and human c-KIT are 93% homologous, their extracellular domains share only 74% homology [33, 34]. For this reason, mouse and human c-KIT do not possess identical ligand binding capabilities. This is due to the fact that the ligand recognition site of human c-KIT, which is located in the second Ig-like domain, whereas the binding site of mouse c-Kit lies in the adjacent but noncontiguous region of the receptor [33, 34]. Furthermore, mouse SCF has high affinity for mouse c-Kit (K_d = 1-5 x 10^{-9} M), but it has reduced affinity for human c-KIT as compared with human SCF [35]. Since *c-KitβTg* mice contain the human *c-KIT* gene in beta-cells, this approach may raise the question of species specificity of ligand-receptor interaction. Nevertheless, *c-KitβTg* mouse islets showed an up-regulation of the PI3K/Akt pathway, which is directly regulated by c-Kit. Our findings indicated that mouse SCF was able to activate human c-KIT and exert its biological function, which is consistent with previous studies showing that the monovalent binding of mouse SCF to mouse c-Kit could induce the formation of human-mouse c-Kit heterodimers through a dimerization site in the receptor itself [35].

Our unpublished data showed that *in vitro* exposure of INS-1 cells to SCF resulted in increased co-localization of c-Kit with insulin receptor, as revealed by double immunofluorescence and co-immunoprecipitation. SCF not only stimulated INS-1 cell proliferation, but also significantly augmented the protein levels of insulin receptor, phospho-insulin receptor substrate 1/2 and Pdx-1. Increased insulin receptor signaling was suppressed by wortmannin (PI3K inhibitor) but not U0126 (MEK inhibitor). These unpublished findings indicate that there is a potential signaling crosstalk between c-Kit and insulin receptor, and this deserves a closer examination for its implication in regulating insulin secretion from beta-cells.

7.2.4 Chapter 6

The limitations of this study are similar to those of the studies discussed in Chapter 3 and 5, specifically in regard to the non-tissue-specific *c-Kit* W^v mutation or the potential leaky expression inherent to the RIP-transgene construct employed in our mouse models. Furthermore, the *c-KitβTg* mouse model is insufficient to determine the direct correlation among c-Kit, VEGF-A, and the subsequent islet vascular formation *in vivo*. A possible future study in this line of work is to examine whether changes in VEGF-A concentration alter islet endothelial cell growth in an *ex vivo* model (e.g. stimulation of isolated *c-Kit*$^{Wv/+}$ mouse islets with VEGF-A) and an *in vivo* model (e.g. knockdown of VEGF-A expression in *c-KitβTg* mouse islets).

In this study one interesting observation was that *c-KIT* overexpression in beta-cells enhanced islet angiogenesis in aged 28-week-old *c-KitβTg* mice. Although the ability of isolated *c-KitβTg* islets to undergo revascularization *in vivo* is unknown. Therefore, it would be interesting to assess the angiogenic capacity of isolated *c-KitβTg* islets following transplantation of these islets in a NOD-SCID mouse model. Another possible study is to examine whether a VEGF-A blocker is able to rescue the hypervascularization-mediated islet inflammatory response seen in *c-KitβTg* mice under HFD conditions. Findings from these future studies will provide a more comprehensive picture of the function of c-Kit in modulating islet vasculature *in vivo*.

7.3 Concluding remarks

In conclusion, the work presented in this thesis has uncovered the mechanisms by which c-Kit modulates beta-cell differentiation, survival, and function *in vivo*. Using the *c-Kit*$^{Wv/+}$ mouse model, we demonstrated that c-Kit through regulation of the downstream Akt/Gsk3β pathway and negatively regulates Fas apoptotic signaling in beta-cells. More convincing evidence showing c-Kit has a primary role in beta-cell survival and function comes from the beta-cell specific c-Kit overexpressing transgenic mouse model (*c-KitβTg* mice). *c-KIT* overexpression not only positively influenced beta-cell proliferation and insulin secretory function under basal and glucose-stimulated conditions in *c-KitβTg* mice, it also improved beta-cell survival and function protecting beta-cells from the detrimental

effects of a HFD. Furthermore, restored c-Kit expression corrected beta-cell failure in *c-Kit*$^{Wv/+}$ mice. The connection between c-Kit and VEGF-A production in beta-cells was also uncovered. Our findings explained the autocrine regulation of islet vascular formation by beta-cells and that it is at least partly regulated by c-Kit-mediated VEGF-A production through the Akt/mTOR pathway. Taken together, the information provided in this work is particularly valuable for advancing our understanding of receptor signaling that regulates beta-cell survival and function, and for the future development of effective therapies against diabetes.

7.4 Future directions

Building on the foundation of this work, further research must be conducted to provide a better understanding of SCF/c-Kit signaling in the beta-cells of normal and diabetic individuals. Some thoughts regarding the future directions in this line of research are as follows: First, multiple c-Kit isoforms that result from alternative splicing. They vary in their ability to control the duration, efficiency, and targets of c-Kit signal transduction. Moreover, it is important to determine the role of mSCF versus sSCF with respect to c-Kit signaling and to see if they are distinct qualitatively as well as quantitatively. Future work must characterize the distinct functional role of these alternative isoforms of c-Kit and SCF *in vivo*. Second, although highly proliferative c-Kit expressing beta-cells may contain a pool of islet progenitors, it should be noted that c-Kit serves as a universal marker for the identification and isolation of stem cells from tissue and multiple types of cancers. With this in mind, it is necessary to identify these unique islet progenitors precisely. Thus, research efforts to develop a specific cocktail of multiple cell surface markers would be an asset in identifying these cell populations with greater specificity. Third, oncogenic c-Kit mutants promote tumorigenesis in contrast to normal c-Kit. Thus, it is important to obtain a complete understanding of the segregation of molecular mechanisms underlying mutant and normal c-Kit. This information can be useful in uncovering the potential downstream signaling targets necessary to maximize the positive effects of c-Kit on islet viability and function, while minimizing the oncogenic effects of c-Kit in other normal and neoplastic tissues. Fourth, the propensity of c-Kit-mediated insulin release and islet angiogenesis presents several potential long-term adverse effects.

For instance, excess insulin release triggered by chronic c-Kit activation on beta-cells may lead to hypoglycemia [36]. Additionally, in obese adults with insulin resistance, c-Kit-mediated islet hypervascularization stimulates an inflammatory response within islets, which contributes to a progressive reduction of beta-cell mass and function leading to T2D. Therefore, it is essential to optimize the time-dependent effect of c-Kit function in preclinical applications when aiming to restore beta-cell survival and function.

7.5 References

1. Krishnamurthy M, Ayazi F, Li J, et al. (2007) c-Kit in early onset of diabetes: a morphological and functional analysis of pancreatic beta-cells in c-KitW-v mutant mice. Endocrinology 148:5520–5530. doi: 10.1210/en.2007-0387

2. Tetsu O, McCormick F (1999) Beta-catenin regulates expression of cyclin D1 in colon carcinoma cells. Nature 398:422–426. doi: 10.1038/18884

3. Shtutman M, Zhurinsky J, Simcha I, et al. (1999) The cyclin D1 gene is a target of the beta-catenin/LEF-1 pathway. Proc Natl Acad Sci USA 96:5522–5527.

4. Feng Z-C, Donnelly L, Li J, et al. (2012) Inhibition of Gsk3β activity improves β-cell function in c-KitWv/+ male mice. Lab Invest 92:543–555. doi: 10.1038/labinvest.2011.200

5. Feng Z-C, Riopel M, Li J, et al. (2013) Downregulation of Fas activity rescues early onset of diabetes in c-Kit(Wv/+) mice. Am J Physiol Endocrinol Metab 304:E557–65. doi: 10.1152/ajpendo.00453.2012

6. Rocha S, Martin AM, Meek DW, Perkins ND (2003) p53 represses cyclin D1 transcription through down regulation of Bcl-3 and inducing increased association of the p52 NF-kappaB subunit with histone deacetylase 1. Mol Cell Biol 23:4713–4727.

7. Schreiber M, Kolbus A, Piu F, et al. (1999) Control of cell cycle progression by c-Jun is p53 dependent. Genes Dev 13:607–619.

8. Feng ZC, Li J, Turco BA, et al. (2012) Critical role of c-Kit in beta cell function: increased insulin secretion and protection against diabetes in a mouse model. Diabetologia 55:2214–2225. doi: 10.1007/s00125-012-2566-5

9. Puputti M, Tynninen O, Pernilä P, et al. (2010) Expression of KIT receptor tyrosine kinase in endothelial cells of juvenile brain tumors. Brain Pathol 20:763–770. doi: 10.1111/j.1750-3639.2009.00357.x

10. Heinke T, Espiríto Santo KSD, Longatto Filho A, Stavale JN (2013) Vascular endothelial growth factor and KIT expression in relation with microvascular density and tumor grade in supratentorial astrocytic tumors. Acta Cir Bras 28:48–54.

11. Amin MM, El-Hawary AK, Farouk O (2012) Relation of CD117 immunoreactivity and microvascular density in invasive breast carcinoma. Indian J Pathol Microbiol 55:456–460. doi: 10.4103/0377-4929.107780

12. Rasmussen BA, Breen DM, Lam TKT (2012) Lipid sensing in the gut, brain and liver. Trends Endocrinol Metab 23:49–55. doi: 10.1016/j.tem.2011.11.001

13. Breen DM, Yang CS, Lam TKT (2011) Gut-brain signalling: how lipids can trigger the gut. Diabetes Metab Res Rev 27:113–119. doi: 10.1002/dmrr.1160

14. King AJF (2012) The use of animal models in diabetes research. Br J Pharmacol 166:877–894. doi: 10.1111/j.1476-5381.2012.01911.x

15. Flanagan DE, Vaile JC, Petley GW, et al. (2007) Gender differences in the relationship between leptin, insulin resistance and the autonomic nervous system. Regul Pept 140:37–42. doi: 10.1016/j.regpep.2006.11.009

16. Rees DA, Alcolado JC (2005) Animal models of diabetes mellitus. Diabet Med 22:359–370. doi: 10.1111/j.1464-5491.2005.01499.x

17. Fraenkel M, Caloyeras J, Ren S-G, Melmed S (2006) Sex-steroid milieu determines diabetes rescue in pttg-null mice. J Endocrinol 189:519–528. doi: 10.1677/joe.1.06656

18. Ostenson CG, Grill V, Roos M (1989) Studies on sex dependency of B-cell susceptibility to streptozotocin in a rat model of type II diabetes mellitus. Exp Clin Endocrinol 93:241–247. doi: 10.1055/s-0029-1210863

19. Bell RC, Khurana M, Ryan EA, Finegood DT (1994) Gender differences in the metabolic response to graded numbers of transplanted islets of Langerhans. Endocrinology 135:2681–2687. doi: 10.1210/endo.135.6.7988458

20. Weksler-Zangen S, Yagil C, Zangen DH, et al. (2001) The newly inbred cohen diabetic rat: a nonobese normolipidemic genetic model of diet-induced type 2 diabetes expressing sex differences. Diabetes 50:2521–2529.

21. Ohno T, Yoshida F, Ichikawa Y, et al. (1998) A new spontaneous animal model of NIDDM without obesity in the musk shrew. Life Sci 62:995–1006.

22. Billimoria FR, Katyare SS, Patel SP (2006) Insulin status differentially affects energy transduction in cardiac mitochondria from male and female rats. Diabetes Obes Metab 8:67–74. doi: 10.1111/j.1463-1326.2005.00470.x

23. Malorni W, Campesi I, Straface E, et al. (2007) Redox features of the cell: a gender perspective. Antioxid Redox Signal 9:1779–1801. doi: 10.1089/ars.2007.1596

24. Davis SN, Galassetti P, Wasserman DH, Tate D (2000) Effects of gender on neuroendocrine and metabolic counterregulatory responses to exercise in normal man. J Clin Endocrinol Metab 85:224–230. doi: 10.1210/jcem.85.1.6328

25. Kunick C, Lauenroth K, Leost M, et al. (2004) 1-Azakenpaullone is a selective inhibitor of glycogen synthase kinase-3 beta. Bioorg Med Chem Lett 14:413–416.

26. Patel S, Doble BW, MacAulay K, et al. (2008) Tissue-specific role of glycogen synthase kinase 3beta in glucose homeostasis and insulin action. Mol Cell Biol 28:6314–6328. doi: 10.1128/MCB.00763-08

27. Cho J, Rameshwar P, Sadoshima J (2009) Distinct roles of glycogen synthase kinase (GSK)-3alpha and GSK-3beta in mediating cardiomyocyte differentiation in murine bone

marrow-derived mesenchymal stem cells. J Biol Chem 284:36647–36658. doi: 10.1074/jbc.M109.019109

28. Liang M-H, Chuang D-M (2006) Differential roles of glycogen synthase kinase-3 isoforms in the regulation of transcriptional activation. J Biol Chem 281:30479–30484. doi: 10.1074/jbc.M607468200

29. Nagata S, Suda T (1995) Fas and Fas ligand: lpr and gld mutations. Immunol Today 16:39–43.

30. Dor Y, Brown J, Martinez OI, Melton DA (2004) Adult pancreatic beta-cells are formed by self-duplication rather than stem-cell differentiation. Nature 429:41–46. doi: 10.1038/nature02520

31. Postic C, Shiota M, Niswender KD, et al. (1999) Dual roles for glucokinase in glucose homeostasis as determined by liver and pancreatic beta cell-specific gene knock-outs using Cre recombinase. J Biol Chem 274:305–315.

32. Herrera PL (2000) Adult insulin- and glucagon-producing cells differentiate from two independent cell lineages. Development 127:2317–2322.

33. Lev S, Blechman J, Nishikawa S, et al. (1993) Interspecies molecular chimeras of kit help define the binding site of the stem cell factor. Mol Cell Biol. 13:2224-2234.

34. Xiang Z, Kreisel F, Cain J, et al. (2007) Neoplasia driven by mutant c-KIT is mediated by intracellular, not plasma membrane, receptor signaling. Mol Cell Biol. 27:267-282.

35. Lev S, Yarden Y, Givol D (1992) Dimerization and activation of the kit receptor by monovalent and bivalent binding of the stem cell factor. J Biol Chem. 267:15970-15977.

36. Schuit F, Van Lommel L, Granvik M, et al. (2012) β-cell-specific gene repression: a mechanism to protect against inappropriate or maladjusted insulin secretion? Diabetes 61:969–975. doi: 10.2337/db11-1564

Appendices

Appendix I. Animal used protocol.

APPROVED2008-038-04::5

To:

Cc:

From:

Western

AUP Number: 2008-038-04
PI Name: Wang, Rennian
AUP Title: Pancreatic Beta Cell Development: The Role Of The C-kit And Integrin Receptors

Approval Date: 10/29/2012

Official Notice of Animal Use Subcommittee (AUS) Approval: Your new Animal Use Protocol (AUP) entitled "Pancreatic Beta Cell Development: The Role Of The C-kit And Integrin Receptors " has been APPROVED by the Animal Use Subcommittee of the University Council on Animal Care. This approval, although valid for four years, and is subject to annual Protocol Renewal.2008-038-04::5

This AUP number must be indicated when ordering animals for this project.
Animals for other projects may not be ordered under this AUP number.
Purchases of animals other than through this system must be cleared through the ACVS office.
Health certificates will be required.

The holder of this Animal Use Protocol is responsible to ensure that all associated safety components (biosafety, radiation safety, general laboratory safety) comply with institutional safety standards and have received all necessary approvals. Please consult directly with your institutional safety officers.

Submitted by: Copeman, Laura
on behalf of the Animal Use Subcommittee
University Council on Animal Care

The University *of* Western Ontario
Animal Use Subcommittee / University Council on Animal Care
Health Sciences Centre, ● London, Ontario ● CANADA – N6A 5C1
PH: :
Email: ● http://www.uwo.ca/animal/website/

1 of 1 12-10-29 12:25 PM

Appendix II. Biosafety approval.

Researcher: Dr. Rennian Wang

Biosafety Approval Number: BIO-LHRI-0046

Expiry Date: April 24, 2017

April 28, 2014

Dear Dr. Wang:

Please note your biosafety approval number listed above. This number is very useful to you as a researcher working with biohazards. It is a requirement for your research grants, purchasing of biohazardous materials and Level 2 inspections.

Research Grants:

- This number is required information for any research grants involving biohazards. Please provide this number to Research Services when requested.

Purchasing Materials:

- This number must be included on purchase orders for Level 1 or Level 2 biohazards. When you order biohazardous material, use the on-line purchase ordering system (www.uwo.ca/finance/people/). In the "Comments to Purchasing" tab, include your name as the Researcher and your biosafety approval number.

Annual Inspections:

- If you have a Level 2 laboratory on campus, you are inspected every year. This is your permit number to allow you to work with Level 2 biohazards.

To maintain your Biosafety Approval, you need to:

- Ensure that you update your Biohazardous Agents Registry Form at least every three years, or when there are changes to the biohazards you are working with.
- Ensure that the people working in your laboratory are trained in Biosafety.
- Ensure that your laboratory follows the University of Western Ontario Biosafety Guidelines and Procedures Manual for Containment Level 1 & 2 Laboratories.
- For more information, please see: www.uwo.ca/hr/safety/biosafety/.

Please let me know if you have questions or comments.

Regards,

Tony Hammoud
Biosafety Coordinator for Western
Support Services Building 4190
Phone:
Fax:

Appendix III. Sequences of primers.

Sequences of primers used in PCR for B6.MRL-Fas^{lpr} mutation genotyping
(The Jackson Laboratory, Bar Harbor, ME, USA)

Primer	sequence 5'->3'	Primer Type
oIMR1678	GTA AAT AAT TGT GCT TCG TCA G	Common
oIMR1679	TAG AAA GGT GCA CGG GTG TG	Mutant
oIMR1680	CAA ATC TAG GCA TTA ACA GTG	Wild type

Sequences of primers used in PCR for c-KitβTg genotyping

Primer	sequence 5'->3'	Primer Type
Globin5	GCT CCT GGG CAA CGT GCT GG	c-Kit
c-Kit	GTG AGA GGA CAG CGG ACC AGC	
eGFP3	CAG TCC GCC CTG AGC AAA GAC C	eGFP
Globin3	GGT ATT TGT GAG CCA GGG CAT TG	

Appendix IV. Sequences of siRNA

A pool of three different c-Kit (r) and Fas (r) siRNA duplexes
(Santa Cruz Biotechnology, Inc., Santa Cruz, CA, USA)

	Sense	**Antisense**
c-Kit siRNA (sc-36533)		
1)	CCAUGUGGAUAAAGUUGAAtt	UUCAACUUUAUCCACAUGGtt
2)	GAUGGUUCUUGCCUACAAAtt	UUUGUAGGCAAGAACCAUCtt
3)	GCAAGAAUAGACUCGUAUAtt	UAUACGAGUCUAUUCUUGCtt
Fas siRNA (sc-270241)		
1)	CCUGAAAGUCUGCCAAUGAtt	UCAUUGGCACACUUUCAGGtt
2)	GCAUUUCUAGUUGCCUAUUtt	AAUAGGCAACUAGAAAUGCtt
3)	CACAGUUAAGUGGUUCAUUtt	AAUGAACCACUUAACUGUGtt

Appendix V. List of antibodies for immunofluorescence.

List of antibodies used for immunofluorescence.

Primary Antibody	Dilution	Source
Mouse anti-insulin	1:1500	Sigma-Aldrich, Saint Louis, Missouri, USA
Guinea pig anti-insulin	1:50	Zymed, San Francisco, CA, USA
Mouse anti-glucagon	1:2000	Sigma-Aldrich, Saint Louis, Missouri, USA
Rabbit anti-Ki67	1:200	Abcam Inc., Cambridge, MA, USA
Guinea pig anti-PDX-1	1:1500	Dr.Wright, University of Vanderbilt, USA
Mouse anti-PAX6	1:300	DHSB, Iowa City, IA, USA
Mouse anti-NKX2.2	1:500	DHSB, Iowa City, IA, USA
Mouse anti-NKX6.1	1:100	DHSB, Iowa City, IA, USA
Rabbit anti-c-Kit	1:50	Abcam Inc., Cambridge, MA, USA
Mouse anti-SCF	1:50	Santa Cruz Biotechnology, Inc., CA, USA
Rabbit anti-Fas	1:200	Santa Cruz Biotechnology, Inc., CA, USA
Mouse anti-cyclin D1	1:200	Cell Signaling, Danvers, MA, USA
Rabbit anti-PECAM-1	1:50	Santa Cruz Biotechnology, Inc., CA, USA
Rabbit anti-MafA	1:100	Bethyl Laboratories, Inc., Montgomery, TX, USA
Rabbit anti-E-Cadherin	1:200	Cell Signaling, Danvers, MA, USA
Rabbit anti-eGFP	1:500	Abcam Inc., Cambridge, MA, USA
In Situ Cell Death (TUNEL)_Tissue	1:20	Roche Applied Science, Mannheim, Germany
In Situ Cell Death (TUNEL)_Cell	1:10	Roche Applied Science, Mannheim, Germany

Appendix VI. List of antibodies for western blot.

List of antibodies used for western blot analyses.

Primary Antibody	Dilution	Source
Mouse anti-β-actin	1:5000	Sigma-Aldrich, Oakville, ON, Canada
Rabbit anti-β-catenin	1:500	Millipore, Billerica, MA, USA
Mouse anti-Calnexin	1:2000	BD Biosciences, Mississauga, ON, Canada
Rabbit anti-Caspase 3	1:1000	Cell signaling, Danvers, MA, USA
Rabbit anti-Cleaved Caspase 3 (D175)	1:2000	Cell signaling, Danvers, MA, USA
Rabbit anti-Caspase 8	1:1000	Cell signaling, Danvers, MA, USA
Mouse anti-Cleaved Caspase 8(D391)	1:1000	Cell signaling, Danvers, MA, USA
Rabbit anti-c-Kit	1:500	Santa Cruz Biotechnology, Inc., CA, USA
Rabbit anti-Fas	1:2000	Santa Cruz Biotechnology, Inc., CA, USA
Mouse anti-P53	1:1000	Cell signaling, Danvers, MA, USA
Rabbit anti-Pdx-1	1:2000	Dr.Wright, University of Vanderbilt, USA
Mouse anti-Phospho-Akt (S473)	1:2000	Cell Signaling, Boston, MA, USA
Mouse anti-Phospho-Akt (T308)	1:2000	Cell Signaling, Boston, MA, USA
Rabbit anti-Akt	1:3000	Cell Signaling, Boston, MA, USA
Rabbit anti-Gsk3β (S9)	1:2000	Cell Signaling, Boston, MA, USA
Rabbit anti-Gsk3β (Y216)	1:2000	Abcam Inc. Cambridge, MA, USA
Rabbit anti-Gsk3β	1:2000	Cell Signaling, Boston, MA, USA
Mouse anti-Cyclin D1	1:2000	Cell Signaling, Boston, MA, USA
Rabbit anti-VEGF	1:2000	Abcam Inc., Cambridge, MA, USA
Mouse anti-P70S6K (T389)	1:1000	Cell Signaling, Boston, MA, USA
Rabbit anti-P70S6K	1:1000	Cell Signaling, Boston, MA, USA
Rabbit anti-NFκBp65 (S536)	1:2000	Cell Signaling, Boston, MA, USA
Rabbit anti-NFκBp65	1:2000	Cell Signaling, Boston, MA, USA
Rabbit anti-GAPDH	1:1000	Santa Cruz Biotechnology, Inc., CA, USA
Rabbit anti-PECAM-1	1:1000	Santa Cruz Biotechnology, Inc., CA, USA
Rabbit anti-E-Cadherin	1:1000	Cell Signaling, Boston, MA, USA
Rabbit anti-Cleaved PARP/PARP	1:1000	Cell Signaling, Boston, MA, USA
Rabbit anti-IL-1β	1:500	Abcam Inc., Cambridge, MA, USA
Mouse anti-Mac-2 (Galectin 3)	1:1000	Abcam Inc., Cambridge, MA, USA
Rabbit anti-TNFα	1:500	Abcam Inc., Cambridge, MA, USA
Rabbit anti-eGFP	1:5000	Abcam Inc., Cambridge, MA, USA

Appendix VII. Sequences of primers for real-time RT-PCR.

Sequences of primers used in real-time RT-PCR

Primer Name	Accession & Definition	Primer Pair Sequence 5'- 3' (*Sense/Antisense*)	Location (*nt*)	Fragment Size(bp)
C-KIT (Homo sapiens)	NM_000222.1	GCA ACG TTG ACT ATC AGT TCA GC TTC ATT CTC AGA CTT GGG ATA AT	904-926 1191-1169	288
Glp1r	NM_021332.2	GGA CTC TCT AGG CTG CCG ACT AAG AGA ATG GGC AAT CGG ATG	673-693 954-934	282
Glucagon (Gcg)	NM_008100.2	GAT CAT TCC CAG CTT CCC AG CGG TTC CTC TTG GTG TTC AT	193-212 355-336	163
Glut2 (Slc2a2)	NM_031197.1	TTG ACT GGA GCC CTC TTG AT ACT TCG TCC AGC AAT GAT GA	466-485 537-518	72
Insulin I&II	NM_008386.3 & NM_008387.3	GGC TTC TTC TAC ACA CCC A CAG TAG TTC TCC AGC TGG TA	322-340 503-484	182
Bax	NM_007527.3	GTT TCA TCC AGG ATC GAG CA CCG TGT CCA CGT CAG CAA TC	209-228 379-360	171
Bcl2	NM_009741.3	AAC CGG GAG ATC GTG ATG AA CAC GAC GGT AGC GAC GAG AG	1441-1460 1732-1713	292
Cflar (c-Flip)	NM_207653.3	TCC AGA ATG GGC GAA GTA AAG TTG CAT ATC GGC GAA CAA TC	1119-1139 1403-1384	285
MafA	NM_194350.1	AGC GCT TCT CCG ACG ACC AG GGC CCG CCA ACT TCT CGT AT	692-711 976-957	285
Neurod1	NM_010894.2	CCC GGT GCA TCC CTA CTC CT CTC GGC GGA TGG TTC GTG TT	739-758 973-954	235
Nkx2.2	NM_010919.1	CGG GCG GAG AAA GGT ATG GA CCG AGC TGT ACT GGG CGT TG	943-962 1144-1125	202
Nkx6.1	NM_144955.2	GAG AGC ACG CTT GGC CTA TT TCG TCA GAG TTC GGG TCC AG	1275-1294 1487-1468	213
Pax4	NM_011038.1	TGA ATC AGC TAG GGG GAC TCT GAC ACC TGT GCG GTA GTA GCG	232-252 404-384	173
Pax6	NM_013627.3	TTC TGG GCA GGT ATT ACG AG GCC CGT TCA ACA TCC TTA GT	636-655 923-904	288
Pdx1	NM_008814.2	CCA CCC CAG TTT ACA AGC TCG GTA GGC AGT ACG GGT CCT CT	252-272 575-556	324
Scf (Kitl)	NM_013598.2	CAG TAC ATG GTG GCT GCT CT CTT GCA CAA GCA AAT CCA GT	2661-2680 2804-2785	144
CyclinD1 (Ccnd1)	NM_007631.2	CTG TGC GCC CTC CGT ATC TTA TCG GGC CGG ATA GAG TTG TCA	343-363 636-616	294
c-Kit(Rat)	NM_022264.1	AGC AAG AGT TAA CGA TTC CG CCA GAA AGG TGT AAG TGC CT	887-906 1230-1216	344
c-Kit(Mouse)	NM_021099.2	TTA CAT AGA CCC GAC GCA ACT T TTT GAG CAT CTT CAC GGC AAC T	1732-1753 1903-1882	172
Fas(Mouse)	NM_007987.1	CCC AGA AAT CGC CTA TGG TT AGC AAT TCT CGG GAT GTA TT	545-564 736-717	192
Fas(Rat)	NM_139194.2	CGG ACC CAG AAT ACC AAG TGC CAT TTG GTG TTG CTG GTT CGT	404-424 540-520	137
Fasl	NM_010177.3	ACC ACC GCC ATC ACA ACC AC GCA AGA CTG ACC CCG GAA GT	375-394 810-791	436
NFkb1	NM_008689.2	TGG TGG AGG CAT GTT CGG TAG CCC TGC GTT GGA TTT CGT GAC	1645-1665 1783-1763	139
NFkb2	NM_019408.3	ACC TGA AGA TCT CCC GAA TGG CGG AAC ACA ATG GCA TAC TGT	989-1009 1178-1158	190
RelA	NM_009045.4	GCA GTA TTC CTG GCG AGA GA TCT GGA TTC GCT GGC TAA TGG	476-495 751-731	276
RelB	NM_009046.2	CAC CGA AGC CAG CAA GAC CCT CAG CTG GAT CTT CCG CTC AAT	601-621 865-845	265
Trp53	NM_011640.3	GCA TGA ACC GCC GAC CTA TC TCT TCT TCT GTA CGG CGG TCT	882-901 1008-988	127
18S	NR_003278.1	GTA ACC CGT TGA ACC CCA TTC CCA TCC AAT CGG TAG TAG CG	1577-1597 1727-1708	151

Appendix VIII. Copyright of Chapter 3.

RightsLink®

Home | Account Info | Help

Title: Inhibition of Gsk3β activity improves β-cell function in *c-Kit*$^{Wv/+}$ male mice

Author: Zhi-Chao Feng, Lisa Donnelly, Jinming Li, Mansa Krishnamurthy, Matthew Riopel, Rennian Wang

Publication: Laboratory Investigation

Publisher: Nature Publishing Group

Date: Jan 16, 2012

Logged in as:
zhi chao Feng

LOGOUT

Creative Commons

The request you have made is considered to be non-commercial/educational. As the article you have requested has been distributed under a Creative Commons license (Attribution-Noncommercial 2.5), you may reuse this material for non-commercial/educational purposes without obtaining additional permission from Nature Publishing Group, providing that the author and the original source of publication are fully acknowledged.

For full terms and conditions of the Creative Commons license, please see the attached link http://creativecommons.org/licenses/by-nc/2.5

BACK | CLOSE WINDOW

Appendix IX. Copyright of Chapter 5.

SPRINGER LICENSE
TERMS AND CONDITIONS

Jun 09, 2014

This is a License Agreement between zhi chao Feng ("You") and Springer ("Springer") provided by Copyright Clearance Center ("CCC"). The license consists of your order details, the terms and conditions provided by Springer, and the payment terms and conditions.

All payments must be made in full to CCC. For payment instructions, please see information listed at the bottom of this form.

License Number	3404911086328
License date	Jun 09, 2014
Licensed content publisher	Springer
Licensed content publication	Diabetologia
Licensed content title	Critical role of c-Kit in beta cell function: increased insulin secretion and protection against diabetes in a mouse model
Licensed content author	Z. C. Feng
Licensed content date	Jan 1, 2012
Volume number	55
Issue number	8
Type of Use	Thesis/Dissertation
Portion	Figures
Author of this Springer article	Yes and you are a contributor of the new work
Order reference number	None
Original figure numbers	Figures 1, 2, 3, 4, 5, 6, 7; Supplemental Figures 1, 2, 3, 4, 5, 6, 7, 8, 9, 10
Title of your thesis / dissertation	THE ROLE OF C-KIT RECEPTOR TYROSINE KINASE IN BETA-CELL PROLIFERATION, FUNCTION, AND SURVIVAL
Expected completion date	Jul 2014
Estimated size(pages)	200
Total	0.00 USD
Terms and Conditions	

Introduction
The publisher for this copyrighted material is Springer Science + Business Media. By

clicking "accept" in connection with completing this licensing transaction, you agree that the following terms and conditions apply to this transaction (along with the Billing and Payment terms and conditions established by Copyright Clearance Center, Inc. ("CCC"), at the time that you opened your Rightslink account and that are available at any time at http://myaccount.copyright.com).

Limited License
With reference to your request to reprint in your thesis material on which Springer Science and Business Media control the copyright, permission is granted, free of charge, for the use indicated in your enquiry.

Licenses are for one-time use only with a maximum distribution equal to the number that you identified in the licensing process.

This License includes use in an electronic form, provided its password protected or on the university's intranet or repository, including UMI (according to the definition at the Sherpa website: http://www.sherpa.ac.uk/romeo/). For any other electronic use, please contact Springer at (permissions.dordrecht@springer.com or permissions.heidelberg@springer.com).

The material can only be used for the purpose of defending your thesis limited to university-use only. If the thesis is going to be published, permission needs to be re-obtained (selecting "book/textbook" as the type of use).

Although Springer holds copyright to the material and is entitled to negotiate on rights, this license is only valid, subject to a courtesy information to the author (address is given with the article/chapter) and provided it concerns original material which does not carry references to other sources (if material in question appears with credit to another source, authorization from that source is required as well).

Permission free of charge on this occasion does not prejudice any rights we might have to charge for reproduction of our copyrighted material in the future.

Altering/Modifying Material: Not Permitted
You may not alter or modify the material in any manner. Abbreviations, additions, deletions and/or any other alterations shall be made only with prior written authorization of the author(s) and/or Springer Science + Business Media. (Please contact Springer at (permissions.dordrecht@springer.com or permissions.heidelberg@springer.com)

Reservation of Rights
Springer Science + Business Media reserves all rights not specifically granted in the combination of (i) the license details provided by you and accepted in the course of this licensing transaction, (ii) these terms and conditions and (iii) CCC's Billing and Payment terms and conditions.

Copyright Notice:Disclaimer
You must include the following copyright and permission notice in connection with any reproduction of the licensed material: "Springer and the original publisher /journal title,

volume, year of publication, page, chapter/article title, name(s) of author(s), figure number(s), original copyright notice) is given to the publication in which the material was originally published, by adding; with kind permission from Springer Science and Business Media"

Warranties: None

Example 1: Springer Science + Business Media makes no representations or warranties with respect to the licensed material.

Example 2: Springer Science + Business Media makes no representations or warranties with respect to the licensed material and adopts on its own behalf the limitations and disclaimers established by CCC on its behalf in its Billing and Payment terms and conditions for this licensing transaction.

Indemnity
You hereby indemnify and agree to hold harmless Springer Science + Business Media and CCC, and their respective officers, directors, employees and agents, from and against any and all claims arising out of your use of the licensed material other than as specifically authorized pursuant to this license.

No Transfer of License
This license is personal to you and may not be sublicensed, assigned, or transferred by you to any other person without Springer Science + Business Media's written permission.

No Amendment Except in Writing
This license may not be amended except in a writing signed by both parties (or, in the case of Springer Science + Business Media, by CCC on Springer Science + Business Media's behalf).

Objection to Contrary Terms
Springer Science + Business Media hereby objects to any terms contained in any purchase order, acknowledgment, check endorsement or other writing prepared by you, which terms are inconsistent with these terms and conditions or CCC's Billing and Payment terms and conditions. These terms and conditions, together with CCC's Billing and Payment terms and conditions (which are incorporated herein), comprise the entire agreement between you and Springer Science + Business Media (and CCC) concerning this licensing transaction. In the event of any conflict between your obligations established by these terms and conditions and those established by CCC's Billing and Payment terms and conditions, these terms and conditions shall control.

Jurisdiction
All disputes that may arise in connection with this present License, or the breach thereof, shall be settled exclusively by arbitration, to be held in The Netherlands, in accordance with Dutch law, and to be conducted under the Rules of the 'Netherlands Arbitrage Instituut' (Netherlands Institute of Arbitration).***OR:***

All disputes that may arise in connection with this present License, or the breach

thereof, shall be settled exclusively by arbitration, to be held in the Federal Republic of Germany, in accordance with German law.

Other terms and conditions:

v1.3

If you would like to pay for this license now, please remit this license along with your payment made payable to "COPYRIGHT CLEARANCE CENTER" otherwise you will be invoiced within 48 hours of the license date. Payment should be in the form of a check or money order referencing your account number and this invoice number 501323712. Once you receive your invoice for this order, you may pay your invoice by credit card. Please follow instructions provided at that time.

Make Payment To:
Copyright Clearance Center
Dept 001
P.O. Box 843006
Boston, MA 02284-3006

For suggestions or comments regarding this order, contact RightsLink Customer Support: customercare@copyright.com or +1-877-622-5543 (toll free in the US) or +1-978-646-2777.

Gratis licenses (referencing $0 in the Total field) are free. Please retain this printable license for your reference. No payment is required.

Curriculum Vitae

Curriculum Vitae

Zhi-Chao Feng

EDUCATION

Ph.D. Pharmacology and Toxicology, expected 09/2009 - 07/2014, Western University
Dissertation: The role of c-Kit receptor tyrosine kinase in beta-cell proliferation, function and survival.

BMSc., **Honors Specialization in Physiology and Pharmacology**, 09/2005 - 04/2009, Western University

SCHOLARSHIPS and AWARDS

Graduate school scholarships

- **Canadian Diabetes Association Doctoral Student Research Award** (Accepted)
  Canada Diabetes Association, Funded Year 2012 - 2015
- **Queen Elizabeth II Graduate Scholarship in Science and Technology** (Declined)
  Government of Ontario, Funded Year 2012 - 2013
- **Schulich Graduate Scholarship** (Accepted)
  Western University, Funded Year 2009 - 2014

Graduate school awards

- **European Association for the Study of Diabetes Travel Grant**
  The European Association for the Study of Diabetes, 2013
- **Graduate Thesis Research Award**
  School of Graduate Studies, Western University, 2013
- **Trainee Travel Award**
  Children's Health Research Institute, 2013
- **Featured Trainee**
  Children's Health Research Institute, 2013
- **Graduate Student Travel Award**
  Department of Physiology and Pharmacology, Western University, 2012
- **Poster Presentation Award, 2nd Prize**
  Department of Physiology and Pharmacology, Western University, 2012
- **Sister Mary Doyle Award for Platform Presentation, Silver medal**
  Lawson Health Research Institute, 2011

RELATED ACADEMIC WORK EXPERIENCE

RELATED ACADEMIC WORK EXPERIENCE

- **Graduate Teaching Assistant – Course: Physiology 3130y**
  Department of Physiology and Pharmacology, Western University, 2009-2014
  - Assisting the professors with the instructional responsibilities in Physiology 3130y course, including teaching students in laboratory, tutorial, discussion sessions.

- **Reviewer Board - Health Science Inquiry (HSI), Issue of Diabetes**
  University of Toronto, 2011-2012
  - Critically evaluating and providing the detailed feedback on submissions received by the journal.

CONFERENCE PROCEEDINGS

- **Feng ZC**, Li J, Silverstein J, Popell A, Yee SP, Wang R. (2013) Long-term overexpression of c-Kit negatively impacts beta-cell function and survival via capillary and inflammatory recruitment in the islet. The European Association for the Study of Diabetes Abstract. Poster presentation 537 to be delivered at EASD, Barcelona, Spain, October, 2013.

- **Feng ZC,** Li J, Silverstein J, Yee SP, Wang R. (2013) Chronic up-regulation of insulin receptor through cross-talk between c-Kit negatively impacts beta-cell proliferation and function in aging *c-KitβTg* mice. The 5th Islet Society Meeting Abstract. Platform presentation to be delivered in Vancouver, Canada, July, 2013.

- **Feng ZC**, Jam A, Li J, Wang R. (2012) Cross-talk between the c-Kit and insulin receptors enhances beta-cell proliferation and function. The European Association for the Study of Diabetes Abstract. Poster presentation 393 to be delivered at EASD, Berlin, Germany, October, 2012.

- Li J, Wong M, **Feng ZC**, Wang R. (2012) Role of Aldehyde dehydrogenase 1 (ALDH1) activity in the developing human pancreas. The European Association for the Study of Diabetes Abstract. Poster presentation 416 to be delivered at EASD, Berlin, Germany, October, 2012.

- **Feng ZC**, Riopel M, Li J, Wang R. (2011) Improved beta-cell proliferation and function in *c-Kit$^{Wv/+}$;Fas$^{lpr/lpr}$* double mutant mice. The 71st Scientific Sessions, American Diabetes Association Abstract. Platform presentation to be delivered at ADA, San Diego, USA, June, 2011. Diabetes, 2011 Suppl (1): A28.

- **Feng ZC**, Li J, Turco BA, Yee SP, Wang R. (2011) Beta-cell specific c-Kit receptor over-expression transgenic mice show improved beta-cell function and resistance to high-fat diet-induced diabetes. The 71st Scientific Sessions, American Diabetes Association Abstract. Poster presentation to be delivered at ADA, San Diego, USA, June, 2011. Diabetes, 2011 Suppl (1): A529.

- **Feng ZC**, Donnelly L, Li J, Krishnamurthy M, Wang R. (2010) Downregulation of Phospho-Akt/GSK3β pathway in early onset of diabetes in *c-Kit$^{Wv/+}$* male mice. The 70th Scientific Sessions, American Diabetes Association Abstract. Poster presentation to be delivered at ADA, Orlando, USA, June, 2010. Diabetes, 2010 Suppl (1): A458.

PEER-REVIEWED PUBLICATIONS

- **Feng ZC**, Popell A, Li J, Yee SP, Wang R. (2014) Chronic up-regulation of insulin receptor through cross-talk between c-Kit negatively impacts beta-cell proliferation and function in aging *c-KitβTg* mice. (*Manuscript in preparation*)

- **Feng ZC**, Popell A, Li J, Silverstein J, Yee SP, Wang R. (2014) c-Kit receptor tyrosine regulates islet microvasculature, beta-cell survival and function *in vivo*. (*Prepared in submission to the journal Cell Metabolism*)

- Li J, **Feng ZC**, Yeung FS, Wong MR, Oakie A, Fellows GF, Goodyer CG, Hess DA, Wang R. (2013) Aldehyde dehydrogenase 1 activity in the developing human pancreas modulates retinoic acid signalling in mediating islet differentiation and survival. *Diabetologia* 57:754-764. IF: 6.487

- Choi J, Diao H, **Feng ZC**, Lau A, Wang R, Jevnikar AM, Ma S. (2013) A fusion protein derived from plants holds promising potential as a new oral therapy for type 2 diabetes. *Plant Biotechnol J.* 12:425-435. IF: 6.279

- **Feng ZC**, Riopel M, Li J, Krishnamurthy M, Wang R. **(**2013) Improved beta-cell proliferation and function in *c-Kit*$^{Wv/+}$*;Fas*$^{lpr/lpr}$ double mutant mice. *Am J Physiol Endocrinol Metab.* 304:E557-E565. IF: 4.514

- **Feng ZC***, Li J*, Turco B, Riopel M, Yee SP, Wang R. (2012) Critical role of c-Kit in beta-cell function: increased insulin secretion and protection against diabetes in a mouse model. *Diabetologia* 55:2214-2225. IF: 6.487 *Equal contribution

  - 'Up front' article that merits special attention in the issue of Diabetologia.
  - Research highlights of diabetes in Nature Reviews Endocrinology. Osorio J. (2012) Diabetes: A Kit for increasing beta-cell function. *Nat Rev Endocrinol*. 8:444.
  - Commissioned commentary. Welsh M. (2012) The PDGF family of tyrosine kinase receptors: A Kit to fix the beta-cell? *Diabetologia* 55:2092-2095.
  - Featured on Schulich School of Medicine & Dentistry web page. A "Kit" for increasing insulin production.

- **Feng ZC**, Donnelly L, Li J, Krishnamurthy M, Riopel M, Wang R. (2012) Inhibition of GSK3β activity improves beta-cell function in *c-Kit*$^{Wv/+}$ male mice. *Lab Invest.* 92:543-555. IF: 3.961

REVIEW ARTICLE

- **Feng ZC,** Riopel M, Popell A, Wang R. (2014) A survival "Kit" for the pancreatic beta-cell: Stem cell factor and c-Kit receptor tyrosine kinase. (*Prepared in submission to the journal Diabetologia*)